ECF-HANFORD-19-0039
Revision 0

Vadose Zone Model for B Complex for Composite Analysis

Prepared for the U.S. Department of Energy
Assistant Secretary for Environmental Management

Contractor for the U.S. Department of Energy
under Contract DE-AC06-08RL14788

CH2MHILL
Plateau Remediation Company

P.O. Box 1600
Richland, Washington 99352

ECF-HANFORD-19-0039
Revision 0

Vadose Zone Model for B Complex for Composite Analysis

Document Type: ECF Program/Project: EPSP

P. Allena
INTERA, Inc.

C. R. Farrow
INTERA, Inc.

G. Tartakovsky
INTERA, Inc.

J. P. McDonald
INTERA, Inc.

Date Published
September 2020

Prepared for the U.S. Department of Energy
Assistant Secretary for Environmental Management

Contractor for the U.S. Department of Energy
under Contract DE-AC06-08RL14788

CH2MHILL
Plateau Remediation Company
P.O. Box 1600
Richland, Washington 99352

APPROVED
By Lynn M. Ayers at 12:23 pm, Sep 30, 2020

Release Approval Date

TRADEMARK DISCLAIMER

Reference herein to any specific commercial product, process, or service by tradename, trademark, manufacturer, or otherwise, does not necessarily constitute or imply its endorsement, recommendation, or favoring by the United States Government or any agency thereof or its contractors or subcontractors.

ENVIRONMENTAL CALCULATION COVER PAGE

SECTION 1 - Completed by the Responsible Manager

Project:
Hanford Site Composite Analysis Update

RELEASE / ISSUE

Date: 05/02/2019

DATE:
Sep 30, 2020
HANFORD RELEASE

Calculation Title and Description:
Vadose Zone Model for B Complex for Composite Analysis

Qualifications Summary

Preparer(s):

Name: Praveena Allena (Model Team Leader; title page identifies all team members)

Degree, Major, Institution, Year: MS, Civil Engineering, New Mexico State University, 2008
BS, Civil Engineering, Andhra University, 1999

Professional Licenses:

Brief Narrative of Experience: Praveena Allena's current focus is on developing and applying groundwater flow and contaminant transport models to support the environmental investigation and remediation of soils and groundwater impacted by past industrial operations and waste disposal practices. Ms. Allena has also worked for several state agencies responsible for the development, management, and protection of water resources, where her activities have included water rights permitting and administration, modeling and monitoring of regional and local groundwater levels, maintaining GIS databases, updating hydrographic and GIS survey maps, and reviewing driller reports and well logs. She also brings experience in assessing the structural damage to buildings caused by earthquakes and performing quality assurance and quality control activities for hte construction of new buildings.

ENVIRONMENTAL CALCULATION COVER PAGE (Continued)

Checker(s):

Name: Jose Lopez (Calculation Process Checking Team Leader)

Degree, Major, Institution, Year: BA, Geography with GIS, Mapping, and Society Focus, University of Washington, 2017

Professional Licenses:

Brief Narrative of Experience: Jose Lopez's experience focuses on collecting, analyzing, manipulating, and developing spatial data pertaining to Geographic Information Systems (GIS). He specializes in analyzing GIS data and using it to identify trends, build geodatabases, and create interactive maps to visualize data changes. He will be applying his skills to support and assist INTERA GIS specialists with map design, GIS analysis, and modeling. Jose is also proficient with ESRI ArcGIS software, Python, Java, and Microsoft Office applications.

Name: Mary Weber (Document Consistency Checker)

Degree, Major, Institution, Year: MS, Geoscience, University of Iowa, 2015
BS, Geoscience, University of Iowa, 2013

Professional Licenses:

Brief Narrative of Experience: Mary Weber focuses her geoscientific skills on the development and application of groundwater flow and contaminant fate and transport models. She uses models to help guide environmental investigation and remediation efforts and to project future water availability as part of developing and managing groundwater resources. Mary currently provides modeling and other technical support for remedial investigations and feasibility studies being performed on one of the largest environmental restoration projects in the world at the U.S. Department of Energy's Hanford Site.

ENVIRONMENTAL CALCULATION COVER PAGE (Continued)

Senior Reviewer(s):

Name: Mart Oostrom

Degree, Major, Institution, Year: PhD, Soil Physics, Auburn University, 1991
MS, Soil Physics and Hydrogeology, Wageningen University, 1986
MA, Teaching (Mathematics), University of Idaho, 2010
BS, Soil Science, Wageningen University, 1984

Professional Licenses:

Brief Narrative of Experience: Mart Oostrom brings specialized expertise in the development and application of numerical models to evaluate groundwater flow and contaminant transport and the effectiveness of various environmental remediation methods and technologies. Some of his recent experience includes quantifying contaminant flux into groundwater at various deep-vadose zone waste disposal sites; conducting reservoir modeling for enhanced oil recovery and CO2 sequestration; remediating the vadose zone using ammonium injection, soil dessication, and/or pore-water extraction; and developing a circulation method to quantify back-diffusion of dissolved contaminants into permeable sediment. Mart is co-author of the STOMP© (Subsurface Flow over Multiple Phase) simulator, a mathematical model used to numerically simulate subsurface (multiphase) flow and transport as well as vadose zone and groundwater remediation. STOMP's target capabilities were guided by proposed or applied remediation activities at sites contaminated with volatile organic compounds and/or radioactive material. The simulator's modeling capabilities address a variety of subsurface environments, including nonisothermal conditions, fractured media, multiple-phase systems, nonwetting fluid entrapment, soil freezing conditions, nonaqueous phase liquids, first-order chemical reactions, radioactive decay, solute transport, dense brines, nonequilibrium dissolution, and surfactant-enhanced dissolution and mobilization of organics. Mart is Associate Editor of the Journal of Contaminant Hydrology and has authored over 100 refereed journal articles and contributed to book chapters on the subjects of multifluid flow, site characterization, remediation, and monitoring.

SECTION 2 - Completed by Preparer

Calculation Number: ECF-HANFORD-19-0039	Revision Number: 0

Revision History

Revision No.	Description	Date	Affected Pages
0	Initial issue	09/17/2020	All

SECTION 3 - Completed by the Responsible Manager

Document Control:

Is the document intended to be controlled within the Document Management Control System (DMCS)? ◉ Yes ○ No

Does document contain scientific and technical information intended for public use? ◉ Yes ○ No

Does document contain controlled-use information? ○ Yes ◉ No

ENVIRONMENTAL CALCULATION COVER PAGE (Continued)

SECTION 4 - Document Review and Approval

Preparer(s):

Praveena Allena	Hydrogeologist	Per Electronic Approval (attached)	
Print First and Last Name	*Position*	*Signature*	*Date*

Checker(s):

Jose Lopez	GIS Analyst	Per Electronic Approval (attached)	
Print First and Last Name	*Position*	*Signature*	*Date*
Mary Weber	Hydrogeologist	Per Electronic Approval (attached)	
Print First and Last Name	*Position*	*Signature*	*Date*

Senior Reviewer(s):

Mart Oostrom	Principal Scientist	Per Electronic Approval (attached)	
Print First and Last Name	*Position*	*Signature*	*Date*

Responsible Manager(s):

Alaa Aly	Risk & Model Integr Mgr	Per Electronic Approval (attached)	
Print First and Last Name	*Position*	*Signature*	*Date*

SECTION 5 - Applicable if Calculation is a Risk Assessment or Uses an Environmental Model

Prior to Initiating Modeling:

Required training for modelers completed:
Integration Lead:

William Nichols	Per Electronic Approval (attached)	
Print First and Last Name	*Signature*	*Date*

Safety Software Approved:
Integration Lead:

William Nichols	Per Electronic Approval (attached)	
Print First and Last Name	*Signature*	*Date*

Calculation Approved:
Risk/Modeling Integration Manager:

Alaa Aly	Per Electronic Approval (attached)	
Print First and Last Name	*Signature*	*Date*

From: PRC SharePoint
To: Nichols, William E
Subject: Electronic Approval has completed for document: ECF-HANFORD-19-0039-R0.
Date: Tuesday, September 22, 2020 2:32:54 PM

Electronic Approval has completed for document: ECF-HANFORD-19-0039-R0.

Please include this email as the Electronic Approval page.

Electronic Approval for document: ECF-HANFORD-19-0039-R0 has successfully COMPLETED.

Electronic Approval started by Nichols, William E on 9/19/2020 2:37 PM
Comment: Please approve release of ECF-HANFORD-19-0039 Rev. 0 (B Complex VZ Model for Composite Analysis)

Approved by Nichols, William E on 9/19/2020 2:39 PM
Comment:

Approved by Aly, Alaa H on 9/21/2020 1:48 PM
Comment:

Approved by Weber, Mary C on 9/22/2020 2:32 PM
Comment:

From: Praveena Allena
To: Nichols, William E; Jose Lopez; Mart Oostrom
Subject: RE: Electronic Approval Tasks - Please approve ECF-HANFORD-19-0039-R0
Date: Monday, September 21, 2020 8:54:47 AM

Approve

From: Nichols, William E <william_e_nichols@rl.gov>
Sent: Saturday, September 19, 2020 2:40 PM
To: Praveena Allena <PAllena@intera.com>; Jose Lopez <JLopez@intera.com>; Mart Oostrom <MOostrom@intera.com>
Subject: Electronic Approval Tasks - Please approve ECF-HANFORD-19-0039-R0

Electronic Approval Task assigned by Nichols, William E on 9/19/2020.

Completing this task acts as your approval in place of a hard copy signature for document: ECF-HANFORD-19-0039-R0.

Due by **9/21/2020 5:00 PM**

Electronic Approval started by Nichols, William E on 9/19/2020 2:37 PM
Comment: Please approve release of ECF-HANFORD-19-0039 Rev. 0 (B Complex VZ Model for Composite Analysis)

To complete this task:
1. Review ECF-HANFORD-19-0039-R0. (note: HLAN link)
2. When review is complete, reply to this email with the word "Approve" to approve release of this document.

From: Jose Lopez
To: Nichols, William E
Subject: RE: Electronic Approval Tasks - Please approve ECF-HANFORD-19-0039-R0
Date: Monday, September 21, 2020 2:49:02 PM

Approve.

From: Nichols, William E <william_e_nichols@rl.gov>
Sent: Saturday, September 19, 2020 2:40 PM
To: Praveena Allena <PAllena@intera.com>; Jose Lopez <JLopez@intera.com>; Mart Oostrom <MOostrom@intera.com>
Subject: Electronic Approval Tasks - Please approve ECF-HANFORD-19-0039-R0

Electronic Approval Task assigned by Nichols, William E on 9/19/2020.

Completing this task acts as your approval in place of a hard copy signature for document: ECF-HANFORD-19-0039-R0.

Due by **9/21/2020 5:00 PM**

Electronic Approval started by Nichols, William E on 9/19/2020 2:37 PM
Comment: Please approve release of ECF-HANFORD-19-0039 Rev. 0 (B Complex VZ Model for Composite Analysis)

To complete this task:
1. Review ECF-HANFORD-19-0039-R0. (note: HLAN link)
2. When review is complete, reply to this email with the word "Approve" to approve release of this document.

From: Mart Oostrom
To: Nichols, William E
Subject: RE: Electronic Approval Tasks - Please approve ECF-HANFORD-19-0039-R0
Date: Monday, September 21, 2020 8:50:33 PM

Approve

From: Nichols, William E <william_e_nichols@rl.gov>
Sent: Saturday, September 19, 2020 2:40 PM
To: Praveena Allena <PAllena@intera.com>; Jose Lopez <JLopez@intera.com>; Mart Oostrom <MOostrom@intera.com>
Subject: Electronic Approval Tasks - Please approve ECF-HANFORD-19-0039-R0

Electronic Approval Task assigned by Nichols, William E on 9/19/2020.

Completing this task acts as your approval in place of a hard copy signature for document: ECF-HANFORD-19-0039-R0.

Due by **9/21/2020 5:00 PM**

Electronic Approval started by Nichols, William E on 9/19/2020 2:37 PM
Comment: Please approve release of ECF-HANFORD-19-0039 Rev. 0 (B Complex VZ Model for Composite Analysis)

To complete this task:
1. Review ECF-HANFORD-19-0039-R0. (note: HLAN link)
2. When review is complete, reply to this email with the word "Approve" to approve release of this document.

Contents

Appendices

Figures

Tables

This page intentionally left blank.

Terms

CA	composite analysis
CCU2	Cold Creek unit – Perched Zone silty sand
CCU3	Cold Creek unit – Perched Zone basal silt
CCUsilt	siltier end member of the upper Cold Creek unit
CCUsand	sandier end member of the upper Cold Creek unit
CCUg	Cold Creek unit gravel
ECF	environmental calculation file
EHM	Equivalent Homogeneous Media
eSTOMP	exascale Subsurface Transport Over Multiple Phases
GIS	geographic information system
Hf1	Hanford formation unit 1
Hf2	Hanford formation unit 2
Hf3	Hanford formation unit 3
HSU	hydrostratigraphic unit
ICF	Integrated Computational Framework
K_d	partition coefficient
P2R	plateau to river
PA	performance assessment
PA-TCT	power-averaging tensorial connectivity-tortuosity
RET	recharge evolution tool
RTD	remove, treat, and dispose
SIM-v2	Hanford Soil Inventory Model
STOMP	Subsurface Transport Over Multiple Phases
TCT	tensorial connectivity-tortuosity
WMA C	Waste Management Area C

This page intentionally left blank.

1 Purpose

The objectives of the vadose modeling for the updated Hanford Site composite analysis (CA) are to simulate the flow and transport of water and radionuclide releases from the surface to the water table and to provide radionuclide transfer rates for the plateau to river (P2R) model, version 8.3 (CP-57037, *Model Package Report: Plateau to River Groundwater Model, Version 8.3*). Water additions include natural recharge and water discharged to the ground as a result of industrial processes associated with Hanford Site operations. Contaminant sources include radionuclides in water discharged to the ground during operations and radionuclides disposed "dry" in solid waste burial grounds or other means. The following 16 radionuclides were selected for this modeling effort; carbon-14 (C-14), chlorine-36 (Cl-36), tritium (H-3), iodine-129 (I-129), neptunium-237 (Np-237), rhenium-187 (Re-187), strontium-90 (Sr-90), technetium-99 (Tc-99), uranium-232 (U-232), uranium-233 (U-233), uranium-234 (U-234), uranium-235 (U-235), uranium-236 (U-236), uranium-238 (U-238), radium-226 (Ra-226), and thorium-230 (Th-230). The simulation time starts in 1943 and ends at 12070, which is 10,000 years after assumed Hanford Site closure in 2070.

The parallel version of the Subsurface Transport Over Multiple Phases (STOMP[1]) simulator officially named the exascale Subsurface Transport Over Multiple Phases (eSTOMP), is used to simulate flow and transport for the vadose models. The documentation for the STOMP code is comprehensive. The theoretical and numerical approaches applied in the STOMP code are documented in a published theory guide (PNNL-12030, *STOMP Subsurface Transport Over Multiple Phases Version 2.0 Theory Guide*). The code has undergone a rigorous verification procedure against analytical solutions, laboratory-scale experiments, and field-scale demonstrations. The application guide (PNNL-11216, *STOMP Subsurface Transport Over Multiple Phases Application Guide*) provides instructive examples in the application of the code to classical groundwater problems. The user's guide (PNNL-15782, *STOMP: Subsurface Transport Over Multiple Phases Version 4.0: User's Guide*) describes the general use, input file formatting, compilation, and execution of the code. The primary output of the vadose zone modeling is radionuclide transfer rates to the groundwater for input into the P2R model. The rates will be summed over the 100 by 100 m P2R grid cells that fall within the vadose zone model source domain.

The Hanford Site Central Plateau was subdivided into 26 individual vadose zone models, with 13 in the 200 East Area and 13 in the 200 West Area. Waste sites that have a completed performance assessment (PA) or past-leak analysis were not included as sources of radionuclides. Instead the vadose zone to groundwater transfer rates of the Environmental Restoration Disposal Facility, Integrated Disposal Facility, US Ecology, and Waste Management Area C (WMA C) PAs and the past-leak analysis for WMA C were used as direct input to the P2R model. Each of the vadose zone models is documented in separate environmental calculation files (ECFs). This ECF describes the B Complex model. The scope of this ECF is to document the development and results of the B Complex vadose zone model. CP-63515, *Model Package Report: Central Plateau Vadose Zone Models*, describes the approach, assumptions, process of determining the number of models required and domain of each model, input data, and processing common to all the models. Additionally, the following documents support inputs to the models:

- CP-60925, *Model Package Report: Central Plateau Vadose Zone Geoframework*, describes the hydrostratigraphic framework.

[1] STOMP is a copyright of Battelle Memorial Institute, Columbus, Ohio, and used under the Limited Government License.

- CP-61786, *Inventory Data Package for the Hanford Site Composite Analysis*, contains the solid waste inventory.
- CP-62184, *Hanford Site Composite Analysis: Radionuclide Selection for Groundwater Pathway Evaluation*, describes the selection of the 16 radionuclides used in these simulations.
- CP-62766, *Model Package Report: Composite Analysis Solid Waste Release Model (CASWR Model)*, describes the mechanisms of release of radionuclides from solid waste based on waste type.
- CP-63883, *Vadose Zone Flow and Transport Parameters Data Package for the Hanford Site Composite Analysis,* describes the process of assigning material properties to the hydrostratigraphic units (HSUs).
- ECF-HANFORD-15-0019, *Hanford Site-wide Natural Recharge Boundary Condition for Groundwater Models*, describes the recharge evolution tool (RET) used to calculate the recharge.
- ECF-HANFORD-17-0079, *Hanford Soil Inventory Model (SIM-v2) Calculated Radionuclide Inventory of Direct Liquid Discharges to Soil in the Hanford Site's 200 Areas*, describes the aqueous sources for the CA modeling effort, which uses the source inventory found in Appendix F of ECF-HANFORD-17-0079.
- ECF-HANFORD-18-0035, *Central Plateau Vadose Zone Geoframework*, describes the updates to the hydrostratigraphy surfaces defined in CP-60925, and defines the hydrostratigraphy surfaces used by this modeling effort.
- ECF-HANFORD-19-0032, *Distribution of Infiltration in the 216-U-10 and 216-B-3 Pond Systems 1944-1997*, estimates the routing of effluent and infiltration between ditches and ponds of the 216-U-10 Pond System and between the main pond and expansion lobes of the 216-B-3 Pond System.
- ECF-HANFORD-19-0094, *Calculation of Moisture-Dependent, Anisotropic Parameters Supporting the Hanford Site's Composite Analysis, Cumulative Impact Evaluation, and Performance Assessments*, describes calculations of moisture-dependent, anisotropy of hydraulic conductivity for the HSUs.
- ECF-HANFORD-19-0112, *Solid Waste Release Calculations for the Composite Analysis Baseline Assessment*, calculates the solid waste annual release rates.
- ECF-HANFORD-19-0121, *Selection of Vadose Zone Flow and Transport Properties with Gravel Fraction Corrections for the Hanford Site Composite Analysis and Cumulative Impact Evaluation*, describes the physical and chemical properties used for these models.
- ECF-HANFORD-20-0006, *Composite Analysis Solid Waste Release Data Reduction of Activity Flux from Waste Sites to the Vadose Zone*, describes the solid waste data reduction.

2 Background

The B Complex model encompasses the region around single-shell tank farms 241-B, 241-BX, and 241-BY, and adjacent cribs, trenches, and burial grounds in the northwestern part of the 200 East Area (Figure 2-1). Sources of waste to this area were primarily from B Plant (221-B), which separated plutonium from irradiated fuel using the bismuth-phosphate process from 1945 to 1956, and U Plant (221-U), which was used for uranium recovery operations (waste from this process was sent to 241-BY Tank Farm) (DOE/RL-97-1047, *Hanford Site Historic District History of the Plutonium Production Facilities 1943-1990*). The bismuth-phosphate process generated large quantities of waste compared to the more efficient continuous solvent extraction processes used later at the Reduction and Oxidation Plant and the Plutonium Uranium Extraction Plant (DOE/RL-97-1047). In addition, the bismuth-phosphate process did not separate uranium. B Plant was reactivated in 1968 and used for strontium and cesium recovery until 1985 (DOE/RL-97-1047). B Plant is located south of B Complex within the B Plant Area model (ECF-HANFORD-19-0040, *Vadose Zone Model for B Plant Area for Composite Analysis*).

High-level liquid wastes containing fission products from B Plant and U Plant were distributed to the tank farms while low-level liquid wastes were distributed to ditches/ponds and cribs. Some of the tanks have leaked. The most substantial were releases from 241-BX-102, which occurred in 1951 and again between 1962 and 1970 (RPP-RPT-47562, *Hanford BX-Farm Leak Assessments Report*). The 1951 release was prior to uranium recovery operations (1952 to 1957 at U Plant), so it included a substantial amount of uranium which has resulted in a groundwater plume (DOE/RL-2018-66, *Hanford Site Groundwater Monitoring Report for 2018*).

Substantial sources of contamination within B Complex also include the BY Cribs (216-B-43 through 216-B-50) located north of the 241-BY Tank Farm. Most of these cribs (216-B-43 through 216-B-49) received supernatant from ferrocyanide scavenging of strontium and cesium in the 241-BY Tank Farm from 1954 to 1956. This process was performed to reduce waste volume in the tanks (DOE/RL-97-1047). The BY Cribs are a substantial source of Tc-99 to groundwater (DOE/RL-2018-66). The 216-B-50 Crib was used from 1965 to 1974 and received process condensate from the 241-BY Tank Farm.

Systems to extract and treat groundwater within a perched zone and the saturated zone are operating at B Complex. The perched zone occurs within a localized silty sand lens of the Cold Creek unit beneath the B Complex. It contains uranium and Tc-99 contamination from 241-BX-102 and nearby cribs, 216-B-7A&B and 216-B-8 (DOE/RL-2014-37, *Removal Action Work Plan for 200-DV-1 Operable Unit Perched Water Pumping / Pore Water Extraction*). A system to extract and treat water from the perched zone began in 2011 as a treatability test and transitioned into a removal action in 2016 (DOE/RL-2018-66). As a conservative assumption, this system is not simulated in the B Complex model. A groundwater extraction and treatment system for the saturated zone began operating as a treatability test in 2015 and transitioned also into a removal action in 2016 (DOE/RL-2018-66).

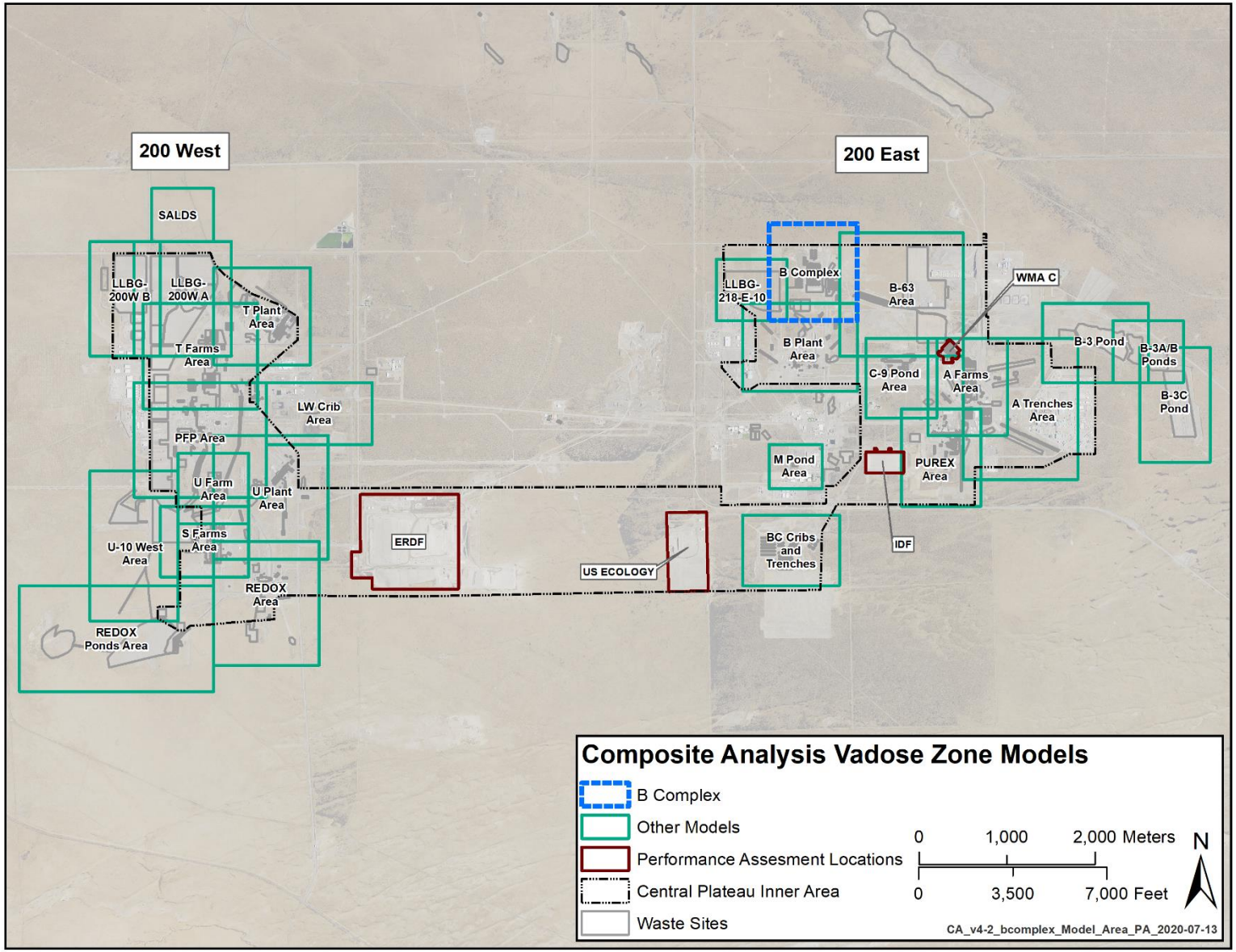

Figure 2-1. Location of the B Complex Model

3 Methodology

This chapter contains a discussion of configuration control, a brief overview of the methodology for creating the B Complex model, and a list of modifications specific to this model.

3.1 Configuration Control

A configuration control system was developed so that all vadose zone models generated for the CA would follow a consistent set of conventions and use only approved input data (e.g., geoframework, hydraulic and contaminant properties, source releases, etc.). This system was manifested as sets of qualified input data, scripts used to construct the models and post-process the results and sets of instructions for building and executing the models. Each script was reviewed, tested, and documented to qualify it for use. A list of scripts developed for the vadose zone modeling effort is found in Section 5.3 of this ECF. Each CA model used the same directory structure. A discussion of the configuration control system is found in CP-63515.

A data configuration quality-control system (hereinafter called the Integrated Computational Framework [ICF]), provides the tools necessary to verify that all model output data are correctly associated with their corresponding input data. The ICF consists of two parts: a file management system and utility scripts to support the file management system.

The ICF houses all data produced by and in support of the CA modeling effort. The ICF file management system ensures that no data can be modified, deleted, or used in a model application without being checked into the ICF, reviewed, and accepted by the ICF administrator. Separating the data flow from the modeling helps prevent accidental modification and guarantees a data review prior to acceptance of any data product into the ICF.

The utility scripts establish a pedigree for any data product stored in the ICF. The ICF allows users to ascertain all the ancestor and derivative products related to any ICF data product. By combining the file structure and software utilities, the ICF provides confidence that the CA output data are associated with a set of versioned input data.

The CA models were constructed on a central computer system, and many of the models contained over one million nodes. Along with the long time period simulated and the release of large volumes of water from liquid waste disposal sites in many of the model domains, the size of the models caused long run times. Thus, the model files were transferred to a high-power computer system, GAIA, for execution. Following completion of model runs, the input and output files were returned to the original computer system for post-processing. File fingerprinting was used to verify this transfer process and to verify that the correct input files were used for each model simulation.

3.2 Model Construction and Execution

This ECF is one of 26 similar ECFs, one for each CA vadose zone model, each of which followed the same general methodology. A detailed description of the general model construction is found in CP-63515. Adjustments are made to the methodology as needed to tailor model development to best represent the area being simulated. The steps were developed to include mass balance checks to verify model performance. A brief outline for the construction and execution of the B Complex model is as follows:

1. Construct the model grid.
2. Assign HSUs and material properties to the model grid nodes.

3. Generate the temporal-spatial recharge distributions for the model using the RET.
4. Execute the steady-state flow simulation to establish the initial conditions for the transient simulations.
5. Conduct post-processing of the steady-state simulation, including calculating the liquid volume balance.
6. Incorporate the transient RET results, radionuclide waste release, and liquid waste release data into the model input file. Generate input files for a historical (1943–2018) simulation and a set of forecast simulations, and a simulation from 1943–12070 with no radionuclide decay which is used to check the mass balance. This model contains waste sites with a disposition to remove, treat, and dispose (RTD), so the forecast simulations were performed in two parts: 2018 to the RTD year, followed by modification of the input file to incorporate the RTD actions, then the RTD year to 12070 was simulated.
7. Modify liquid waste releases as necessary, for example, averaging releases to improve model convergence.
8. Execute the mass balance simulation. This requires two simulations because the 16 radionuclides simulated are divided into two groups, Radionuclide Group 1 and Radionuclide Group 2, as shown in Table 3-1.
9. Conduct post-processing of the radionuclide mass balance simulations, including calculating the mass balance.
10. Execute the historical radionuclide transport simulations (1943–2018) for Radionuclide Group 1 and Radionuclide Group 2.
11. Execute the forecast radionuclide transport simulations from 2018–RTD year, then RTD year–12070 for Radionuclide Group 1 and Radionuclide Group 2.
12. Conduct post-processing of the radionuclide transport simulations to generate contaminant transfer rates to groundwater for the P2R model.

Table 3-1. List of Modeled Radionuclides in Radionuclide Group 1 and Radionuclide Group 2

Radionuclide Group 1	Radionuclide Group 2
C-14	U-232
Cl-36	U-233
H-3	U-234
I-129	U-235
Np-237	U-236
Re-187	U-238
Sr-90	Ra-226
Tc-99	Th-230

All model inputs were checked during production. Checking documentation is found in Appendix A.

3.3 Model-Specific Modifications

Model-specific changes were required for some models. This model required model-specific modifications. These modifications are as follows:

- A separate simulation was conducted for to allow for a mobile (partition coefficient [K_d] = 0 ml/g) uranium fraction in the 241-BX-102 tank leak. This is discussed in Section 4.5.1.1.
- Averaged aqueous sources over a number of years. This is discussed in Section 4.5.2.1.

This page intentionally left blank.

4 Assumptions and Inputs

The domain and structure of the B Complex model, hydraulic properties, boundary and initial conditions, source releases, the types of simulations performed, and assumptions are described in this chapter.

4.1 Model Domain and Grid

The B Complex model was constructed to simulate radionuclide contaminant transport through the vadose zone from the waste sites at and around the B Complex in the 200 East Area. The extents and grid spacing of this model are shown in Figure 4-1. A general approach to grid spacing for the CA vadose zone models, both horizontal and vertical, is discussed in CP-63515. The B Complex model grid is aligned with the P2R model grid (CP-57037) as shown in Figure 4-2. The B Complex model has 100 columns from west to east (X-nodes), 127 rows from south to north (Y-nodes), and 258 layers in the vertical dimension (Z-nodes), for a total of 3,276,600 nodes. The total extent of the model is 1,000 m in the east-west direction and 1,100 m in the north-south direction. The southwest corner of the domain has coordinates of 573,100 m east and 136,900 m north (Washington State Plane, South Zone [4602]). The model extends vertically from the approximate water table elevation to the ground surface. Grid spacing for each model was determined through multiple iterations based on geologic layer thickness, plume extent, waste site alignment, and mass balance considerations. Preliminary model runs were used to evaluate spatial discretization, and refinements were made as necessary (e.g., to better represent source zone geometry and plume migration). Vertical spacing is 0.5 m and 0.1 m. The grid was discretized to 0.1 m in the vertical dimension around the siltier end member of the upper Cold Creek unit (CCUsilt) to properly capture the unit, as it was smaller than 0.5 m thick in some places and would not have shown up as a unit in the model otherwise.

This model has a source zone and a buffer zone. The dashed blue line in Figure 4-1 indicates the separation between the source and buffer zones. These regions are distinguished by how the radionuclide inventory from waste sites is distributed. Water and radionuclide releases were simulated for waste sites in the source zone, whereas only water volume releases were simulated for waste sites in the buffer zone. Water volume releases in the buffer zone were included so that their hydraulic effect on flow beneath the source zone is accounted for. Waste sites with radionuclide releases located in the buffer zone are included in the source zones of other models.

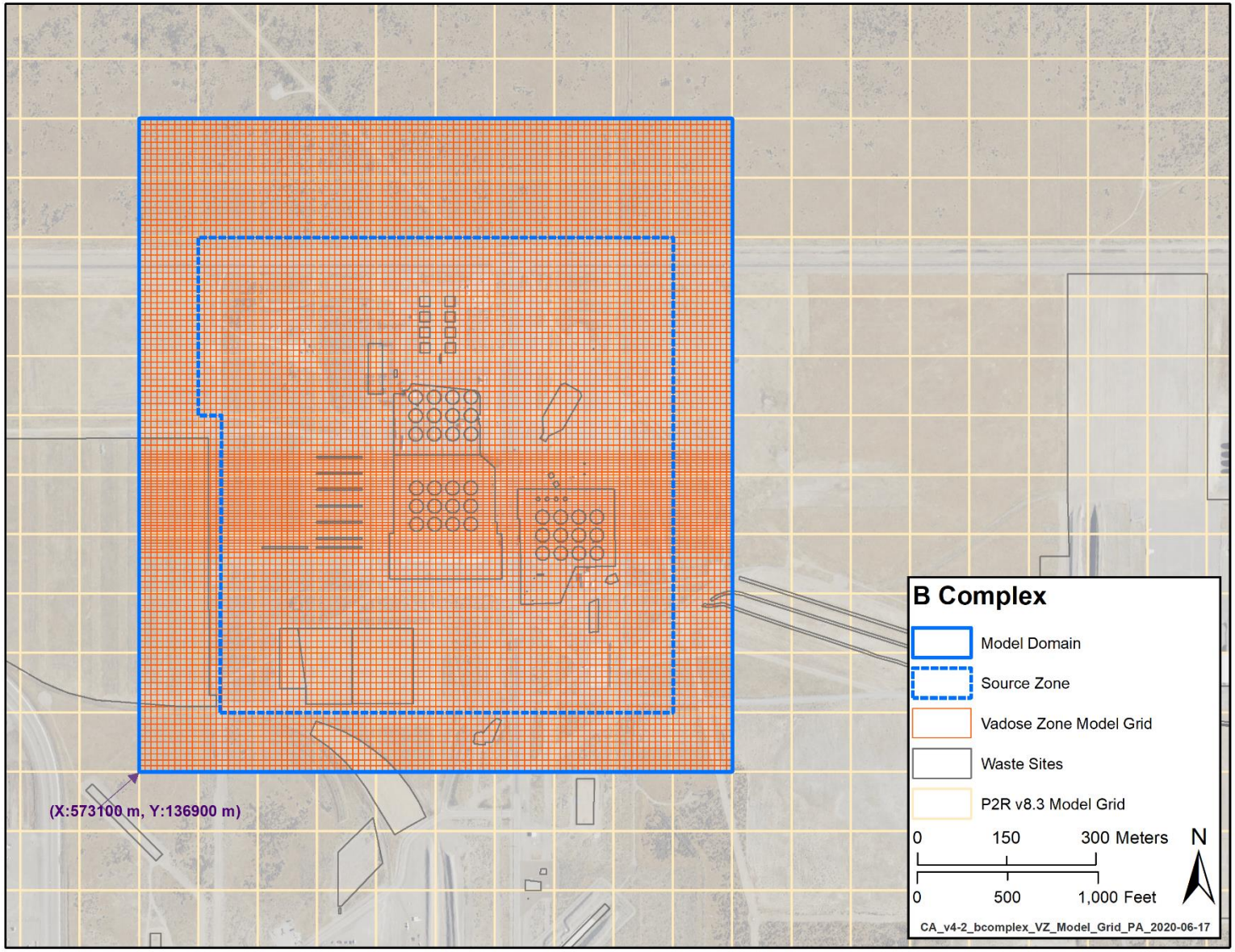

Figure 4-1. Plan View of the B Complex Model Grid Overlain on the P2R Grid Cells

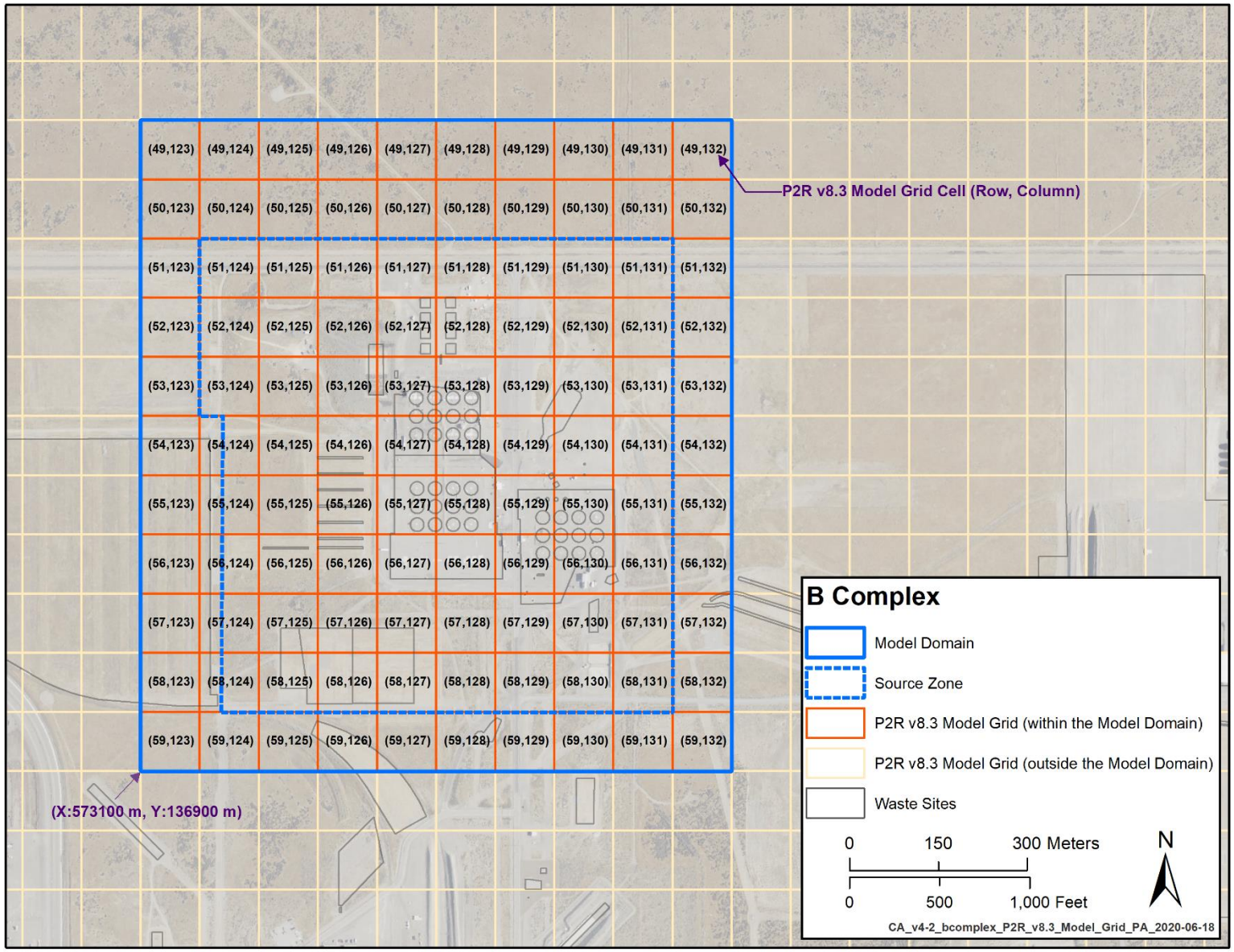

Figure 4-2. Plan View of the P2R Grid Cells in the B Complex Model

4.2 Model Hydrostratigraphy

The B Complex model includes 10 HSUs: Backfill, Hanford formation unit 1 (Hf1), Hanford formation unit 2 (Hf2), Hanford formation unit 3 (Hf3), CCUsilt, sandier end member of the upper Cold Creek unit (CCUsand), Cold Creek unit – Perched Zone silty sand (CCU2), Cold Creek unit – Perched Zone basal silt (CCU3), Cold Creek unit gravel (CCUg), and Columbia River Basalt (hereinafter referred to as Basalt), in descending sequence. HSU designations were assigned to each grid node based on the surfaces in the geoframework model (ECF-HANFORD-18-0035). Properties assigned to each HSU are presented in ECF-HANFORD-19-0121 and are described in Section 4.3. CP-63515 provides a detailed description of the hydrostratigraphy for the CA vadose zone models. Figure 4-3 through Figure 4-6 show the hydrostratigraphic framework for the B Complex model from various orientations. A progression of cross-sections from west to east and south to north through the model are shown in Appendix B of this ECF.

The CCUsilt and CCUsand represent a lateral facies change in the Cold Creek Unit in the 200 East Area between the finer-grained CCUsilt and the coarser, sand-dominated CCUsand (ECF-HANFORD-18-0035). As noted in Section 4.1, the vertical gridding is reduced in some areas to 0.1 m to characterize the CCUsilt. Hf1 dips sharply in the northeast corner of the model. A feature of the hydrostratigraphy of this model is the Perched Zone, which is discussed in ECF-200DV1-18-0036, *B-Complex Perched Zone Geoframework, 200 East, Hanford Site*. This feature is defined by CCU2 and CCU3. The extent of the Perched Zone is shown in Figure 4-7. The oldest formation is basalt, with a small pinch in the northwestern part of the model.

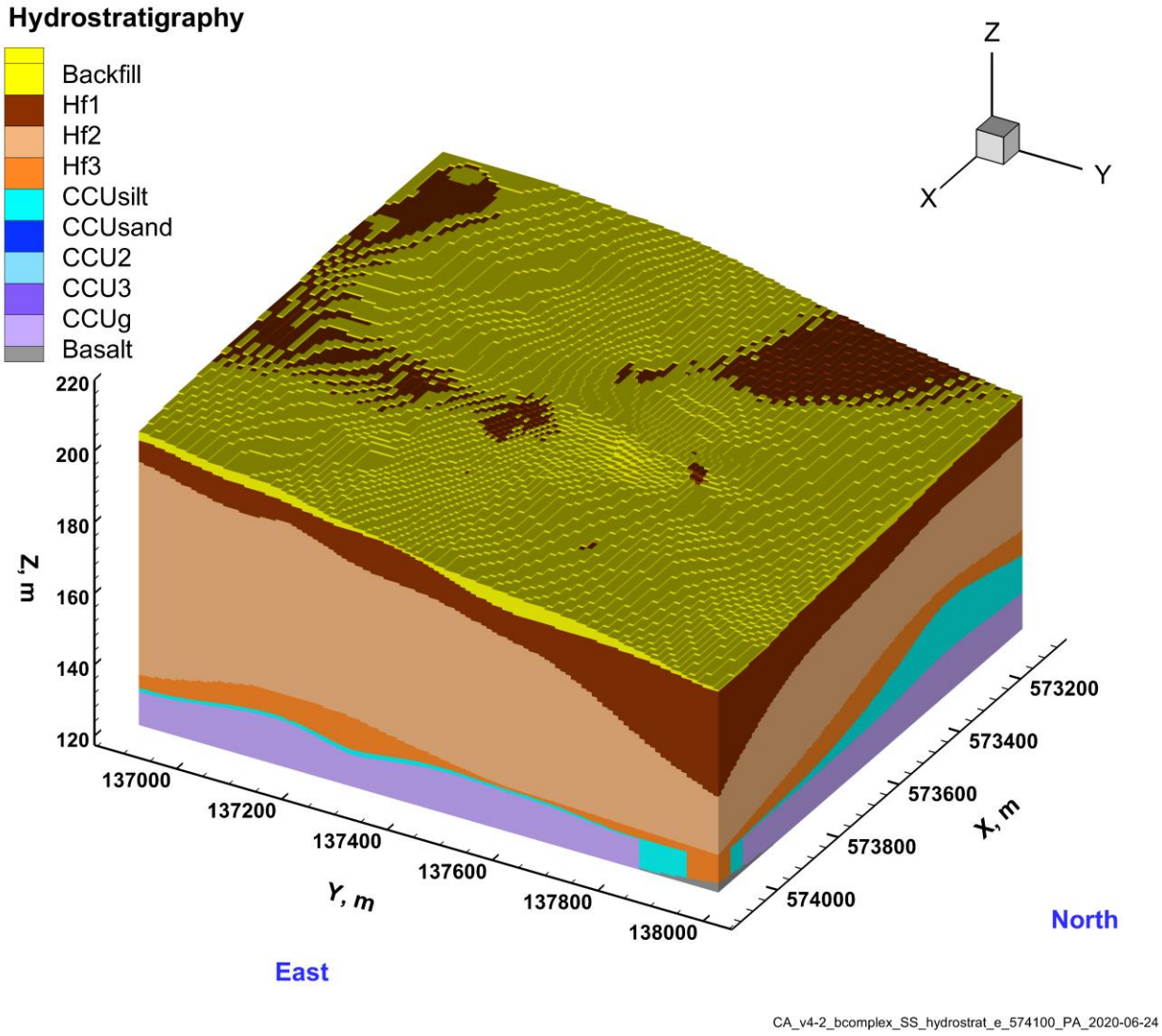

Figure 4-3. Model Hydrostratigraphy Three-Dimensional View Showing the North and East Faces

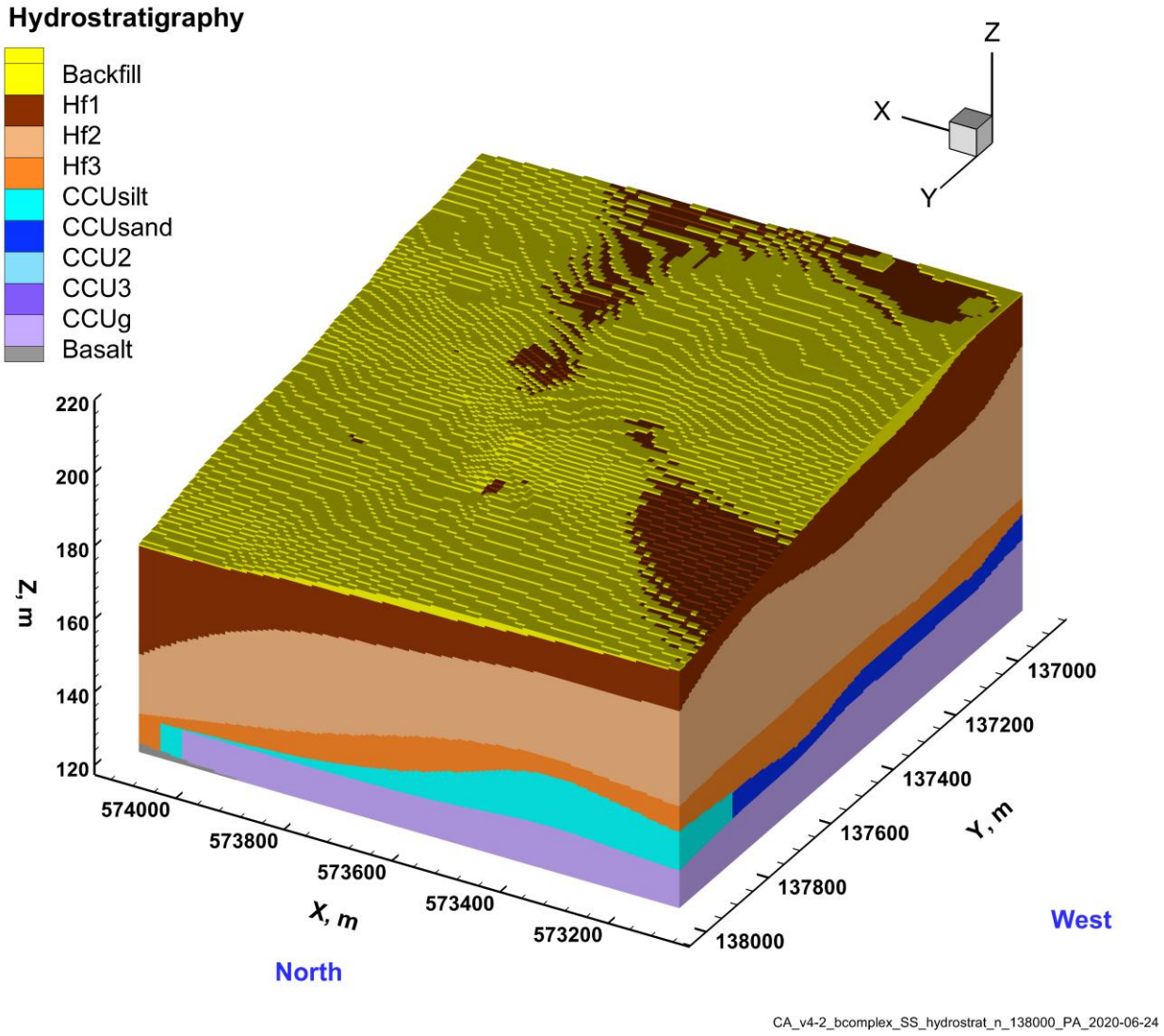

Figure 4-4. Model Hydrostratigraphy Three-Dimensional View Showing the North and West Faces

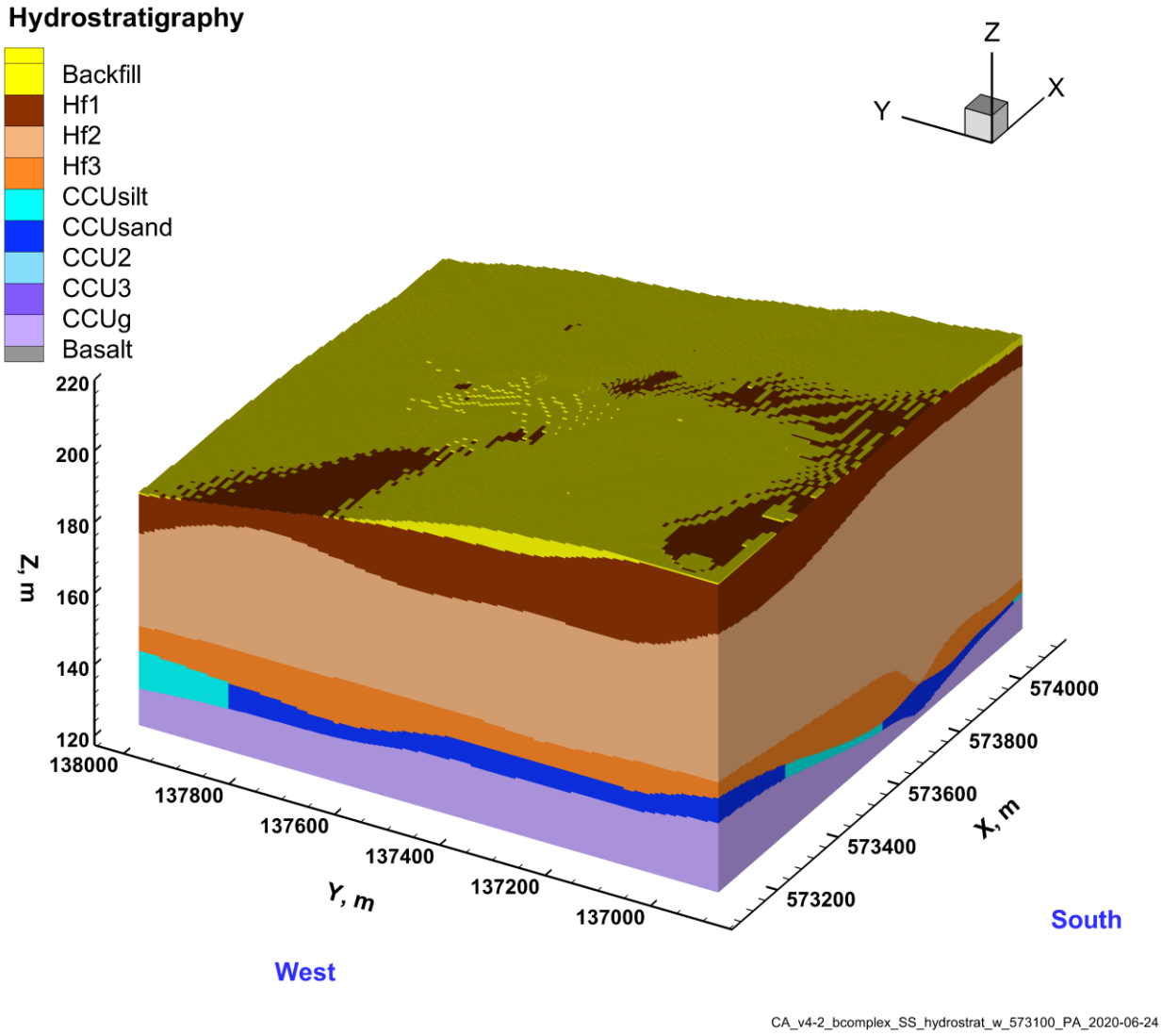

Figure 4-5. Model Hydrostratigraphy Three-Dimensional View Showing the South and West Faces

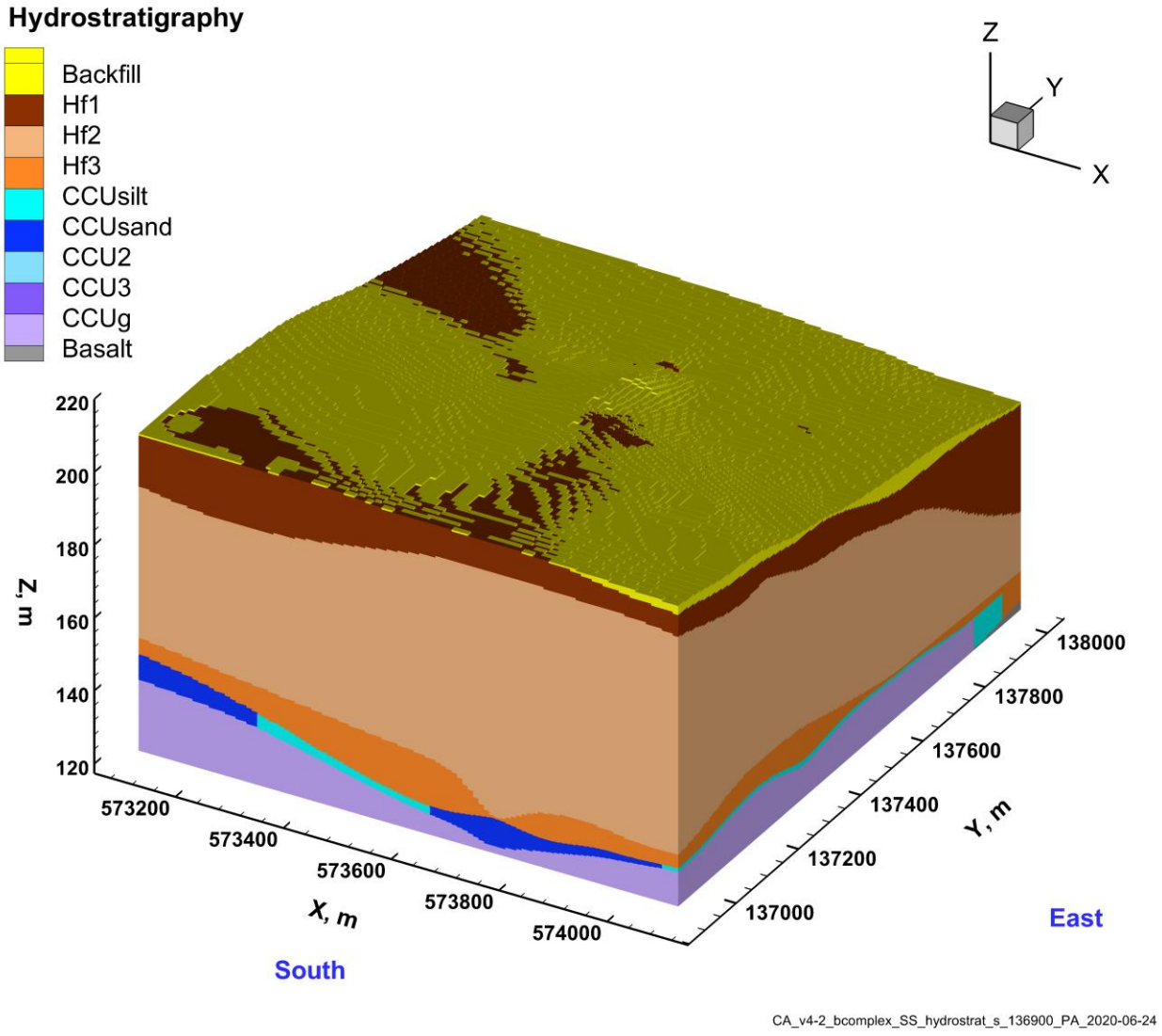

Figure 4-6. Model Hydrostratigraphy Three-Dimensional View Showing the South and East Faces

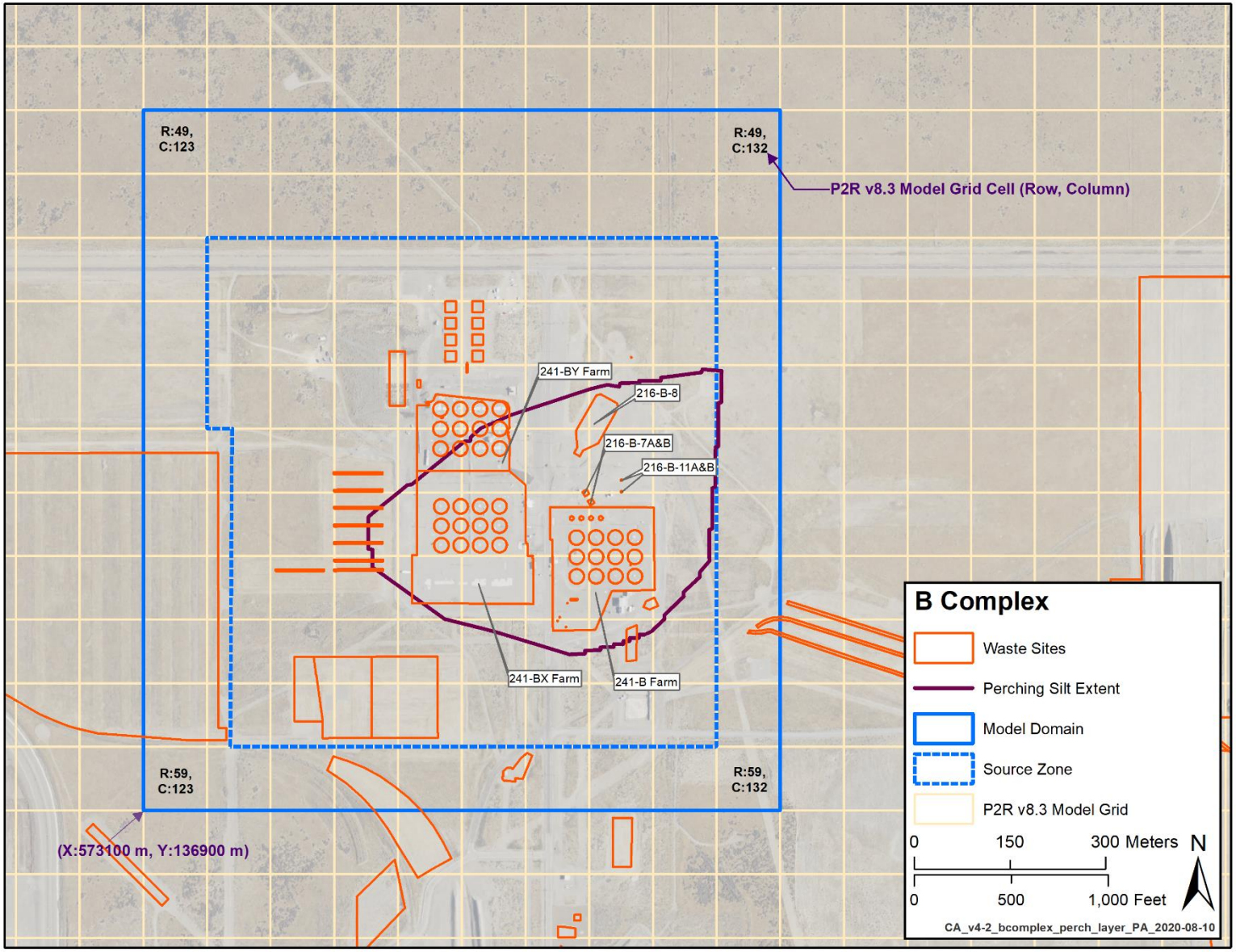

Figure 4-7. Extent of the Perched Zone

4.3 Hydraulic Properties

Hydraulic properties for the B Complex HSUs are shown in Tables 3, 4, 6, and 7 of ECF-HANFORD-19-0121. For most of the HSUs, hydraulic property estimates in ECF-HANFORD-19-0121 were obtained from CP-63883, which contains a detailed description of the development of these parameters for the unconsolidated sediments overlying the basalt HSU in the Central Plateau. Properties for the perched zone units and the basalt HSU were obtained from other sources.

HSUs were assumed to follow the van Genuchten (van Genuchten, 1980, "A Closed-form Equation for Predicting the Hydraulic Conductivity of Unsaturated Soils") moisture-retention constitutive relation and the Mualem-van Genuchten relative-permeability constitutive relation (Mualem, 1976, "A New Model for Predicting the Hydraulic Conductivity of Unsaturated Porous Media"), requiring values to be specified in STOMP for the following items:

- Saturated hydraulic conductivity
- Saturated moisture content
- Residual saturation, equal to the residual moisture content divided by the saturated moisture content
- van Genuchten α, proportional to the inverse of the air entry matric potential
- The dimensionless van Genuchten *n* fitting parameter
- The tensorial connectivity-tortuosity (TCT) parameters for moisture dependent anisotropy (discussion of the TCT parameters is in CP-63515 and ECF-HANFORD-19-0094).

4.4 Transport Parameters

In addition to the hydraulic properties discussed in Section 4.3, the transport simulations also require particle density, molecular diffusion rate, longitudinal and transverse dispersivity, solid-aqueous K_d, and radionuclide half-life. Tables 5, 8, 9, 10, 13, 15, and 16 of ECF-HANFORD-19-0121 list the transport properties for the HSUs present in the modeled area. A detailed description of the transport properties used for the CA vadose zone models can be found in ECF-HANFORD-19-0121.

4.5 Source Releases

Within the source zone, the transport models consider radionuclide releases from both solid and liquid sources. Sources within the buffer zone are simulated as water-only releases (i.e., the radionuclide inventory is not included; these sites are included in the source zones of other models). Some sites within a model's source zone lack a radionuclide inventory and are also simulated as water-only releases (e.g., septic systems). An index of waste sites contributing releases to the model are shown in Table 4-1. The waste sites contributing liquid releases within this model are shown in Figure 4-8, and the solid waste sites contributing releases of radionuclides are shown in Figure 4-9. Section 4.5.1 contains a discussion of the radionuclide inventory released from waste sites in the model; liquid waste sites are addressed in Section 4.5.1.2 and solid waste sites are addressed in Section 4.5.1.3. Section 4.5.2 addresses liquid (volume) releases from waste sites, including water-only release sites.

Table 4-1. Waste Sites Included in the B Complex Model

Source Zone – Liquid Waste Sites with Radionuclide Releases (40)					
200-E-60	216-B-40	216-B-47	216-B-8	241-BX-102*	UPR-200-E-73
216-B-11A&B	216-B-41	216-B-48	241-B-101*	241-BY-103*	UPR-200-E-74
216-B-35	216-B-42	216-B-49	241-B-105*	UPR-200-E-105	UPR-200-E-75
216-B-36	216-B-43	216-B-50	241-B-107*	UPR-200-E-108	UPR-200-E-79
216-B-37	216-B-44	216-B-51	241-B-110*	UPR-200-E-109	UPR-200-E-9
216-B-38	216-B-45	216-B-57	241-B-153	UPR-200-E-110	
216-B-39	216-B-46	216-B-7A&B	241-BX-101*	UPR-200-E-38	
Source Zone – Liquid Waste Sites with No Radionuclide Releases (i.e., Liquid Only) (3)					
216-BY-201	2607-E9	2607-EB			
Source Zone – Solid Waste Sites (46)					
218-E-2	241-B-106	241-B-202	241-BX-105	241-BX-ANC	241-BY-108
218-E-5	241-B-107*	241-B-203	241-BX-106	241-BY-101	241-BY-109
218-E-5A	241-B-108	241-B-204	241-BX-107	241-BY-102	241-BY-110
241-B-101*	241-B-109	241-B-ANC	241-BX-108	241-BY-103*	241-BY-111
241-B-102	241-B-110*	241-BX-101*	241-BX-109	241-BY-104	241-BY-112
241-B-103	241-B-111	241-BX-102*	241-BX-110	241-BY-105	241-BY-ANC
241-B-104	241-B-112	241-BX-103	241-BX-111	241-BY-106	
241-B-105*	241-B-201	241-BX-104	241-BX-112	241-BY-107	
Buffer Zone – Waste Sites (Liquid Only) (3)					
UPR-200-E-78	216-B-2-1	216-B-2-2			

* Site is a source of both liquid and solid waste.

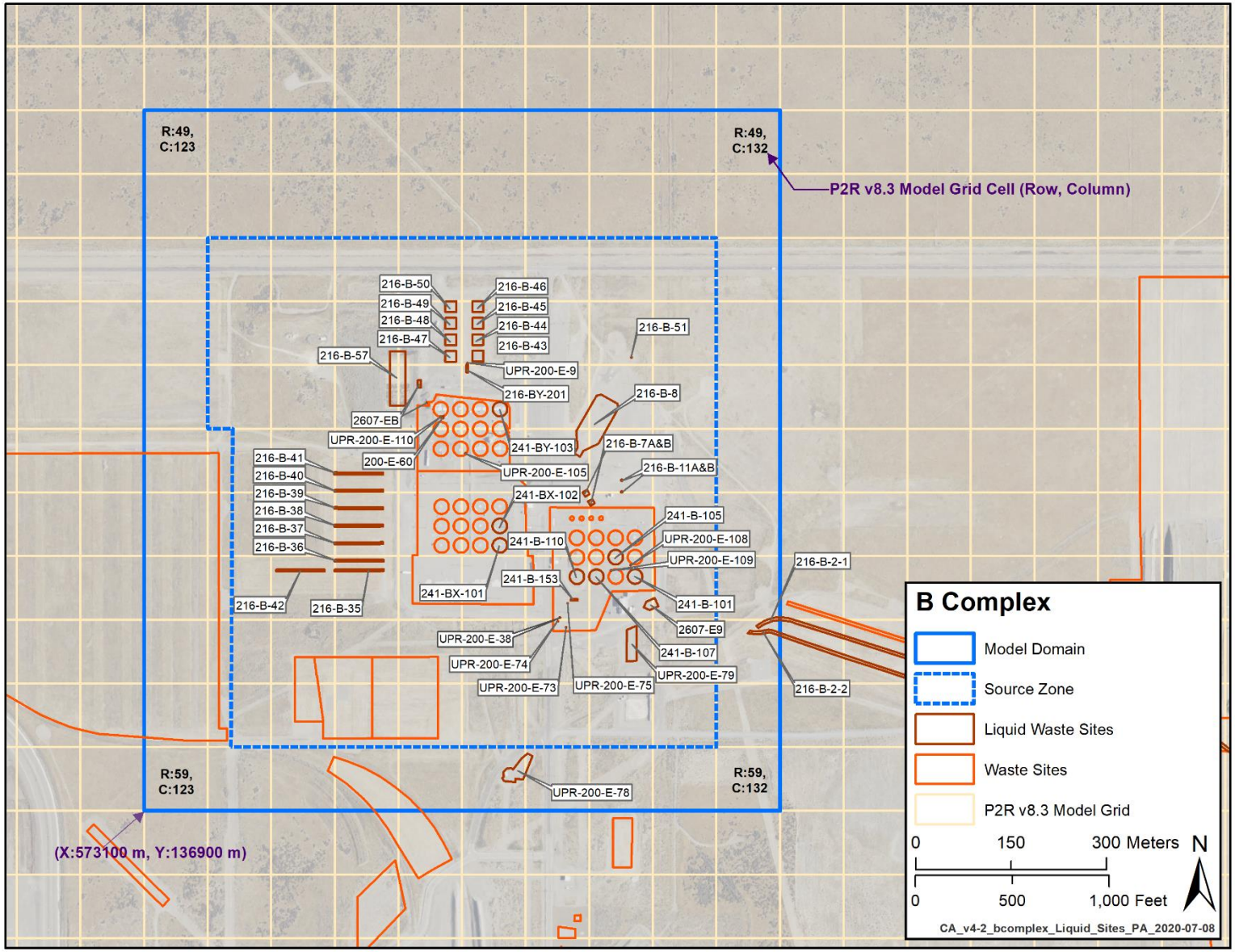

Figure 4-8. Waste Sites in the B Complex Model with Liquid Source Inventory

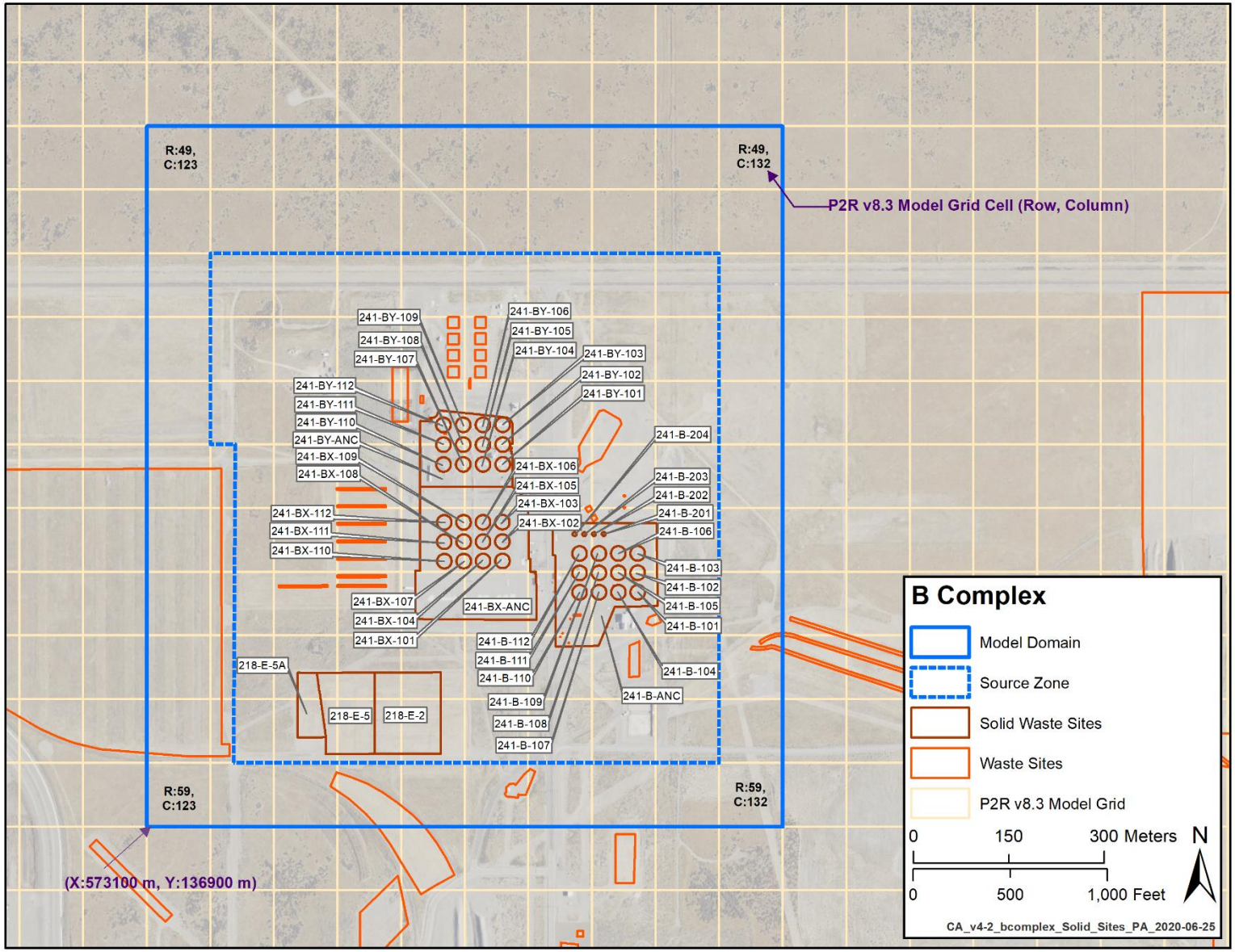

Figure 4-9. Waste Sites in the B Complex Model with Solid Source Inventory

The radionuclides included in the CA vadose zone models were determined through a screening process based on prior modeling studies. CP-62184 discusses this screening process. This process identified 16 radionuclides for simulation. For computational reasons, transport of radionuclides for the CA vadose zone modeling effort was modeled in two separate groups, Radionuclide Group 1 and Radionuclide Group 2, as shown in Table 3-1. Transport properties and half-lives of the radionuclides are described in CP-62184. Not all 16 radionuclides are present in every model. No inventory is present at the waste sites in this model domain for Cl-36 and Re-187; therefore, they were not simulated. Ra-226 and Th-230 are present as both sources and decay products of U-234. Radionuclide activities released in the model (from liquid and solid waste sites separately, as well as the total) are shown in Table 4-2.

Table 4-2. Released Radionuclide Activities in the B Complex Model

Radionuclide	Total (Ci)	Liquid Waste (Ci)	Solid Waste (Ci)
Radionuclide Group 1			
C-14	1.126E+01	1.120E+01	6.057E-02
Cl-36	0.000E+00	0.000E+00	0.000E+00
H-3	5.913E+03	5.913E+03	3.909E-02
I-129	2.704E-01	2.580E-01	1.245E-02
Np-237	1.217E+00	1.210E+00	6.295E-03
Re-187	0.000E+00	0.000E+00	0.000E+00
Sr-90	2.836E+04	2.745E+04	9.072E+02
Tc-99	1.888E+02	1.716E+02	1.723E+01
Radionuclide Group 2			
U-232	3.198E-02	3.153E-02	4.565E-04
U-233	1.454E+00	1.336E+00	1.176E-01
U-234	3.899E+00	3.828E+00	7.117E-02
U-235	1.748E-01	1.718E-01	3.066E-03
U-236	3.908E-02	3.804E-02	1.046E-03
U-238	4.012E+00	3.862E+00	1.495E-01
Th-230	1.090E-04	0.000E+00	1.090E-04
Ra-226	1.078E-03	0.000E+00	1.080E-03

4.5.1 Contaminant (Activity) Releases

This section describes the releases of radionuclides to the subsurface included in this model. Simulations for the CA consider both liquid and solid waste sites and both are present in the source zone of this model. Releases from liquid waste sites are described in Section 4.5.1.2 and solid waste releases are described in Section 4.5.1.3. Releases were input to the model as annual average release rates.

4.5.1.1 241-BX-102 Uranium

According to PNNL-19277, *Conceptual Model of Uranium in the Vadose Zone for Acidic and Alkaline Wastes Discharged at the Hanford Site Central Plateau,* the current uranium plume below B Complex results from the 241-BX-102 overflow event in 1951. The conceptual model provided by PNNL-19277 suggests that uranium from that source started to reach groundwater in the early 1990s. Initial simulations of the B Complex model did not result in substantial releases of uranium isotopes to the groundwater beneath the tank, in contradiction to the PNNL-19277 conceptual model and groundwater sampling results over several years (see, for instance, DOE/RL-2018-66, *Hanford Site Groundwater Monitoring Report for 2018*). The vadose zone simulations used a nominal K_d of 0.8 mL/g uniformly for all uranium isotopes (ECF-HANFORD-19-0121). The nominal K_d value is corrected for the gravel content, modifying the effective values applied to the B Complex HSUs to values ranging from 0.27 to 0.8 mL/g.

Mechanisms to accelerate simulated migration in the vadose include incorporating anthropogenic recharge (e.g., effluent discharge, dust water suppression water, pipeline leaks, storm water management water) from adjacent locations and a reduction of the K_d values. There is no evidence of adjacent anthropogenic recharge that could accelerate uranium transport in the vadose zone. However, PNNL-19277 and PNNL-17031, *A Site-Wide Perspective on Uranium Geochemistry at the Hanford Site*, both suggest that part of the released uranium would likely be mobile (i.e., have a K_d = 0.0 mL/g) to explain the presence of large amounts of uranium in the deep vadose zone. The results of a mass-balance evaluation for the 241-BX-102 subsurface, shown in Table 9.2 of PNNL-19277, indicate that approximately 1/3 of the released uranium inventory related to the overflow event is mobile. For that reason, the assumption has been implemented for the B-Complex vadose zone model that 33% of the 241-BX-102 uranium inventory is considered to be mobile (K_d = 0.0 mL/g), and 67% non-mobile (nominal K_d = 0.8 mL/g). The inventory details for the 241-BX-102 uranium isotopes are shown in Table 4-3.

Table 4-3. Released Total, Non-Mobile, and Mobile Uranium Inventory from 241-BX-102 Overflow Event

Radionuclide	Total Released Inventory (Ci)	Released Non-Mobile Inventory (Ci)	Released Mobile Inventory (Ci)
U-232	2.483E-04	1.664E-04	8.194E-05
U-233	1.321E-02	8.852E-03	4.360E-03
U-234	3.184E+00	2.134E+00	1.051E+00
U-235	1.437E-01	9.627E-02	4.742E-02
U-236	2.722E-02	1.824E-02	8.984E-03
U-238	3.239E+00	2.170E+00	1.069E+00

4.5.1.2 Liquid Waste Site Releases

Liquid waste sites are sites where liquid wastes, often containing radionuclides, are released to the vadose zone. A map of aqueous waste sites in the B Complex model is shown in Figure 4-8. The waste site inventory was retrieved from ECF-HANFORD-17-0079. The radionuclides discharged to this model from liquid waste sites are shown as site totals in Figure 4-10 through Figure 4-21, and by waste site by year in Figure 4-22 through Figure 4-33. Waste sites that contributed less than 0.1% of the total radionuclide

release were not included in the images for Figure 4-10 through Figure 4-21. Radionuclide releases in ECF-HANFORD-17-0079 were decayed to 2001; these were undecayed for input to the B Complex model.

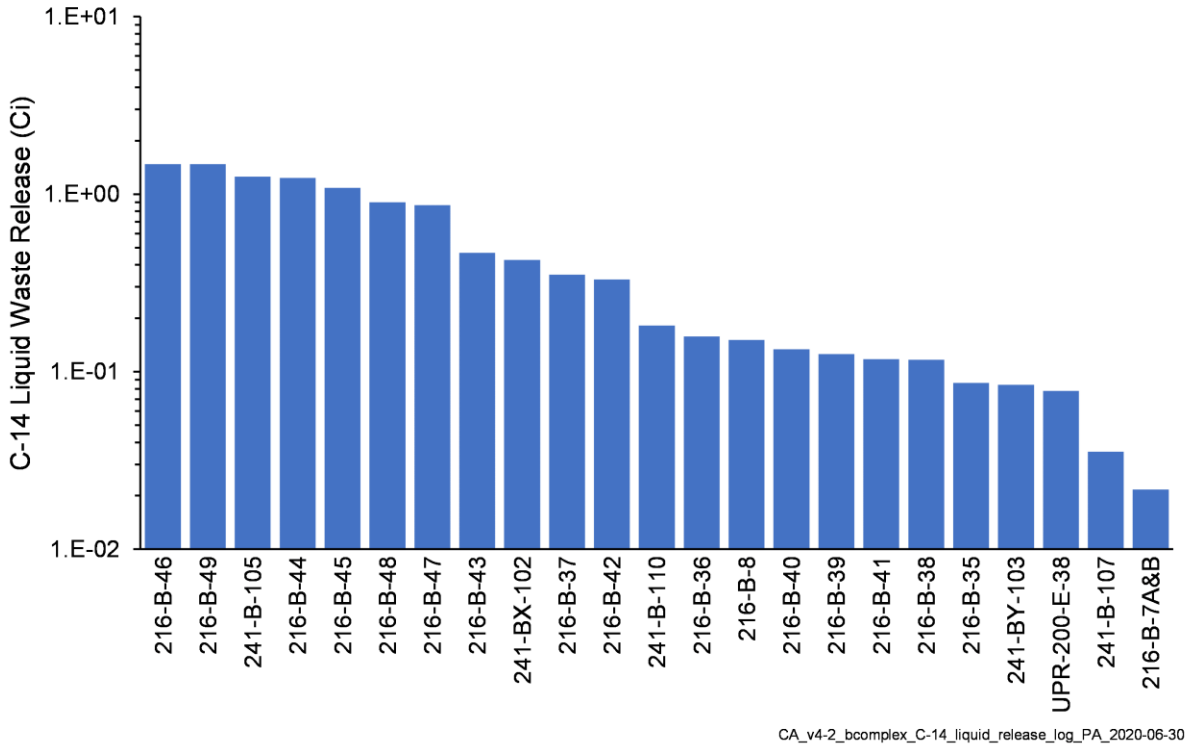

Figure 4-10. Total C-14 Activity Released from Liquid Waste Sites in the B Complex Model

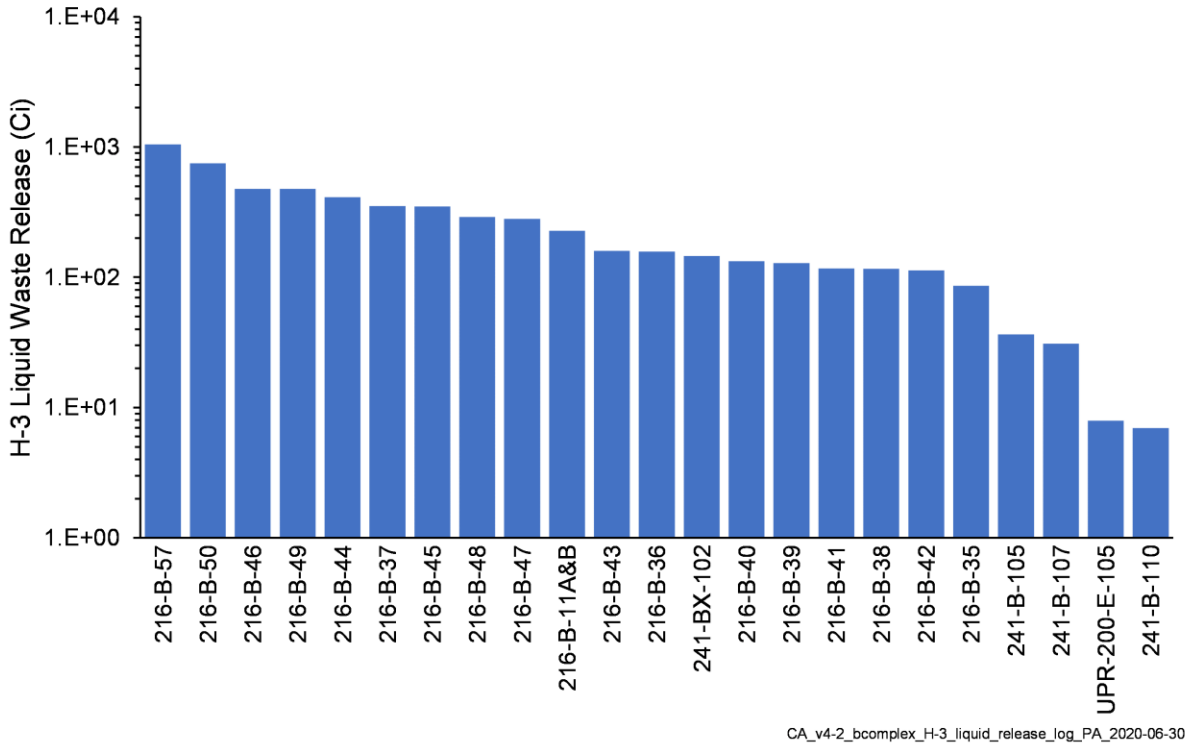

Figure 4-11. Total H-3 Activity Released from Liquid Waste Sites in the B Complex Model

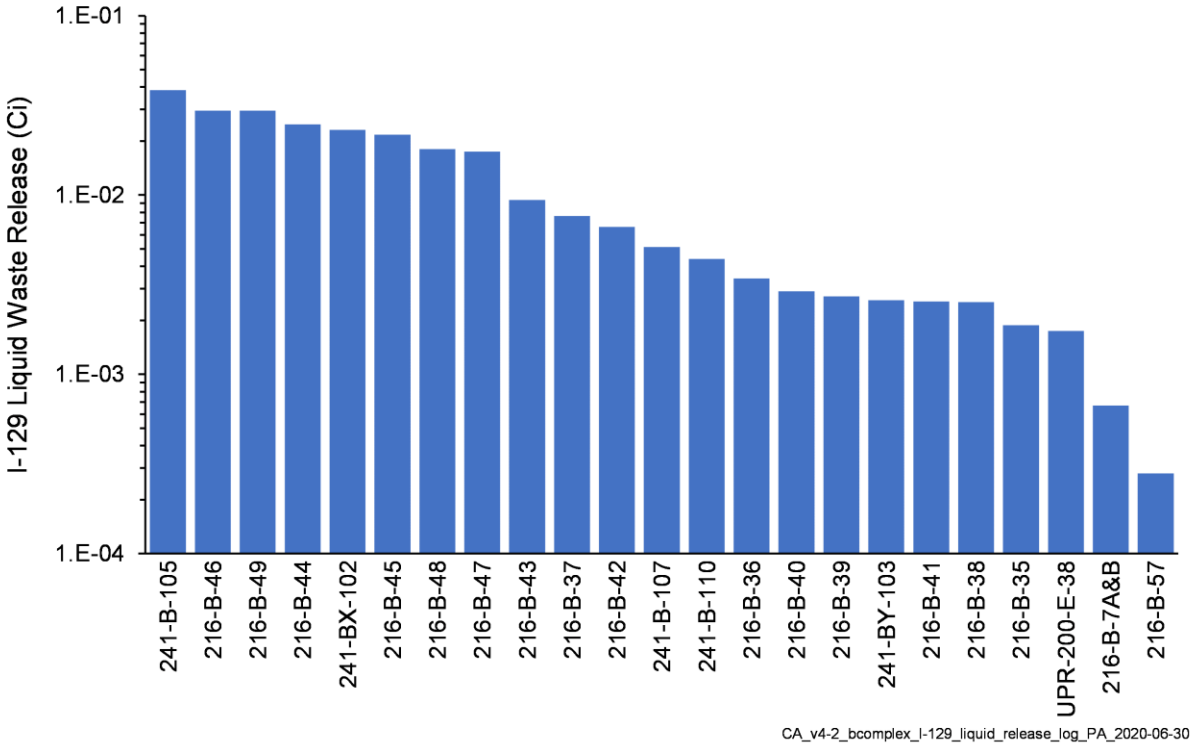

Figure 4-12. Total I-129 Activity Released from Liquid Waste Sites in the B Complex Model

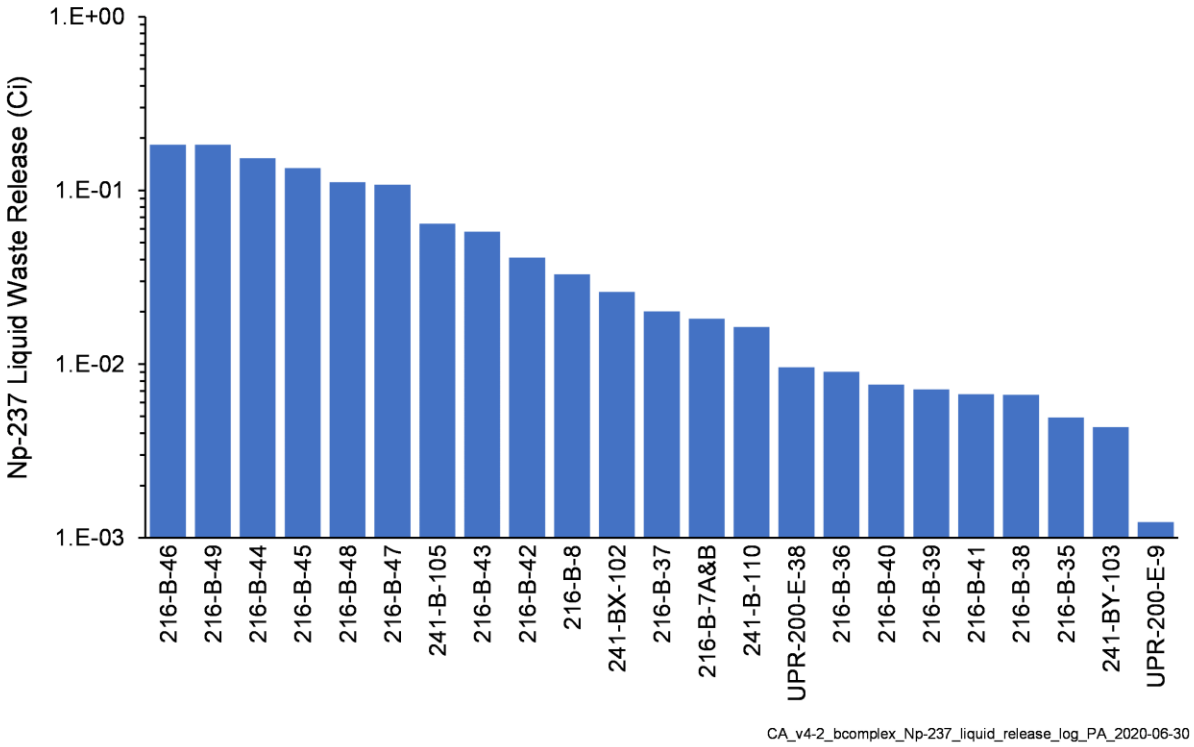

Figure 4-13. Total Np-237 Activity Released from Liquid Waste Sites in the B Complex Model

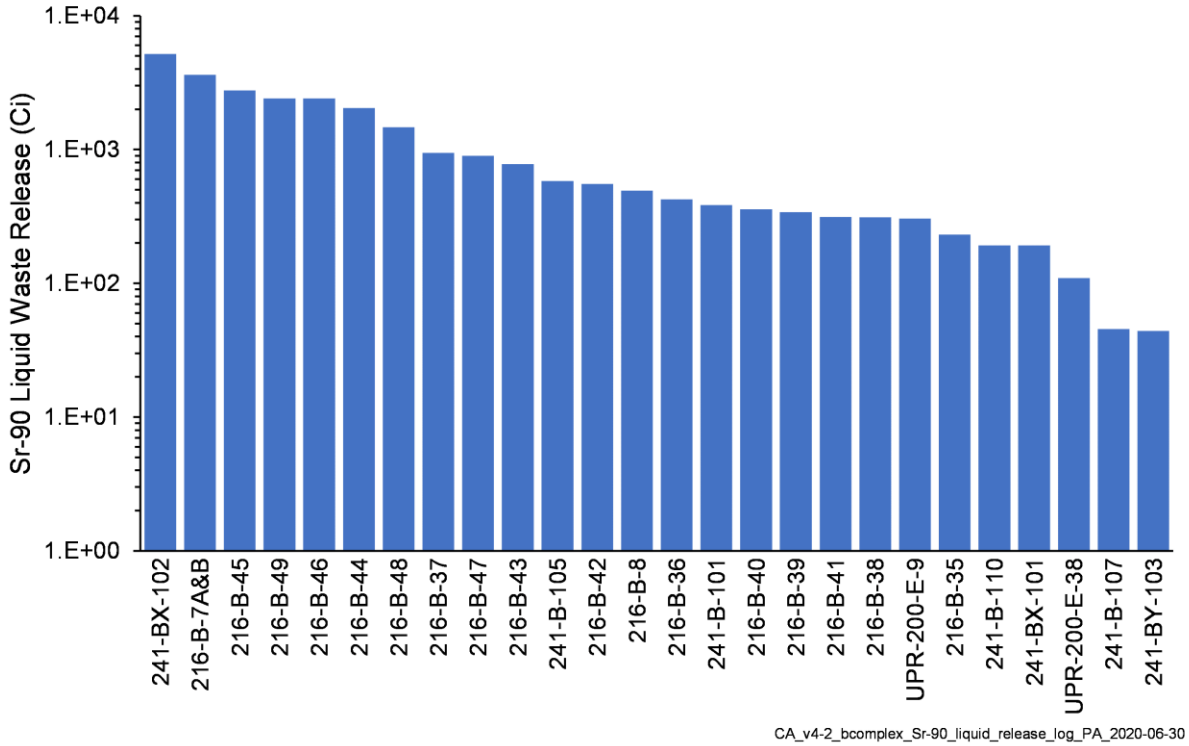

Figure 4-14. Total Sr-90 Activity Released from Liquid Waste Sites in the B Complex Model

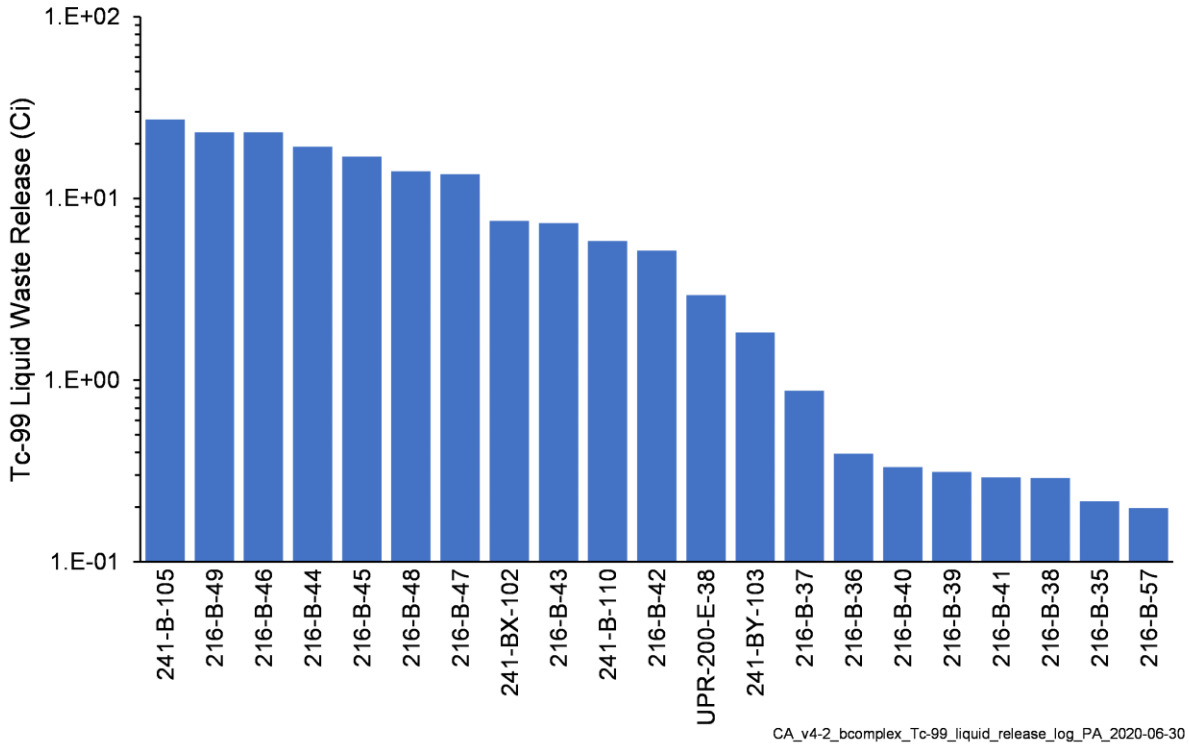

Figure 4-15. Total Tc-99 Activity Released from Liquid Waste Sites in the B Complex Model

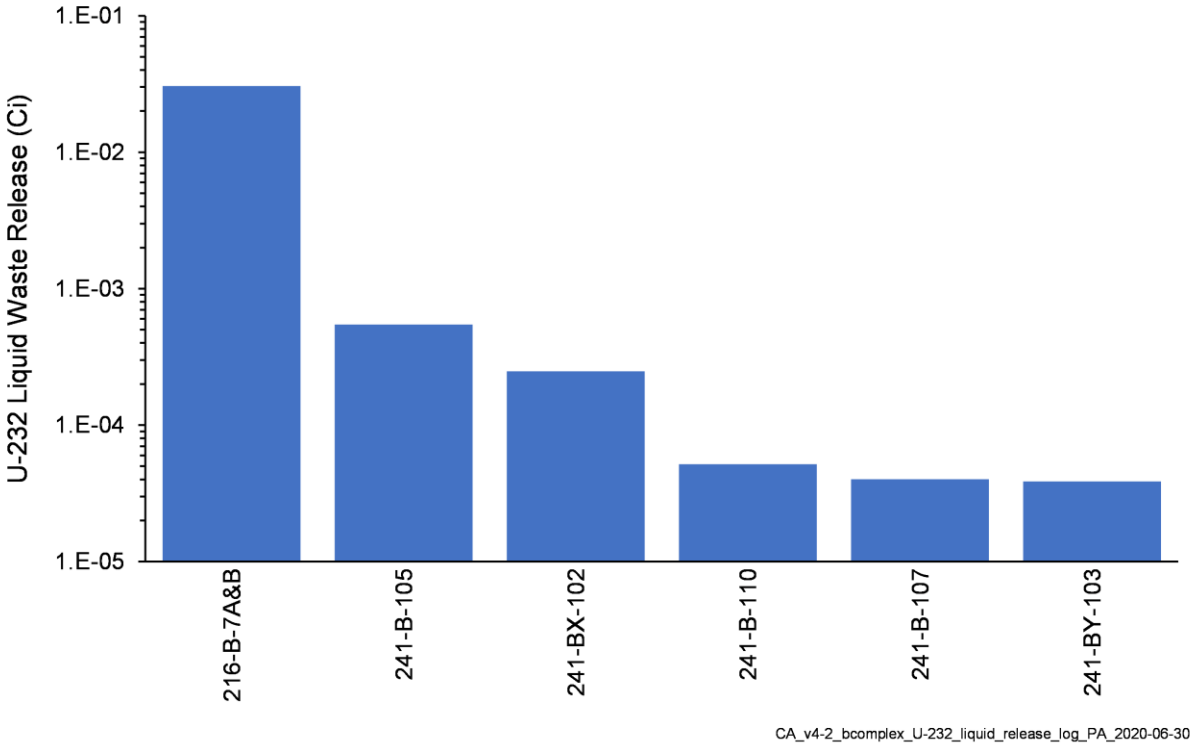

Figure 4-16. Total U-232 Activity Released from Liquid Waste Sites in the B Complex Model

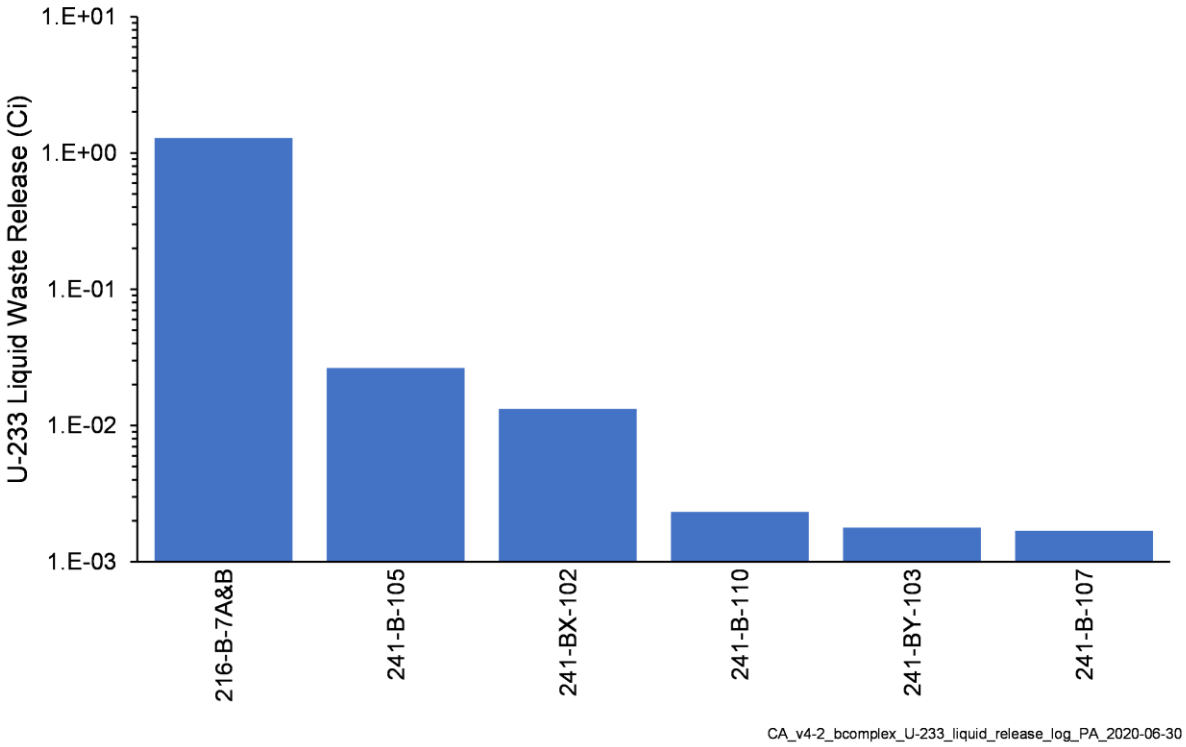

Figure 4-17. Total U-233 Activity Released from Liquid Waste Sites in the B Complex Model

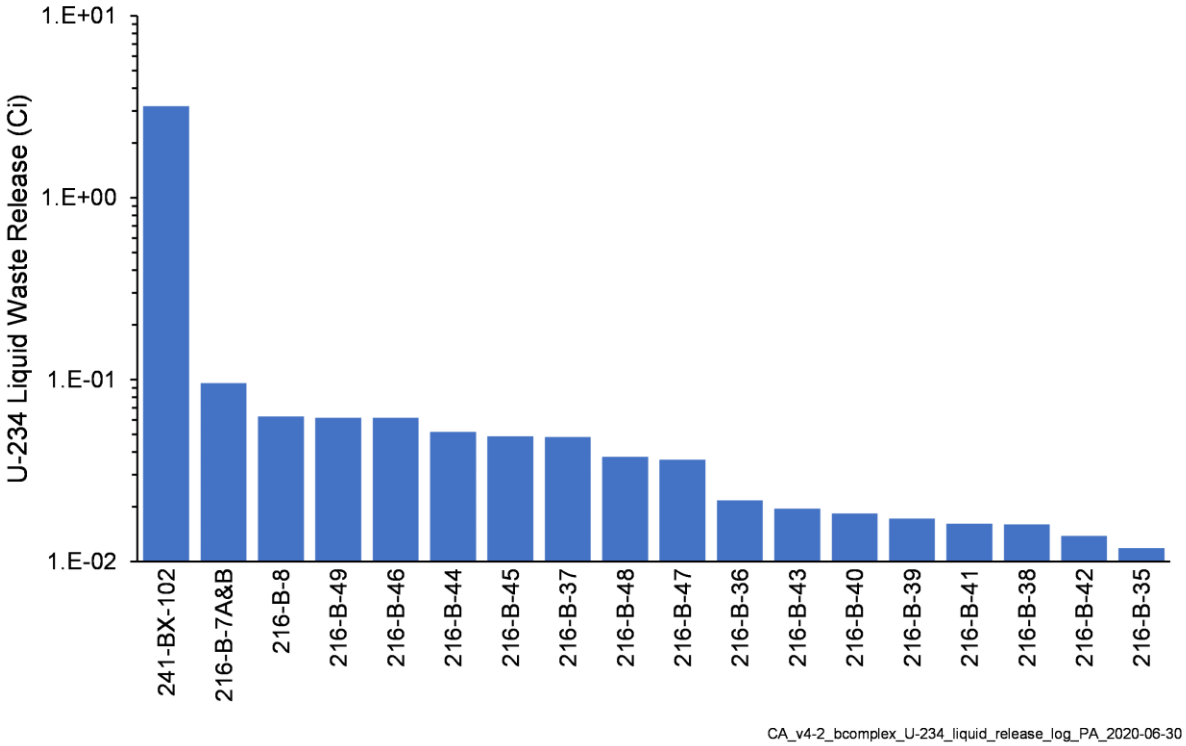

Figure 4-18. Total U-234 Activity Released from Liquid Waste Sites in the B Complex Model

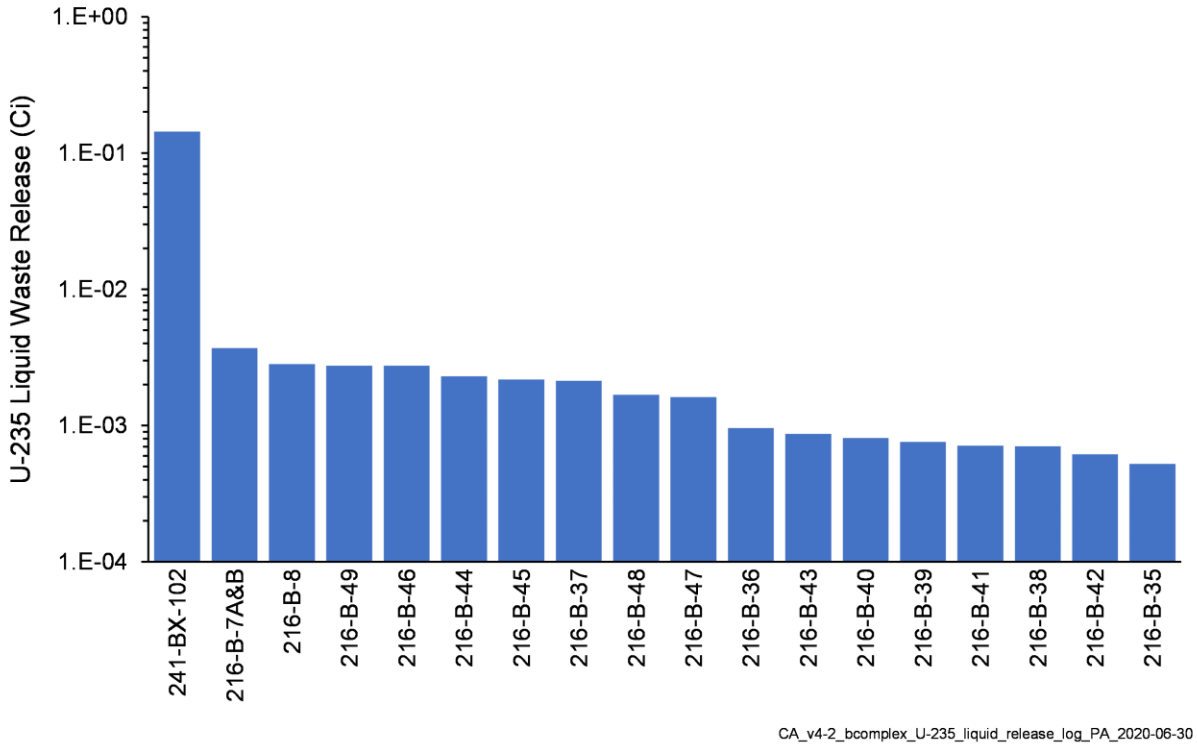

Figure 4-19. Total U-235 Activity Released from Liquid Waste Sites in the B Complex Model

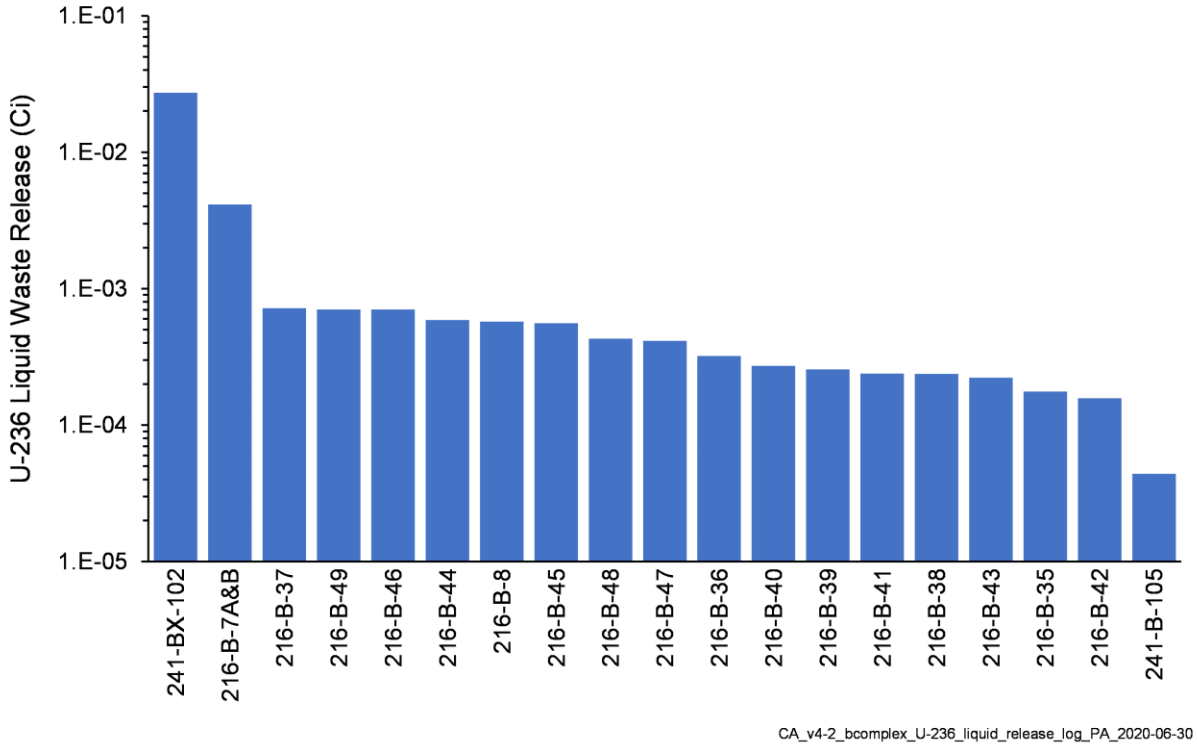

Figure 4-20. Total U-236 Activity Released from Liquid Waste Sites in the B Complex Model

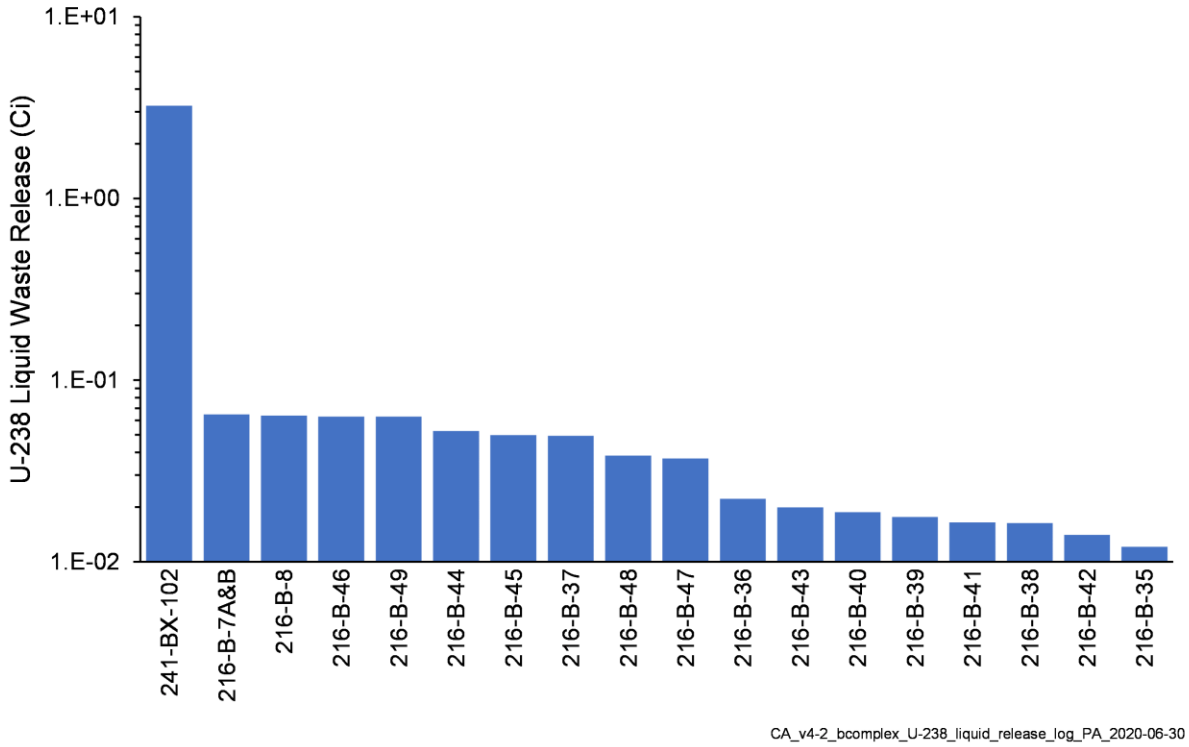

Figure 4-21. Total U-238 Activity Released from Liquid Waste Sites in the B Complex Model

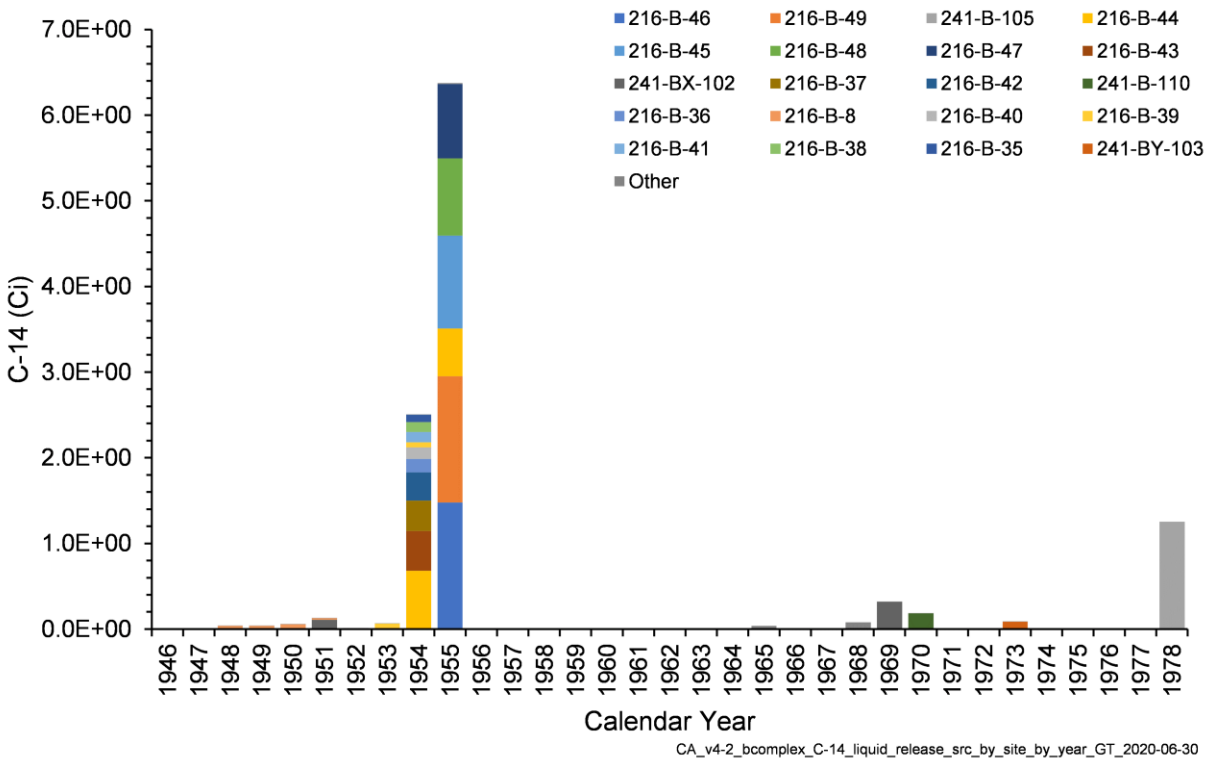

Figure 4-22. Annual C-14 Activity Released from Liquid Waste Sites in the B Complex Model

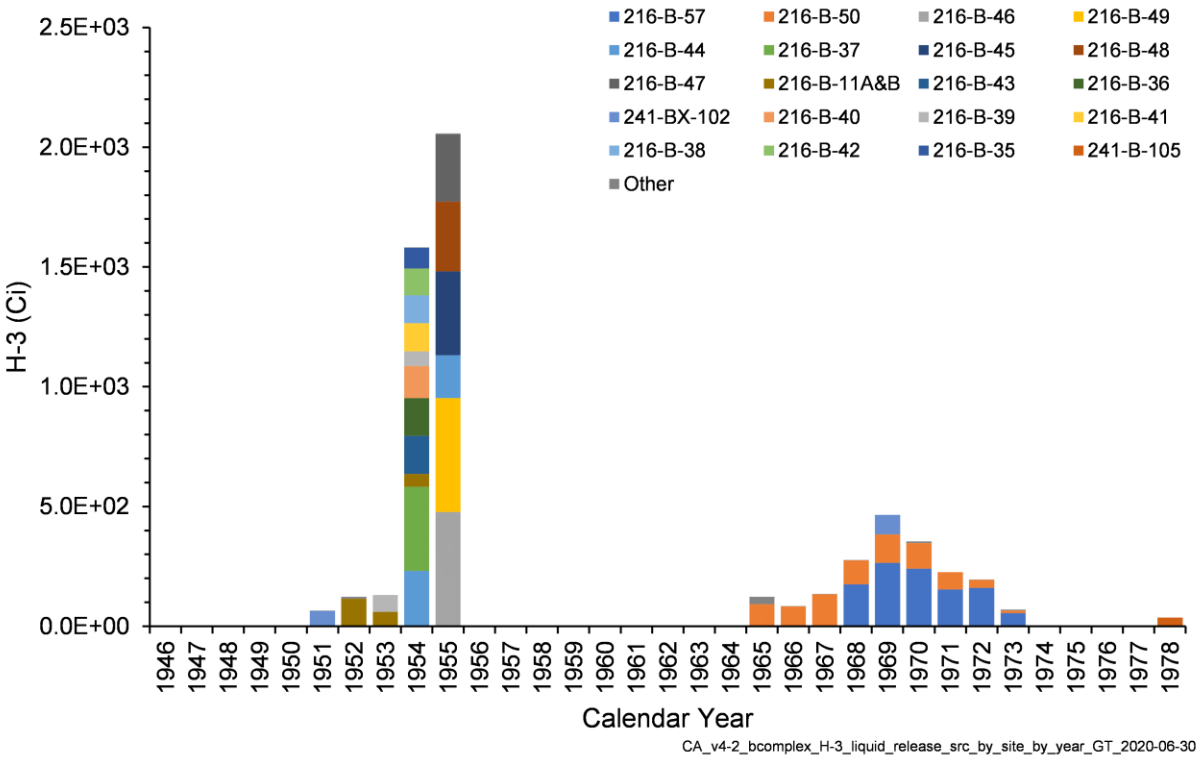

Figure 4-23. Annual H-3 Activity Released from Liquid Waste Sites in the B Complex Model

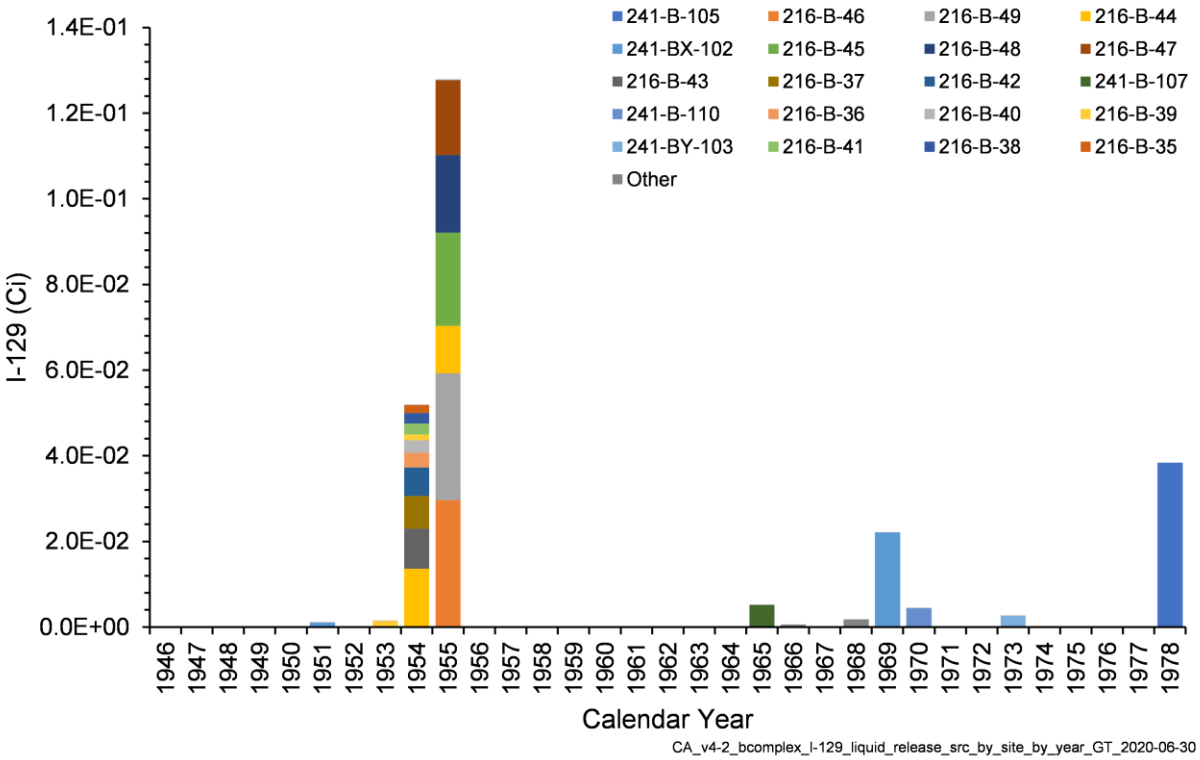

Figure 4-24. Annual I-129 Activity Released from Liquid Waste Sites in the B Complex Model

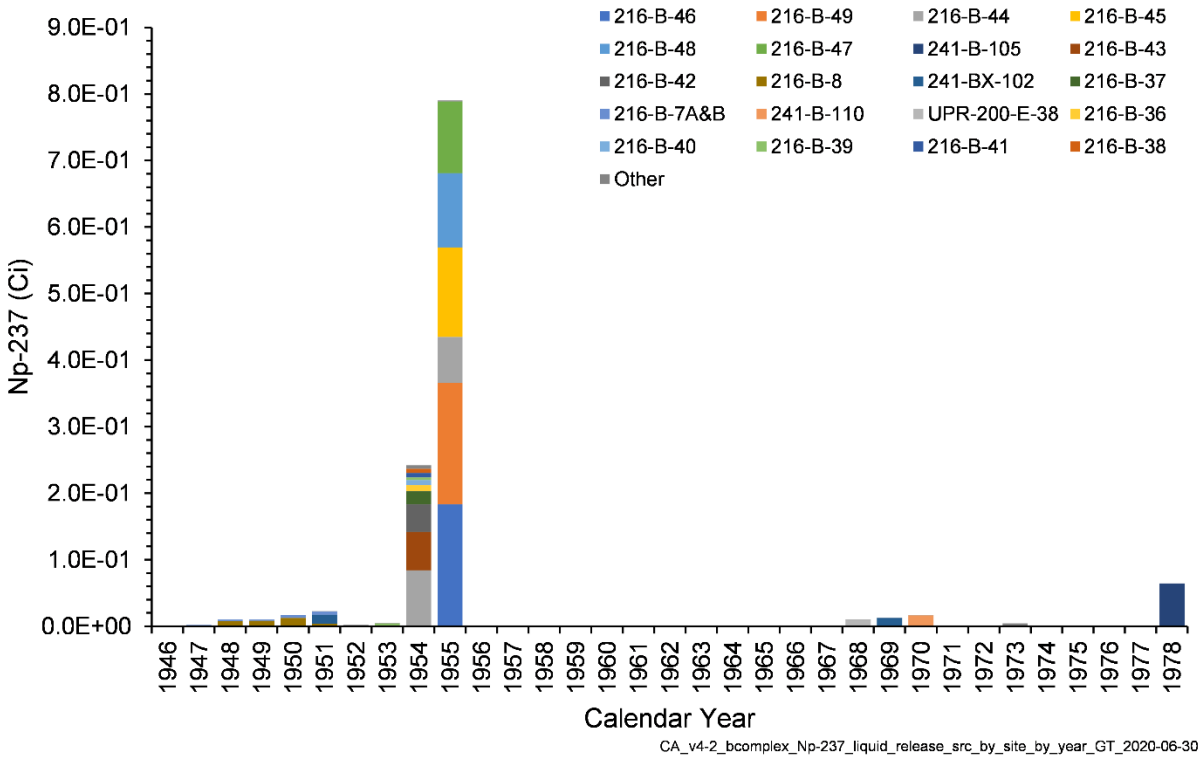

Figure 4-25. Annual Np-237 Activity Released from Liquid Waste Sites in the B Complex Model

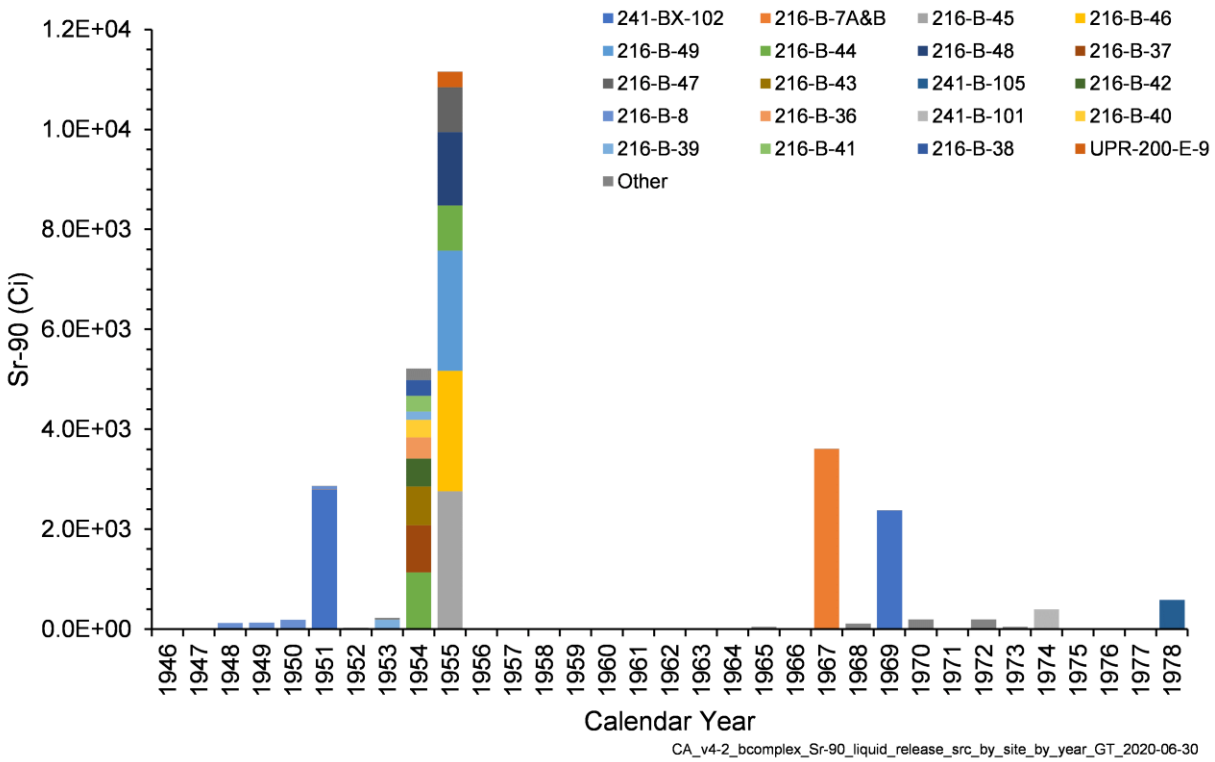

Figure 4-26. Annual Sr-90 Activity Released from Liquid Waste Sites in the B Complex Model

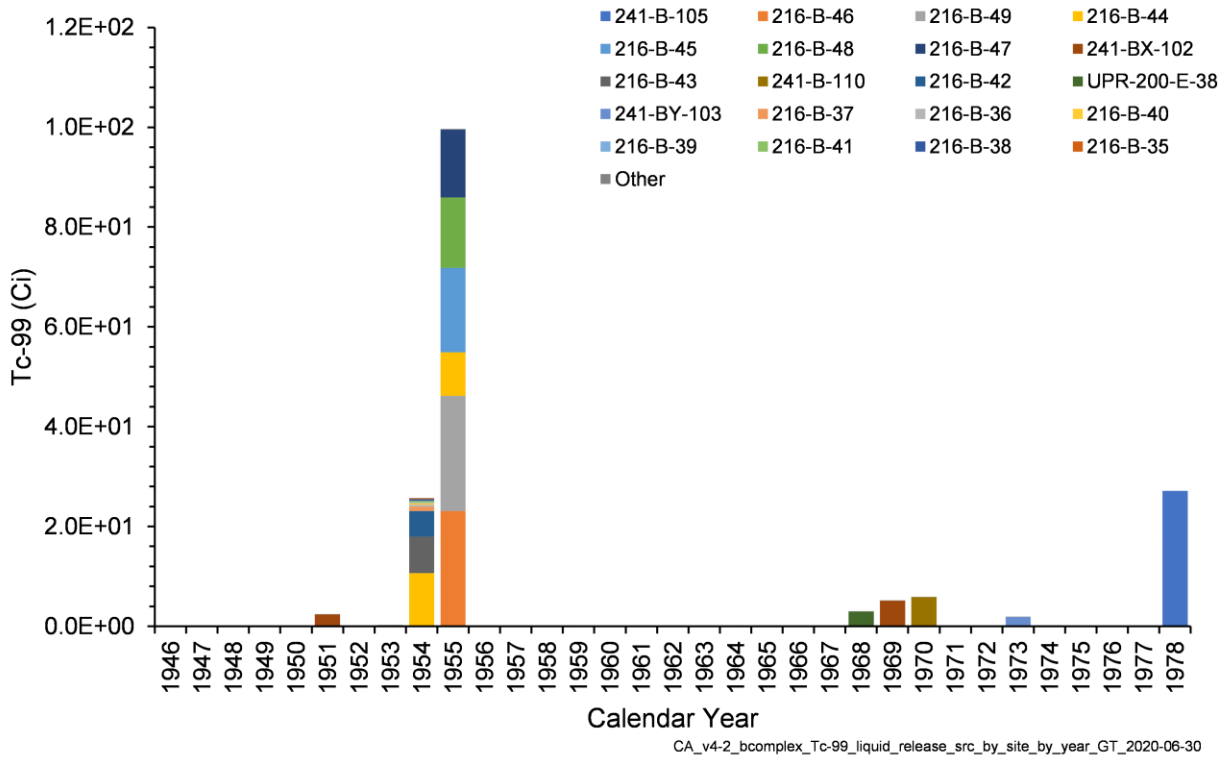

Figure 4-27. Annual Tc-99 Activity Released from Liquid Waste Sites in the B Complex Model

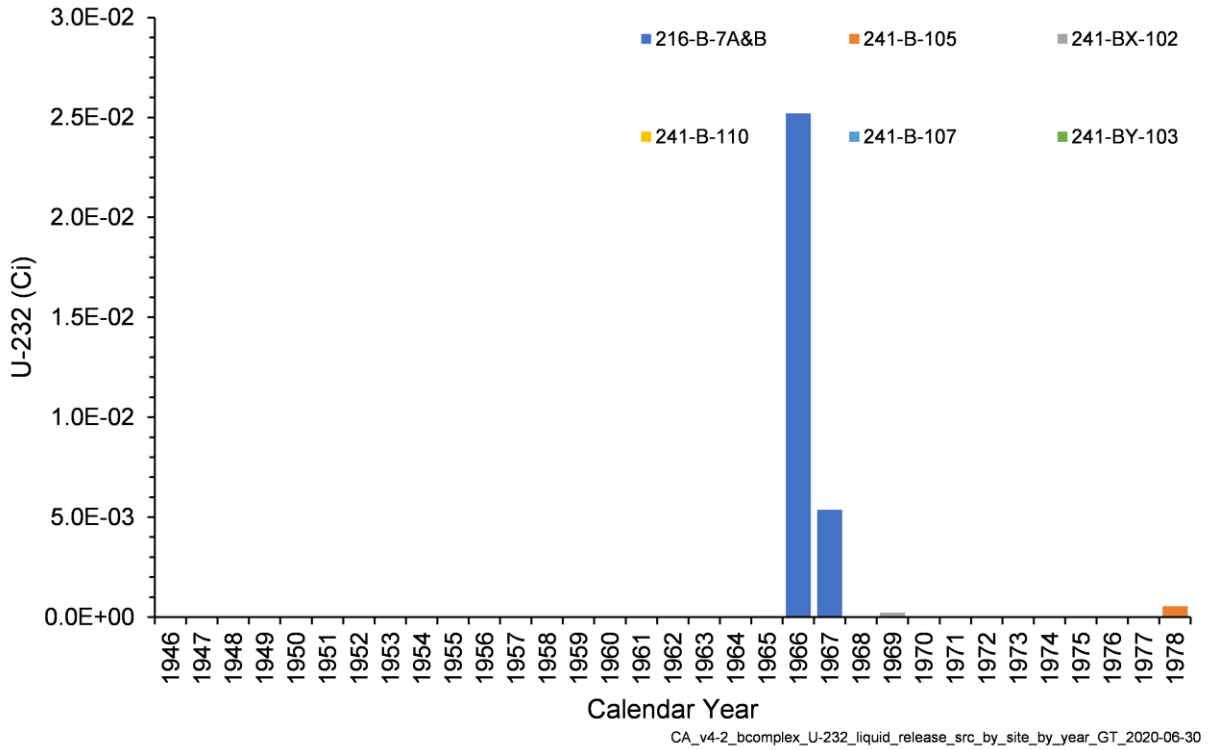

Figure 4-28. Annual U-232 Activity Released from Liquid Waste Sites in the B Complex Model

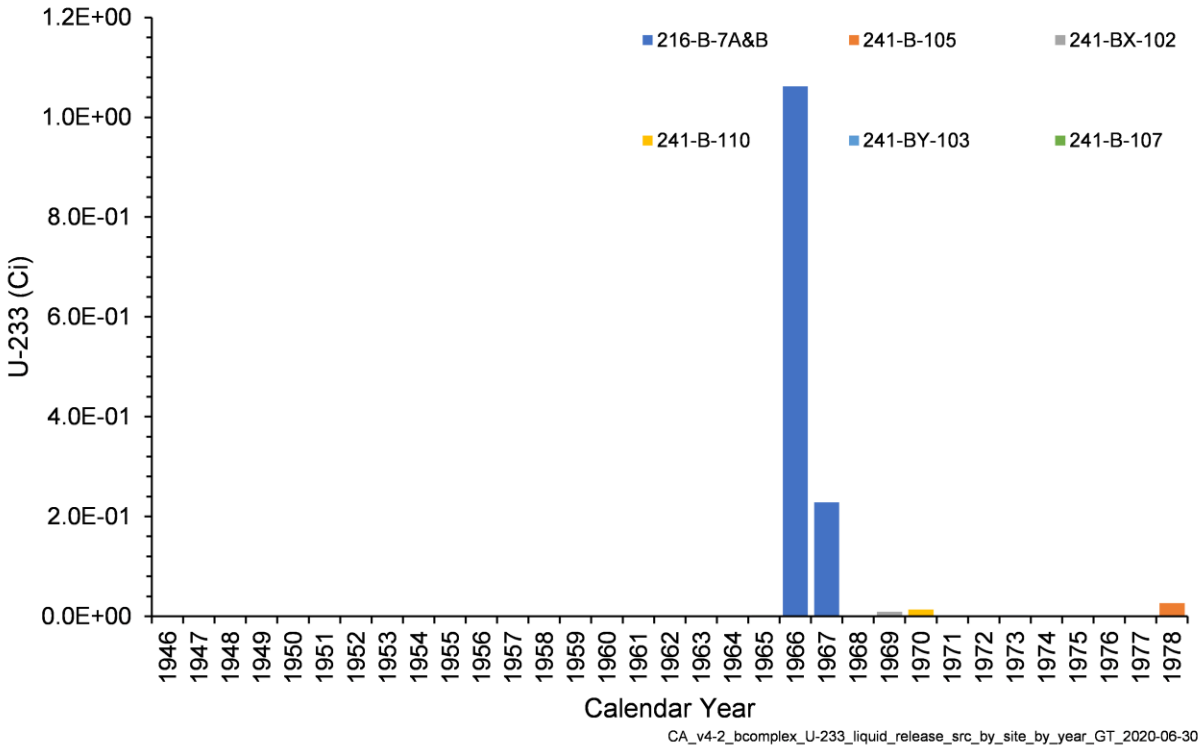

Figure 4-29. Annual U-233 Activity Released from Liquid Waste Sites in the B Complex Model

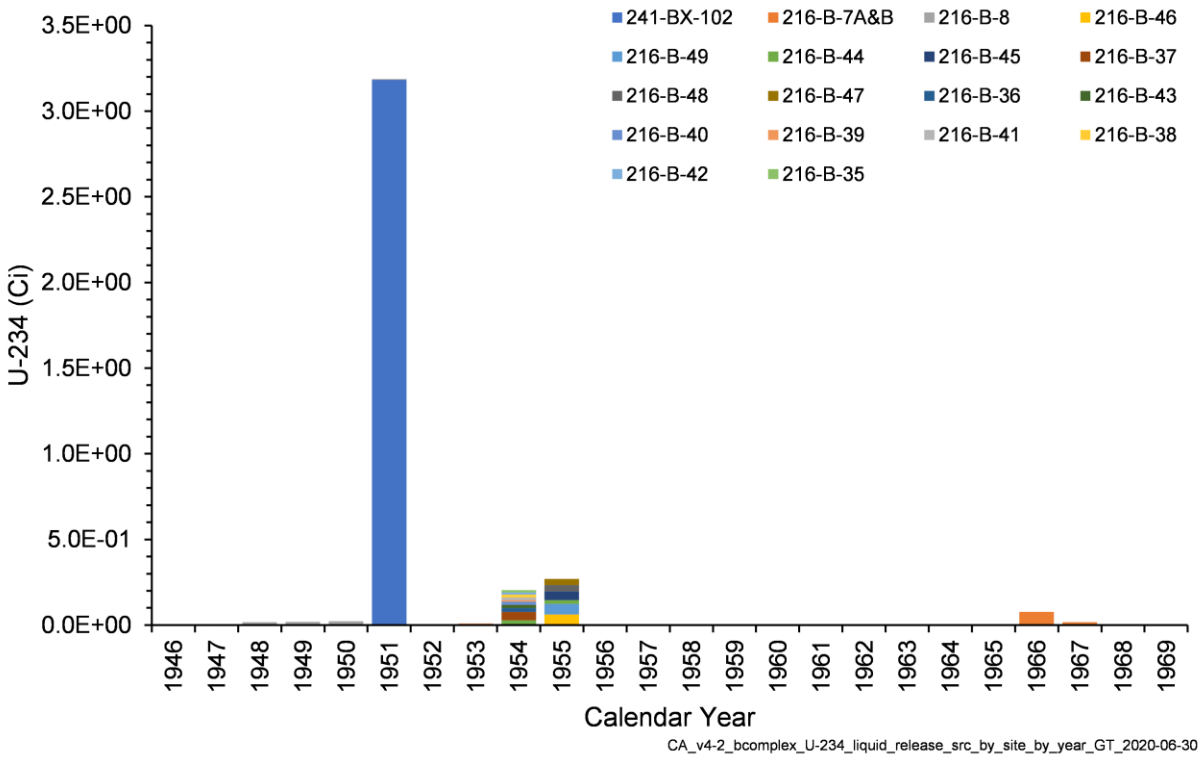

Figure 4-30. Annual U-234 Activity Released from Liquid Waste Sites in the B Complex Model

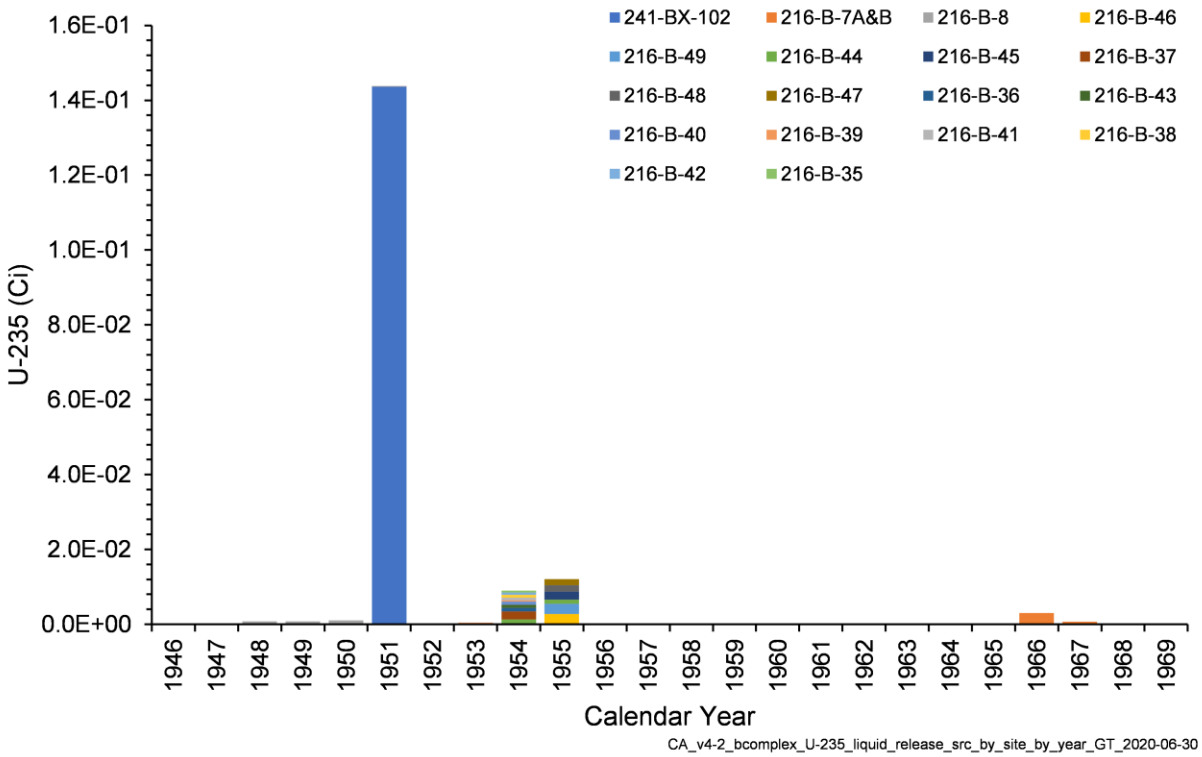

Figure 4-31. Annual U-235 Activity Released from Liquid Waste Sites in the B Complex Model

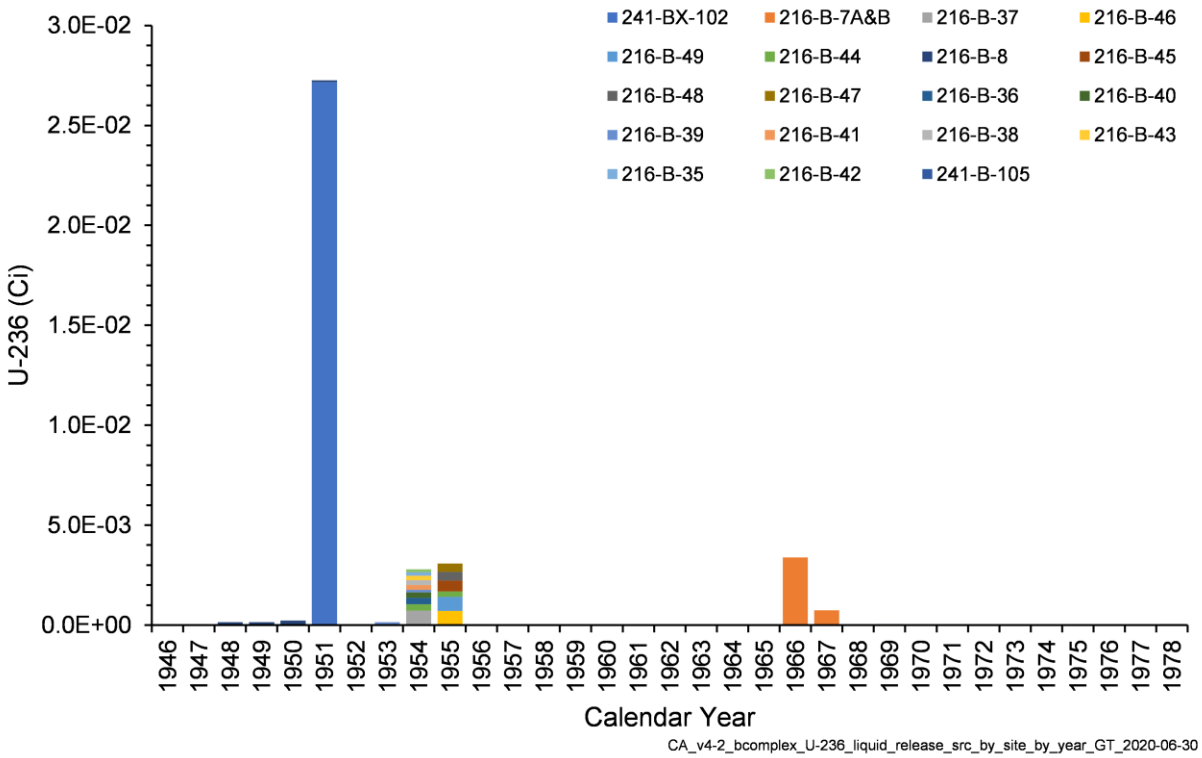

Figure 4-32. Annual U-236 Activity Released from Liquid Waste Sites in the B Complex Model

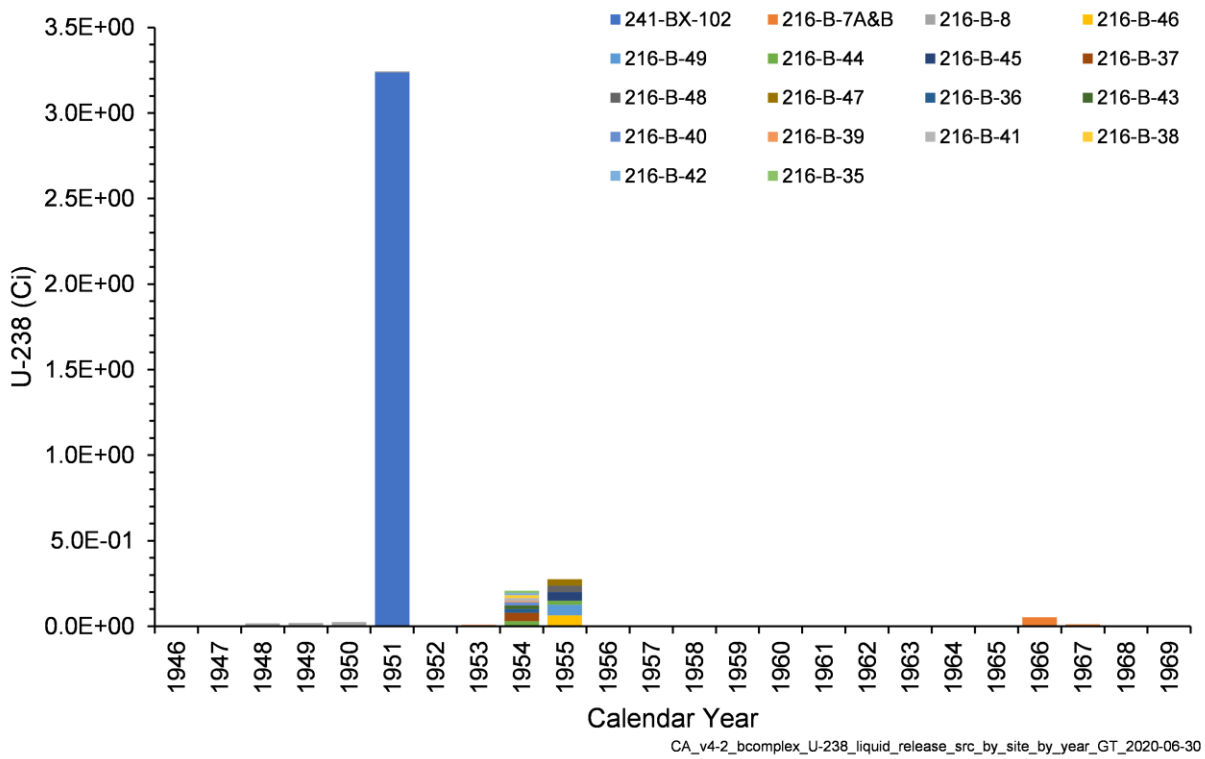

Figure 4-33. Annual U-238 Activity Released from Liquid Waste Sites in the B Complex Model

4.5.1.3 Solid Waste Site Releases

Solid wastes are contaminated materials that have the potential to release radionuclides to the vadose zone. Solid waste sites in the B Complex model are shown in Figure 4-9. Radionuclide inventories for the solid waste sites were originally designated in CP-61786. Waste form type (e.g., surplus reactor block, cement, soil-debris, grouted residual waste, and ancillary equipment) and release mechanisms are discussed in detail in CP-62766 with the supporting calculated annual release rates documented in ECF-HANFORD-19-0112. The total activities of radionuclides discharged to this model from those waste sites are shown in Figure 4-34 through Figure 4-47. Waste sites that contributed less than 0.1% of the total radionuclide release were not included in the images for Figure 4-34 through Figure 4-47. The annual release rates of radionuclide activities and the cumulative activities released to the model by waste site by year is shown in Figure 4-48 through Figure 4-75. The radionuclide releases in ECF-HANFORD-19-0112 are decayed to their year of release, so no decay corrections were needed for input to the B Complex model.

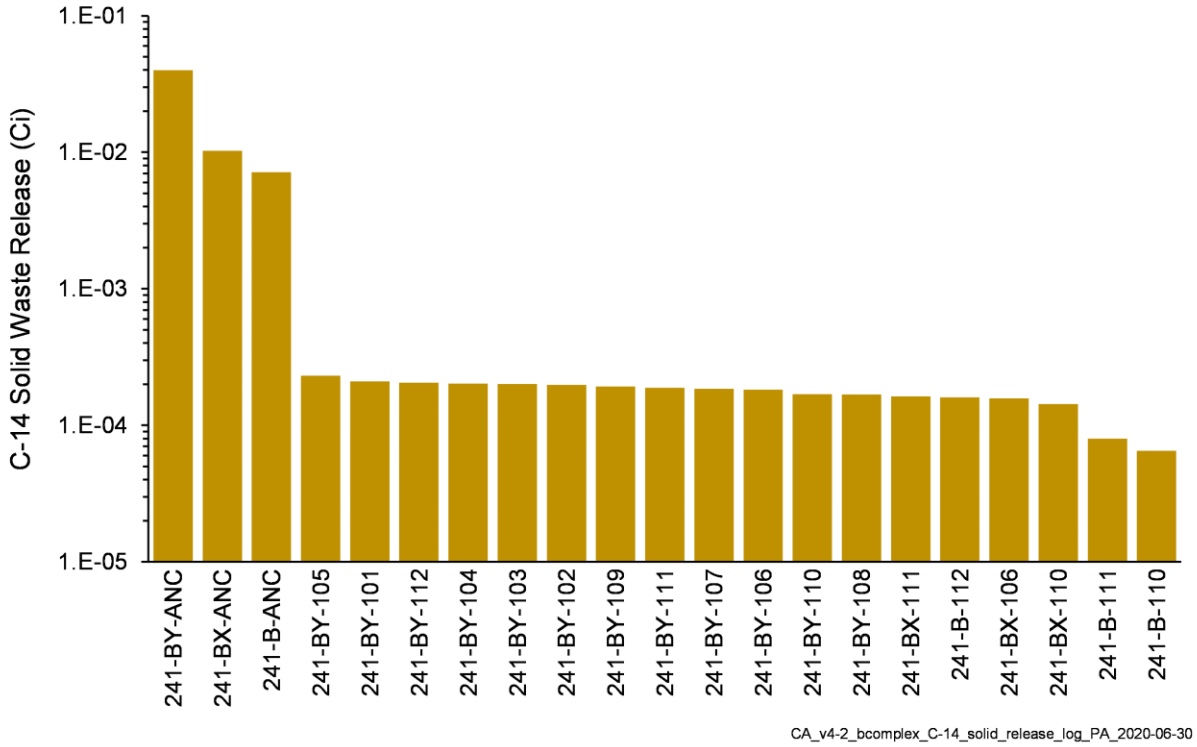

Figure 4-34. Total C-14 Activity Released from Solid Waste Sites in the B Complex Model

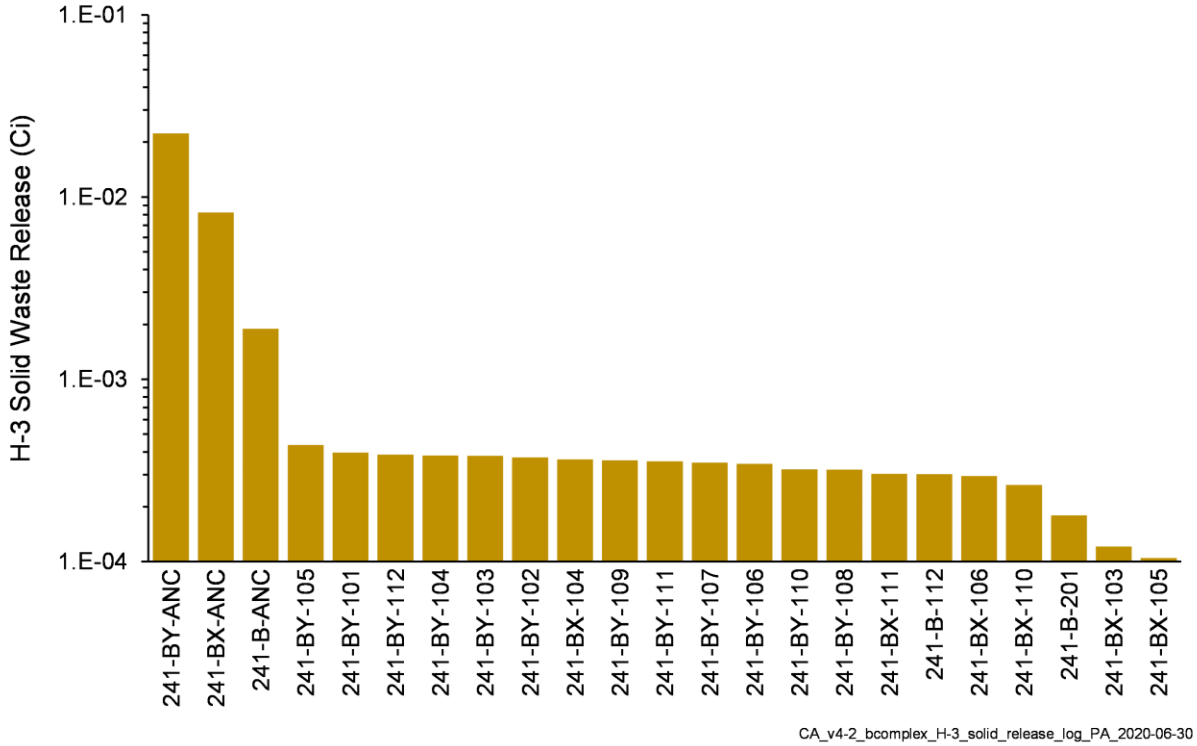

Figure 4-35. Total H-3 Activity Released from Solid Waste Sites in the B Complex Model

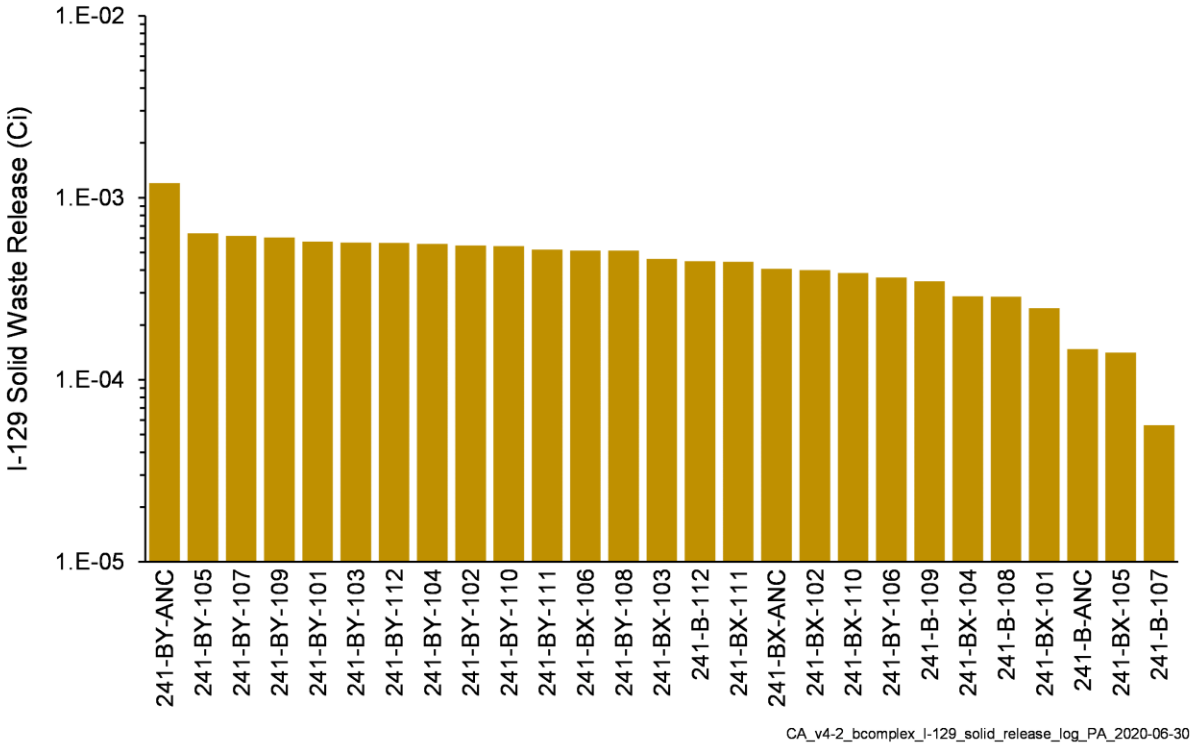

Figure 4-36. Total I-129 Activity Released from Solid Waste Sites in the B Complex Model

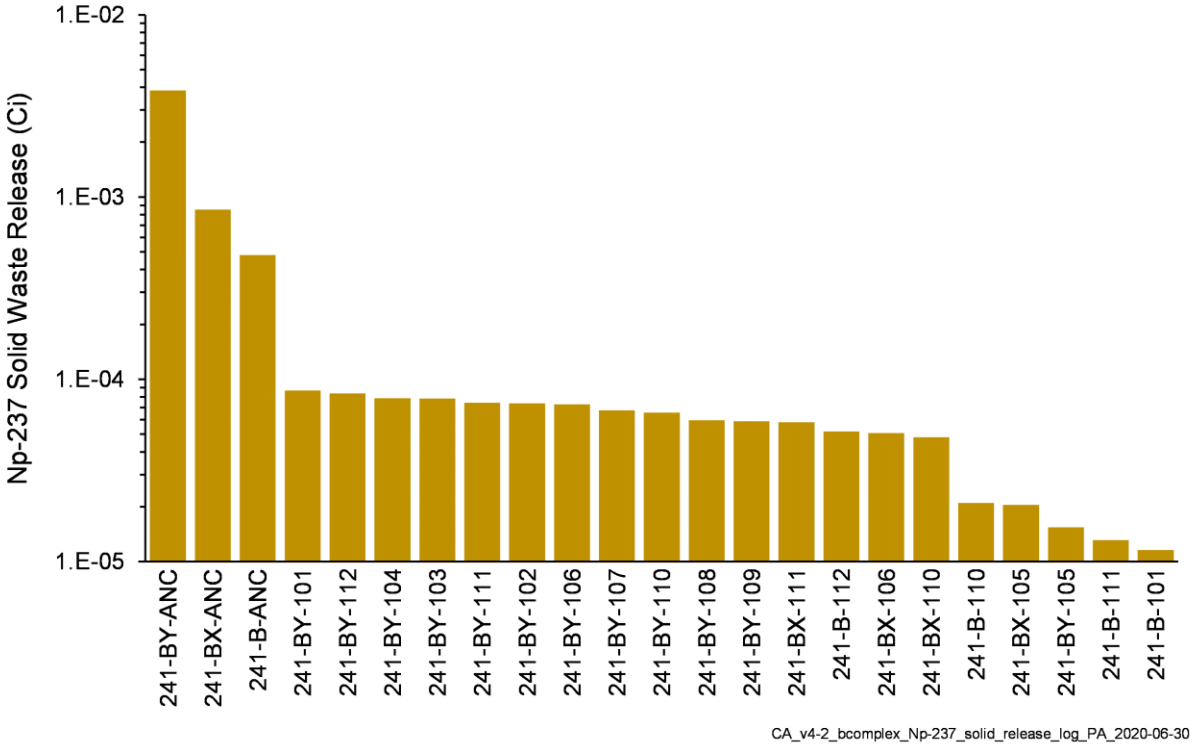

Figure 4-37. Total Np-237 Activity Released from Solid Waste Sites in the B Complex Model

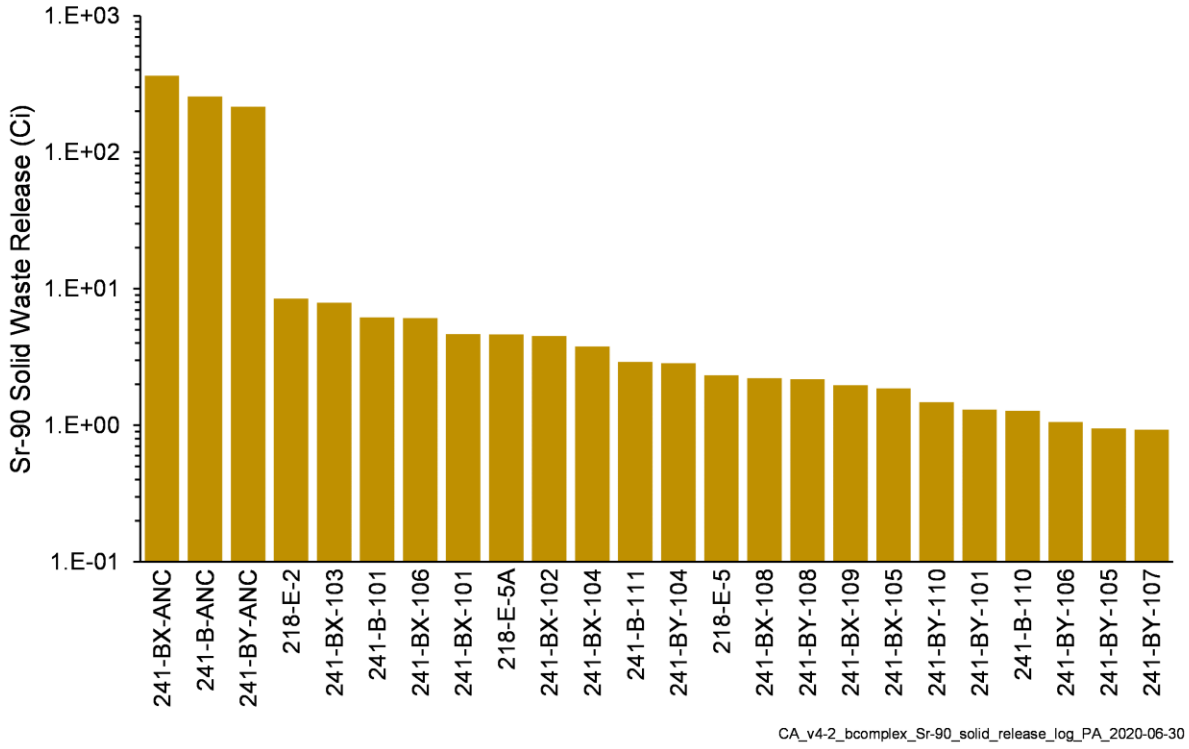

Figure 4-38. Total Sr-90 Activity Released from Solid Waste Sites in the B Complex Model

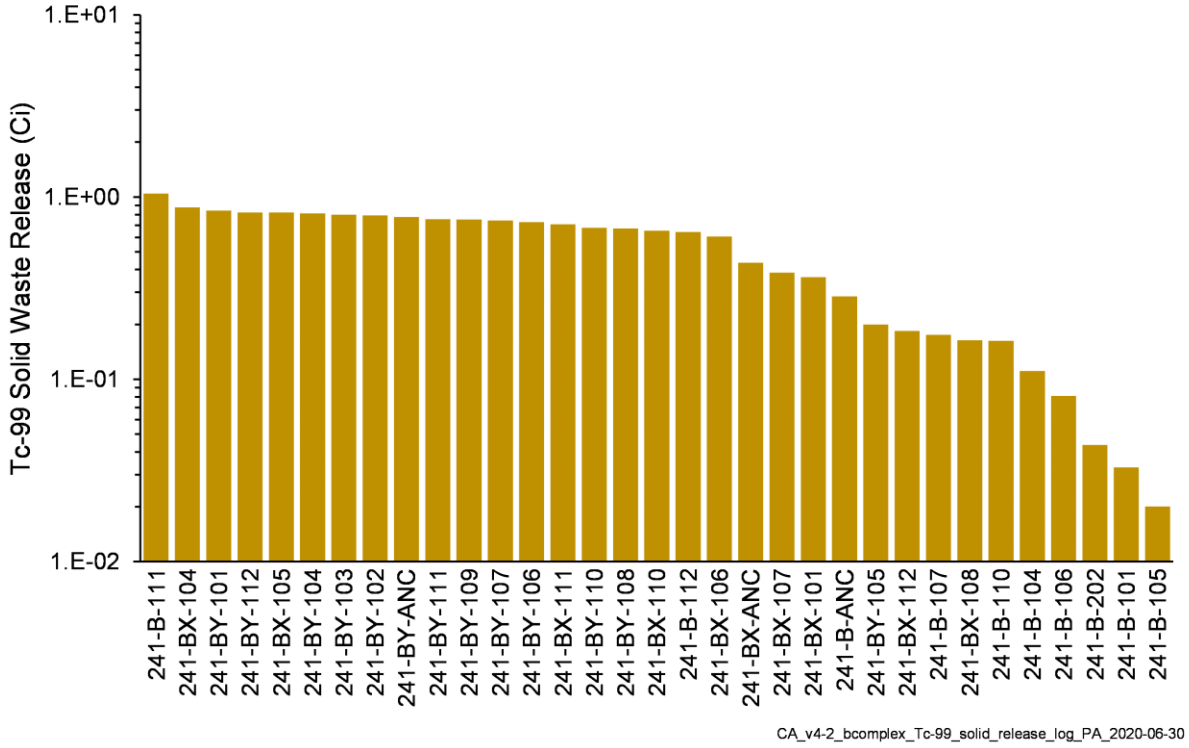

Figure 4-39. Total Tc-99 Activity Released from Solid Waste Sites in the B Complex Model

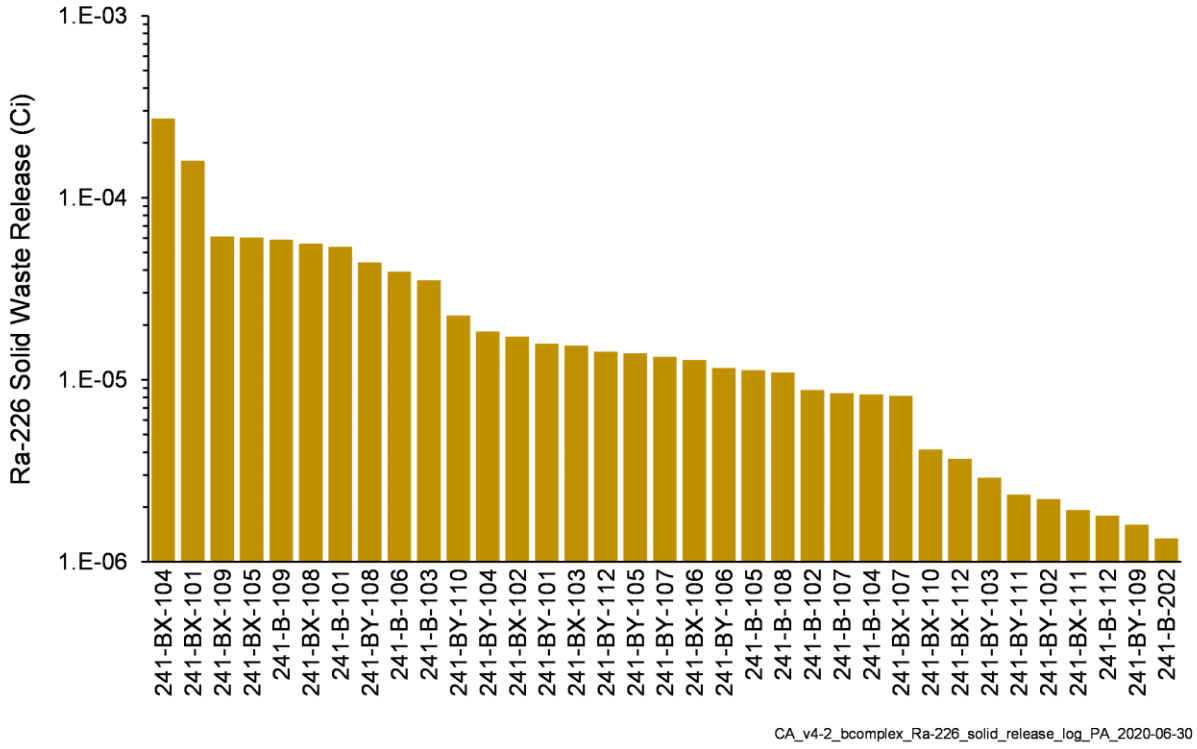

Figure 4-40. Total Ra-226 Activity Released from Solid Waste Sites in the B Complex Model

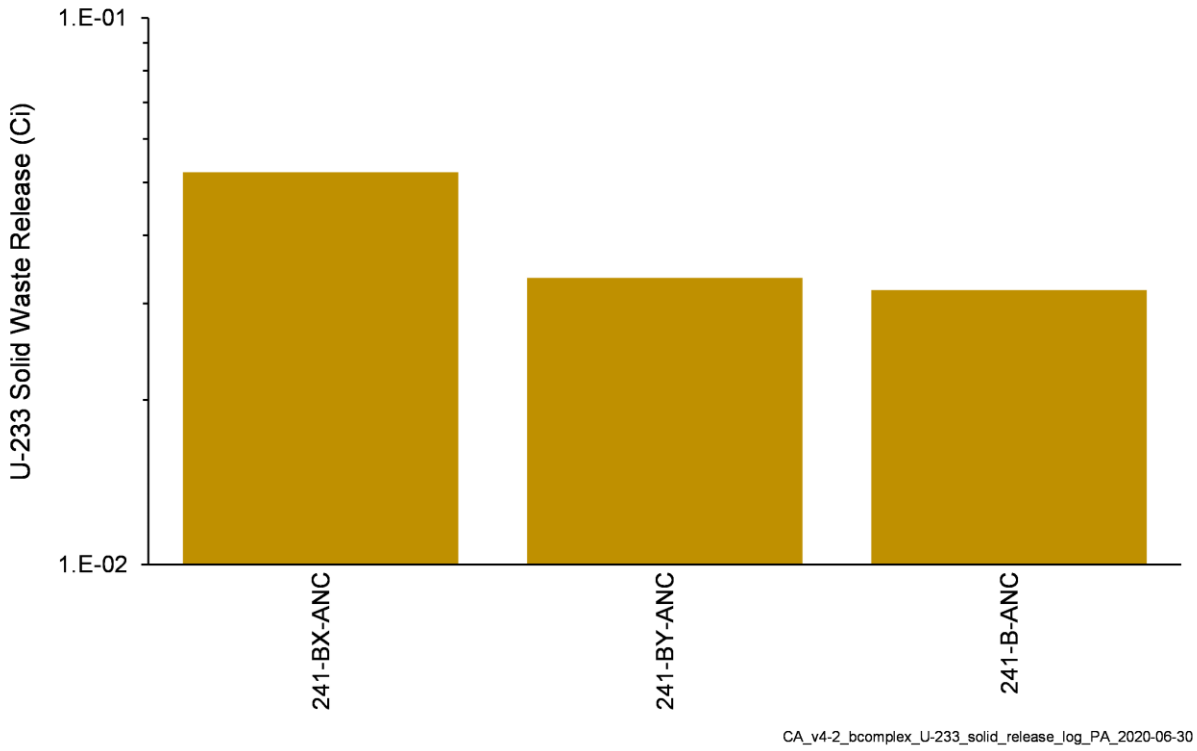

Figure 4-41. Total Th-230 Activity Released from Solid Waste Sites in the B Complex Model

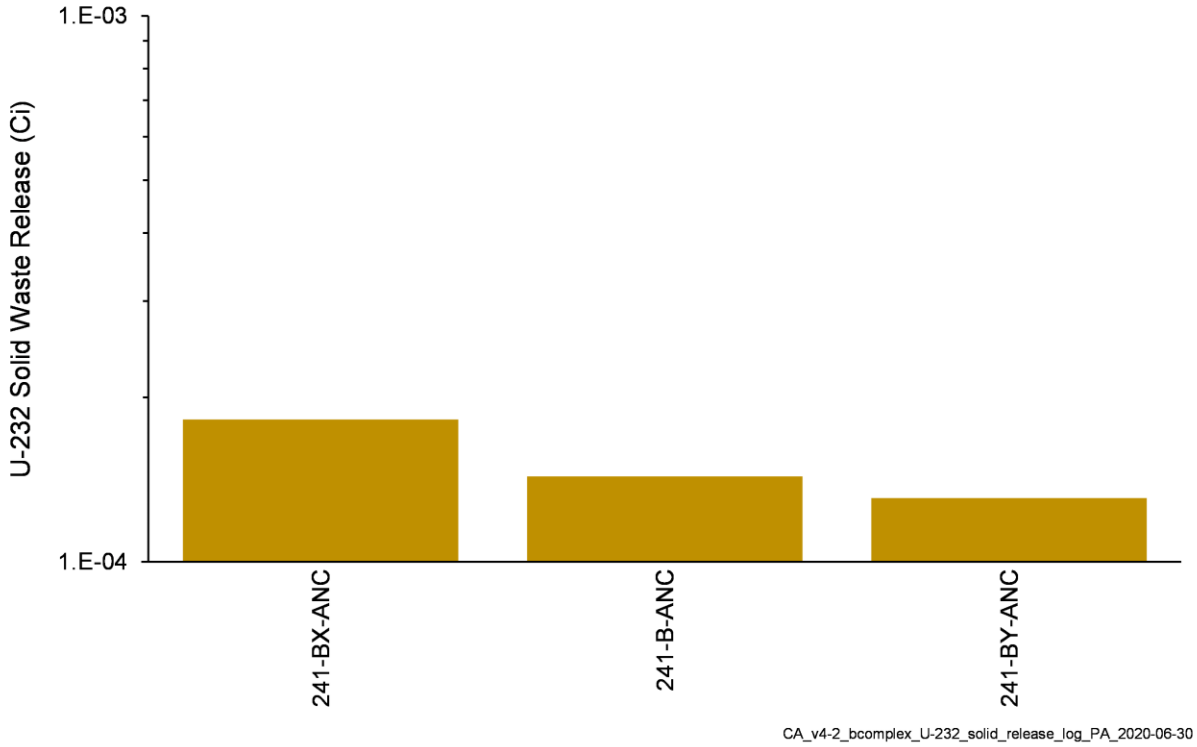

Figure 4-42. Total U-232 Activity Released from Solid Waste Sites in the B Complex Model

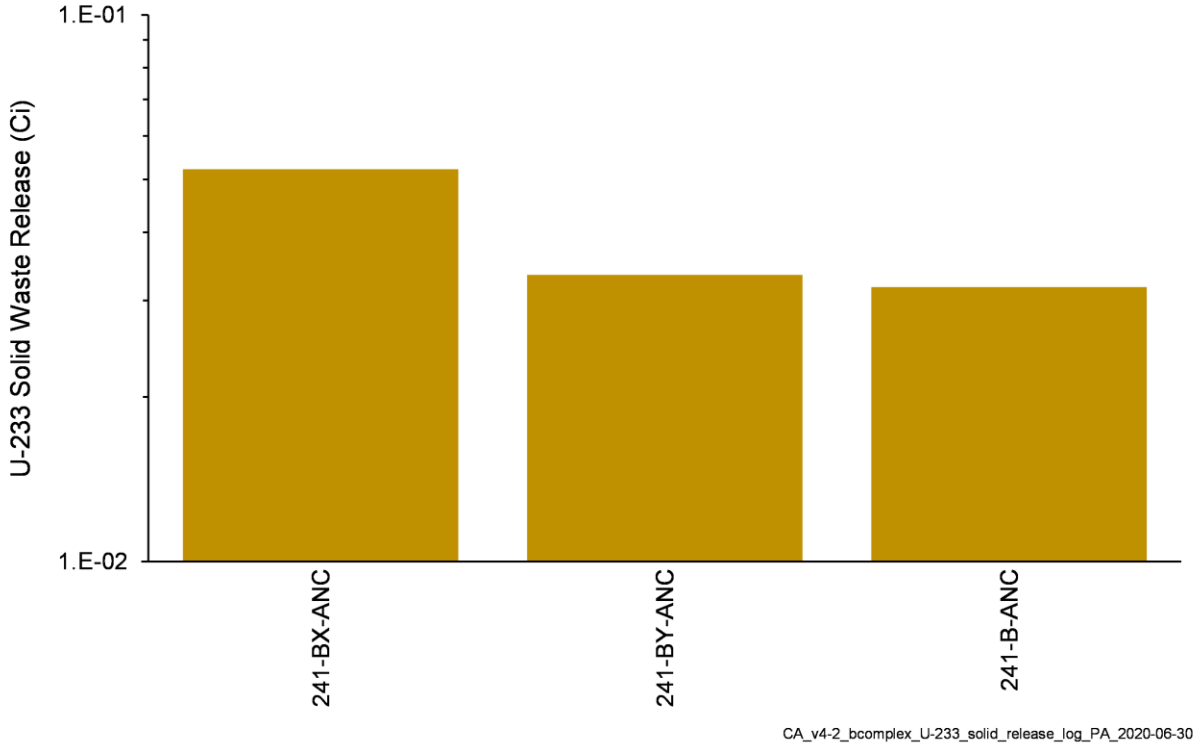

Figure 4-43. Total U-233 Activity Released from Solid Waste Sites in the B Complex Model

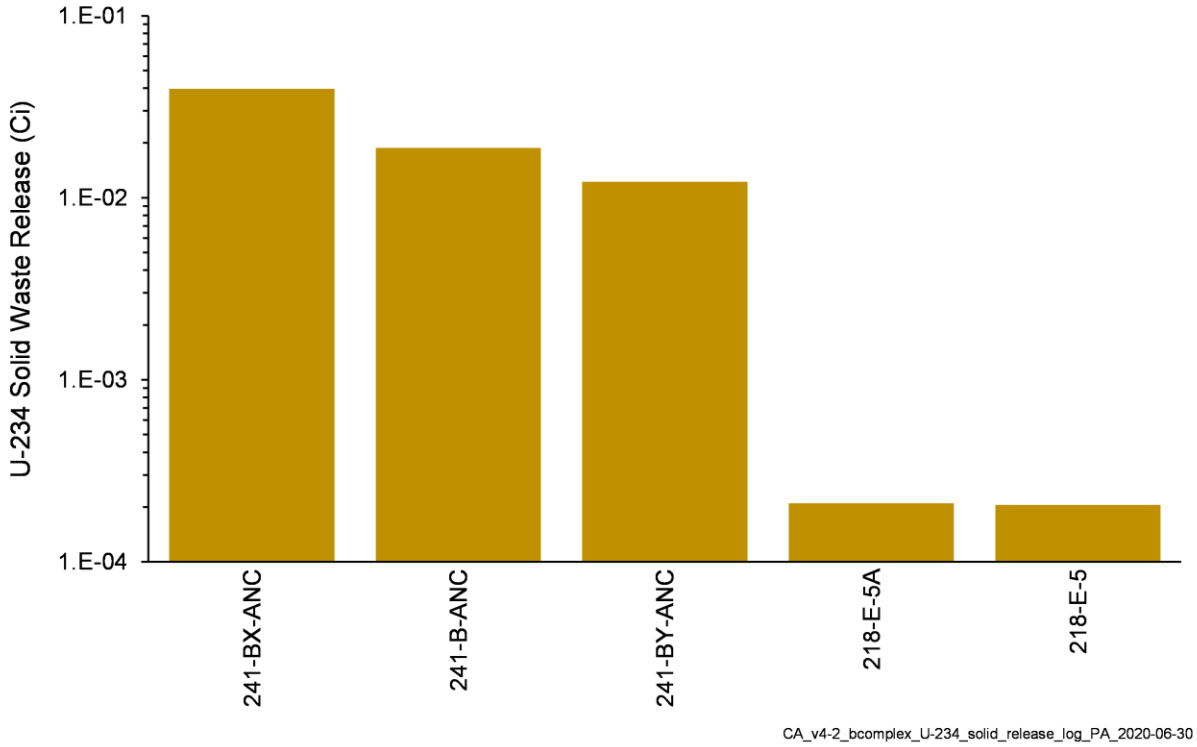

Figure 4-44. Total U-234 Activity Released from Solid Waste Sites in the B Complex Model

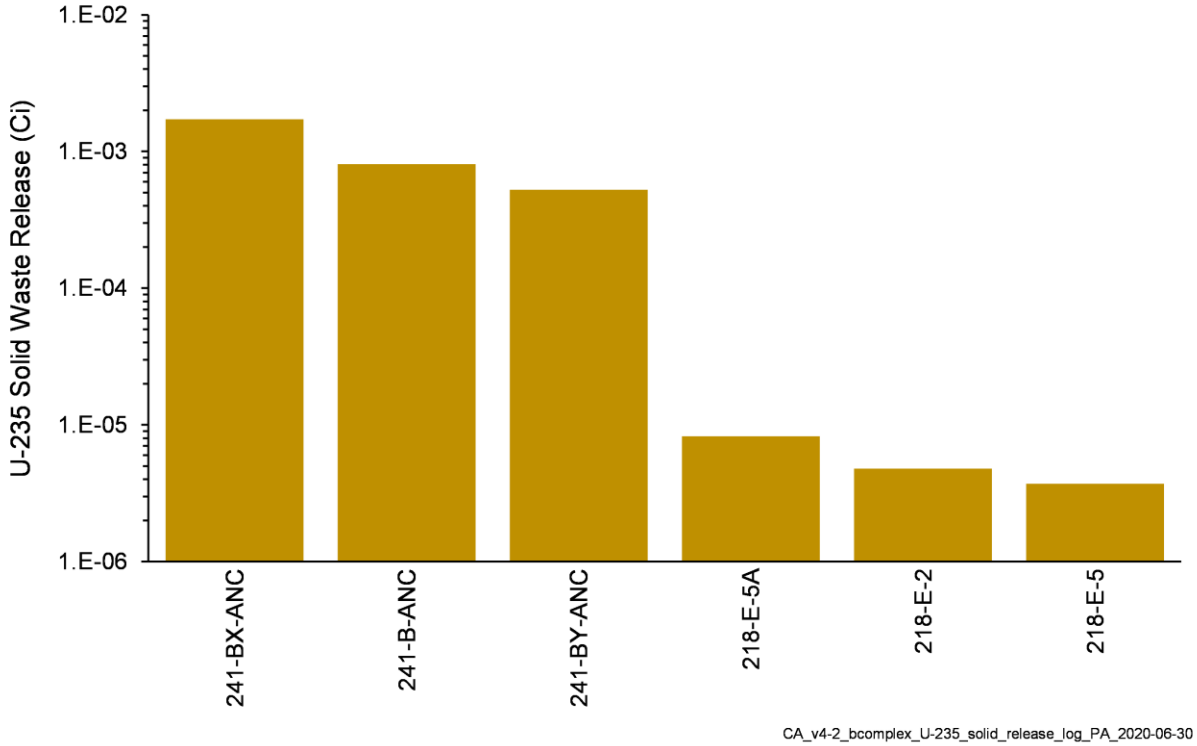

Figure 4-45. Total U-235 Activity Released from Solid Waste Sites in the B Complex Model

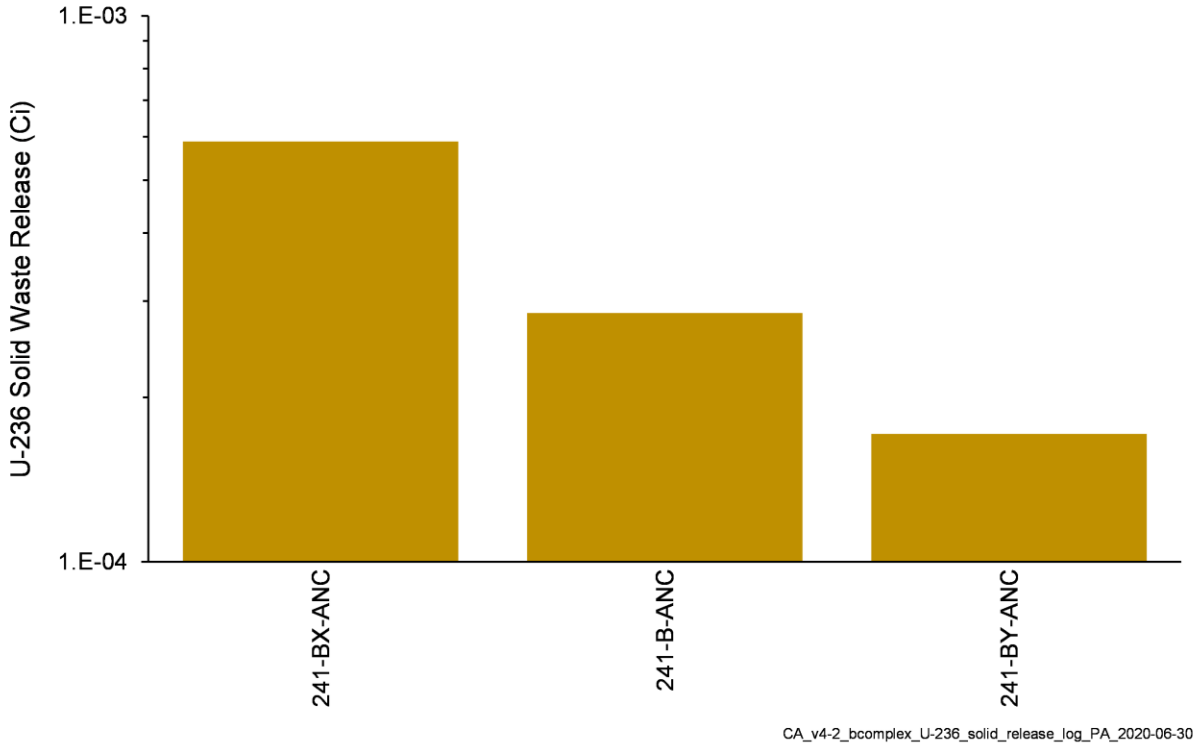

Figure 4-46. Total U-236 Activity Released from Solid Waste Sites in the B Complex Model

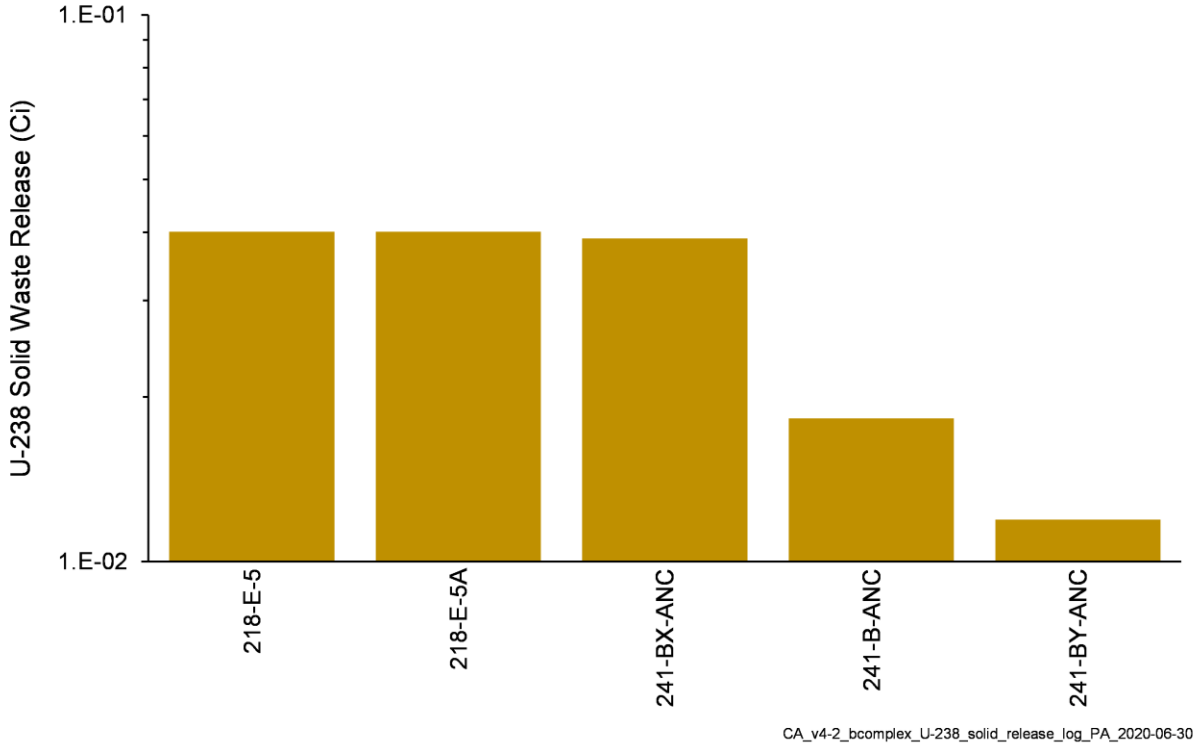

Figure 4-47. Total U-238 Activity Released from Solid Waste Sites in the B Complex Model

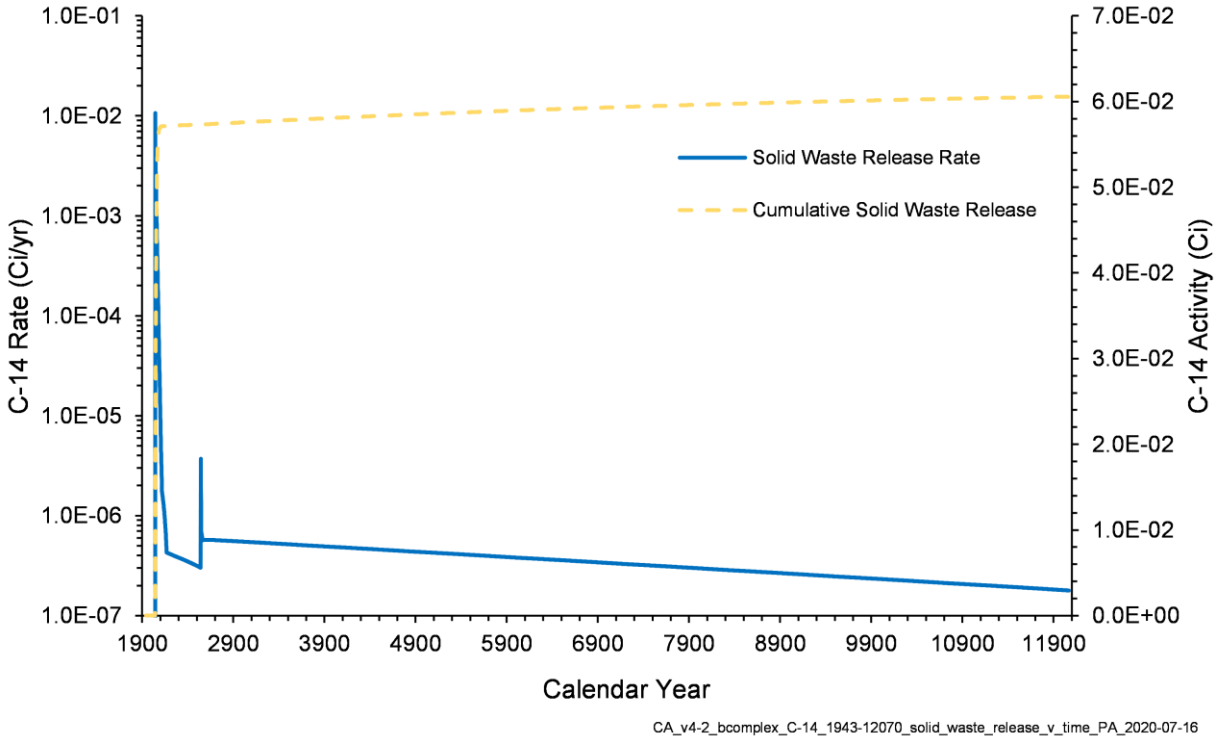

Figure 4-48. C-14 Release Rate and Cumulative Activity from Solid Waste in the B Complex Model, 1943–12070

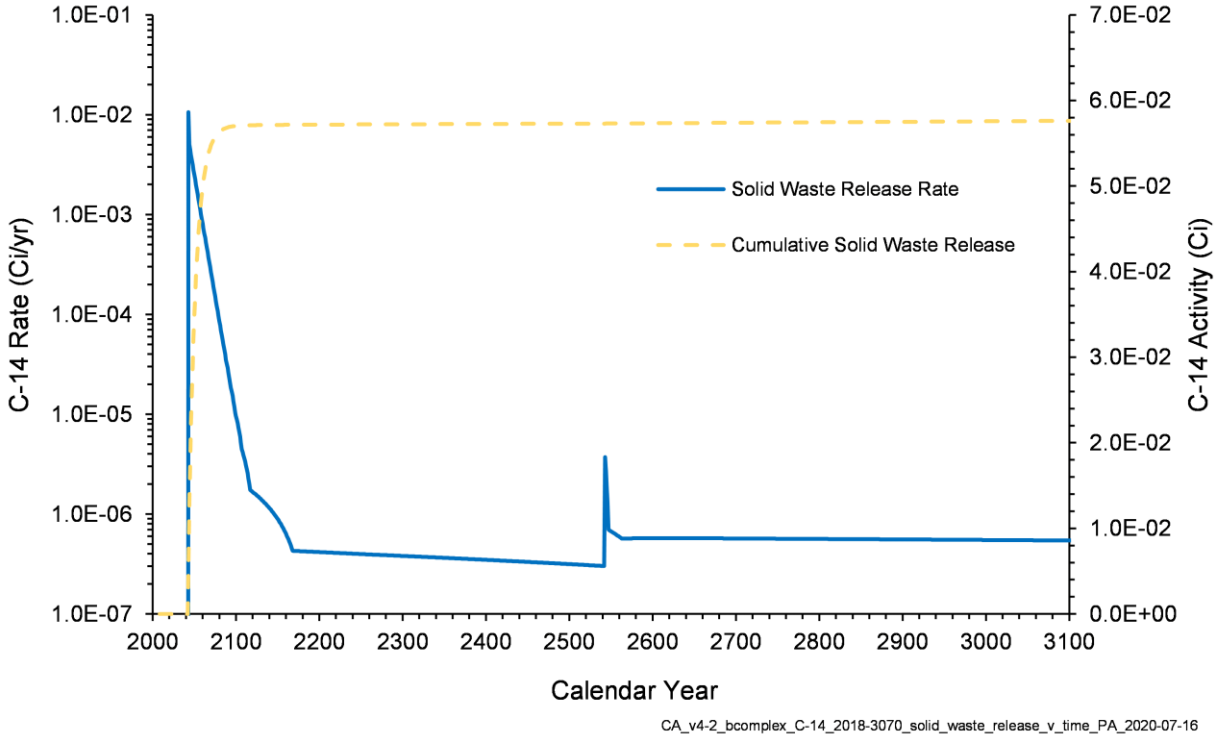

Figure 4-49. C-14 Release Rate and Cumulative Activity from Solid Waste in the B Complex Model, 2018–3070

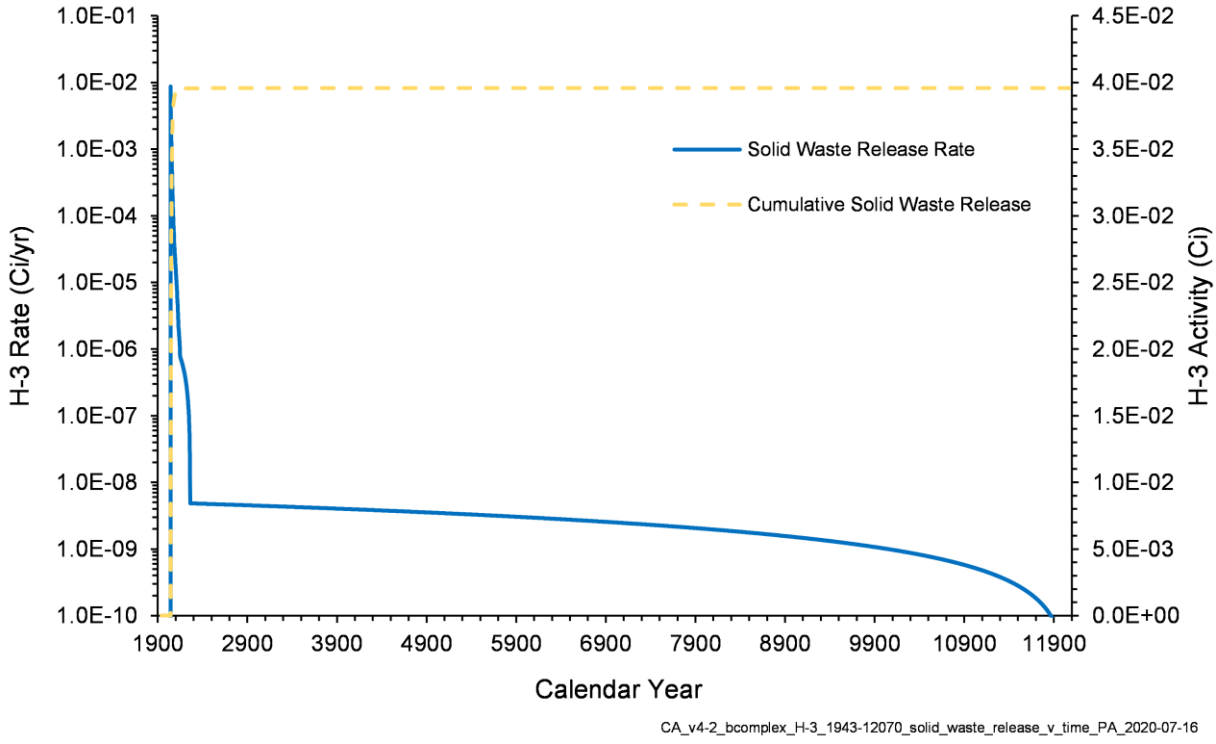

Figure 4-50. H-3 Release Rate and Cumulative Activity from Solid Waste in the B Complex Model, 1943–12070

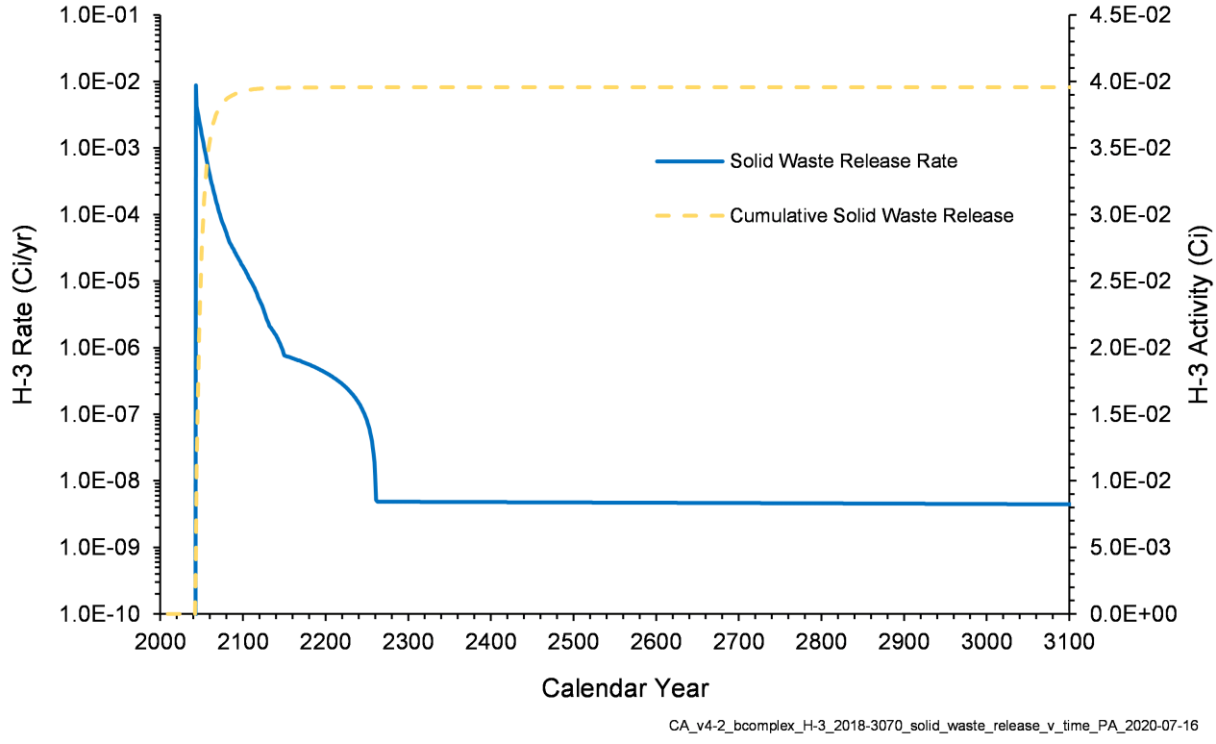

Figure 4-51. H-3 Release Rate and Cumulative Activity from Solid Waste in the B Complex Model, 2018–3070

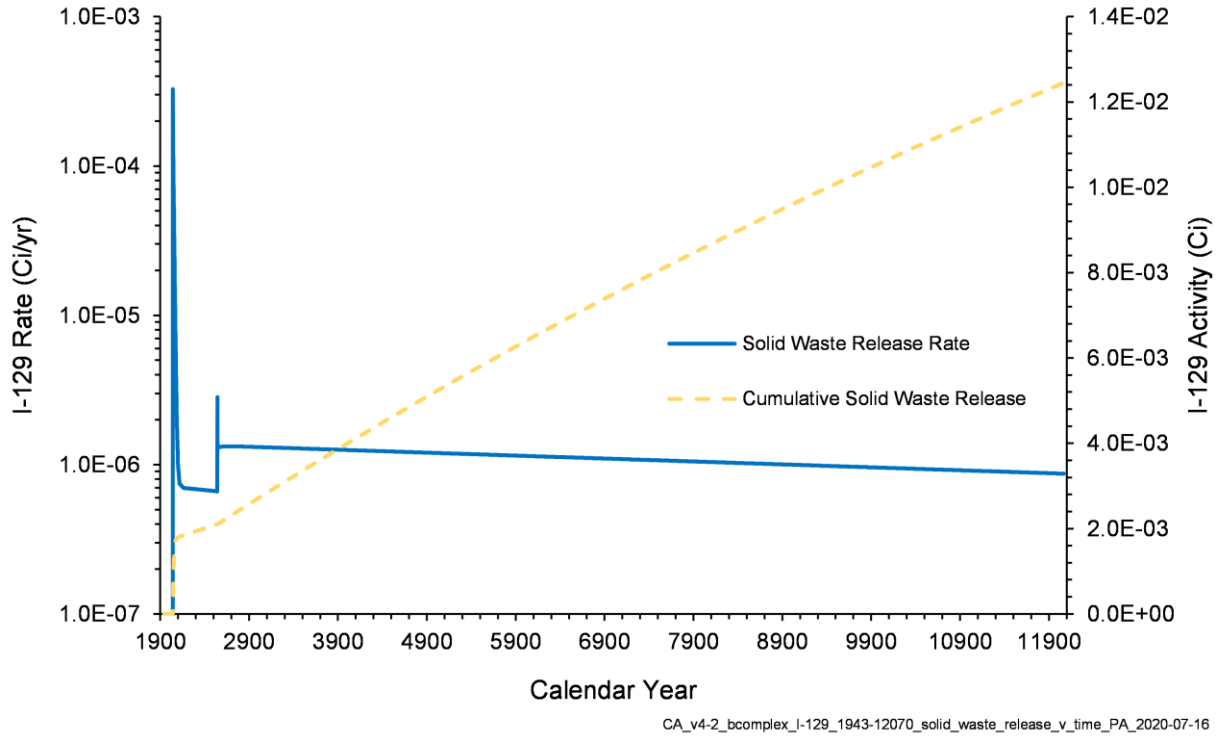

Figure 4-52. I-129 Release Rate and Cumulative Activity from Solid Waste in the B Complex Model, 1943–12070

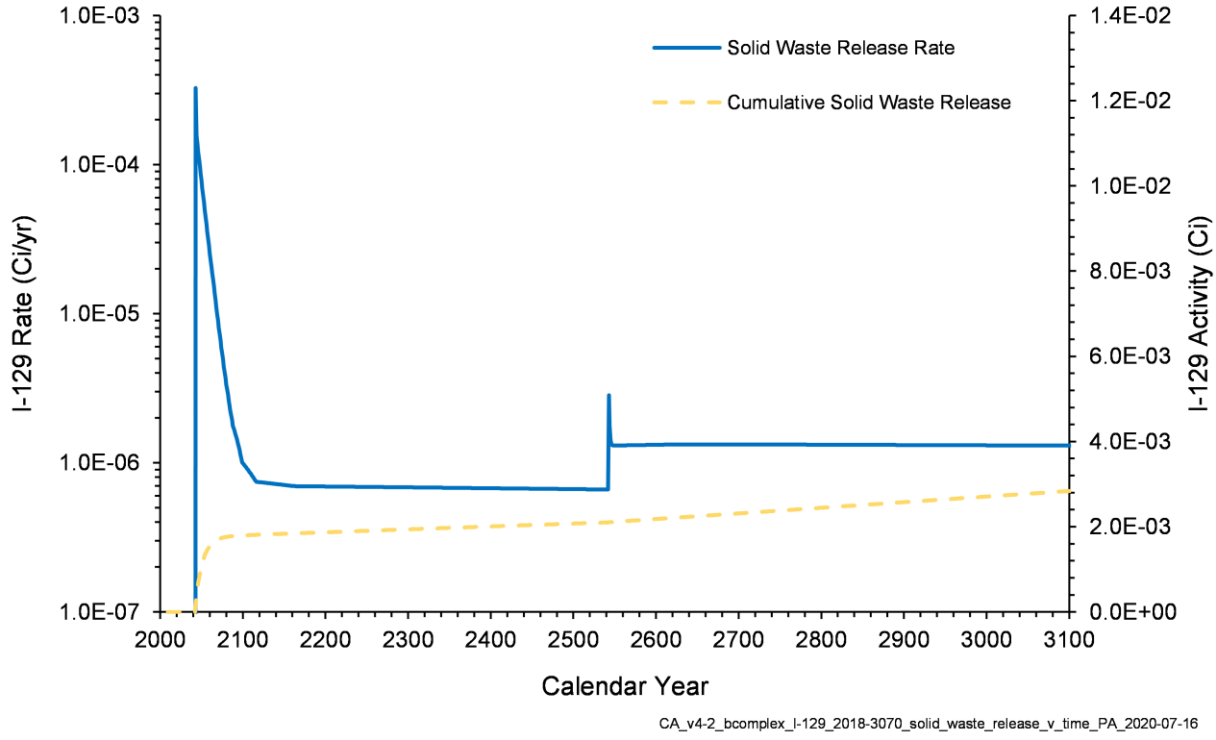

Figure 4-53. I-129 Release Rate and Cumulative Activity from Solid Waste in the B Complex Model, 2018–3070

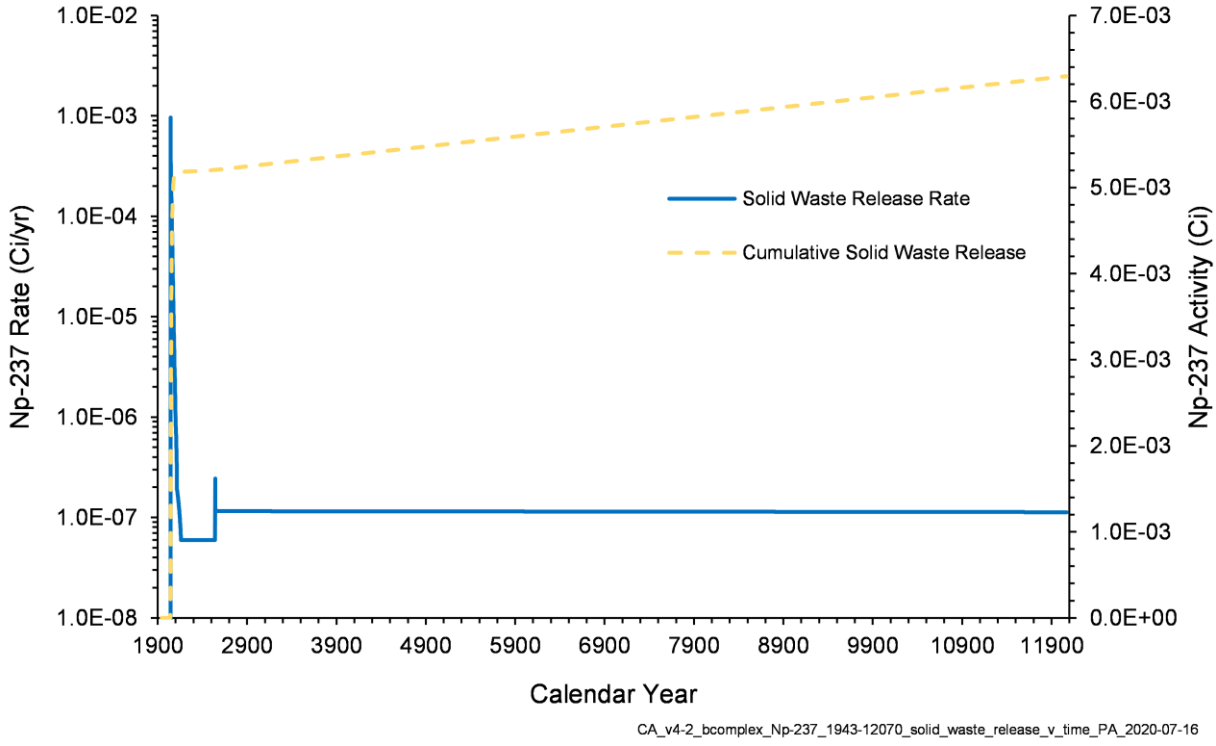

Figure 4-54. Np-237 Release Rate and Cumulative Activity from Solid Waste in the B Complex Model, 1943–12070

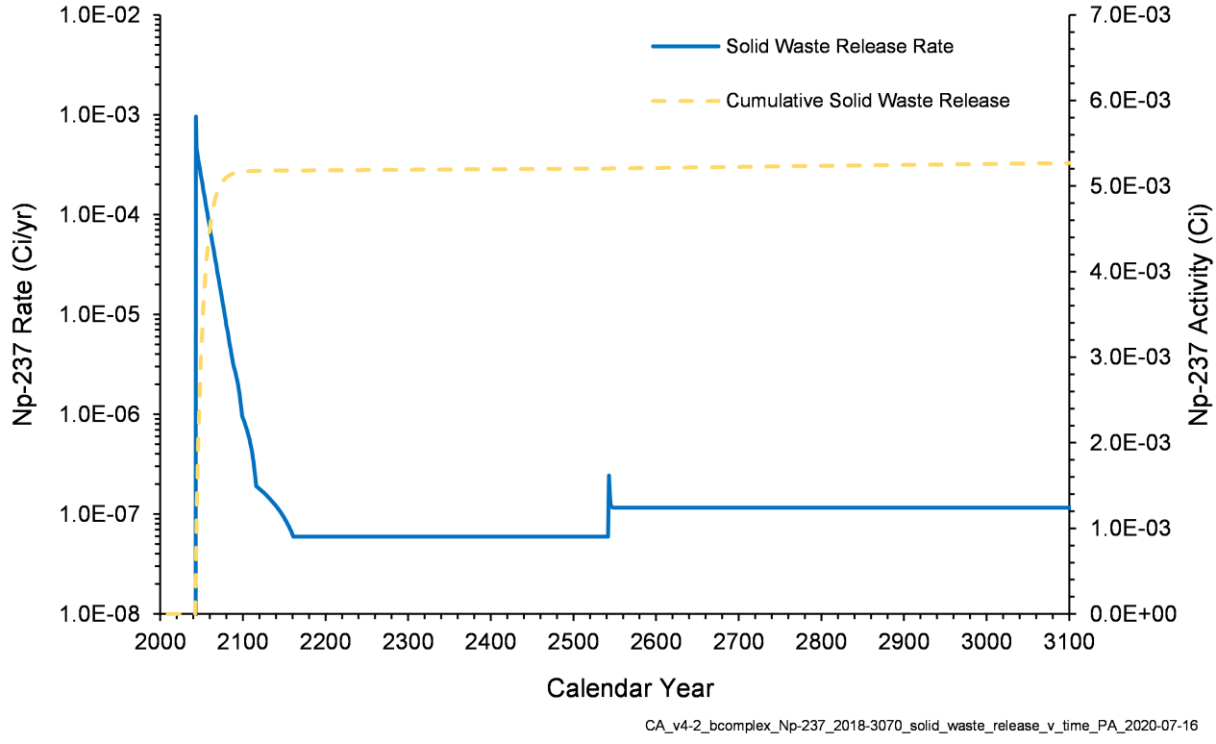

Figure 4-55. Np-237 Release Rate and Cumulative Activity from Solid Waste in the B Complex Model, 2018–3070

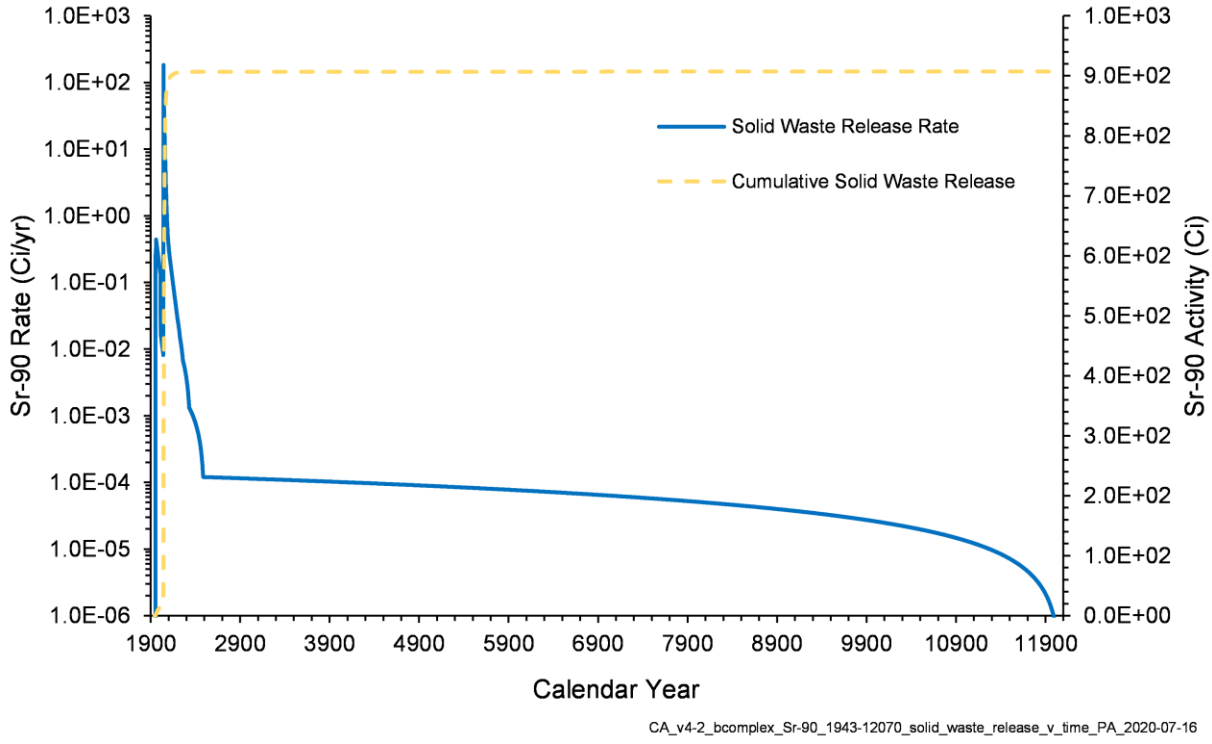

Figure 4-56. Sr-90 Release Rate and Cumulative Activity from Solid Waste in the B Complex Model, 1943–12070

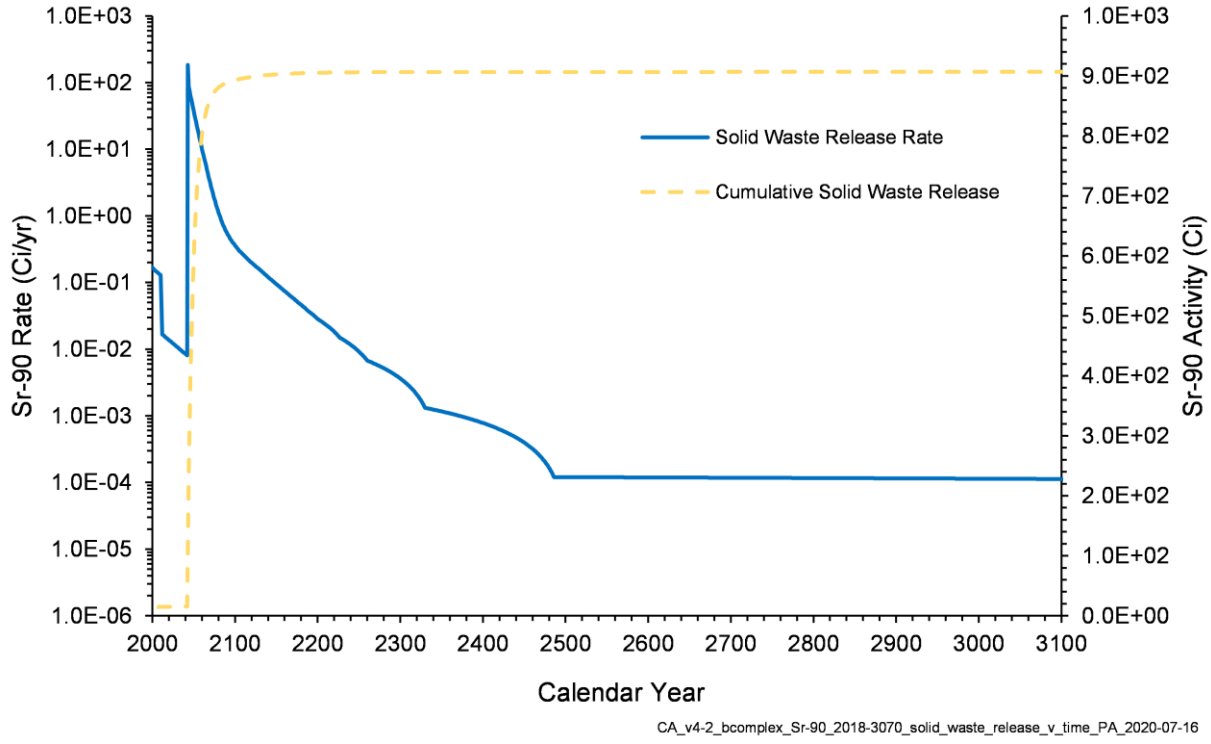

Figure 4-57. Sr-90 Release Rate and Cumulative Activity from Solid Waste in the B Complex Model, 2018–3070

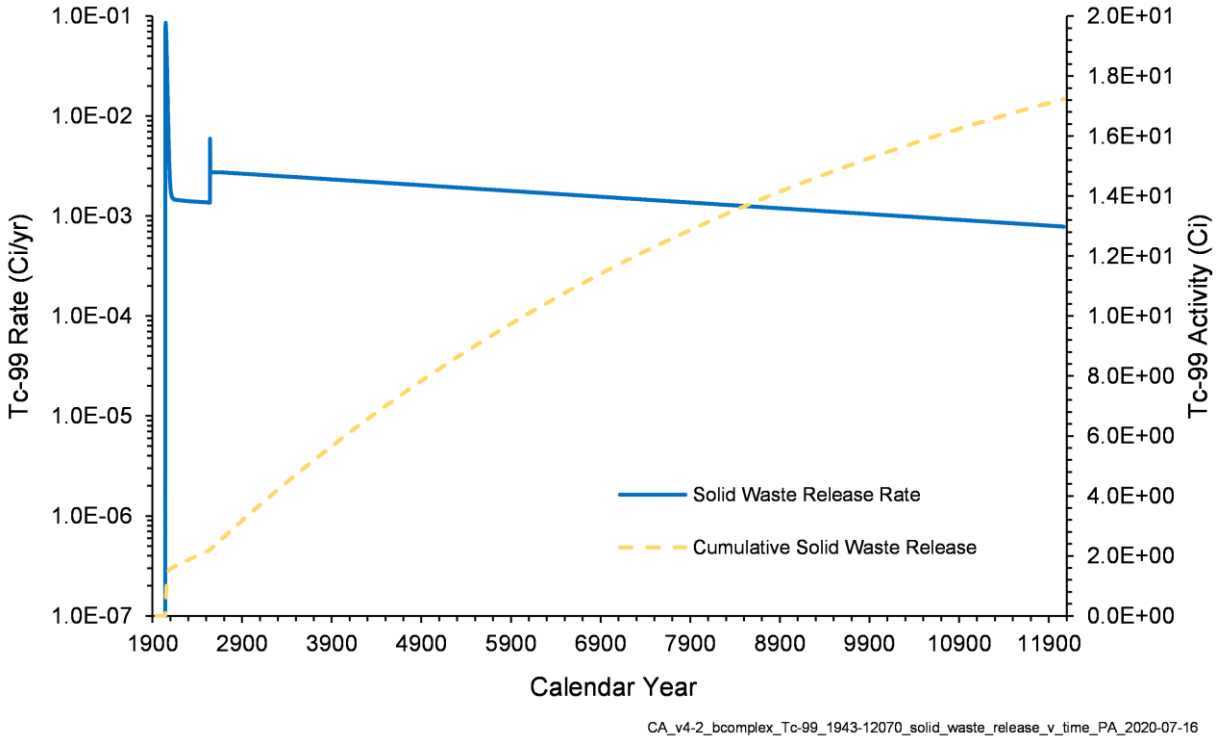

Figure 4-58. Tc-99 Release Rate and Cumulative Activity from Solid Waste in the B Complex Model, 1943–12070

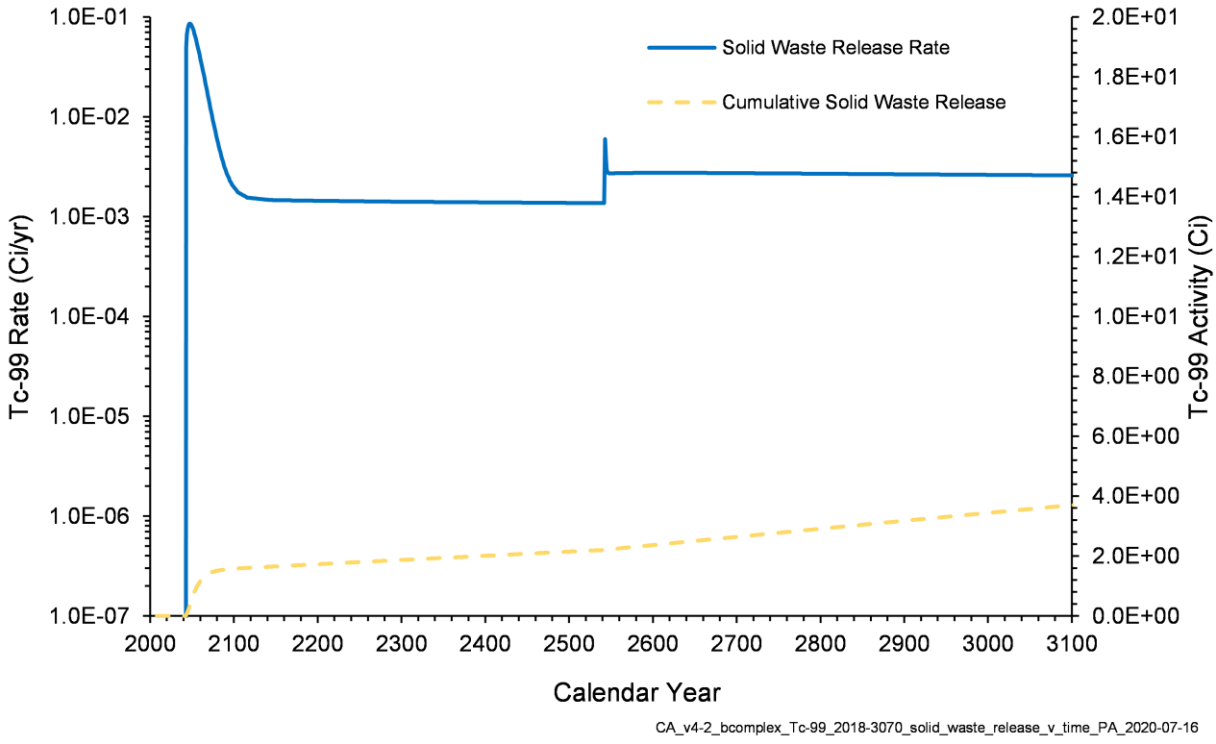

Figure 4-59. Tc-99 Release Rate and Cumulative Activity from Solid Waste in the B Complex Model, 2018–3070

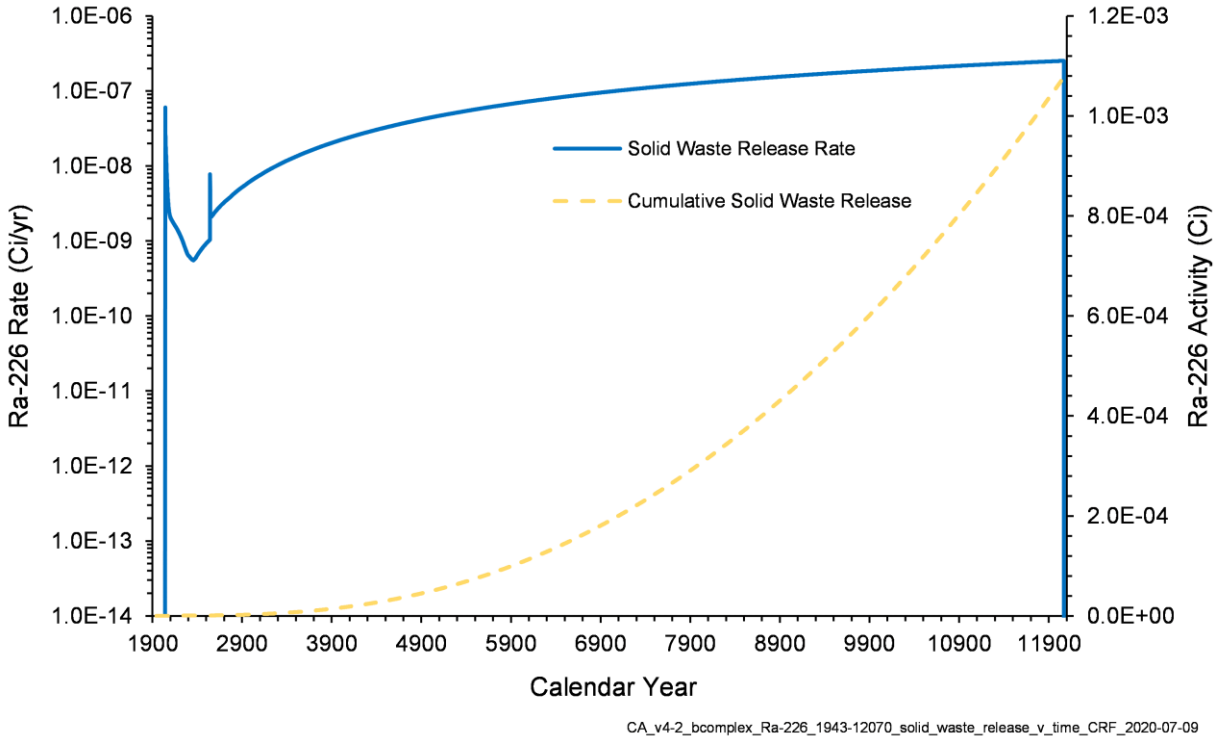

Figure 4-60. Ra-226 Release Rate and Cumulative Activity from Solid Waste in the B Complex Model, 1943–12070

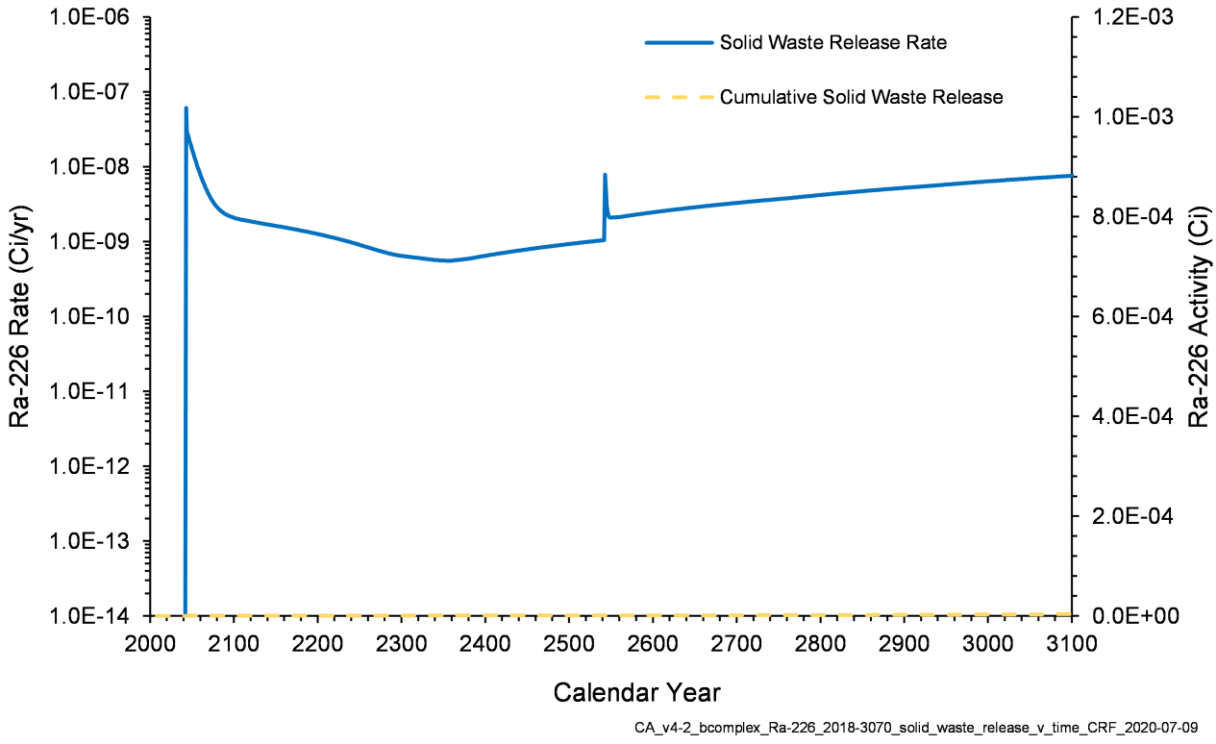

Figure 4-61. Ra-226 Release Rate and Cumulative Activity from Solid Waste in the B Complex Model, 2018–3070

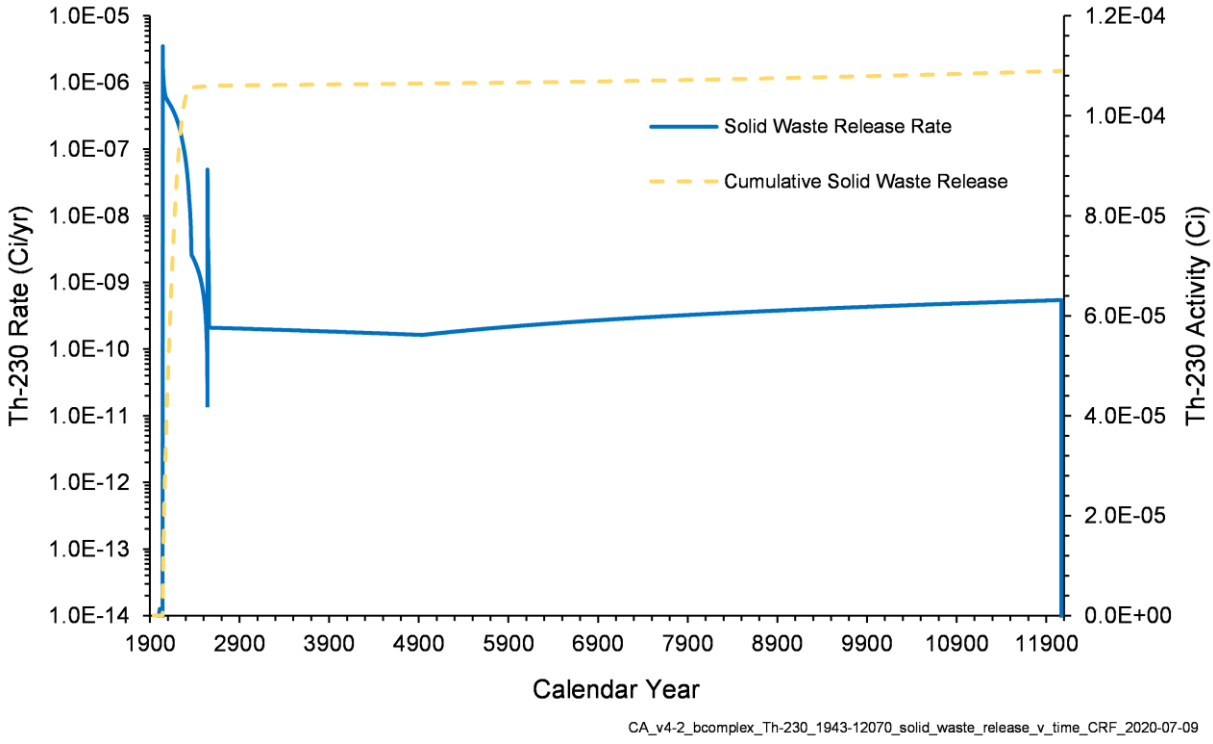

Figure 4-62. Th-230 Release Rate and Cumulative Activity from Solid Waste in the B Complex Model, 1943–12070

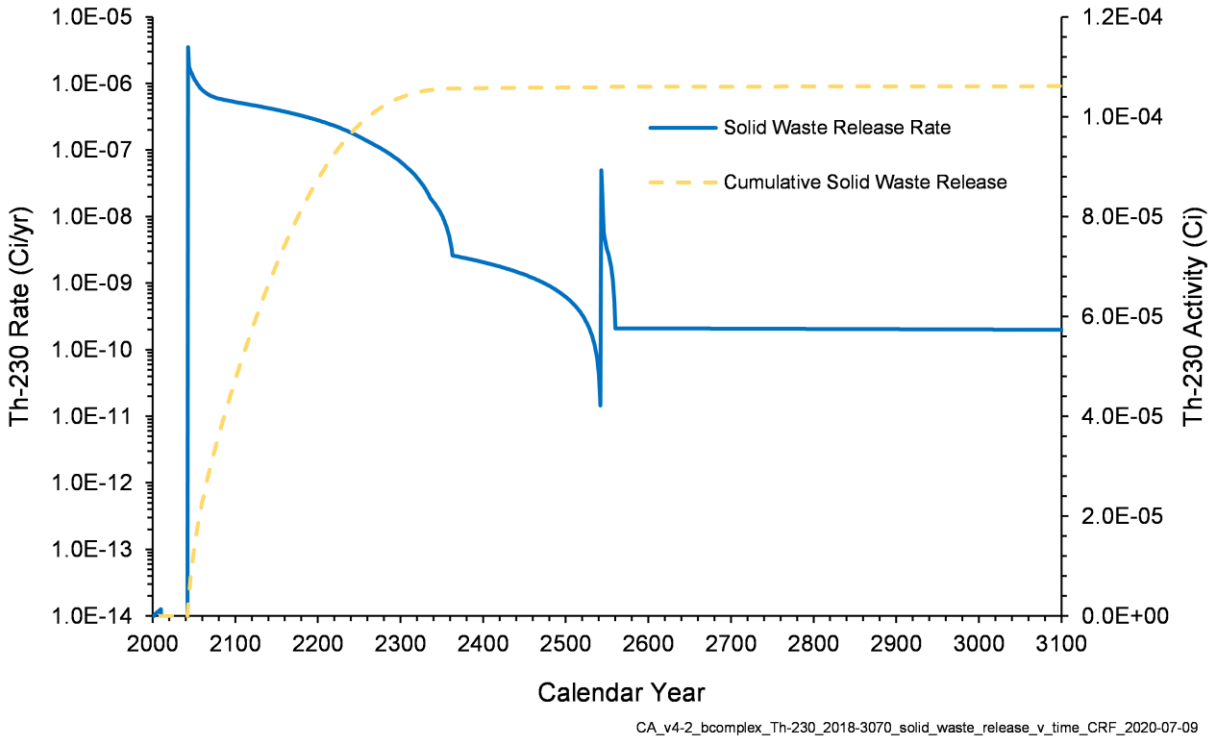

Figure 4-63. Th-230 Release Rate and Cumulative Activity from Solid Waste in the B Complex Model, 2018–3070

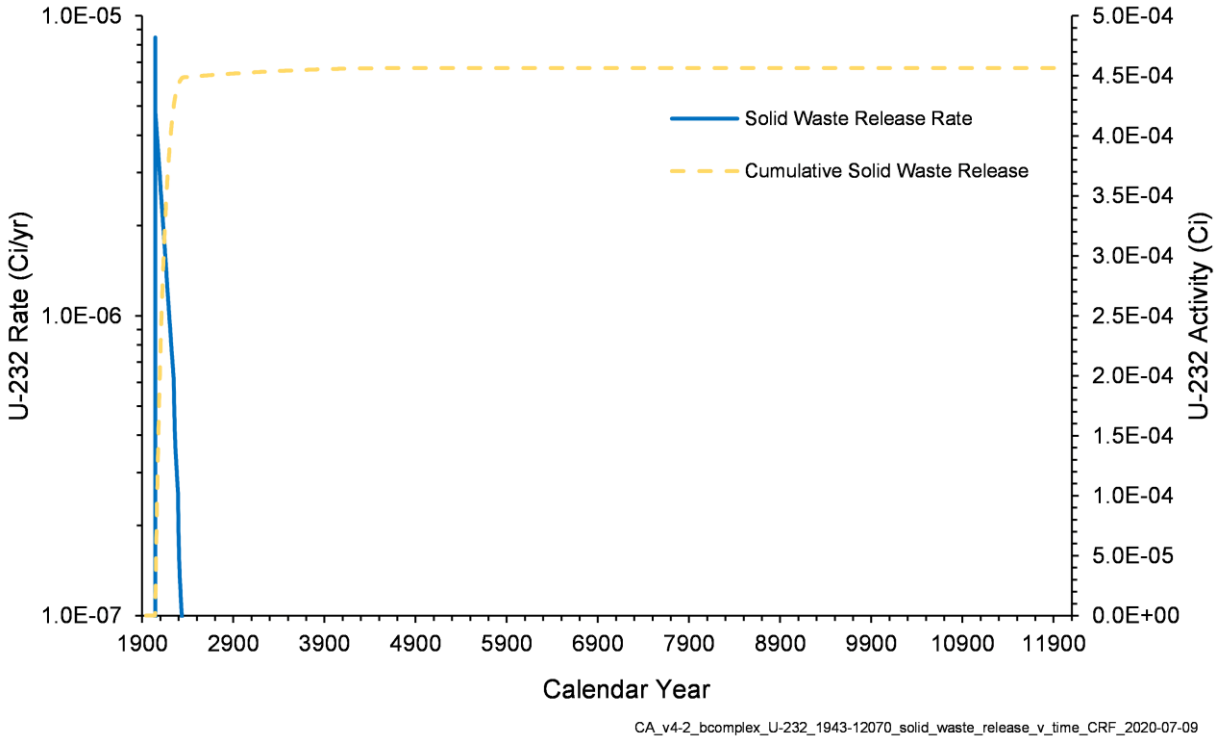

Figure 4-64. U-232 Release Rate and Cumulative Activity from Solid Waste in the B Complex Model, 1943–12070

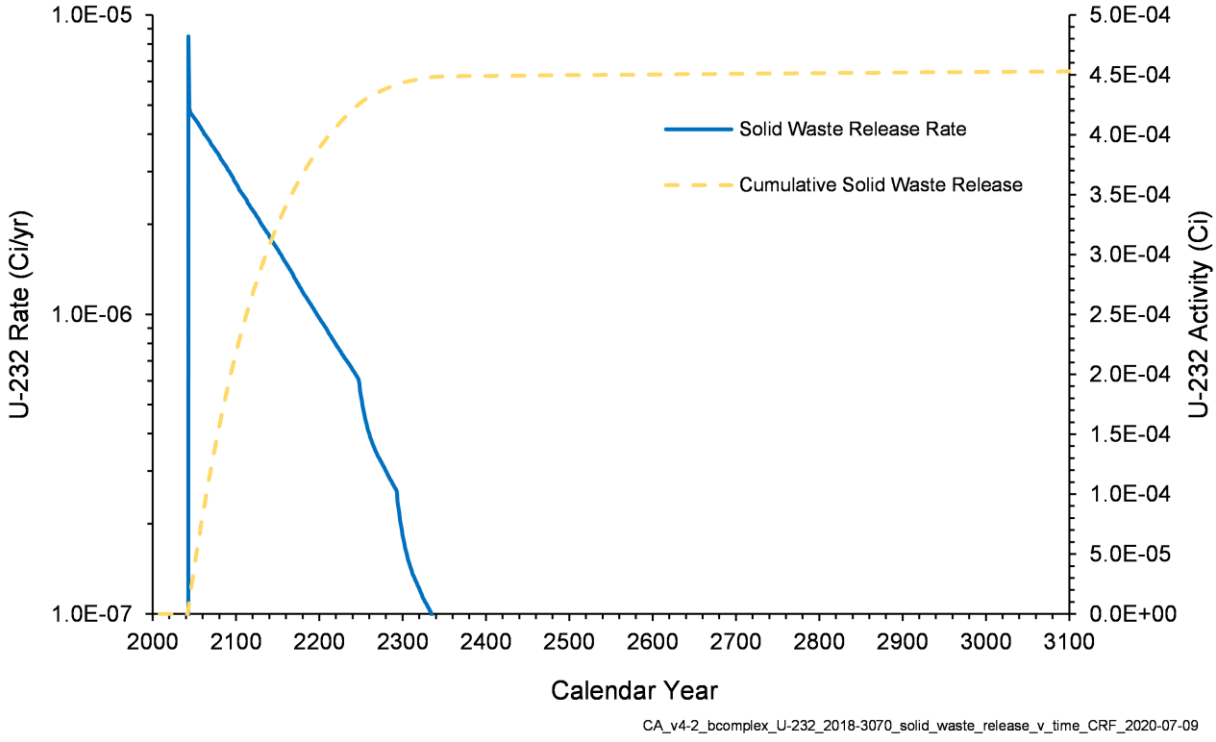

Figure 4-65. U-232 Release Rate and Cumulative Activity from Solid Waste in the B Complex Model, 2018–3070

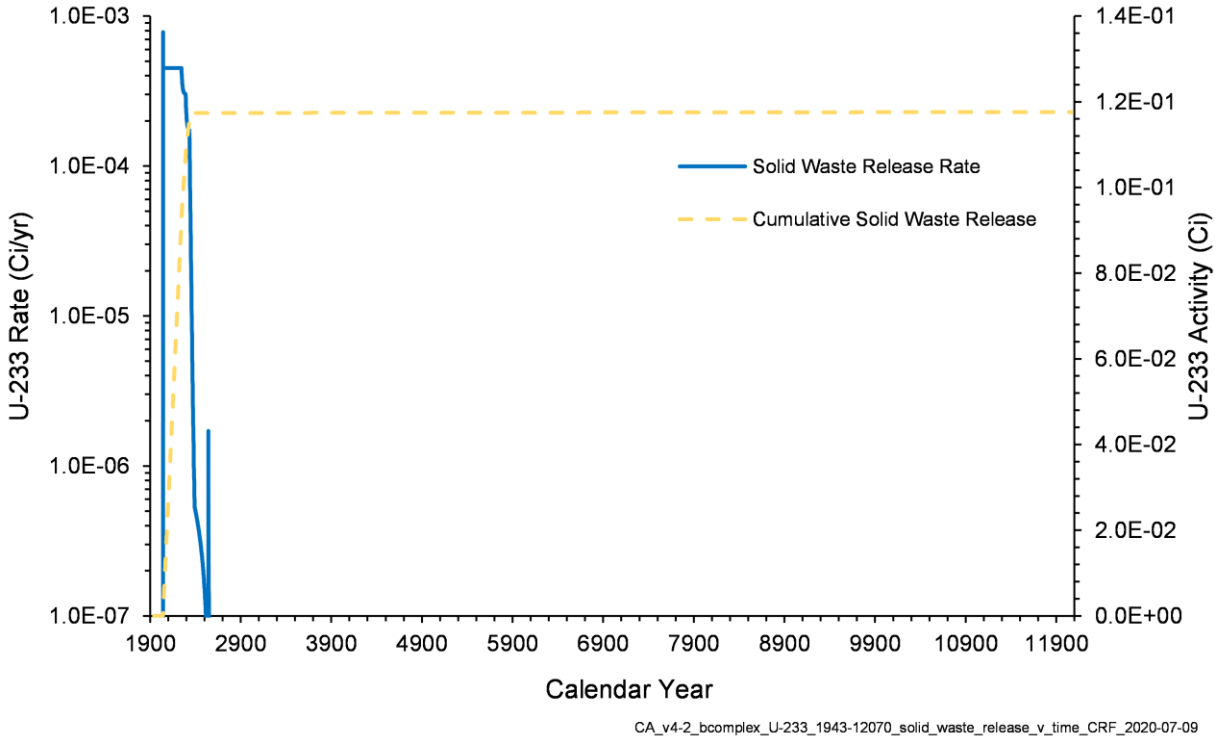

Figure 4-66. U-233 Release Rate and Cumulative Activity from Solid Waste in the B Complex Model, 1943–12070

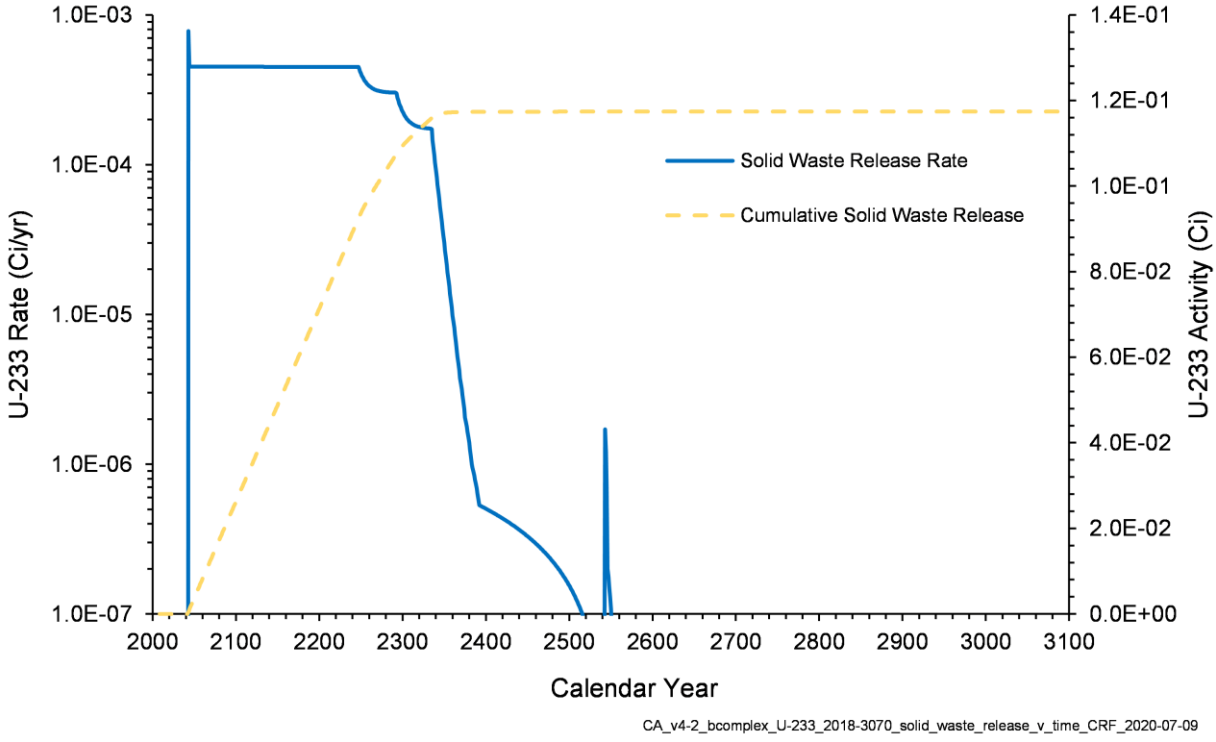

Figure 4-67. U-233 Release Rate and Cumulative Activity from Solid Waste in the B Complex Model, 2018–3070

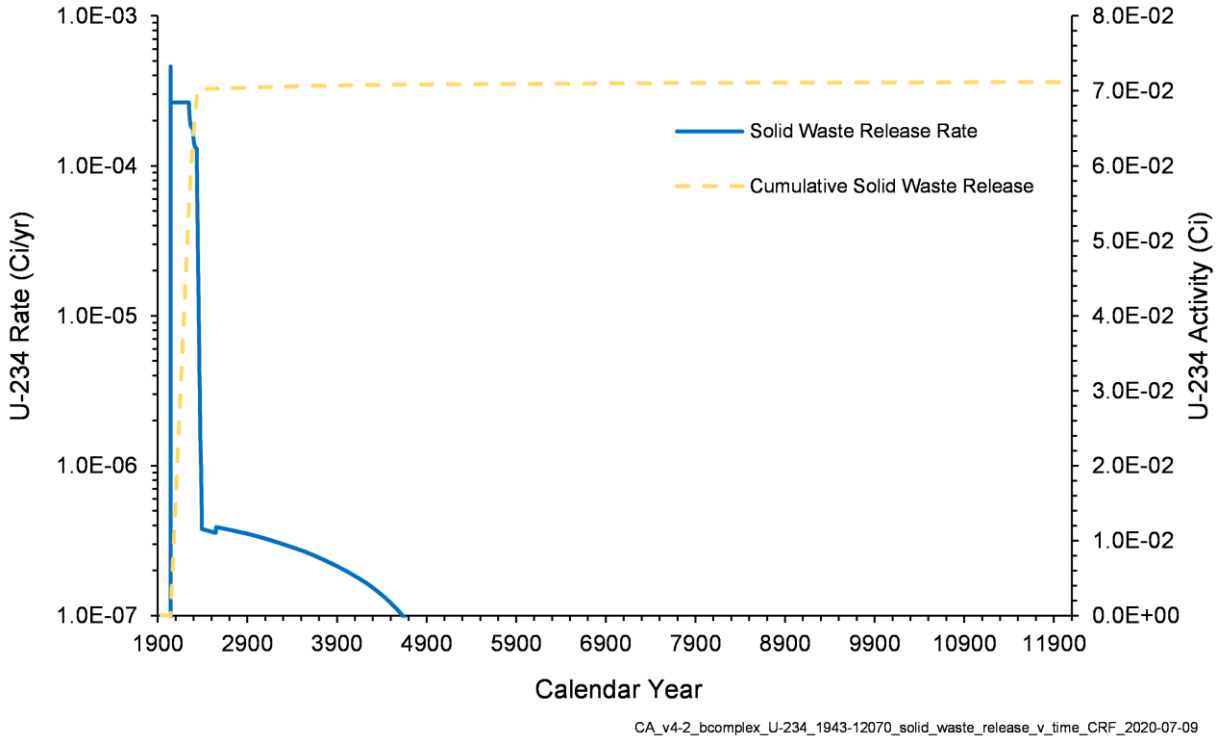

Figure 4-68. U-234 Release Rate and Cumulative Activity from Solid Waste in the B Complex Model, 1943–12070

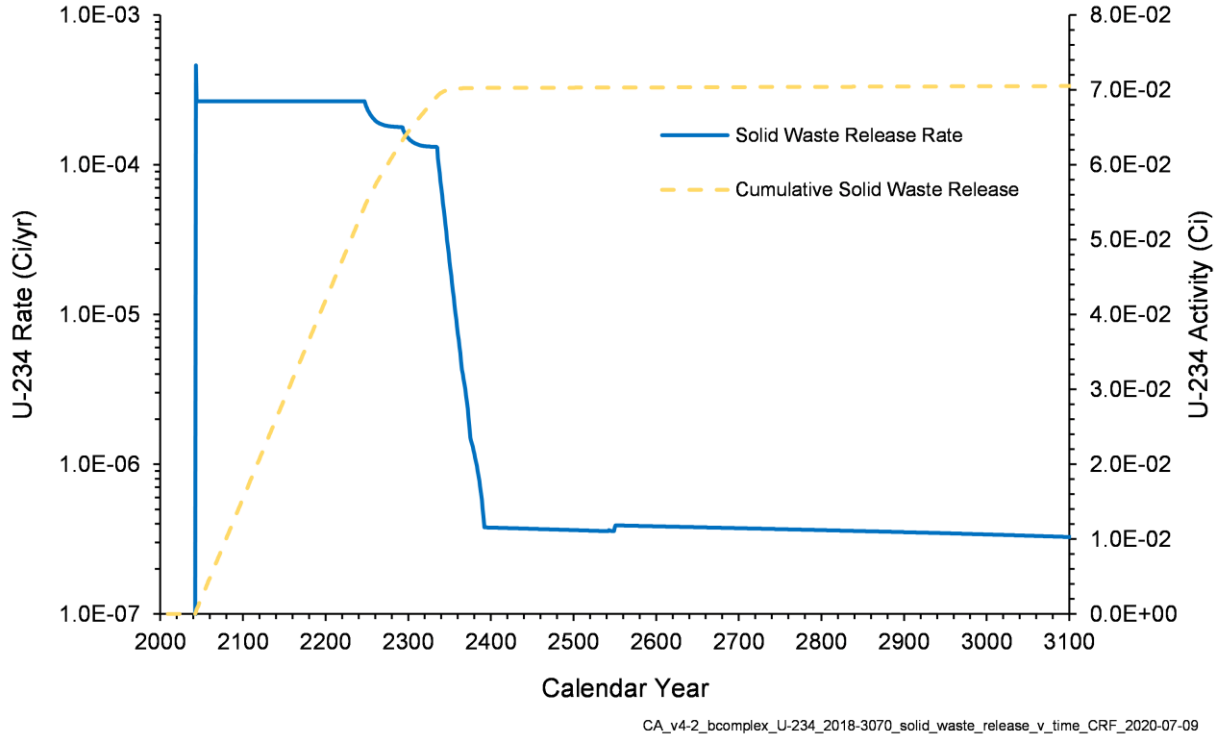

Figure 4-69. U-234 Release Rate and Cumulative Activity from Solid Waste in the B Complex Model, 2018–3070

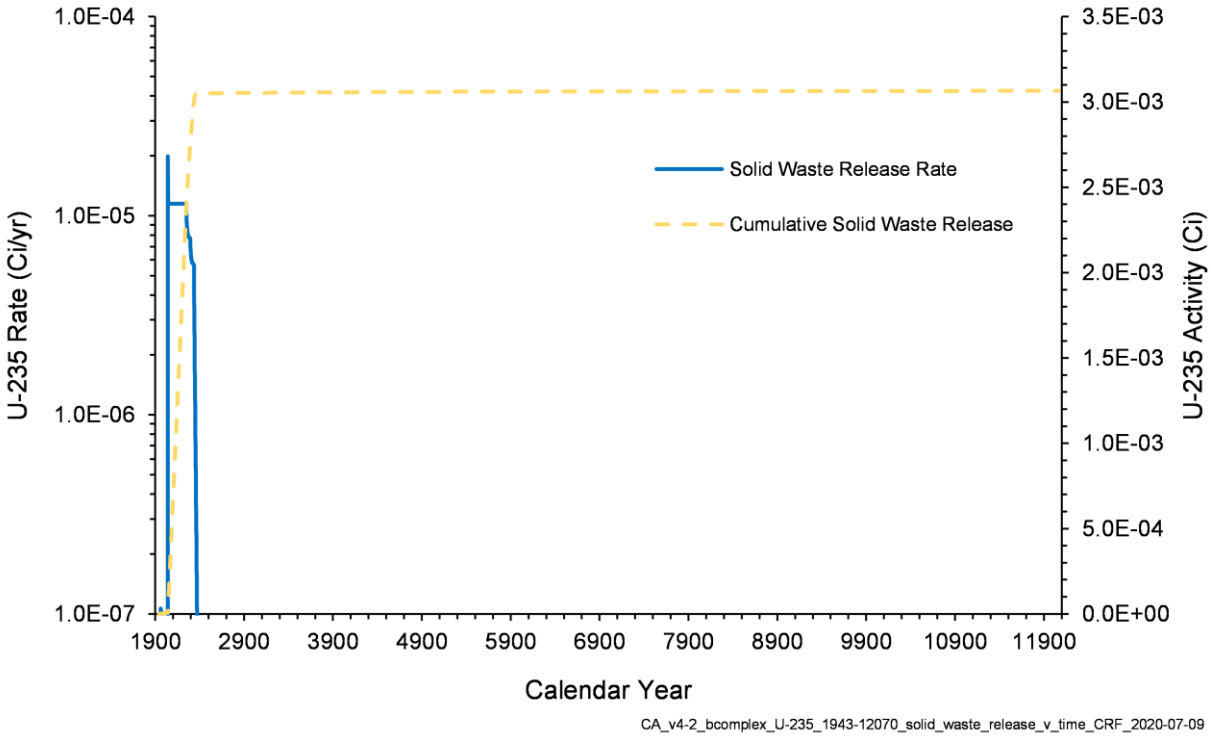

Figure 4-70. U-235 Release Rate and Cumulative Activity from Solid Waste in the B Complex Model, 1943–12070

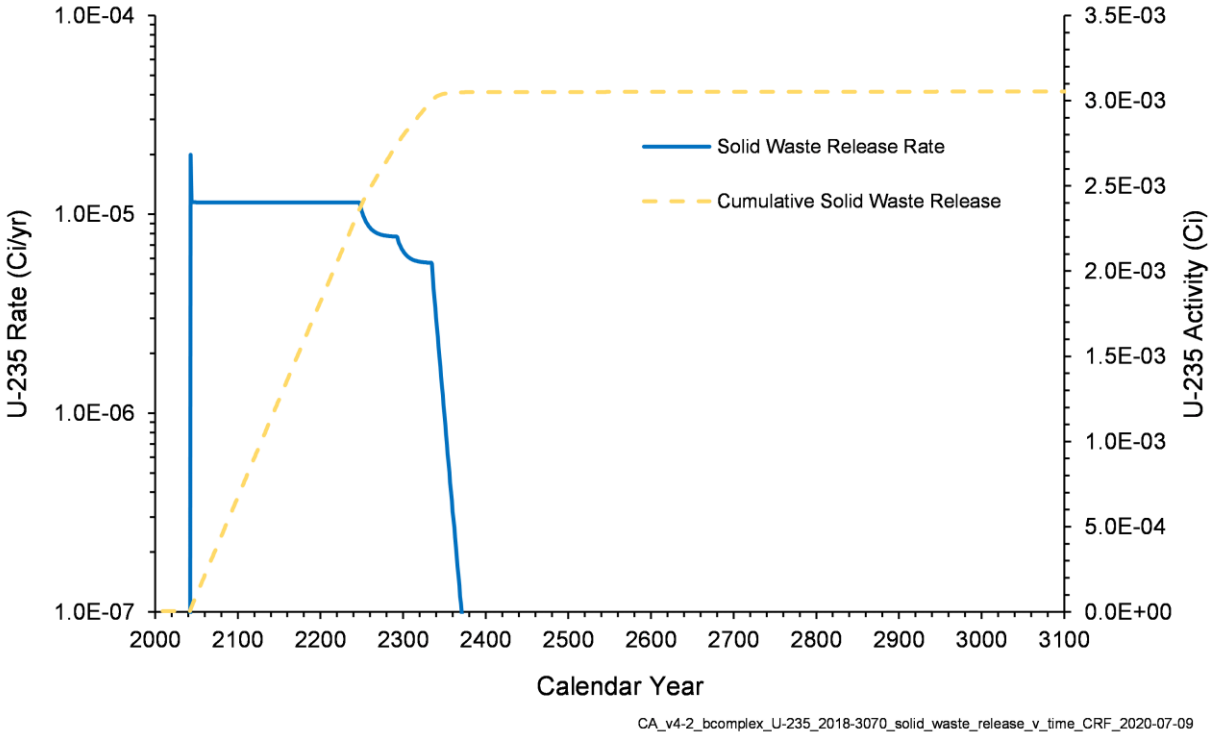

Figure 4-71. U-235 Release Rate and Cumulative Activity from Solid Waste in the B Complex Model, 2018–3070

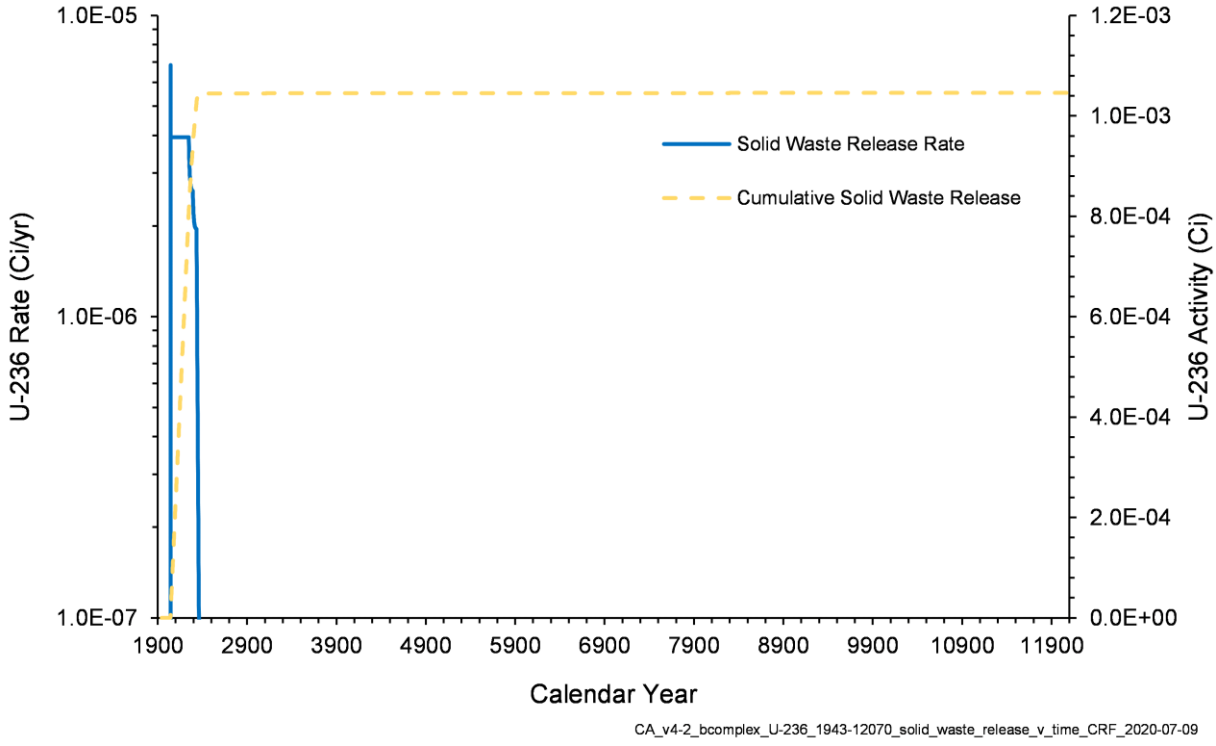

Figure 4-72. U-236 Release Rate and Cumulative Activity from Solid Waste in the B Complex Model, 1943–12070

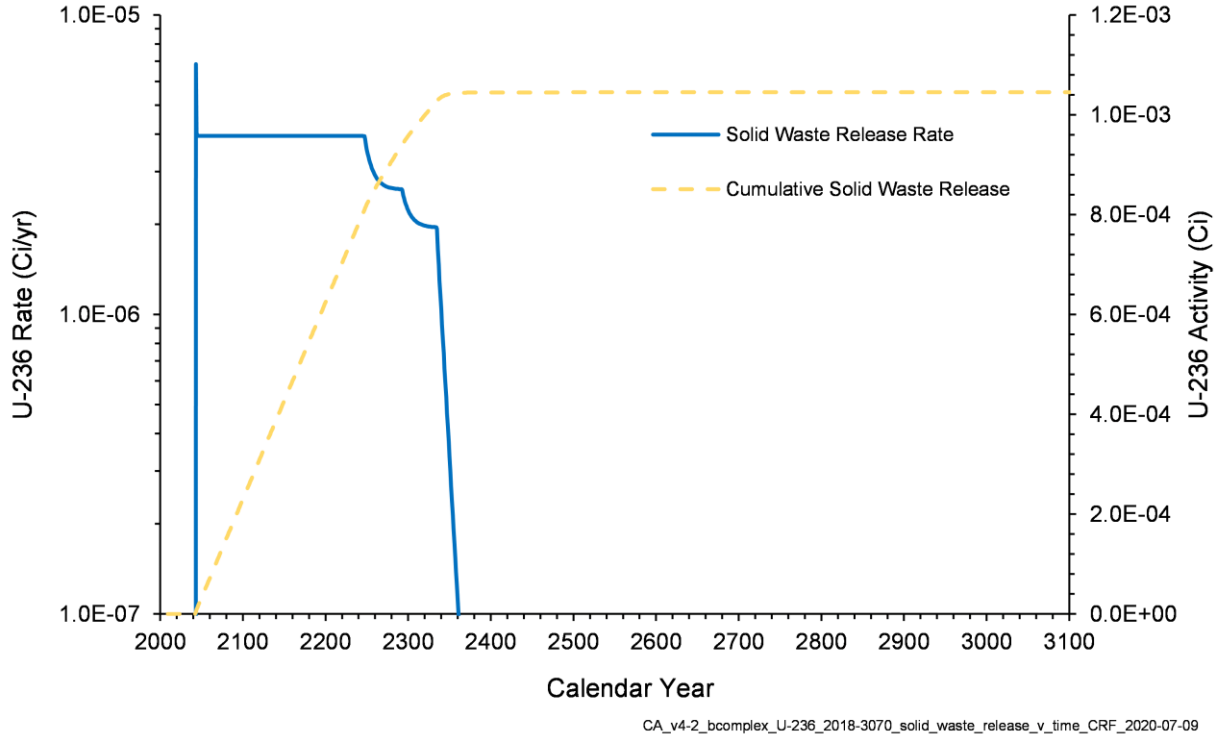

Figure 4-73. U-236 Release Rate and Cumulative Activity from Solid Waste in the B Complex Model, 2018–3070

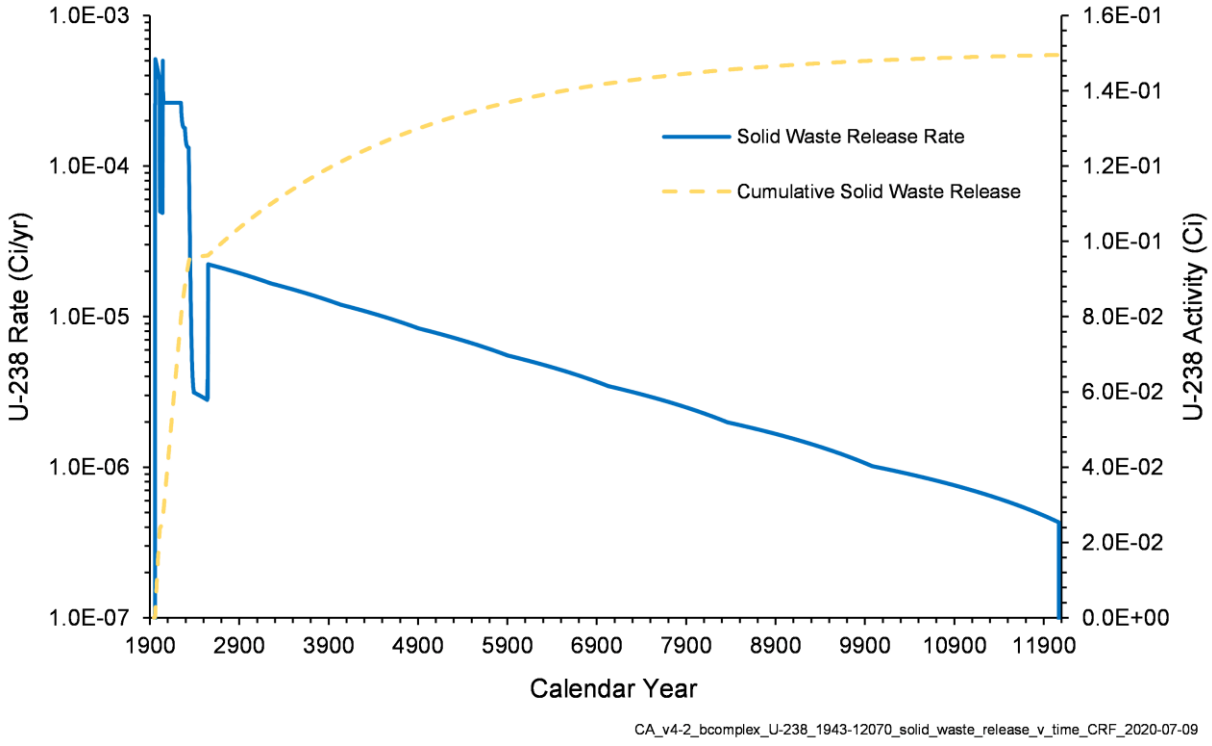

Figure 4-74. U-238 Release Rate and Cumulative Activity from Solid Waste in the B Complex Model, 1943–12070

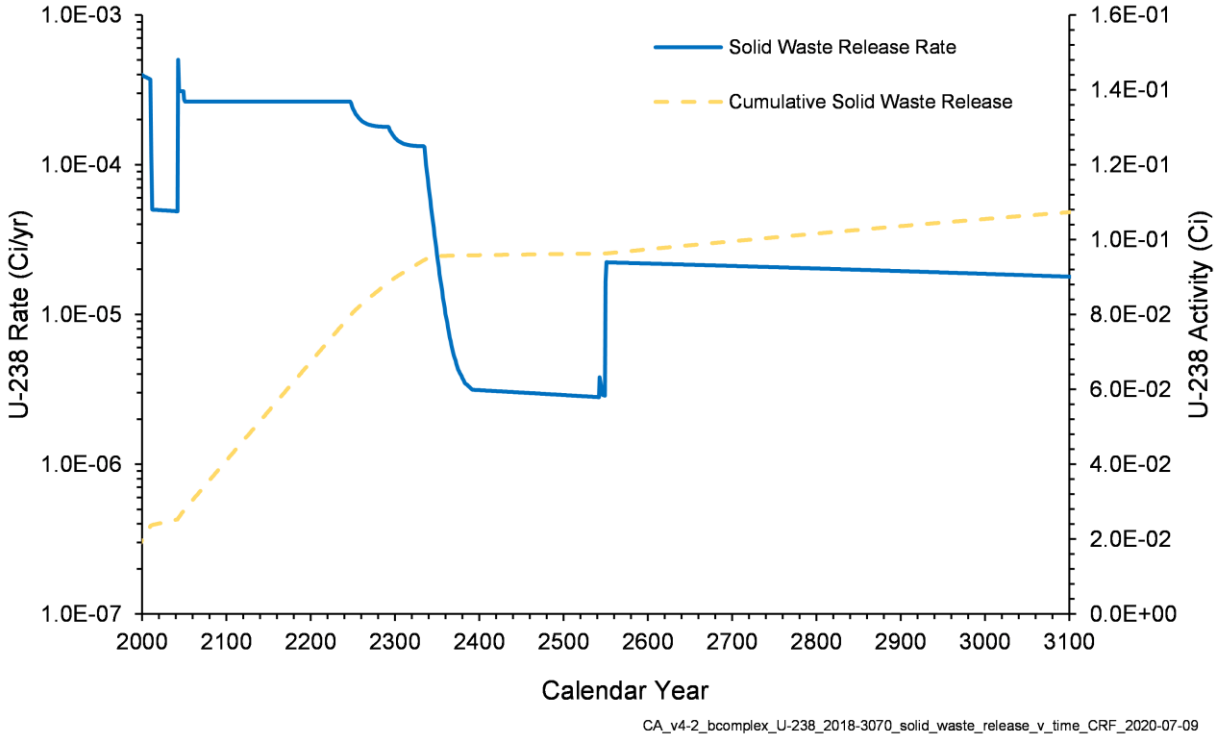

Figure 4-75. U-238 Release Rate and Cumulative Activity from Solid Waste in the B Complex Model, 2018–3070

4.5.2 Liquid (Volume) Releases

This section provides information on liquid volumes released within the domain of the B Complex model. These liquids can act as a driving force for the movement of radionuclides deeper into the subsurface. Table 4-4 shows an overview of the total liquids released in the model. Figure 4-76 shows the volume of water released within the model domain by waste site, and Figure 4-77 shows the total volume of water released by year.

Table 4-4. Released Liquid Volumes in the B Complex Model

Total	Source Zone	Buffer Zone
301,526	298,854	2,672

Note: all values reported in m^3

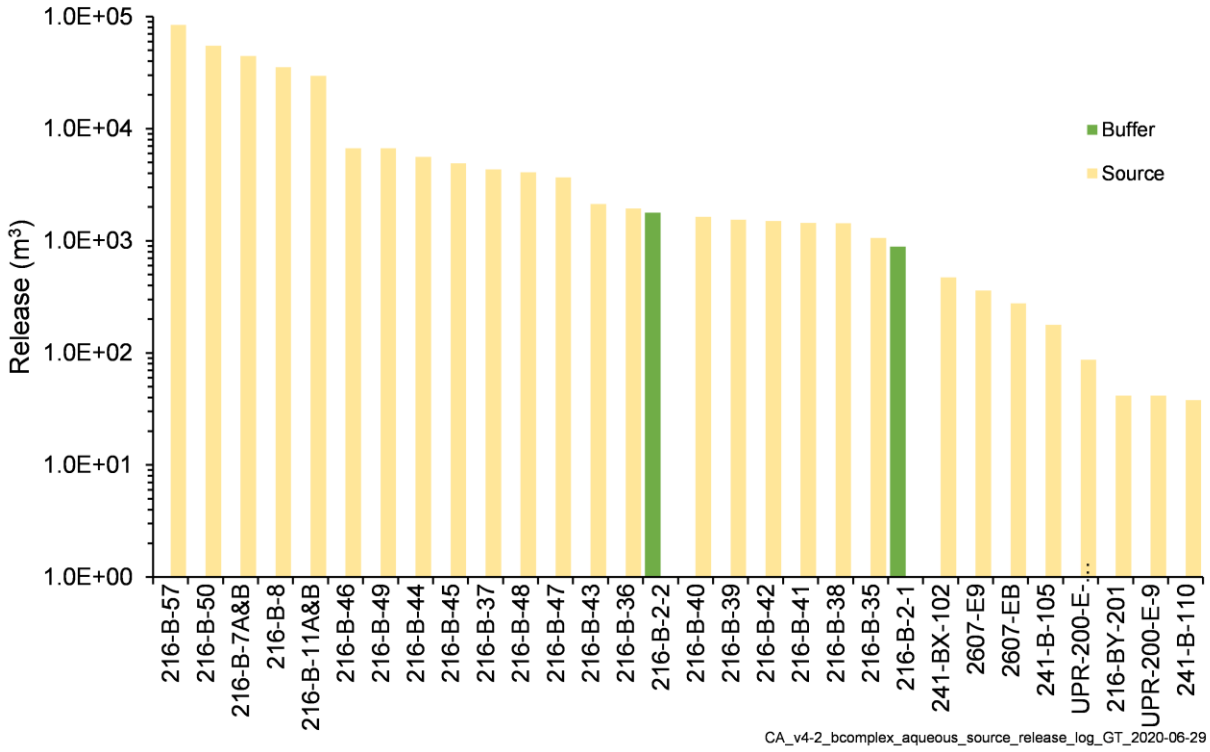

Figure 4-76. Total Volume of Water Released from Liquid Waste Sites in the B Complex Model

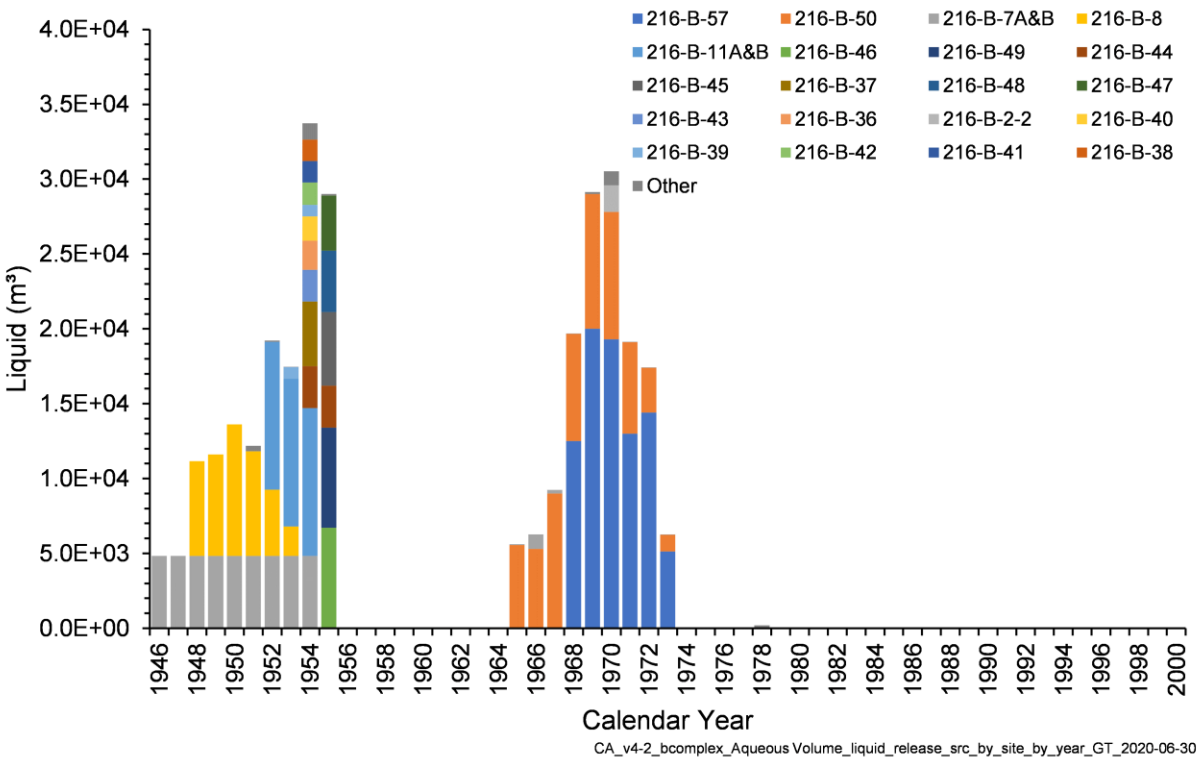

Figure 4-77. Total Volume of Water Released by Year from Liquid Waste Sites in the B Complex Model

4.5.2.1 Liquid Release Modifications

For some models, modifications to liquid release volumes were needed to help with convergence of the numerical solution or to provide for more representative transport through the vadose zone.

Model Convergence Resolution

This model required that the water at 216-B-7A&B and 216-B-11A&B be averaged so the numerical solution of the model governing equation may converge. For each waste site, the water discharged over a specified time period was summed, averaged, and evenly dispersed throughout the same time period, or if needed, an extended time period. The time period over which the discharge was averaged for each waste site is shown in Table 4-5. Liquid discharged from 216-B-7A&B was averaged from 1946 to 1954 and evenly distributed, and liquid discharged from 216-B-11A&B was averaged from 1952 to 1954 and evenly distributed.

Table 4-5. Liquid Release Modifications for the B Complex Model

Site Name	Model Zone	Original Start Year	Original End Year	Modified Start Year	Modified End Year	Averaged Release Rate (m^3/yr)
216-B-7A&B	Source	1946	1954	1946	1954	4,830
216-B-11A&B	Source	1952	1954	1952	1954	9,874

4.6 Simulations

Three different types of simulations were performed. Constant recharge conditions were used in a flow-only simulation to set the initial aqueous pressure conditions in the model. A mass balance simulation was conducted to evaluate model performance, and transport simulations were performed to estimate radionuclide activity entering the saturated zone. These are discussed in the following sections.

4.6.1 Flow-Only (Steady-State) Simulation

The flow-only simulation was performed using recharge estimated for 1943, which was prior to the start of Hanford Site operations. This was a transient simulation, but it is referred to hereinafter as the steady-state simulation because recharge was held constant at the 1943 values and the simulation was run for 10,000 years to ensure steady-state conditions were achieved within the model domain. The results were used as the initial aqueous pressure conditions for the radionuclide transport simulations starting in 1943.

4.6.2 Mass/Activity Balance Simulation

A mass/activity balance simulation was conducted to evaluate model performance. This simulation was run for 10,000 years using the source releases described in Section 4.5 and the initial aqueous pressure conditions from the steady-state simulation, but radionuclide half-lives were set to 1.0E+20 years to eliminate radiological decay and allow for the mass/activity balance to be evaluated directly. The mass/activity of each constituent leaving the model over 10,000 years and the mass/activity present in the model at the end of the simulation were summed, and the results were compared to the mass/activity released from the sources.

4.6.3 Transport Simulations

Transport simulations were performed to estimate the radionuclide activity entering the saturated zone. These were done in stages. The time period for the CA evaluation is 2018 to 12070. To set the initial radionuclide concentrations in the model domain for simulations of that time period (i.e., forecast period), a historical simulation of radionuclide releases was performed from 1943 up to but not including 2018. The radionuclide distribution in the model domain at the end of this simulation became the starting concentrations for the forecast runs.

The forecast simulations were performed for 2018 to 12070. The forecast simulation was performed in two stages because this model contains a waste site with a disposition of RTD. This waste site is scheduled to be excavated to a pre-determined depth and the removed contaminated soil will be transported to an appropriate disposal facility (CP-63386, *Hanford Site Disposition Baseline for Composite Analysis*). The excavated area will then be filled with clean soil. This process was simulated in the forecast runs by stopping model execution at the year excavation is scheduled, setting the model domain concentrations from the waste site to the RTD depth to zero, and restarting the model at that year. A map of the RTD site is shown in Figure 4-78. The RTD site, the planned RTD year, the modeled RTD year, and the excavated depth are shown in Table 4-6.

Table 4-6. RTD Site Information for the B Complex Model

RTD Site Name	Excavated Depth (ft)	Planned RTD Year	Simulated RTD Year
216-B-51	15	2024	2024

RTD = remove, treat, dispose

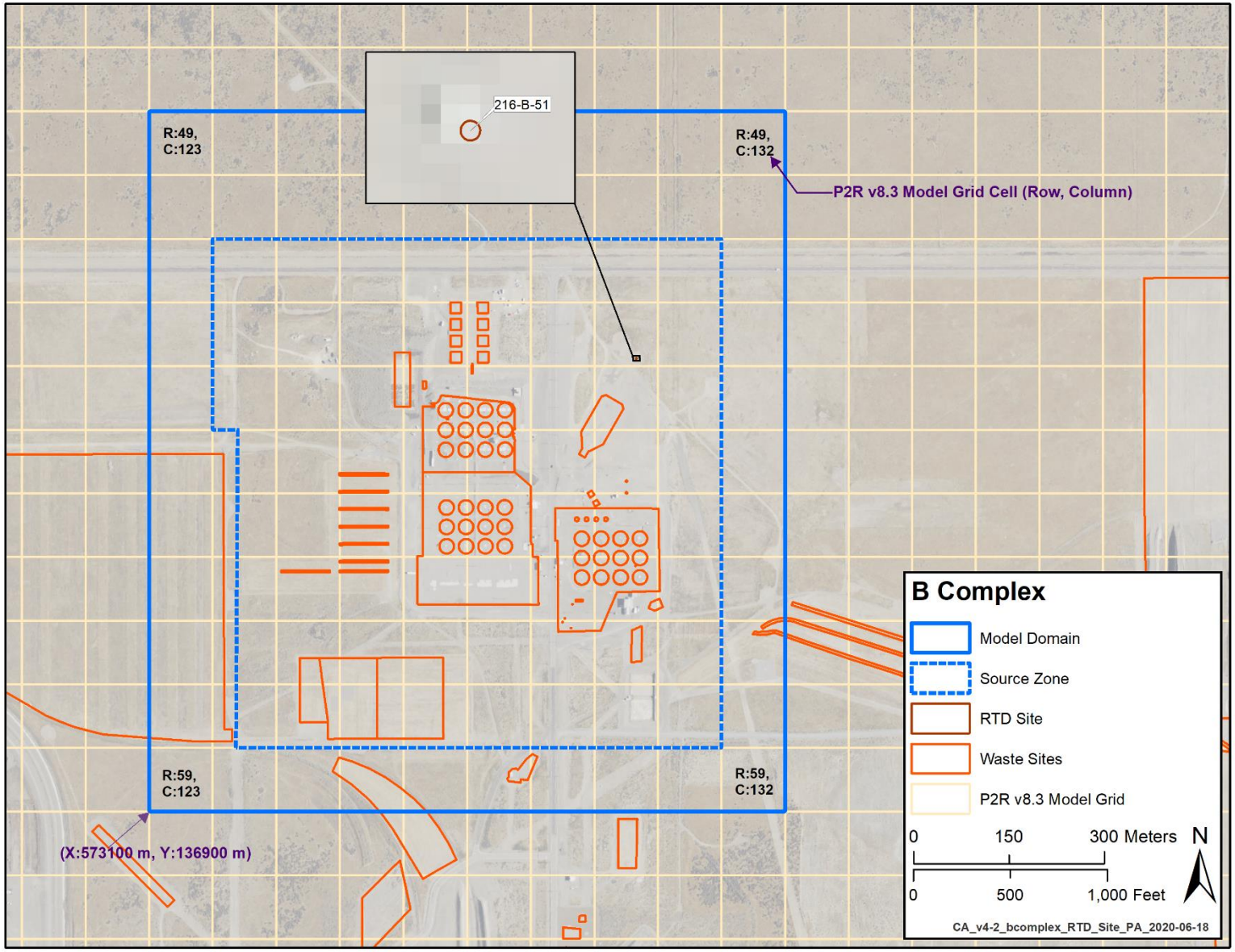

Figure 4-78. Map of the RTD Sites in the B Complex Model

4.7 Initial Conditions

The simulations performed for the B Complex model require that initial aqueous pressure conditions and radionuclide concentrations in the model domain be specified, depending on the simulation. Initial aqueous pressure conditions for the steady-state, flow-only simulation are based on hydrostatic conditions assuming that the base of the model is at the water table. This is input to STOMP as an aqueous pressure of 101,325 Pa at the water table and a z-direction gradient of -9,793.52 Pa/m.

For the historical transient simulations (i.e., 1943 to 2018), initial aqueous pressure conditions are the steady-state conditions taken from the end of the steady-state simulation. Since the purpose of the historical simulations was to define the starting radionuclide concentrations and aqueous pressure conditions for the forecast runs by simulating source release during the entirety of Hanford Site operations, the initial radionuclide concentrations were zero.

Aqueous pressure conditions and radionuclide concentration results of the historical simulation were used as the initial conditions for the forecast simulations. This model contains an RTD site, so model execution was stopped at the year designated for the RTD action as indicated by Table 4-6. The resulting aqueous pressure conditions became the starting conditions when execution of the model was resumed from the RTD year. The resulting radionuclide concentrations became the starting conditions when model execution was resumed, except that concentrations were set to zero where RTD had occurred.

4.8 Boundary Conditions

Boundary conditions for the B Complex model include recharge to the top of the model, water table conditions at the base of the model, and no-flow conditions along the sides of the model. The boundary conditions are described in further detail in the rest of this section.

4.8.1 Natural Recharge – Top Boundary Condition

Model recharge was estimated using the RET (ECF-HANFORD-15-0019). The RET assigns soil infiltration rates for the CA vadose zone models based on land use, surface cover information from multiple sources (including existing buildings and structures, waste site footprints, and natural vegetative cover), and soil survey information. Planned future actions for waste site closure are used to develop future recharge estimates through the end of the modeling period. The RET generates spatial representations of recharge estimates for each year from 1943 until recharge reaches a final post-closure condition. These yearly recharge estimates for the model domain are then post-processed to generate the STOMP boundary condition input. The steady-state simulation uses the 1943 RET recharge values for the entire simulation under the assumption that the 1943 recharge is representative of pre-Hanford Site conditions. Recharge rates from every output year from the RET are used as the transient boundary conditions.

Natural recharge within the model domain is spatially variable. Figures of the spatial distribution of RET recharge estimates for the B Complex model are shown for every year there is a change in any recharge estimate in Appendix C. Figure 4-79 to Figure 4-86 show the RET recharge estimates for the B Complex model for 1943, 1948, 1978, 1994, 2031, 2043, 2050 and 2550. The pre-Hanford Site recharge rate distribution is determined by the soil types Ephrata Sandy Loam and Rupert Sand covered with mature shrub-steppe plant communities (Figure 4-79). The recharge rates for these soils with mature vegetation are 1.5 and 4.0 mm/yr, respectively. The model area is mostly covered by Ephrata Sandy Loam, with an area of Rupert Sand in the southeast of the model. As shown in Figure 4-8 and Figure 4-9, numerous waste sites, tank farms, and associated buildings were constructed after 1943, resulting in highly variable

recharge rates over time. Construction, including excavation, caused surface disturbances resulting in increased recharge rates. The construction activities for the three tanks farms (241-B, 241-BX, and 241-BY), including emplacement of gravel, caused infiltration rates to increase to 100 mm/yr starting in 1948 (Figure 4-80). The maximum average recharge rate for the model domain is obtained in 1978 (Figure 4-81) with estimated recharge rates of 100 mm/yr for the tank farms with disturbed gravel surfaces, and 63 mm/yr for other waste sites with major disturbances. The considerable activity during the operations period left only a few areas undisturbed.

In 1994, the Hanford Prototype Barrier became operational at the location of the previous 216-B-57 waste site, just west of the 216-BY Cribs. The reduction in recharge rate to 0.5 mm/yr for this barrier, with a design life of 500 years, is shown in Figure 4-82. A series of interim barriers and evaporation covers are planned for parts of the three tanks farms, with emplacement complete by 2031 (Figure 4-83). The interim barriers will be replaced by larger barriers in 2043 (Figure 4-84). In addition to the tank farms, the construction of multiple surface barriers, with an assumed recharge rate of 0.5 mm/yr, is planned to cover several other waste sites. For this model, these remediation activities are planned to be completed by 2050, affecting large surface areas (Figure 4-85). Post remediation, the surface barriers are assumed to have a design life of 500 years, after which the affected areas return to natural conditions with an assigned recharge rate of 4.0 mm/yr (Figure 4-86).

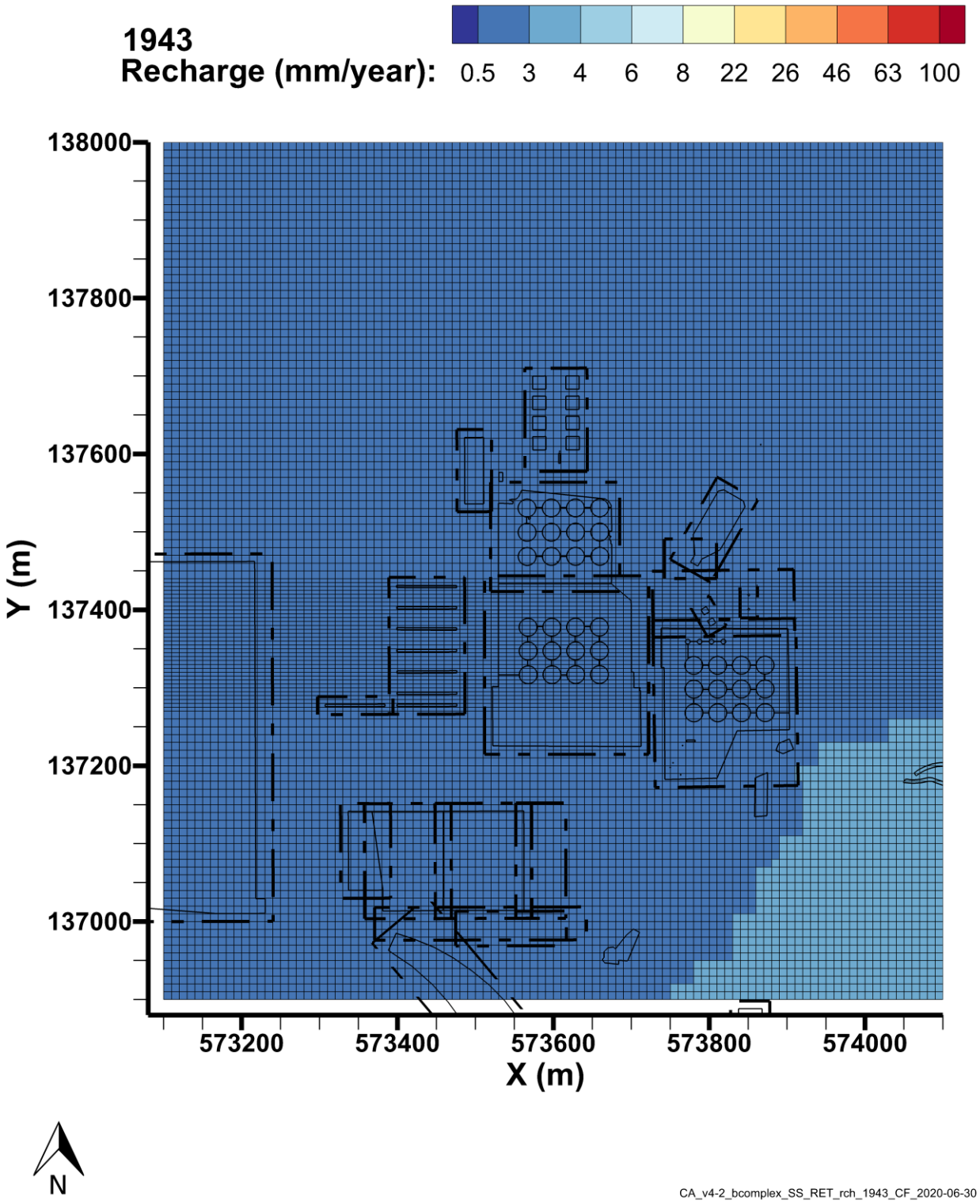

Figure 4-79. Transient Recharge Estimates for the B Complex Model, 1943

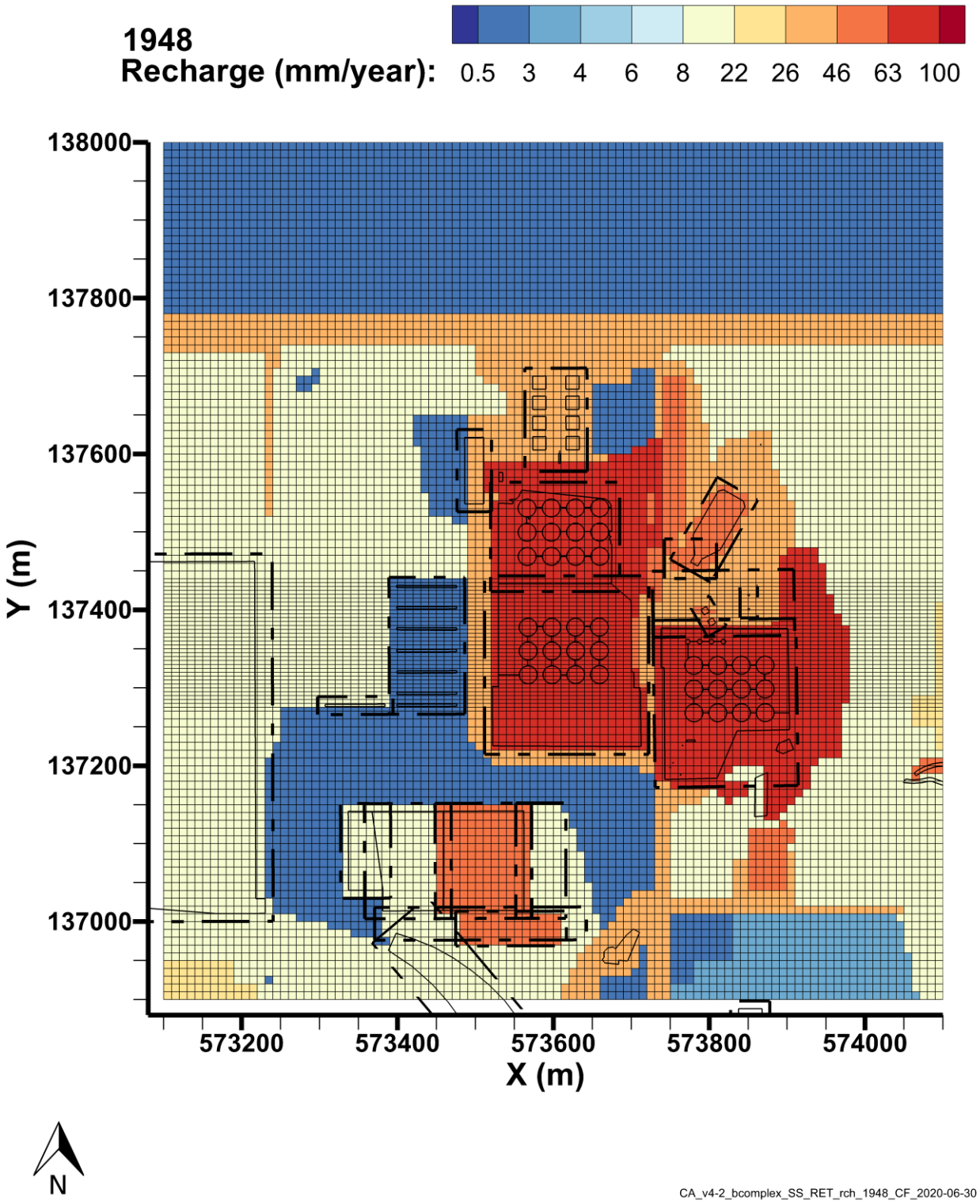

Figure 4-80. Transient Recharge Estimates for the B Complex Model, 1948

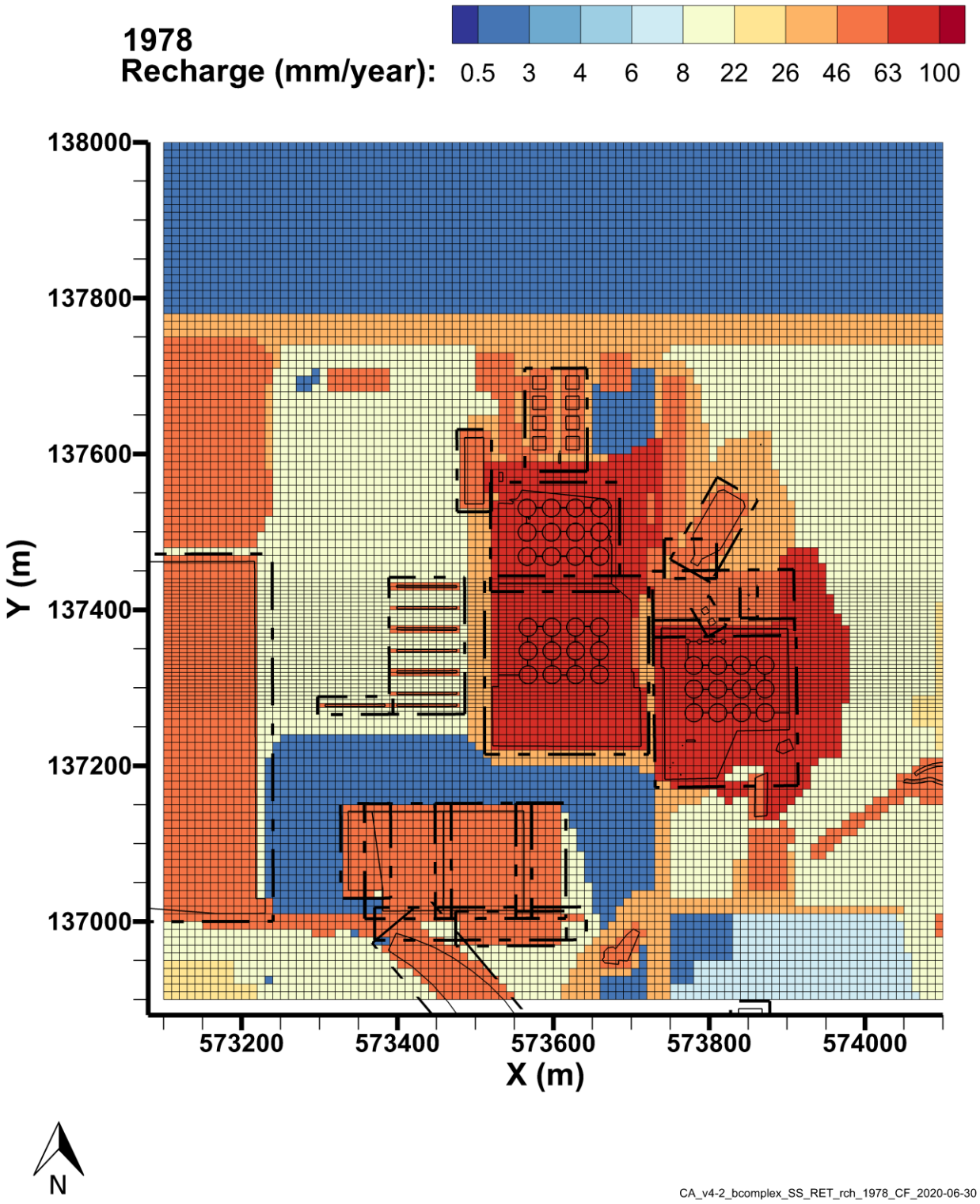

Figure 4-81. Transient Recharge Estimates for the B Complex Model, 1978

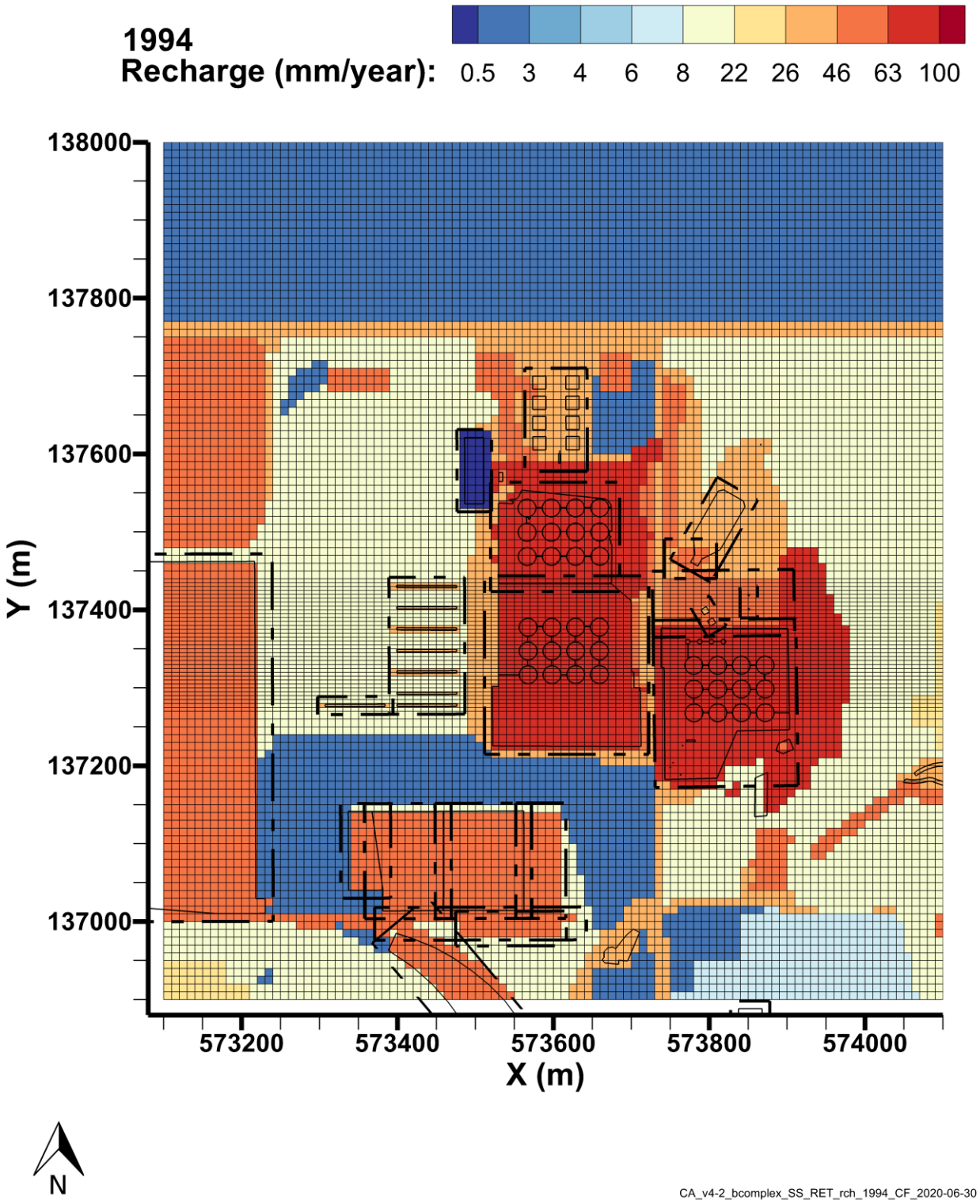

Figure 4-82. Transient Recharge Estimates for the B Complex Model, 1994

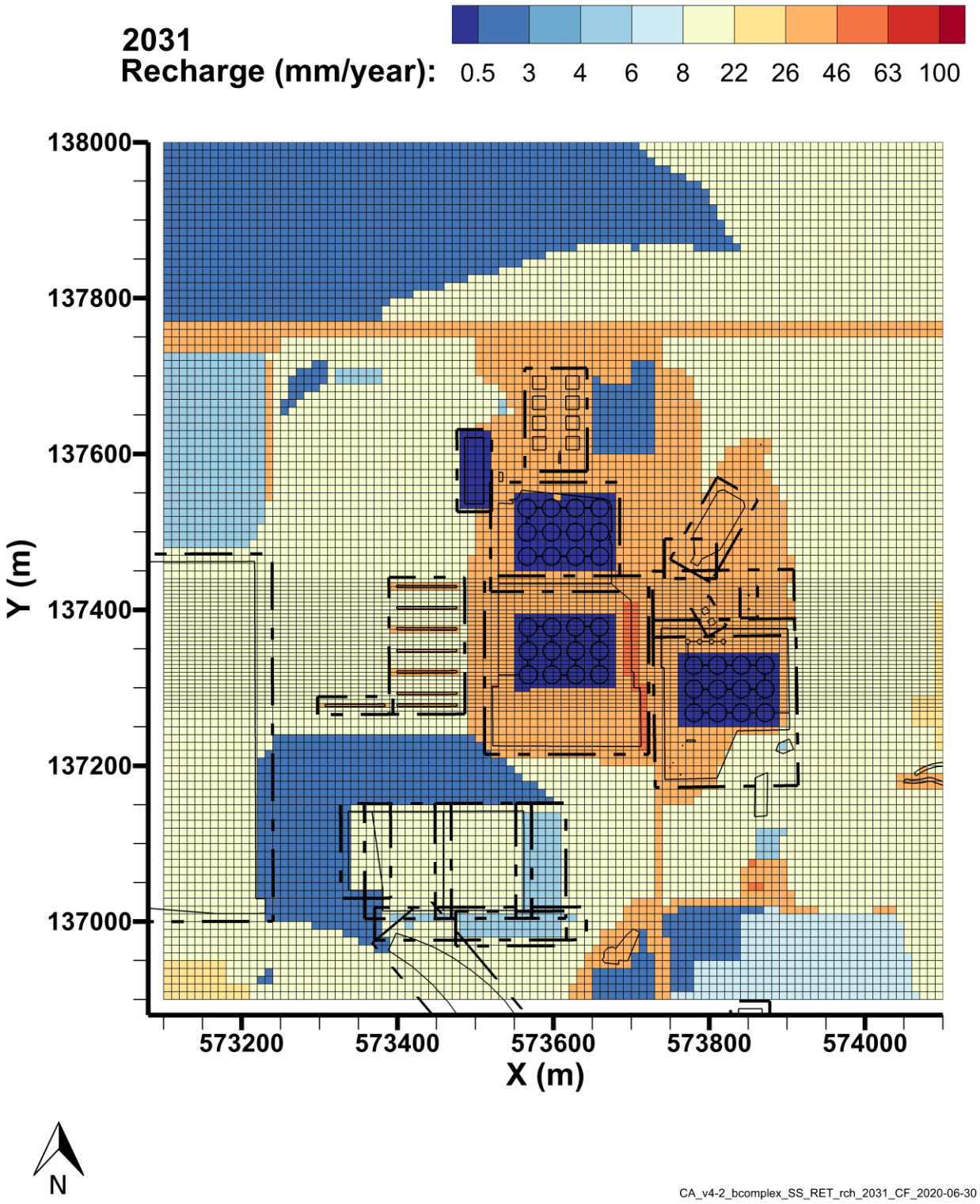

Figure 4-83. Transient Recharge Estimates for the B Complex Model, 2031

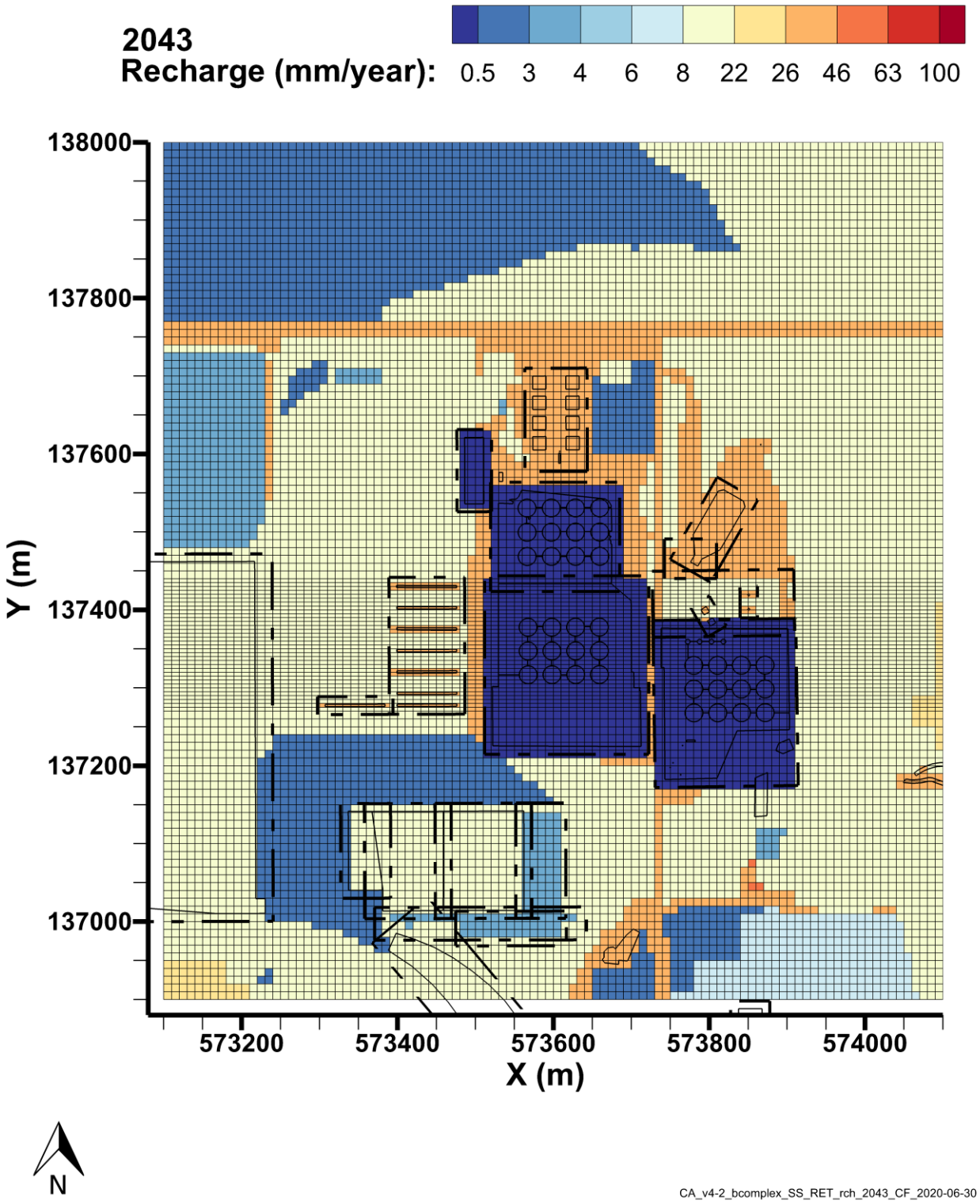

Figure 4-84. Transient Recharge Estimates for the B Complex Model, 2043

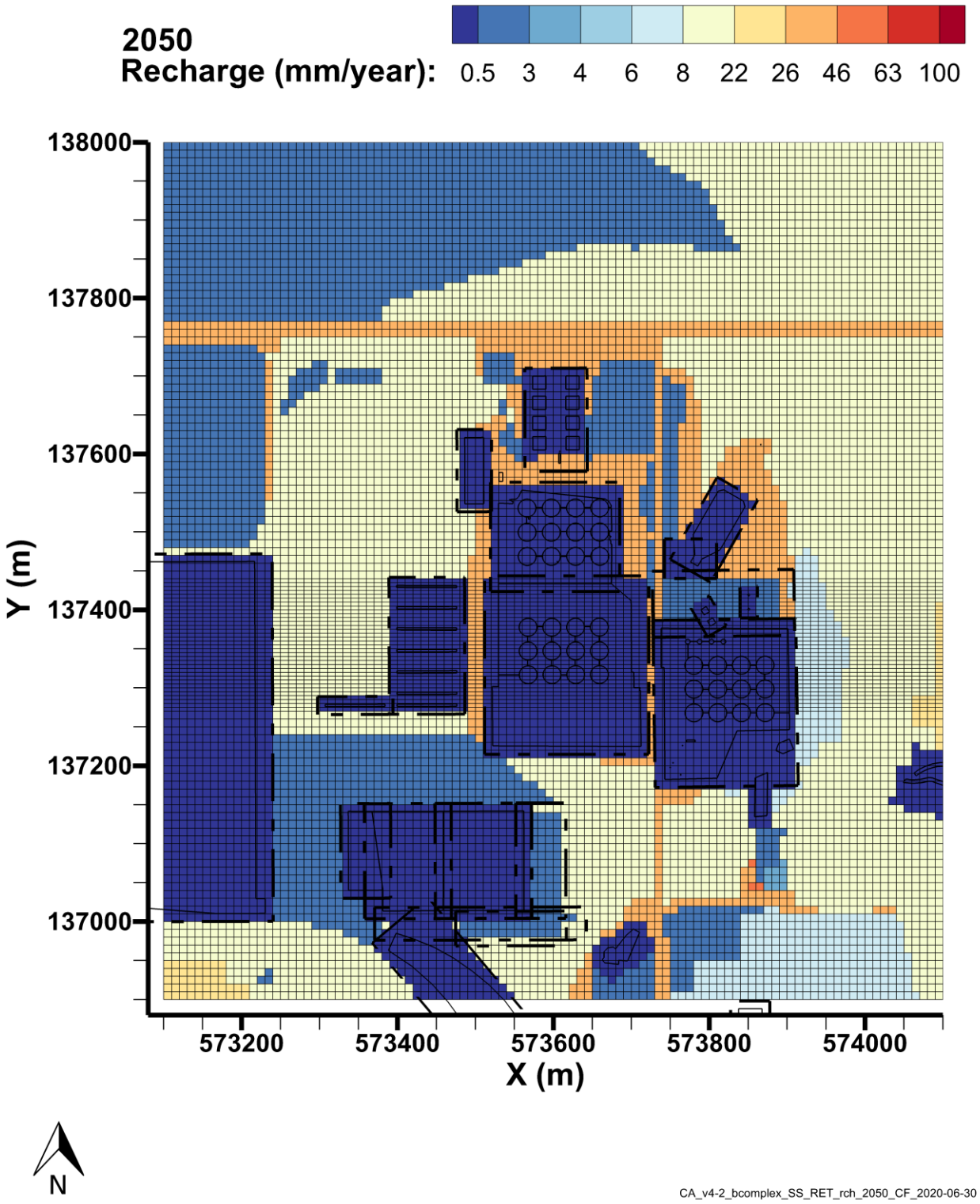

Figure 4-85. Transient Recharge Estimates for the B Complex Model, 2050

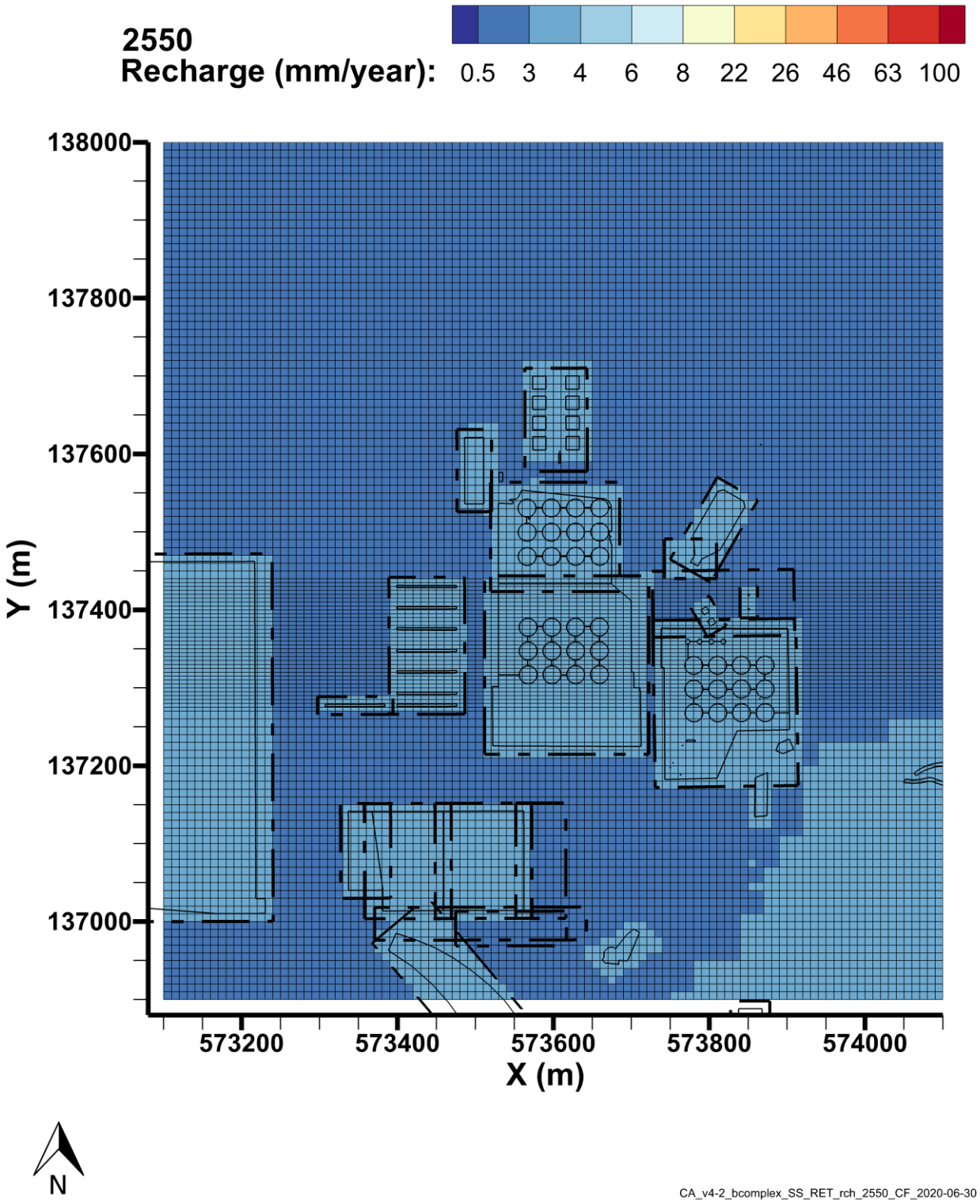

Figure 4-86. Transient Recharge Estimates for the B Complex Model, 2550

Example time series charts of natural recharge rates for selected locations within the model domain (locations shown in Figure 4-87) are shown in Figure 4-88 through Figure 4-96. Several of the locations on Figure 4-87 represent non-tank farm waste sites (location C, 216-B-57, Figure 4-90; location D,

216-B-49, Figure 4-91; location G, 216-B-7A&B, Figure 4-94; location I, 216-B-8, Figure 4-96). The pre-Hanford Site recharge rates at these sites of either 4.0 and 1.5 mm/yr are determined by the soil types Rupert Sand or Ephrata Sandy Loam, respectively, covered with mature shrub-steppe plant communities. After 1943, an initial increase in recharge occurred depending on the activities that took place within the waste site boundary. At all the selected waste site locations, a disposition of "disturbed sand" due to excavation activities and other disturbances is reached at some time, with an assigned recharge rate of 63 mm/yr. This value is consistent with rates measured in unvegetated sands (Table 4.15 in PNNL-14702, *Vadose Zone Hydrogeology Data Package for Hanford Assessments*). Before reaching a value of 63 mm/yr, some of the waste sites (e.g., location C, 216-B-57, Figure 4-90) are affected by adjacent disturbances, with an assigned recharge rate of 46 mm/yr. After the period with the 63 mm/yr recharge rate, some of the waste sites go through a phase of partial revegetation (cheatgrass over gravel), with an assigned recharge rate of 46 mm/yr. Location D (216-B-49, Figure 4-91) is an example of a site with partial revegetation after site operations. At the end of the remediation period, barriers will be installed with an assumed rate of 0.5 mm/yr for an expected design life of 500 years. After the expected design life, a final estimated recharge rate of 4.0 mm/yr is assumed.

Three of the locations on Figure 4-87 are tank farms (location E, 241-BY, Figure 4-91; location F, 241-BX, Figure 4-93; location H, 241-B, Figure 4-95). After construction of the tank farms and prior to installation of surface infiltration barriers, the recharge rate is assumed to be 100 mm/yr. Before reaching this value, some of the tank farms (e.g., location E, 241-BY, Figure 4-92) are affected by adjacent disturbances or excavations, with an assigned recharge rate of 46 mm/yr. After the high recharge rate period, all tank farm surfaces go through a phase of partial revegetation (cheatgrass over gravel), with an assigned recharge rate of 46 mm/yr. All three locations will be covered by an interim barrier with a recharge rate of 0.0 mm/yr until emplacement of the final barriers at 2043. At the end of the remediation period, barriers will be emplaced on the three locations with an assumed rate of 0.5 mm/yr for an expected design life of 500 years. After the expected design life, a final estimated recharge rate of 4.0 mm/yr is assumed.

Locations A (Figure 4-88) and B (Figure 4-89) are not located on a waste site or tank farm. The recharge rate during the operation period for both locations initially increased to 8.5 mm/yr due to the appearance of a cheatgrass cover on Ephrata Sandy Loam. For location A, a revegetation cycle with a linear rate decrease over 30 years down to 1.5 mm/yr is imposed in 2070. There is no infiltration barrier emplaced at this location and the 1.5 mm/yr rate was therefore used until 12070. Location B, just south of the 216-B-38 crib, is in an area that will receive a barrier in 2050. After the expected design life, a final estimated recharge rate of 4.0 mm/yr is assumed after 2550.

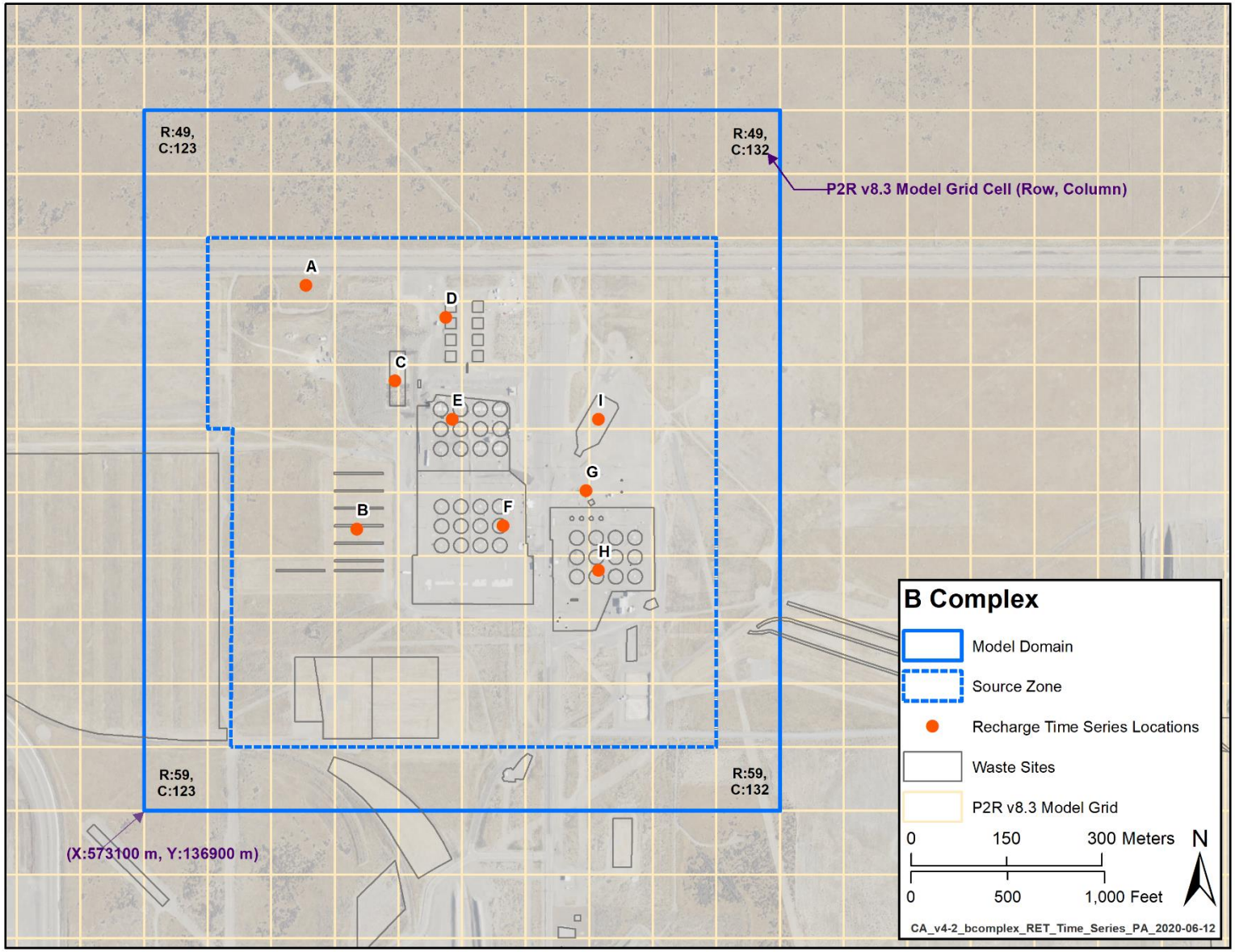

Figure 4-87. Locations of Recharge Rate Time Series Examples

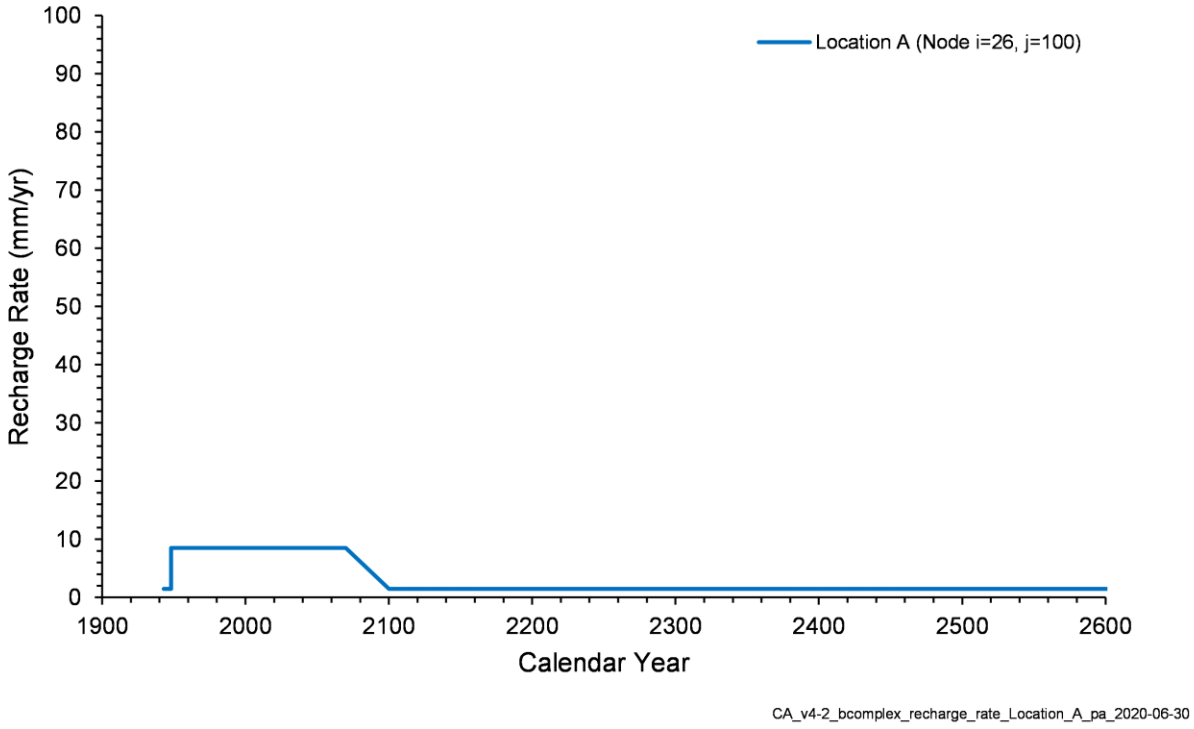

Figure 4-88. Time Series of Natural Recharge Rates, Location A

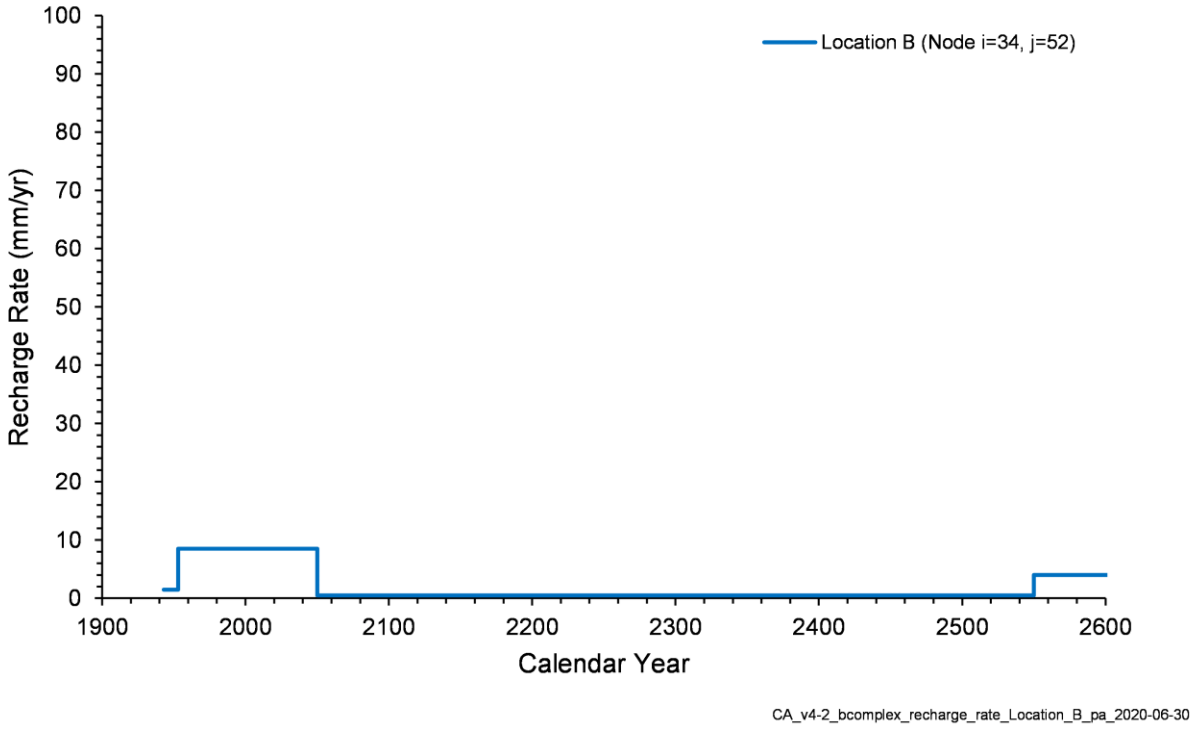

Figure 4-89. Time Series of Natural Recharge Rates, Location B

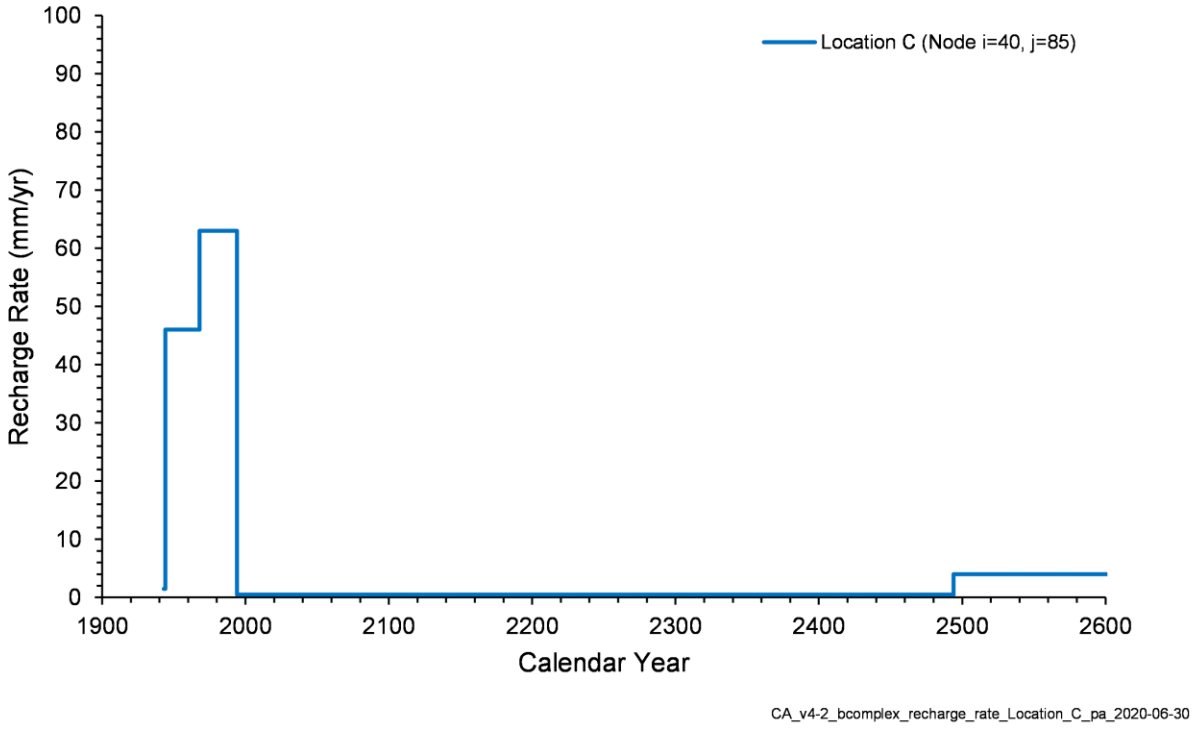

Figure 4-90. Time Series of Natural Recharge Rates, Location C

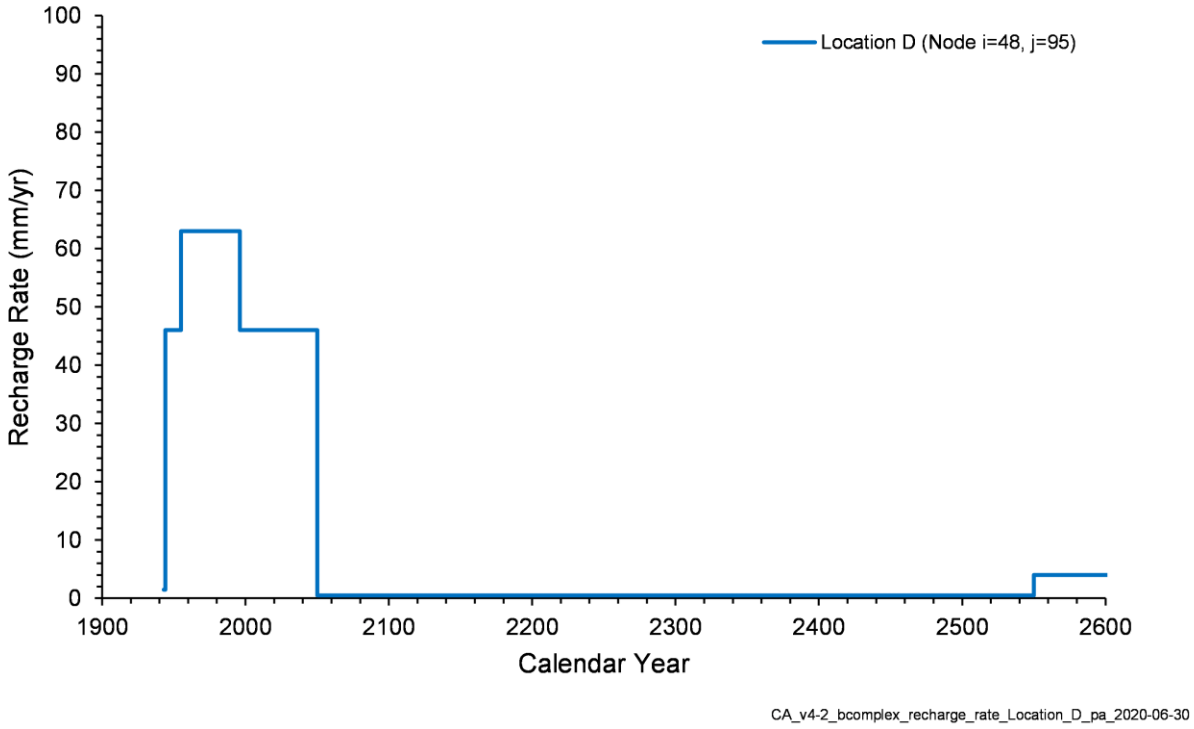

Figure 4-91. Time Series of Natural Recharge Rates, Location D

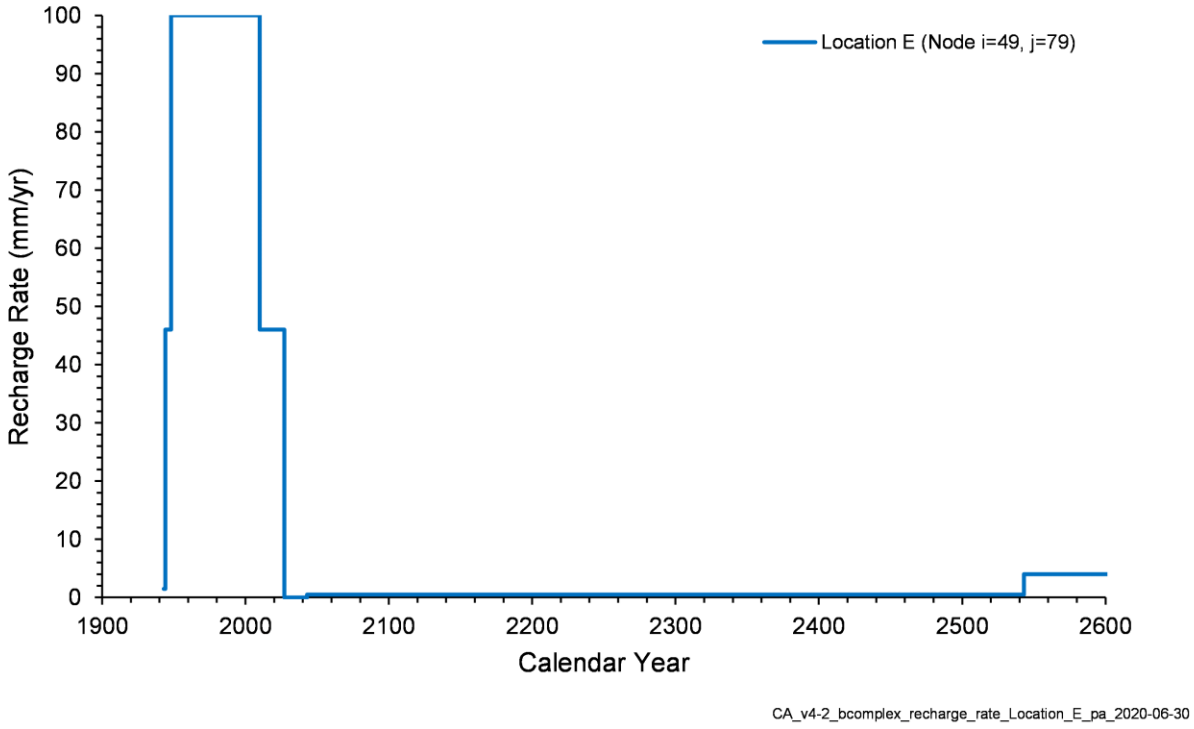

Figure 4-92. Time Series of Natural Recharge Rates, Location E

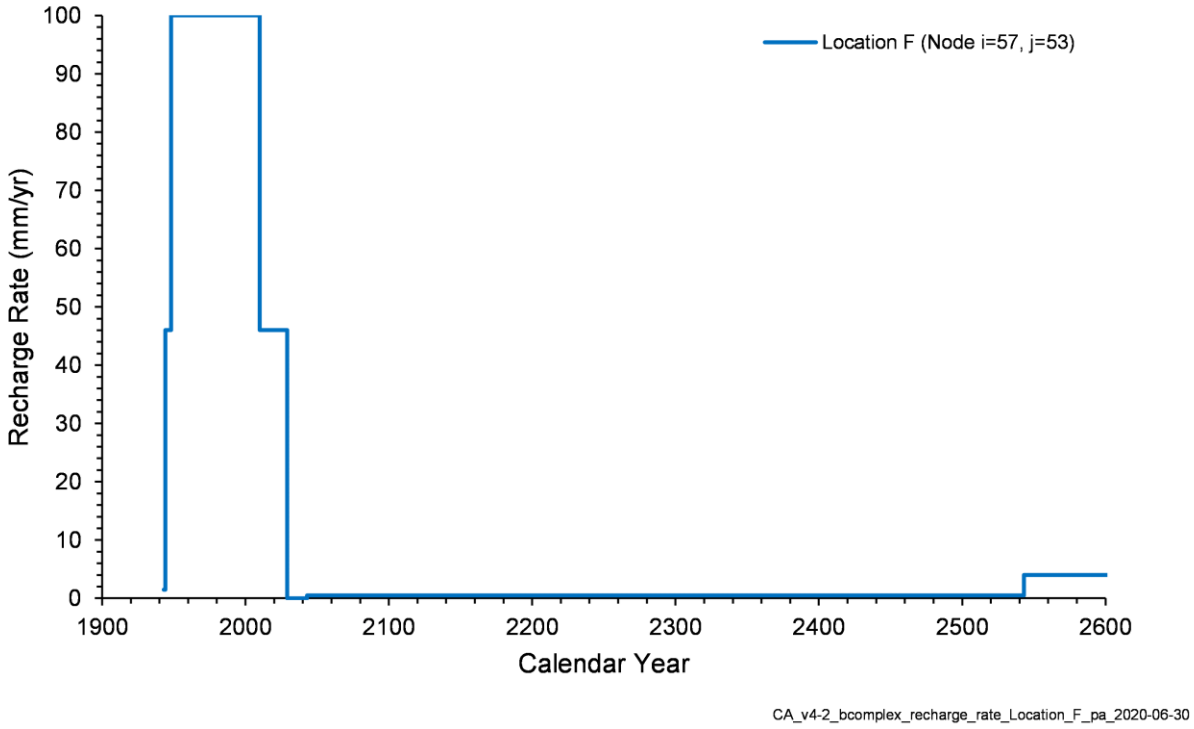

Figure 4-93. Time Series of Natural Recharge Rates, Location F

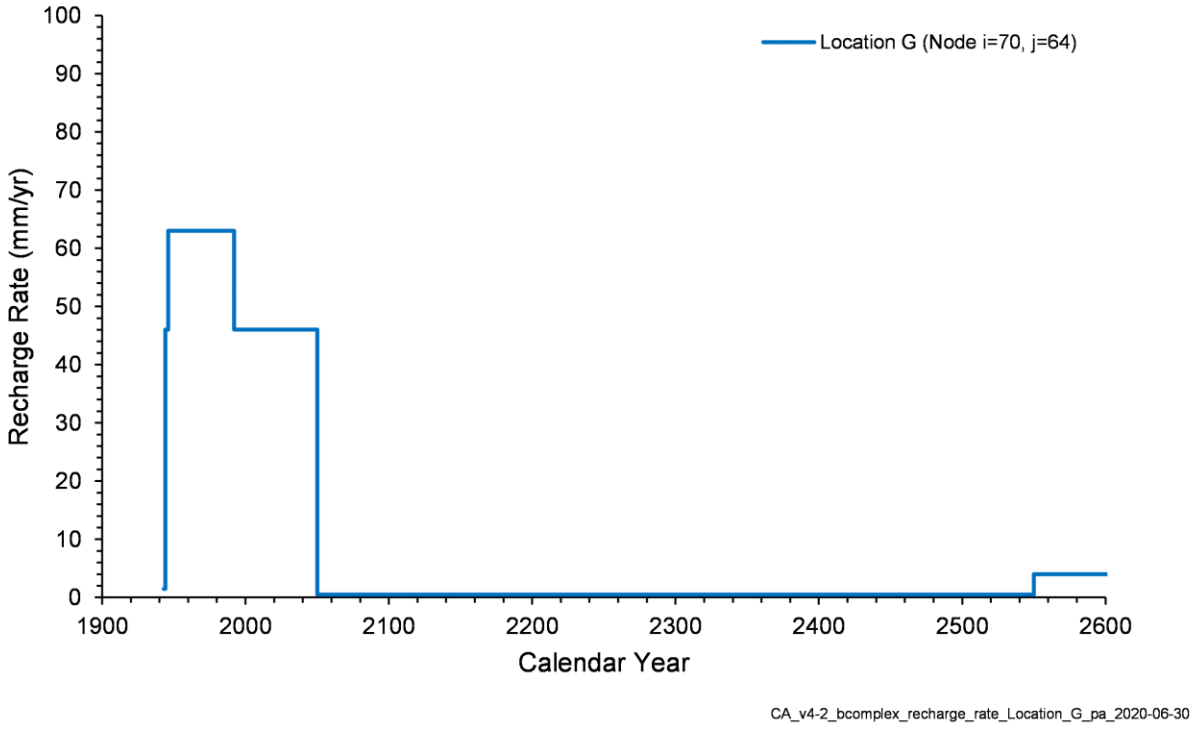

Figure 4-94. Time Series of Natural Recharge Rates, Location G

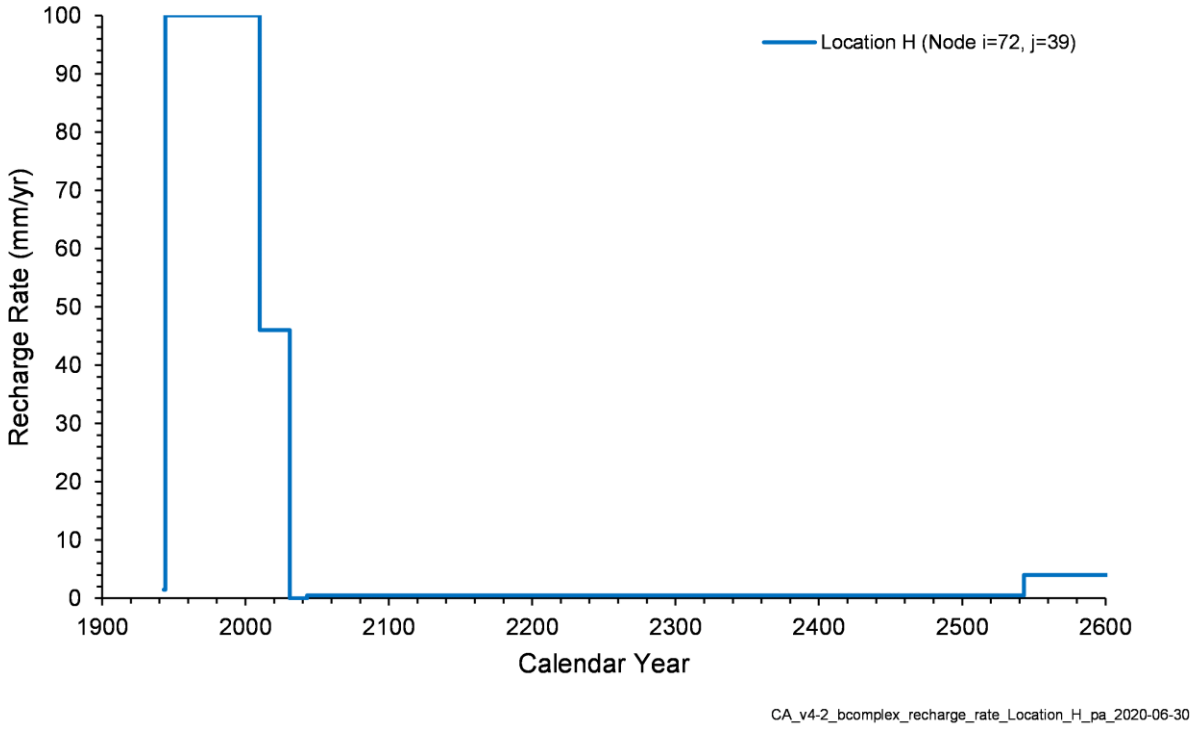

Figure 4-95. Time Series of Natural Recharge Rates, Location H

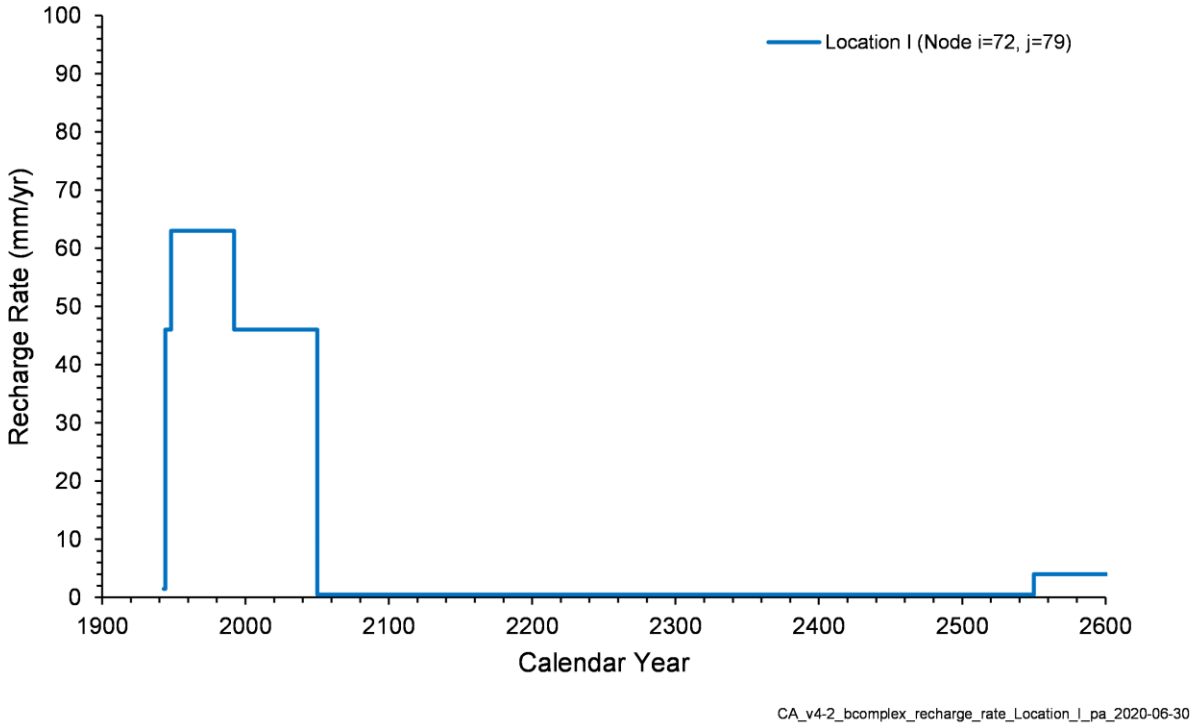

Figure 4-96. Time Series of Natural Recharge Rates, Location I

4.8.2 Lateral and Bottom Boundaries

Lateral boundaries for the model are assumed to be zero-flux boundaries for both contaminant transport and water flow. The locations of the lateral boundaries were selected in an iterative procedure to ensure that the contaminant plumes would not reach the model boundary. Source zone waste sites with radionuclide and liquid releases were at least 100 m away from the model boundary so that the releases would not affect soil moisture or contents at or near the boundary. For elongated waste sites extending into adjacent models, the assumption is that bifurcation of a waste site by a model boundary does not lead to soil moisture gradients across the boundary and that zero-flux boundaries are therefore appropriate for such waste sites.

The bottom of the model was assumed to be coincident with the water table at the model location, as estimated from the 2017 water table elevation (ECF-HANFORD-17-0120, *Preparation of the March 2017 Hanford Site Water Table and Potentiometric Surface Maps*). This boundary was represented by a Dirichlet boundary condition with a pressure of 101,325 Pa.

4.9 Source Nodes

Radionuclides and water discharged from waste sites are introduced to this model at source nodes. The distribution of these source nodes is shown in Figure 4-97. The STOMP Source Cards (i.e., specific information on source location and releases in the STOMP input file) were built using waste site footprints, source inventory, and the model grid. A discussion of the source node allocation process is found in CP-63515.

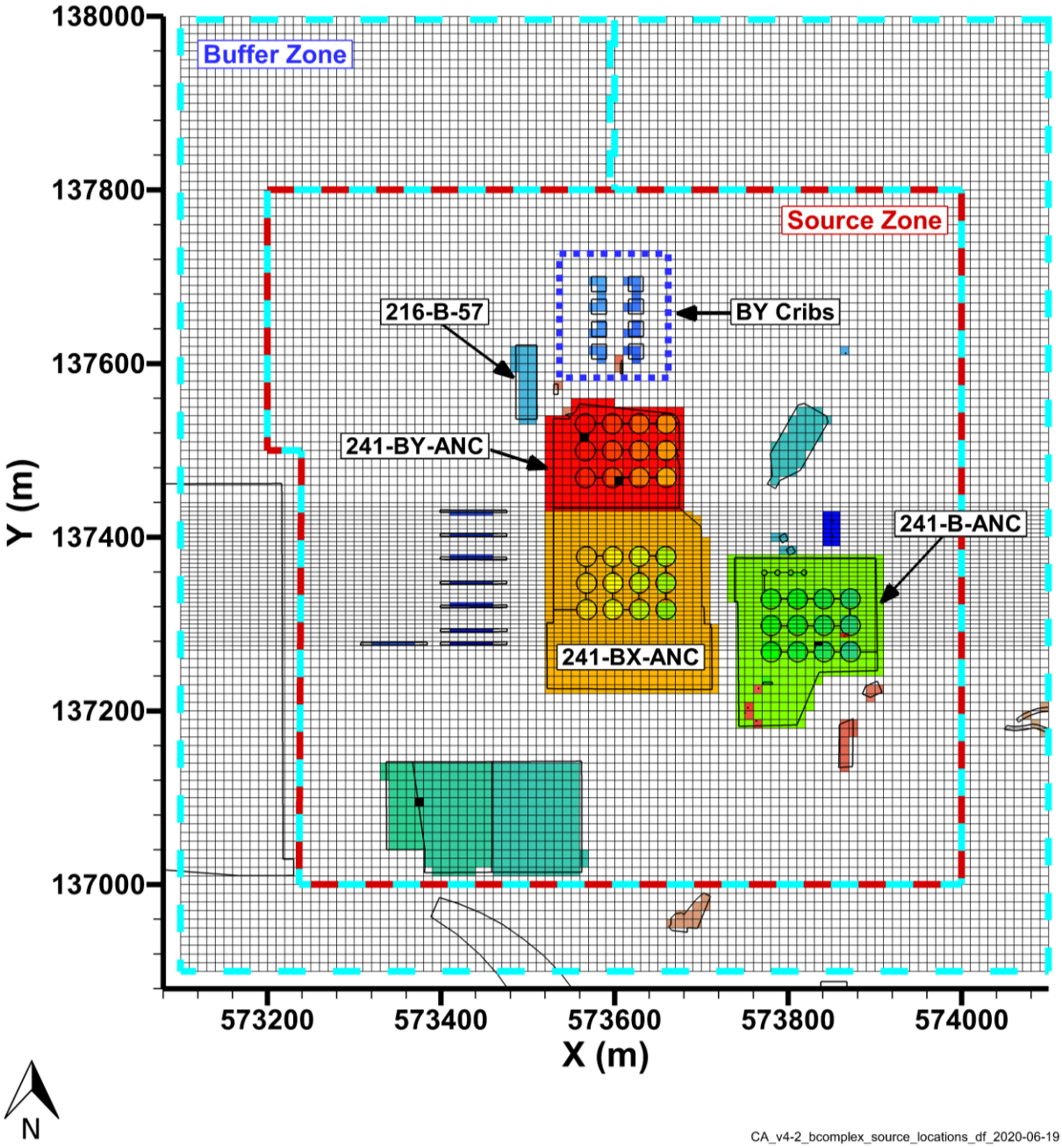

Note: Black cells indicate source nodes with input from multiple sites.

Figure 4-97. Distribution of Source Nodes in the B Complex Model

4.9.1 Data Reduction

The solid waste inventory from ECF-HANFORD-19-0112 described in Section 4.5.1.3 is released over approximately 10,000 years, with the total release timespan varying by waste site. These long release periods had many timesteps, resulting in large STOMP Source Cards. To accommodate the size limitations of STOMP Source Cards, the original inventory datasets were modified to release the solid waste inventory in a number of timesteps that is compatible with the Source Card size limitations. The

reduced datasets were checked to ensure they adequately represent the original inventory amounts and release rates. Additional information regarding the data reduction methodology is documented in ECF-HANFORD-20-0006.

4.10 Modeling Assumptions

The development of the B Complex model required several conceptual and simulation assumptions. The major assumptions are as follows:

- The vadose zone model consists of a system of HSUs derived from the Central Plateau Vadose Zone Geoframework Model (CP-60925). The geoframework is a three-dimensional representation of the subsurface beneath the Central Plateau, vertically extending from the ground surface to the top of the Columbia River Basalt Group. The geoframework model is constructed using a combination of lithologic and sequence stratigraphic interpretations, leading to the definition of a series of HSUs. With this approach, correlated, hydraulically significant units are mapped while still representing the interpretations of lithologically heterogeneous features. The HSU surfaces used in generating the B Complex model are from an update to CP-60925, ECF-HANFORD-18-0035.

- The anisotropic Equivalent Homogeneous Media (EHM) approach is used to simulate flow and transport in the heterogeneous Central Plateau HSUs. The EHM approach is recommended by Yeh et al., 2015, "Flow Through Heterogeneous Geologic Media," for systems with large-scale HSUs. With this approach, an HSU has two main characteristics: (1) representative hydraulic property and parameter values are applied that are equivalently homogeneous (i.e., constant) in space, and (2) the effects of heterogeneity on flow are described using an anisotropic unsaturated hydraulic conductivity. An important feature of an anisotropic EHM model representation is that it captures the mean or the bulk flow characteristics of the vadose zone moisture plumes, as demonstrated by Zhang and Khaleel, 2010, "Simulating Field-Scale Moisture Flow Using a Combined Power-Averaging and Tensorial Connectivity-Tortuosity Approach." Therefore, the contaminant peak arrival time under recharge-dominated flow conditions is adequately captured by an anisotropic EHM model representation. The anisotropic EHM approach is commonly used to model flow and transport at the Hanford Site. For instance, recent PA vadose modeling for WMA C (RPP-ENV-58782, *Performance Assessment of Waste Management Area C, Hanford Site, Washington*) used this approach to simulate subsurface flow and transport.

- For simulation of flow in unsaturated Hanford Site sediments, the soil water retention relation (i.e., the relation between soil moisture content and capillary pressure) and the unsaturated hydraulic conductivity relation (i.e., the relation between moisture content and unsaturated hydraulic conductivity) need to be provided. The unsaturated hydraulic conductivity is the product of the saturated hydraulic conductivity and the aqueous phase relative permeability. The nonhysteretic van Genuchten equation (van Genuchten, 1980) is used for the soil water retention relation. The Mualem relation (Mualem, 1976) is used for the unsaturated hydraulic conductivity relation.

- For the heterogeneous stratified sediments at the Central Plateau, upscaled hydraulic properties based on small-scale laboratory measurements are used to simulate the large, field-scale behavior. This assumption requires that each heterogeneous HSU be replaced by an anisotropic EHM with upscaled hydraulic properties. The hydraulic properties used in the CA model are on a grid-block scale which are much larger than the cores that are typically analyzed in the laboratory.

- The upscaled grid-block-scale parameter values for the water retention and relative permeability relations are obtained by applying averaging procedures to core-scale data. For the soil water retention relation, the linear upscaling scheme (Green et al., 1996, "Upscaled Soil-Water Retention

Using Van Genuchten's Function") is applied. For the unsaturated hydraulic conductivity, the power-averaging tensorial connectivity-tortuosity (PA-TCT) method (Zhang et al., 2003, "A Tensorial Connectivity–Tortuosity Concept to Describe the Unsaturated Hydraulic Properties of Anisotropic Soils"; Zhang and Khaleel, 2010) is used to determine directionally-dependent saturated hydraulic conductivity and relative permeability tortuosity parameters that are functions of the soil moisture content. The PA-TCT upscaling method leads to a soil-moisture-dependent anisotropic unsaturated hydraulic. Applying the PA-TCT method allows for an assessment of the effects of heterogeneity on lateral flow and contaminant spreading, including plume commingling at the HSU scale. The method has been successfully applied to evaluate various water infiltration tests performed at the Sisson and Lu field experiment site in the 200 East Area (Ye et al., 2005, "Stochastic Analysis of Moisture Plume Dynamics of a Field Injection Experiment"; Zhang and Khaleel, 2010). The field applications of the upscaled vadose zone property values based on the PA-TCT method suggests that it provides a reasonable framework for upscaling core-scale measurements, as well as an accurate simulation of moisture flow in the heterogeneous vadose zone under the Central Plateau.

- The CA vadose zone models use a "forward" modeling approach for contaminant transport in the subsurface: model transport simulations initiate at a time when contamination is not present in the subsurface, and the contaminant activity is introduced in the models as sources over time. This approach has been used to simulate Hanford Site contaminant transport resulting from liquid waste disposal (e.g., Oostrom et al., 2017, "Deep Vadose Zone Contaminant Flux Evaluation at the Hanford BY-Cribs Site Using Forward and Imposed Concentration Modeling Approaches") and past leaks (RPP-RPT-59197, "Analysis of Past Waste Tank Leaks and Losses in the Vicinity of Waste Management Area C, Hanford Site, Washington").

- Contaminant activity is assumed to be transported in the vadose zone by advection and hydrodynamic dispersion, which is the sum of molecular diffusion and mechanical dispersion. The two components of hydrodynamic dispersion are described by a single hydrodynamic dispersion coefficient and treated as a diffusive flux proportional to the concentration gradient. Advective transport and mechanical dispersion are computed using the flow field obtained when solving the water conservation equation. The contaminants are considered to be solutes, without affecting fluid properties like density and viscosity.

- Mechanical dispersion is assumed to be directionally dependent with a constant macroscopic macrodispersivity value for each HSU. The use of a constant (asymptotic) macrodispersivity for large-scale vadose zone CA modeling is considered appropriate (NUREG/CR-5965, *Modeling Field Scale Unsaturated Flow and Transport Processes*). Macrodispersivity values for the HSUs in the longitudinal direction, are obtained from Hanford Site field-scale numerical simulations and field experiments. Hanford Site-specific datasets include Khaleel et al., 2002, "Upscaled Flow and Transport Properties for Heterogeneous Unsaturated Media"; and PNNL-25146, *Scale-Dependent Solute Dispersion in Variably Saturated Porous Media*. In the absence of unsaturated media experimental data, the CA transport models used a transverse macrodispersivity value that is 1/10th of the obtained longitudinal value.

- Contaminant sorption is simulated using a reversible linear sorption isotherm with a linear K_d. The linear sorption model approach is assumed to be adequate for modeling transport at the Hanford Site (PNNL-13895, *Hanford Contaminant Distribution Coefficient Database and Users Guide*). An important benefit of the linear adsorption assumption is that an extensive database of K_d values applicable to Hanford Site sediments is available for the contaminants of most concern over a broad range of conditions (e.g., PNNL-17154, *Geochemical Characterization Data Package for the Vadose Zone in the Single-Shell Tank Waste Management Areas at the Hanford Site*). Use of reversible linear

K_d isotherms is computationally efficient and appropriate for the scale of the CA problem. Recognizing that experimental K_d values are mostly determined using sediment grain sizes <2 m, corrections for gravel content using equations provided in PNNL-17154 are used to adjust measured values for the finer fraction applicable to HSUs with considerable gravel content.

- The spatial and temporal variable natural recharge rate is used to define the upper boundary conditions for the water conservation equation. The natural recharge rate is a term applied to define the net infiltration that migrates through the vadose zone to reach the water table. At the Hanford Site, this rate is primarily a function of the surface soil type and type/density of vegetative cover. Effects of climate change on natural recharge over the next 10,000 years are not accounted for in the simulations.
- No moisture or contaminants are allowed to migrate across the lateral boundaries of the model domain. During development of the model domain, the proper locations of the zero flux lateral boundaries were determined in an iterative procedure.
- The simulations use a fixed water table representing 2018 conditions to increase efficiency and reduce complexity during implementation of the vadose zone models. The effects of the transient water table on contaminant transfer after 2018 to the aquifer were evaluated to validate this approach in Farrow et al., 2019, "Prediction of Long-Term Contaminant Flux from the Vadose Zone to Groundwater for Fluctuating Water Table Conditions at the Hanford Site." Simulations for selected vadose zone models with continuing sources demonstrated that a simplification of the water table boundary condition (i.e., a static water table), could be adequately used to compute long-term predictions of contaminant flux to groundwater.
- The liquid volumes and waste site inventories are obtained from the Hanford Soil Inventory Model (SIM-v2) (ECF-HANFORD-17-0079). Non-radiological site liquid volumes were obtained from site-specific literature. Using geometry information, waste and non-radiological site shapes were assigned to vadose zone model grid surfaces, according to EMDT-GR-0035, *Waste Site and Structure Footprint Shapefiles for Inclusion in Updated Composite Analysis*. Water volumes and SIM-v2 contaminant inventories were assigned to the model grid cells at the lowest topographic location within the site footprints.

5 Software Applications

Three types of calculation software are used in this modeling effort: the numerical modeling simulator eSTOMP, support software (spreadsheet and geographic information system [GIS] applications), and custom utility calculation software. Custom utility calculations software is documented under CHPRC-04032, *Composite Analysis / Cumulative Impact Evaluation (CACIE) Utility Codes Integrated Software Management Plan* and described in further detail in Section 5.3 of this ECF.

5.1 Approved Software

The eSTOMP numerical simulator has been used for the flow and transport calculations reported in this ECF. The application of the simulator is managed under the requirements of CHPRC-00176, *STOMP Software Management Plan*. Use of this software is consistent with the intended uses of STOMP at the Hanford Site as defined in CHPRC-00222, *STOMP Functional Requirements Document*. The STOMP software is actively managed by the CH2M HILL Plateau Remediation Company and approved for use at the Hanford Site as Level C software under a procedure that implements the requirements of DOE O 414.1D, *Quality Assurance*.

Build 6 of the STOMP software was used in the implementation of the model described in this document. This version was approved for use at the Hanford Site based on acceptance testing results reported in CHPRC-00515, *STOMP Acceptance Test Report*. The status of requirements for this software are maintained in CHPRC-00269, *STOMP Software Requirements Traceability Matrix*. All acceptance testing was performed to the requirements of CHPRC-00211, *STOMP Software Test Plan*. Installation testing is also required for any computer system on which STOMP is run. The installation test is specified in CHPRC-00211.

The STOMP simulator was developed by Pacific Northwest National Laboratory to simulate flow and transport over multiple phases in a subsurface environment. The water mode of the simulator uses numerical approximation techniques to solve partial differential equations that describe the conservation of aqueous mass and radionuclide activity in variably saturated porous media. These governing conservation equations, along with a corresponding set of constitutive relations that relate variables within the conservation equations, are solved numerically by using integrated-volume, finite-difference discretization to the physical domain and first- or second-order Euler discretization to the time domain. The resulting equations are nonlinear, coupled algebraic equations that are solved using the Newton-Raphson iteration.

The theoretical and numerical approaches applied in the STOMP simulator are documented in a published theory guide (PNNL-12030). The simulator has undergone a rigorous verification procedure against analytical solutions, laboratory-scale experiments, and field-scale demonstrations. The application guide (PNNL-11216) provides instructive examples in the application of the code to classical groundwater and vadose zone flow and transport problems. The user's guide (PNNL-15782) describes the general use, input file formatting, compilation, and execution of the code.

- Software Title: STOMP, parallel implementation (eSTOMP), executable eSTOMP1-chprc06-20200204-g.x
- Software Version: CHPRC Build 6
- Hanford Information System Inventory Identification Number: 2471

- Workstation type and property number (from which software is run): GAIA Subsurface Flow and Transport Modeling Platform, Nodes compute-0-0 through compute-0-8 inclusive, property tags: WF32991, WF32992, WF32993, WF32994, WF32995, WF32996, WF32997, WF32998, WF32999

5.1.1 Software Installation and Checkout

The software installation and checkout form for STOMP simulation software is provided as Appendix D to this ECF.

5.1.2 Statement of Valid Software Application

The application of the eSTOMP software to the vadose zone flow and transport systems is correct. The software has been used within the limits discussed in the simulator's theory guide (PNNL-12030) and user's guide (PNNL-15782). The water mode of the STOMP simulator is designed to simulate flow and transport over multiple phases in a subsurface environment, including unsaturated systems like the Hanford Site vadose zone. The simulator solves partial differential equations describing conservation of aqueous mass and radionuclide activity in variably saturated porous media, consistent with aqueous flow and contaminant transport in Hanford Site sediments. The STOMP code has been executed at research institutions and universities to address vadose zone flow and contaminant transport problems comparable to the CA unsaturated systems.

The STOMP code, including the eSTOMP parallel implementation, is developed and tested to NQA-1, *Quality Assurance Requirements for Nuclear Facility Applications*, standards by Pacific Northwest National Laboratory "by option" wherein testing conducted option by option. Therefore, an "NQA-1 Options Analysis" is provided for the model application documented in this ECF (as well as other related model applications) in CP-63515 to demonstrate that all eSTOMP code options used in this model are NQA-1 qualified.

5.2 Support Software

The following programs are classified as Support Software:

- **Microsoft® Excel®** (version 2010): The tool was used to generate inventory plots and contaminant release and transfer timeseries.
- **ArcGIS®** (version 10.3.1): The tool was used to create of spatial model discretization and waste site location maps.
- **Tecplot® 360 EX** (version 2018R1): The tool was used to generate source location, recharge distribution, and mass transfer to groundwater plots.

5.3 Support Scripts

Generation of model input files and post-processing of model results was mostly performed with utility codes (scripts) that are managed, tested, and controlled in accordance with CHPRC-04032. CHPRC-04032 provides a common foundation for the management of several custom-developed scripts to manage pre- and post-processing operations and inter-facet information passing between major software packages efficiently for the CA. It also provides direction for electronic management of

® Microsoft and Excel are registered trademarks of the Microsoft Corporation in the United States and other countries.

® ArcGIS® is a registered trademark of the Environmental Systems Research Institute, Inc., Redlands, California.

® Tecplot is a registered trademark or trademarks of Tecplot, Inc. in the United States and other countries.

documentation requirements at the script level with respect to individual tool functional requirements, software requirements specification, software design description, requirements tracing, test plans and reporting, and user documentation. The utility scripts developed for this project, in alphabetical order, are as follows:

- **aq_mod_avg.exe:** The Aqueous Source Averaging Tool averages aqueous source rates for user-specified waste sites and times.
- **ca_build_surface_flux.py:** The Build Surface Flux Tool maps the STOMP grid into the MODFLOW grid.
- **ca-dups.pl:** The Duplicate Source Nodes Tool identifies any source nodes that overlap spatially and writes information regarding the duplicate source node(s) to an output file.
- **ca-getmod_srf.pl:** The Surface File to P2R Tool aggregates solute flux and cumulative discharge data exiting the vadose zone model by P2R grid cell.
- **ca-ipp.pl:** The Inventory Pre-Processor Tool creates a comprehensive dataset consisting of radionuclide and aqueous volume releases as a function of time for Central Plateau sites. The dataset is input for the SRC2STOMP Tool.
- **ca-merge_srf.pl:** The STOMP Surface Merge Tool merges STOMP surface file data from two consecutive STOMP simulations (e.g., surface files for the 2018 to 12070 simulation).
- **ca-patchbowl.pl:** The Patchbowl Tool modifies STOMP soil zonation files to patch holes in the silt layers of the perching silt layer in the 200 East Area.
- **ca_RET2STOMP.py**: The RET2STOMP Tool generates the natural recharge Boundary Condition Cards for the STOMP model input file using output generated by the RET.
- **ca-rtdic.pl:** The RTD Initial Conditions Card Tool generates Initial Conditions Cards at RTD years for models with RTD sites using an input source card file and a steady-state STOMP input file.
- **ca-src2stomp.pl**: The SRC2STOMP Tool combines the site spatial information with the corresponding radionuclide inventory and creates a STOMP-readable Source Card file containing grid cell definitions of solute and/or liquid sources.
- **K2S_ROCSAN.exe:** The Kingdom2Stomp Tool reads an input file representing each node in the model and generates an output file like the input file with the addition of which geologic formation each model node represents.
- **ModelSetupFY18.jar:** The Composite Analysis STOMP Tool is a graphical user interface tool that produces STOMP input files based on user input model dimensions and material properties.
- **OC_SS_gen.exe:** The Steady-State Output Card Generator Tool reads files generated by the Composite Analysis STOMP Tool and generates a STOMP Output Control Card for the steady-state simulation.
- **OC_rad_gen.exe:** The Transport Output Card Generator Tool Creates a STOMP Output Control Card used for mass balance and transport production simulations.
- **reroute_sources.exe:** The Source Rerouting Tool redistributes wastewater volumes and contaminant inventories for the 216-U-10 Pond System and the 216-B-3 Pond System.

- **splitKingdomLayer.pl:** The SplitKingdomLayer Tool is used to split one geology surface layer file into two sub-unit surface layer files based on the information specified in the polygon file.
- **srcloc_modify.exe:** The Source Node Moving Tool moves source nodes from the locations selected by the SRC2STOMP Tool.
- **SS_input_gen.exe*:*** The Steady-State STOMP Input File Generator Tool generates the STOMP input file for the steady-state simulation.
- **xprt_2018_input_gen.exe:** The 2018 STOMP Input File Generator Tool generates the 1943–2018 STOMP transport input file.
- **xprt_12070_input_gen.exe:** The 12070 STOMP Input File Generator Tool generates the 2018 (or RTD year if the model has RTD remediation sites)–12070 STOMP transport input file. This code reads and modifies the 1943–2018 STOMP input file created by the 2018 STOMP Input File Generator Tool.
- **xprt_mb_input_gen.exe:** The Mass Balance STOMP Input File Generator Tool generates the mass balance STOMP transport input file. This code reads and modifies the STOMP input file created by the 2018 STOMP Input File Generator Tool.
- **xprt_RTD_input_gen.exe:** The RTD STOMP Input File Generator tool generates the 2018 – RTD year STOMP transport input file. This code reads and modifies the 1943–2018 STOMP input file created by the 2018 STOMP Input File Generator Tool.

6 Calculation

The fate and transport calculations for the B Complex model were performed using a suite of STOMP simulations: a steady-state simulation, mass balance transport simulations, and historical and forecast transport simulations (as discussed in Section 4.6). This section describes the mass balance calculations for the steady-state and transport simulations.

6.1 Steady-State Simulation

The purpose of the steady-state simulation was to verify model performance and to generate the initial primary variable (i.e., aqueous pressure) conditions within the model domain for the historical transport simulations, as discussed in Section 4.6.1. Contaminants are not simulated in the steady-state simulation, only flow. Pre-Hanford Site boundary conditions (i.e, natural recharge rates for 1943) are applied for a period of 10,000 years (from year zero to 10,000) to allow the simulation to reach steady-state conditions. Figure 6-1 compares the steady-state recharge flux into the top of the model to the flux leaving the base of the model, which represents discharge to groundwater from the model. Conditions reach equilibrium (i.e. flux in equals flux out) and remain unchanged through the end of the simulated time period, indicating that steady-state conditions have been achieved.

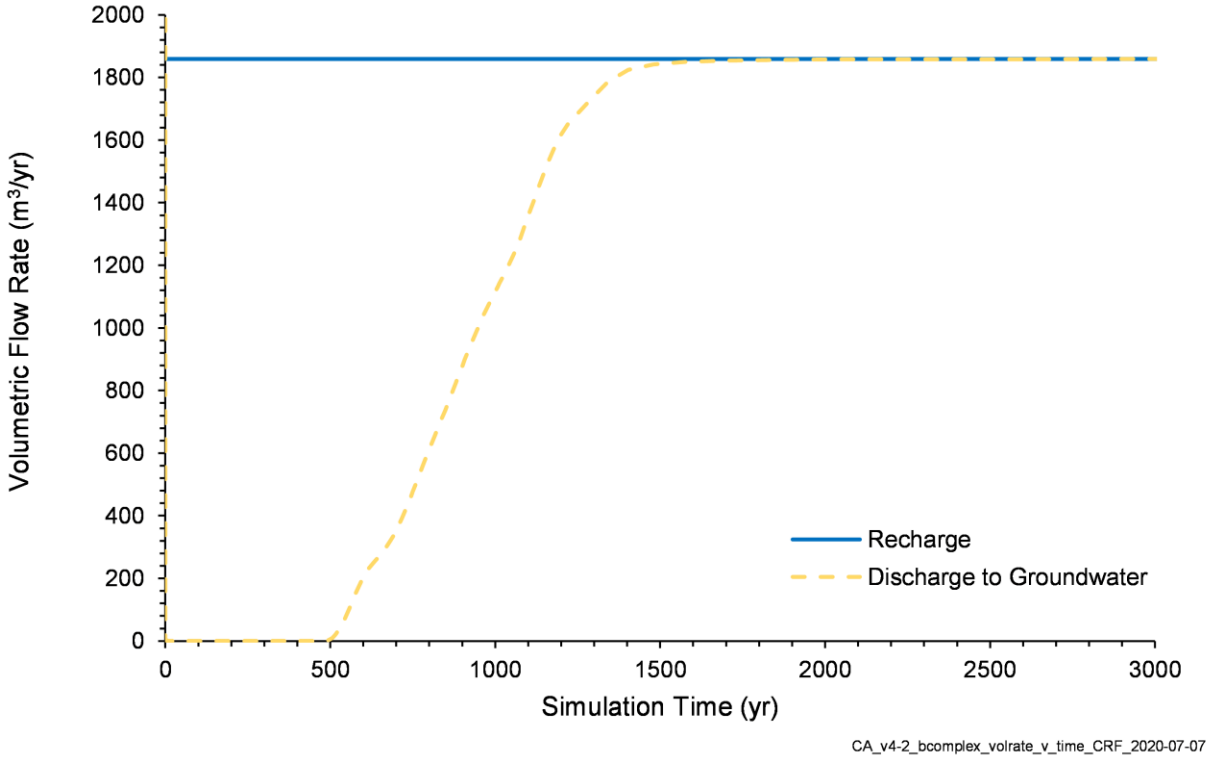

Figure 6-1. Steady-State Recharge Compared to Discharge to Groundwater Over Time

The steady-state liquid volume balance (also called mass balance) error (E) is calculated as shown in Equation 6-1 (all variables have units of volume):

$$E = (S + O) - R_P \quad \textbf{(Eq. 6-1)}$$

where:

E = liquid volume balance error

S = change in liquid storage within the model domain
O = total liquid outflow from the model domain
R_P = total pre-Hanford Site natural recharge.

The percent relative error (*%RE*) of the aqueous volume balance is calculated as shown in Equation 6-2:

$$\%RE = 100|E/R_P| \quad \textbf{(Eq. 6-2)}$$

where %RE is the liquid volume percent relative error.

Change in liquid storage (*S*) is the difference between liquid in the model at year 10,000 and year 0. Total liquid water outflow from the model (*O*) is the cumulative liquid volume that passed through the bottom of the model boundary at the end of 10,000 years. The pre-Hanford Site natural recharge (R_P) is the cumulative volume of recharge applied to the top layer of the model during the simulation. The flow-only steady-state liquid volume balance is shown in Table 6-1.

Table 6-1. Liquid Volume Balance for the B Complex Model Steady-State Simulation

Natural Recharge (*RP*) [a]	Change in Liquid Storage (*S*) [a,b]	Total Liquid Outflow (*O*) [a,b]	Error (*E*) [a]	Percent Relative Error (*%RE*)
18,587,500	1,713,073	16,874,860	433	2.332E-03

STOMP is a copyright of Battelle Memorial Institute, Columbus, Ohio, and used under the Limited Government License.

a. Volume units in m^3.

b. Calculated by STOMP.

%RE = liquid volume percent relative error
E = liquid volume balance error
O = total liquid outflow from the model domain
R_P = total pre-Hanford Site natural recharge
S = change in liquid storage within the model domain
STOMP = Subsurface Transport Over Multiple Phases

6.2 Radionuclide Transport Volume and Activity Simulations

Transient simulations were used to calculate liquid volume and activity balances, also referred to as mass balances. These simulations use the steady-state model final aqueous pressure distribution as initial aqueous pressure conditions, the transient natural recharge described in Section 4.8.1, and the waste site sources described in Section 4.5. Although run as single simulations for each radionuclide group, two sets of radionuclide activity balance evaluations were performed: the first for the historical time period from 1943 to 2018, and the second for the entire transient model duration from 1943 to 12070. Radionuclide half-life values were set to 1.0E+20 years to virtually eliminate radioactive decay. Therefore, decay corrections were not necessary, and the radionuclide activity balance could be evaluated directly.

The liquid volume balance error (*E*) is calculated as shown in Equation 6-3 (all variables have units of volume):

$$E = (S + O) - (I + R) \quad \textbf{(Eq. 6-3)}$$

where:

E = liquid volume balance error

S = change in liquid storage within the model domain
O = total liquid outflow from the model domain
I = liquid inventory entering the model domain from liquid waste site releases
R = total natural recharge.

The percent relative error (*%RE*) of liquid volume balance is calculated as shown in Equation 6-4:

$$\%RE = 100|E/(I + R)| \quad \textbf{(Eq. 6-4)}$$

where %RE is the liquid volume percent relative error.

The change in liquid storage within the model domain (*S*) is the difference between the volume of water in the model at the beginning of the simulation (1943) and the end of the mass balance analysis period (either 2018 or 12070). The total liquid outflow from the model domain (*O*) is the cumulative liquid volume that passed through the bottom of the model boundary by the end of the mass balance analysis period. The liquid inventory entering the model domain from liquid waste site releases (*I*) is the cumulative volume of liquids released to the model from liquid waste sites in the source and buffer zones during the mass balance analysis period. The natural recharge (*R*) is the cumulative volume of liquid applied to the top of the model from natural recharge during the mass balance analysis period. The liquid volume balance for the B Complex model for the simulation for Radionuclide Group 1 is shown in Table 6-2, the liquid volume balance for Radionuclide Group 2 is not included as it is functionally the same.

Table 6-2. Transient Liquid Volume Balances for the B Complex Model Radionuclide Group 1 Simulations

Liquid Inventory (*I*) [a]	Natural Recharge (*R*) [a]	Change in Liquid Storage (*S*) [a,b]	Total Liquid Outflow (*O*) [a,b]	Error (*E*) [a]	Percent Relative Error (*%RE*)
1943–2018					
301,526	2,268,388	1,283,608	1,286,633	326	1.270E-02
1943–12070					
301,526	27,996,064	140,572	28,156,930	-89	3.151E-04

STOMP is a copyright of Battelle Memorial Institute, Columbus, Ohio, and used under the Limited Government License.

a. Volume units in m^3.

b. Calculated by STOMP.

%RE = liquid volume percent relative error
E = liquid volume balance error
I = liquid inventory entering the model domain from liquid waste site releases
O = total liquid outflow from the model domain
R = total natural recharge
S = change in liquid storage within the model domain
STOMP = Subsurface Transport Over Multiple Phases

The radionuclide activity balance error (E_R) is calculated as shown in Equation 6-5 (all variables have units of activity):

$$E_R = (S_R + O_R) - I_R \quad \textbf{(Eq. 6-5)}$$

where:

E_R = radionuclide activity balance error
S_R = radionuclide storage within the model domain at the end of the simulation
O_R = total radionuclide outflow from the model domain
I_R = radionuclide inventory entering the model domain from waste site releases.

The percent relative error ($\%RE_R$) of the radionuclide activity balance is calculated as shown in Equation 6-6:

$$\%RE_R = 100|E_R/I_R| \quad \textbf{(Eq. 6-6)}$$

where $\%RE_R$ is the radionuclide activity balance percent relative error.

The total radionuclide outflow (O_R) is the cumulative activity of a particular radionuclide that migrated through the bottom boundary of the vadose zone model from the beginning of the simulation (1943) to the end of the mass balance analysis period (either 2018 or 12070). The radionuclide storage (S_R) is the difference in total activity of a particular radionuclide in the model from the beginning of the simulation (1943) and the end of the mass balance analysis period (2018 or 12070). Because there were no radionuclides in the model from anthropogenic sources in 1943, this can be understood as the change in total activity of a radionuclide in the model domain. The radionuclide inventory that entered the model domain from waste site releases (I_R) is the cumulative activity of the radionuclide released to the model from the solid and liquid waste release sites in the source zone. Table 6-3 and Table 6-4 show the activity balance for the B Complex model no-decay transport simulations for Radionuclide Group 1 and Radionuclide Group 2, respectively.

Table 6-3. Transient No-Decay Activity Balances for the B Complex Model Radionuclide Group 1 Simulations

Radionuclide	Released Radionuclide Inventory (I_R) [a]	Radionuclide Storage (S_R) [a,b]	Radionuclide Outflow (O_R) [a,b]	Error (E_R) [a]	Relative Error ($\%RE_R$)
1943–2018					
C-14	1.120E+01	7.192E+00	4.020E+00	1.178E-02	1.051E-01
Cl-36	0.000E+00	0.000E+00	0.000E+00	See note c	See note c
H-3	5.913E+03	3.153E+03	2.760E+03	1.084E-01	1.834E-03
I-129	2.580E-01	2.530E-01	5.335E-03	3.298E-04	1.278E-01
Np-237	1.210E+00	1.210E+00	0.000E+00	-5.498E-08	4.543E-06
Re-187	0.000E+00	0.000E+00	0.000E+00	See note c	See note c
Sr-90	2.747E+04	2.747E+04	0.000E+00	-2.978E-04	1.084E-06
Tc-99	1.716E+02	1.105E+02	6.142E+01	2.840E-01	1.655E-01

Table 6-3. Transient No-Decay Activity Balances for the B Complex Model Radionuclide Group 1 Simulations

Radionuclide	Released Radionuclide Inventory (I_R) [a]	Radionuclide Storage (S_R) [a,b]	Radionuclide Outflow (O_R) [a,b]	Error (E_R) [a]	Relative Error ($\%RE_R$)
1943–12070					
C-14	1.126E+01	4.451E-03	1.125E+01	-1.067E-02	9.477E-02
Cl-36	0.000E+00	0.000E+00	0.000E+00	See note c	See note c
H-3	5.913E+03	1.306E-01	5.906E+03	-6.468E+00	1.094E-01
I-129	2.704E-01	1.047E-02	2.601E-01	1.718E-04	6.351E-02
Np-237	1.217E+00	1.217E+00	0.000E+00	1.163E-04	9.563E-03
Re-187	0.000E+00	0.000E+00	0.000E+00	See note c	See note c
Sr-90	2.836E+04	2.836E+04	0.000E+00	-2.339E-01	8.248E-04
Tc-99	1.888E+02	1.361E+00	1.874E+02	-1.165E-01	6.167E-02

a. Units are in Curies.

b. Calculated by STOMP.

c. The radionuclide has no inventory.

$\%RE_R$ = percent relative error of the radionuclide activity balance

E_R = radionuclide activity balance error

I_R = radionuclide inventory entering the model domain from waste site releases

O_R = total radionuclide outflow from the model domain

S_R = radionuclide outflow from the model domain

STOMP = Subsurface Transport Over Multiple Phases

Table 6-4. Transient No-Decay Activity Balances for the B Complex Model Radionuclide Group 2 Simulations

Radionuclide	Released Radionuclide Inventory (I_R) [a]	Radionuclide Storage (S_R) [a,b]	Radionuclide Outflow (O_R) [a,b]	Error (E_R) [a]	Relative Error ($\%RE_R$)
1943–2018					
U-232	3.153E-02	3.153E-02	4.632E-07	1.694E-07	5.373E-04
U-233	1.336E+00	1.336E+00	4.721E-06	6.556E-06	4.906E-04
U-234	3.828E+00	3.792E+00	3.947E-02	2.969E-03	7.756E-02
U-235	1.718E-01	1.701E-01	1.780E-03	1.340E-04	7.801E-02
U-236	3.804E-02	3.772E-02	3.406E-04	2.529E-05	6.650E-02
U-238	3.887E+00	3.849E+00	4.015E-02	3.019E-03	7.767E-02
Th-230	3.193E-13	3.193E-13	1.114E-25	-5.795E-17	1.815E-02
Ra-226	1.365E-13	1.364E-13	0.000E+00	-1.341E-17	9.826E-03
1943–12070					
U-232	3.198E-02	3.192E-02	8.123E-05	2.041E-05	6.382E-02
U-233	1.454E+00	1.450E+00	4.304E-03	6.277E-04	4.317E-02
U-234	3.899E+00	2.848E+00	1.057E+00	5.285E-03	1.355E-01
U-235	1.748E-01	1.274E-01	4.767E-02	2.547E-04	1.457E-01
U-236	3.908E-02	3.009E-02	9.041E-03	4.996E-05	1.278E-01
U-238	4.012E+00	2.943E+00	1.075E+00	5.390E-03	1.343E-01
Th-230	1.090E-04	1.090E-04	1.338E-21	-1.230E-08	1.129E-02
Ra-226	1.078E-03	1.078E-03	0.000E+00	2.351E-09	2.181E-04

a. Units are in Curies.

b. Calculated by STOMP.

$\%RE_R$ = percent relative error of the radionuclide activity balance

E_R = radionuclide activity balance error

I_R = radionuclide inventory entering the model domain from waste site releases

O_R = total radionuclide outflow from the model domain

S_R = radionuclide outflow from the model domain

STOMP = Subsurface Transport Over Multiple Phases

7 Results

This chapter presents the results of the transport simulations. These results include the calculation of cumulative radionuclide activity transferred to the groundwater and the cumulative activity remaining in the vadose zone at the end of the historical simulation (1943–2018) and the CA evaluation (i.e., forecast) simulation (2018–12070). The removal of radionuclides by RTD remediation is also presented.

For each of the 16 radionuclides, Table 7-1 and Table 7-2 list the total activity discharged to the groundwater and the total activity remaining in the vadose zone. Table 7-1 shows these data at the end of the historical simulation (1943–2018), and Table 7-2 shows these data at the end of the forecast simulation (2018–12070). This model has one RTD site. The activity of each radionuclide removed from the RTD waste site due to removal actions of RTD remediation in this model is shown in Table 7-3.

The data presented in Table 7-1 and Table 7-2 are presented graphically in Section 7.1 through 7.16. These sections each present the data for one radionuclide. The cumulative activity of radionuclides discharged to the groundwater presented in Table 7-1 are shown spatially, aggregated by P2R grid cell, in Figure 7-1 and similar figures. The cumulative activity discharged to groundwater and the cumulative inventory released to the model shown in Table 7-1 for 1943–2018 and Table 7-2 for 2018–12070, is shown through time, first by figures which show the data from 1943–2018 (like Figure 7-3) and then by figures which show the data from 1943–12070 (like Figure 7-4). Additional figures showing radionuclide arrival to the groundwater through time for P2R grid cells in this model are shown in Appendix E.

Table 7-1. B Complex Model Radionuclide Activity Transfer to Groundwater from 1943–2018 and Remaining Activity in the Vadose Zone at 2018

Radionuclide	1943–2018 Inventory Released to Vadose Zone (Ci)	1943–2018 Activity Transferred to Groundwater (Ci)	1943–2018 Percent Activity Transferred to Groundwater [a]	Activity Remaining in Vadose Zone at 2018 (Ci)	Percent Activity Remaining in Vadose Zone at 2018 [a]
Radionuclide Group 1					
C-14	1.120E+01	4.008E+00	35.8	7.141E+00	63.8
Cl-36	0.000E+00	0.000E+00	See note b	0.000E+00	See note b
H-3	5.913E+03	1.528E+03	25.8	1.178E+02	2.0
I-129	2.580E-01	5.335E-03	2.1	2.530E-01	98.1
Np-237	1.210E+00	0.000E+00	0.0	1.210E+00	100.0
Re-187	0.000E+00	0.000E+00	See note b	0.000E+00	See note b
Sr-90	2.747E+04	0.000E+00	0.0	6.681E+03	24.3
Tc-99	1.716E+02	6.141E+01	35.8	1.105E+02	64.4

Table 7-1. B Complex Model Radionuclide Activity Transfer to Groundwater from 1943–2018 and Remaining Activity in the Vadose Zone at 2018

Radionuclide	1943–2018 Inventory Released to Vadose Zone (Ci)	1943–2018 Activity Transferred to Groundwater (Ci)	1943–2018 Percent Activity Transferred to Groundwater [a]	Activity Remaining in Vadose Zone at 2018 (Ci)	Percent Activity Remaining in Vadose Zone at 2018 [a]
Radionuclide Group 2					
U-232	3.153E-02	2.905E-07	<0.1	1.886E-02	59.8
U-233	1.336E+00	4.720E-06	<0.1	1.336E+00	>99.9
U-234	3.828E+00	3.946E-02	1.0	3.791E+00	99.0
U-235	1.718E-01	1.780E-03	1.0	1.701E-01	99.0
U-236	3.804E-02	3.406E-04	0.9	3.772E-02	99.2
U-238	3.887E+00	4.015E-02	1.0	3.849E+00	99.0
Th-230	3.193E-13	4.618E-11	See note c	7.096E-04	See note c
Ra-226	1.365E-13	1.253E-13	See note c	2.128E-07	See note c

a. The percentage or sum of percentages could differ slightly from 100 due to numerical error.

b. The radionuclide has no 1943–2018 inventory.

c. Th-230 and Ra-226 are present as source inventory and daughter products of U-234. Activity percentages are therefore not calculated as they may be greater than 100.

Table 7-2. B Complex Model Radionuclide Activity Transfer to Groundwater from 2018–12070 and Remaining Activity in the Vadose Zone at 12070

Radionuclide	1943–12070 Inventory Released to Vadose Zone (Ci)	2018–12070 Activity Transferred to Groundwater (Ci)	2018–12070 Percent Activity Transferred to Groundwater [a]	Activity Remaining in Vadose Zone at 12070 (Ci)	Percent Activity Remaining in Vadose Zone at 12070 [a]
Radionuclide Group 1					
C-14	1.126E+01	6.815E+00	60.5	1.477E-03	<0.1
Cl-36	0.000E+00	0.000E+00	See note b	0.000E+00	See note b
H-3	5.913E+03	1.243E+01	0.2	1.116E-10	<0.1
I-129	2.704E-01	2.547E-01	94.2	1.047E-02	3.9
Np-237	1.217E+00	0.000E+00	0.0	1.213E+00	99.7
Re-187	0.000E+00	0.000E+00	See note b	0.000E+00	See note b
Sr-90	2.836E+04	0.000E+00	0.0	2.035E-05	<0.1
Tc-99	1.888E+02	1.257E+02	66.6	1.353E+00	0.7
Radionuclide Group 2					
U-232	3.198E-02	2.208E-05	0.1	0.000E+00	0.0
U-233	1.454E+00	4.318E-03	0.3	1.388E+00	95.5
U-234	3.899E+00	1.017E+00	26.1	2.768E+00	71.0
U-235	1.748E-01	4.590E-02	26.2	1.274E-01	72.9
U-236	3.908E-02	8.700E-03	22.3	3.008E-02	77.0
U-238	4.012E+00	1.035E+00	25.8	2.943E+00	73.3
Th-230	1.090E-04	5.203E-07	See note c	7.689E-02	See note c
Ra-226	1.078E-03	5.273E-07	See note c	1.705E-03	See note c

a. The percentage or sum of percentages could differ slightly from 100 due to numerical error.

b. The radionuclide has no 1943–12070 inventory.

c. Th-230 and Ra-226 are both be present as source inventory and daughter products of U-234. Activity percentages are therefore not calculated as they may be greater than 100.

Table 7-3. Activity Removed Due to RTD Remediation in the B Complex Model

216-B-51			
Radionuclide	**Activity Removed (Ci)**	**Radionuclide**	**Activity Removed (Ci)**
C-14	0.000E+00	U-232	4.896E-11
Cl-36	0.000E+00	U-233	0.000E+00
H-3	0.000E+00	U-234	4.970E-06
I-129	2.200E-10	U-235	2.219E-07
Np-237	3.174E-05	U-236	5.680E-08
Re-187	0.000E+00	U-238	5.066E-06
Sr-90	1.598E-02	Th-230	1.733E-09
Tc-99	0.000E+00	Ra-226	5.763E-13
Total			
Radionuclide	**Activity Removed (Ci)**	**Radionuclide**	**Activity Removed (Ci)**
C-14	0.000E+00	U-232	4.896E-11
Cl-36	0.000E+00	U-233	0.000E+00
H-3	0.000E+00	U-234	4.970E-06
I-129	2.200E-10	U-235	2.219E-07
Np-237	3.174E-05	U-236	5.680E-08
Re-187	0.000E+00	U-238	5.066E-06
Sr-90	1.598E-02	Th-230	1.733E-09
Tc-99	0.000E+00	Ra-226	5.763E-13

RTD = remove treat, and dispose.

Further description of the fate and transport of each radionuclide is outlined in Sections 7.1 through 7.16. Results presented in the sections show cumulative activity of the radionuclide discharged to groundwater over the historical (1943–2018) and forecast (2018–12070) simulations, and figures showing the cumulative activity released from the sources compared to the transfer rate to groundwater for the historical (1943–2018) and entire (1943–12070) modeled periods. For H-3, I-129, Tc-99, and mobile U-238, constituents with a relatively large inventory that could potentially contribute to dose, additional figures were included detailing the radionuclide flux to groundwater.

7.1 C-14 Fate and Transport Results

This model simulated the release and transport of C-14. The cumulative discharge of C-14 into groundwater is shown aggregated by P2R grid cell in Figure 7-1 and Figure 7-2 for 1943–2018 and 2018–12070, respectively. The inventory released to the B Complex model and the transfer of C-14 to groundwater are shown from 1943–2018 in Figure 7-3 and from 1943–12070 in Figure 7-4.

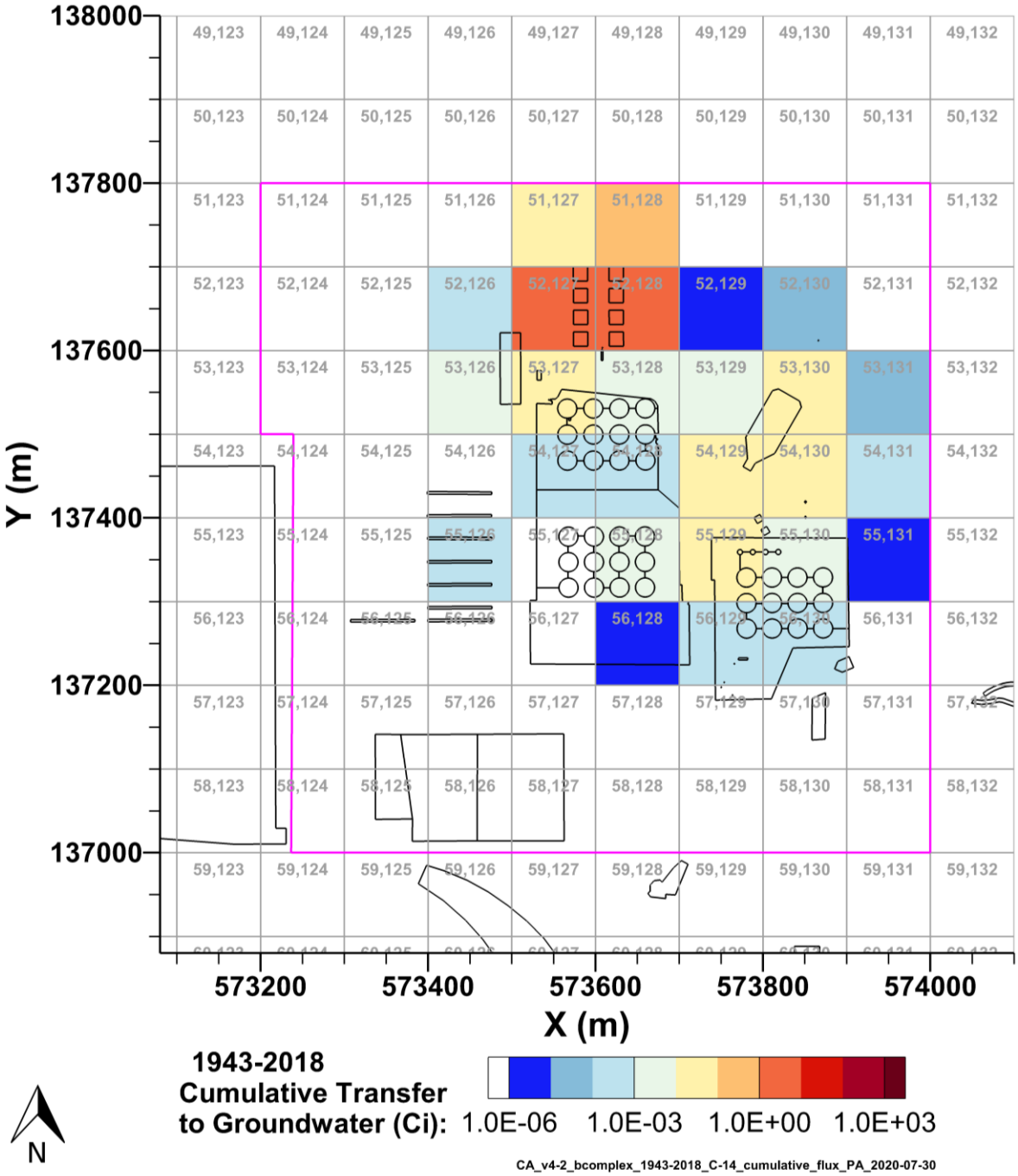

Note: source zone outlined in pink.

Figure 7-1. Cumulative C-14 Activity Discharged to Groundwater from the B Complex Model from 1943–2018 per P2R Grid Cell

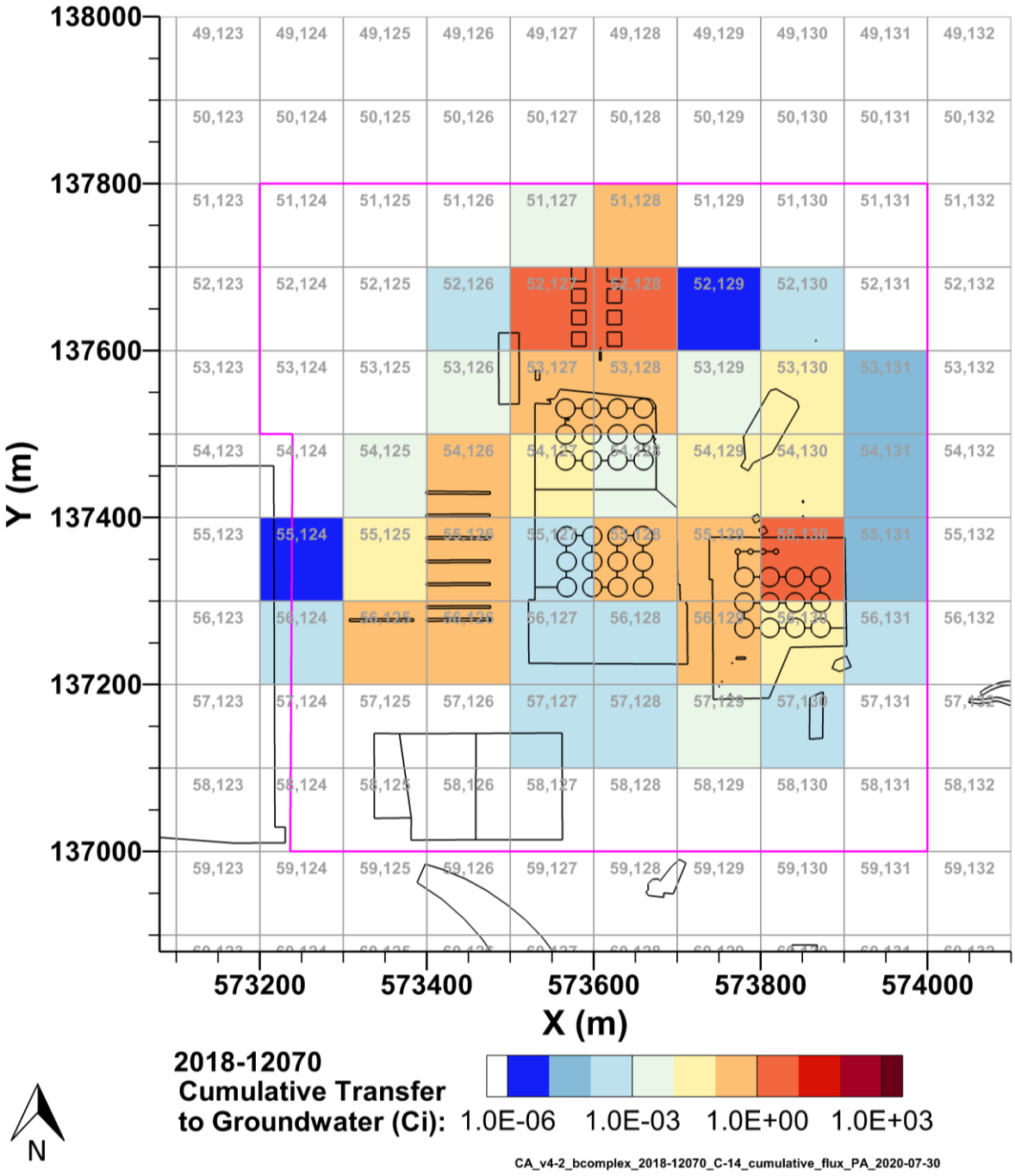

Note: source zone outlined in pink.

Figure 7-2. Cumulative C-14 Activity Discharged to Groundwater from the B Complex Model from 2018–12070 per P2R Grid Cell

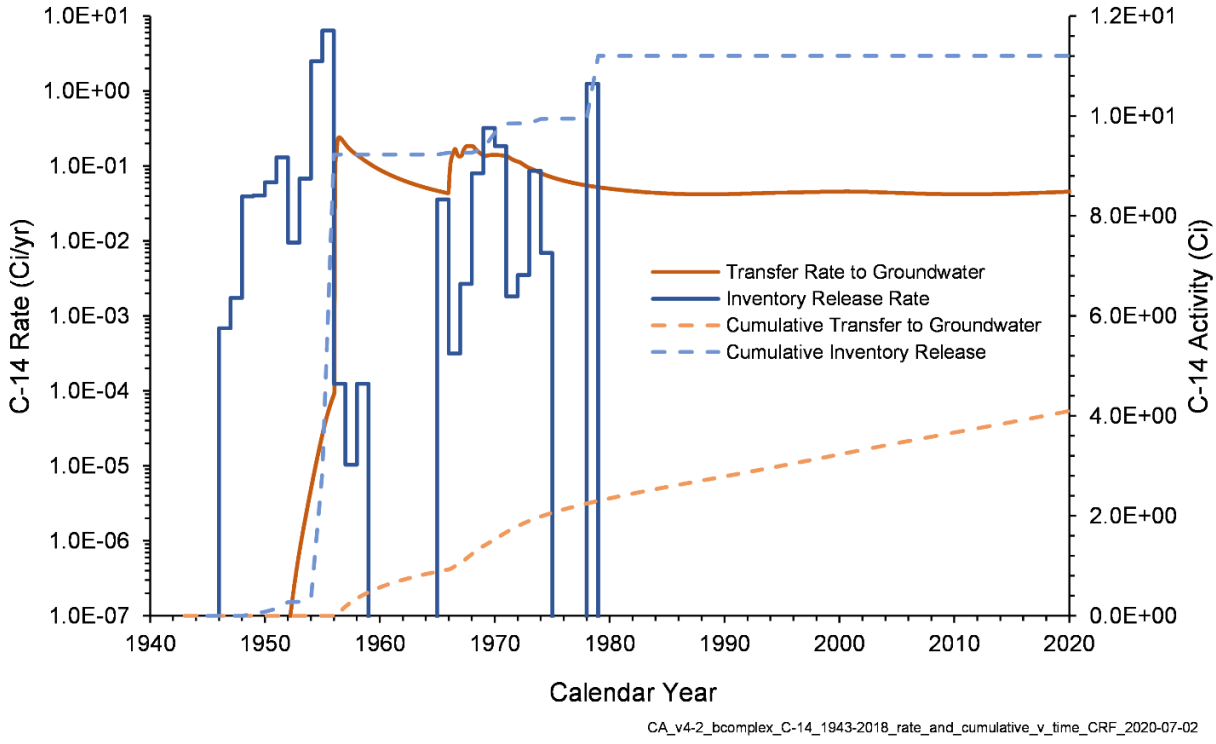

Figure 7-3. C-14 Inventory Release from Waste Sites and Transfer to Groundwater for the B Complex Model from 1943–2018

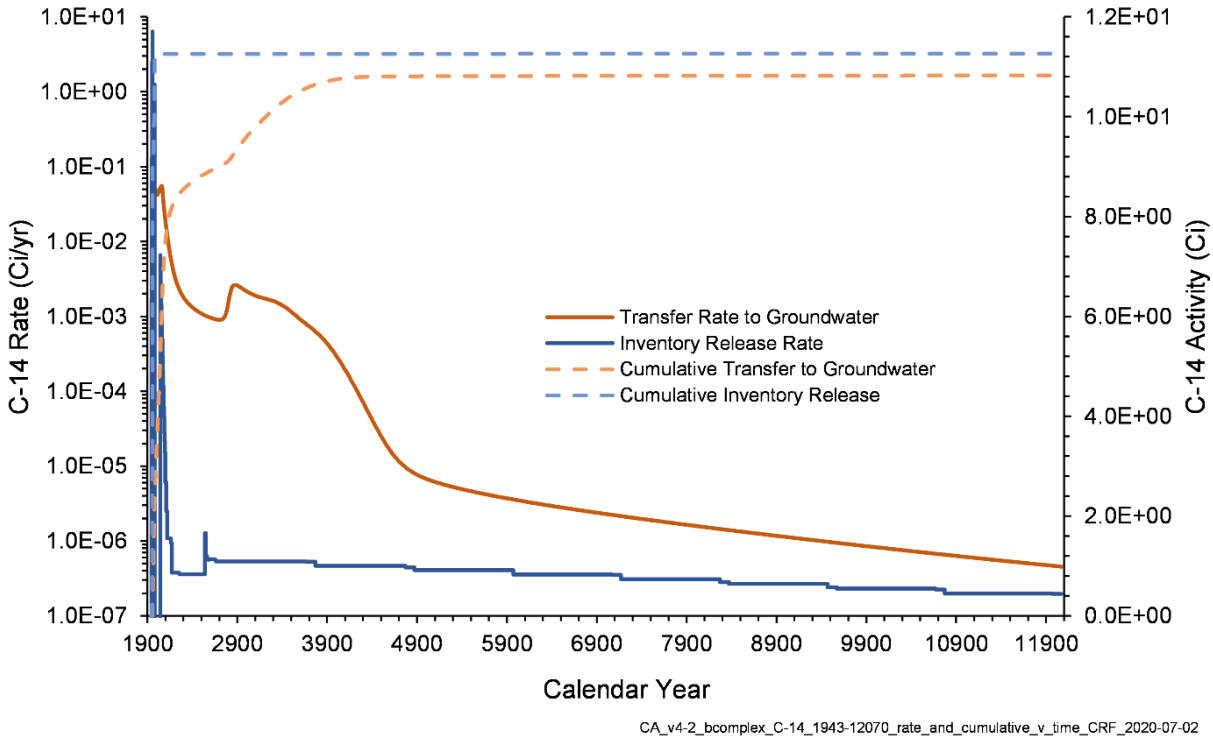

Figure 7-4. C-14 Inventory Release from Waste Sites and Transfer to Groundwater for the B Complex Model from 1943–12070

7.2 Cl-36 Fate and Transport Results

Due to a lack of inventory, transport of Cl-36 was not calculated in this model.

7.3 H-3 Fate and Transport Results

This model simulated release and transport of H-3. The cumulative discharge of H-3 into groundwater is shown aggregated by P2R grid cell in Figure 7-5 and Figure 7-6 for 1943–2018 and 2018–12070, respectively. The inventory released to the B Complex model and the transfer of H-3 to groundwater are shown from 1943–2018 in Figure 7-7 and from 1943–12070 in Figure 7-8. Figure 7-9 through Figure 7-16 show the flux of H-3 to groundwater in Ci/yr. These figures are generated at times with peak fluxes (local maxima) and during periods with gradual decline, as shown in Figure 7-7 and Figure 7-8. A figure for 2018, Figure 7-13, is also included to demonstrate the initial flux conditions for the 2018–12070 simulation.

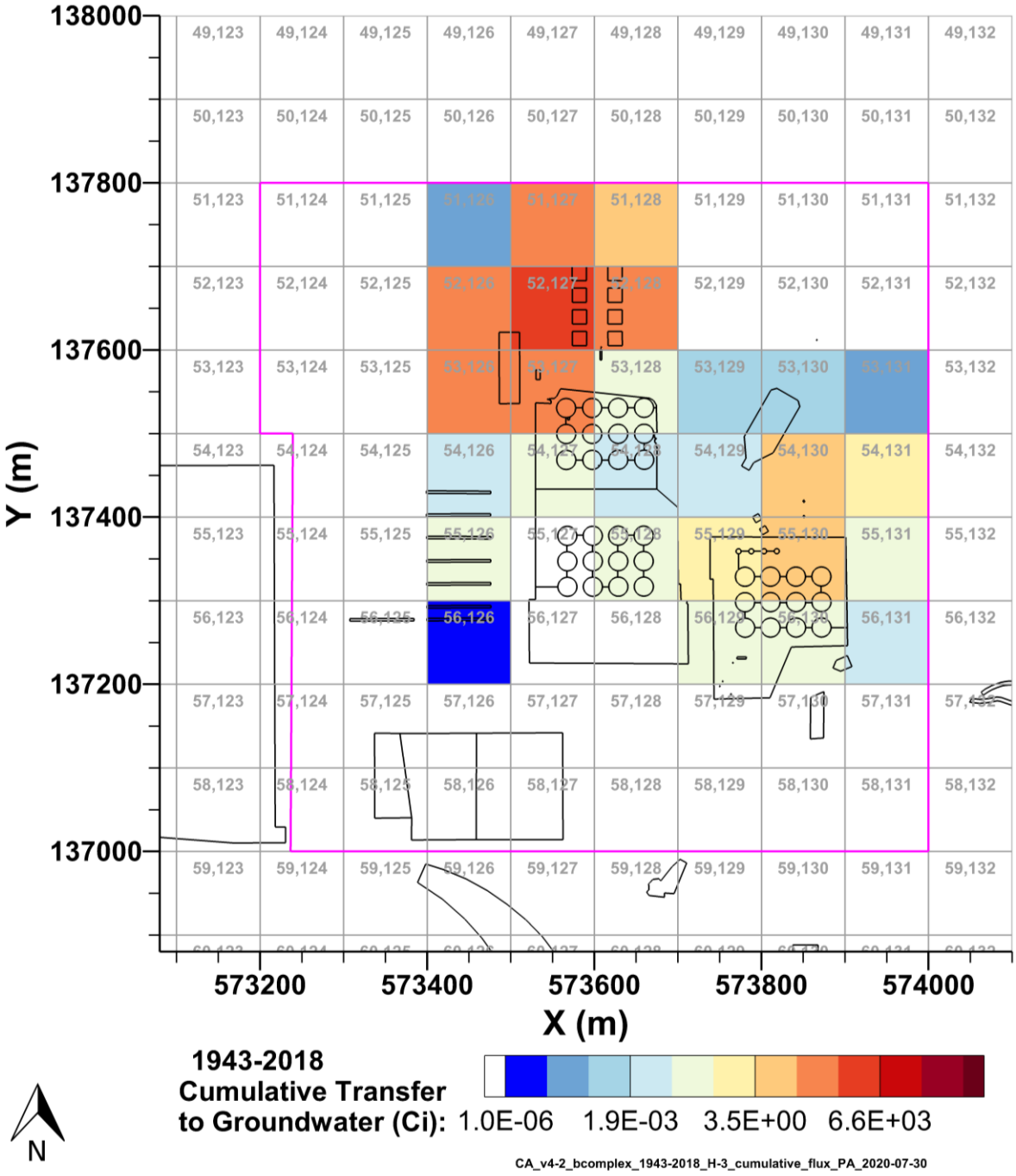

Note: source zone outlined in pink.

Figure 7-5. Cumulative H-3 Activity Discharged to Groundwater from the B Complex Model from 1943–2018 per P2R Grid Cell

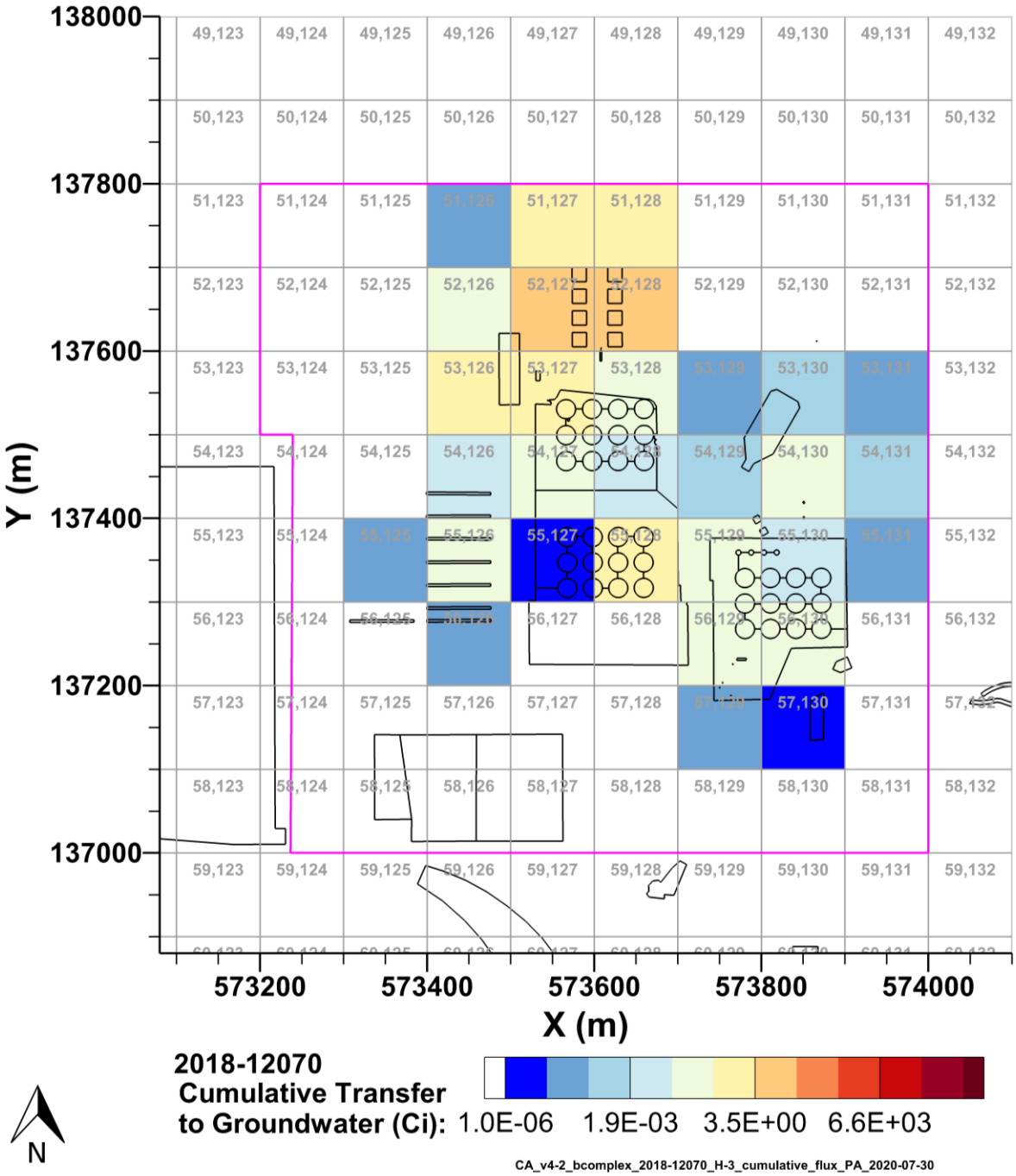

Note: source zone outlined in pink.

Figure 7-6. Cumulative H-3 Activity Discharged to Groundwater from the B Complex Model from 2018–12070 per P2R Grid Cell

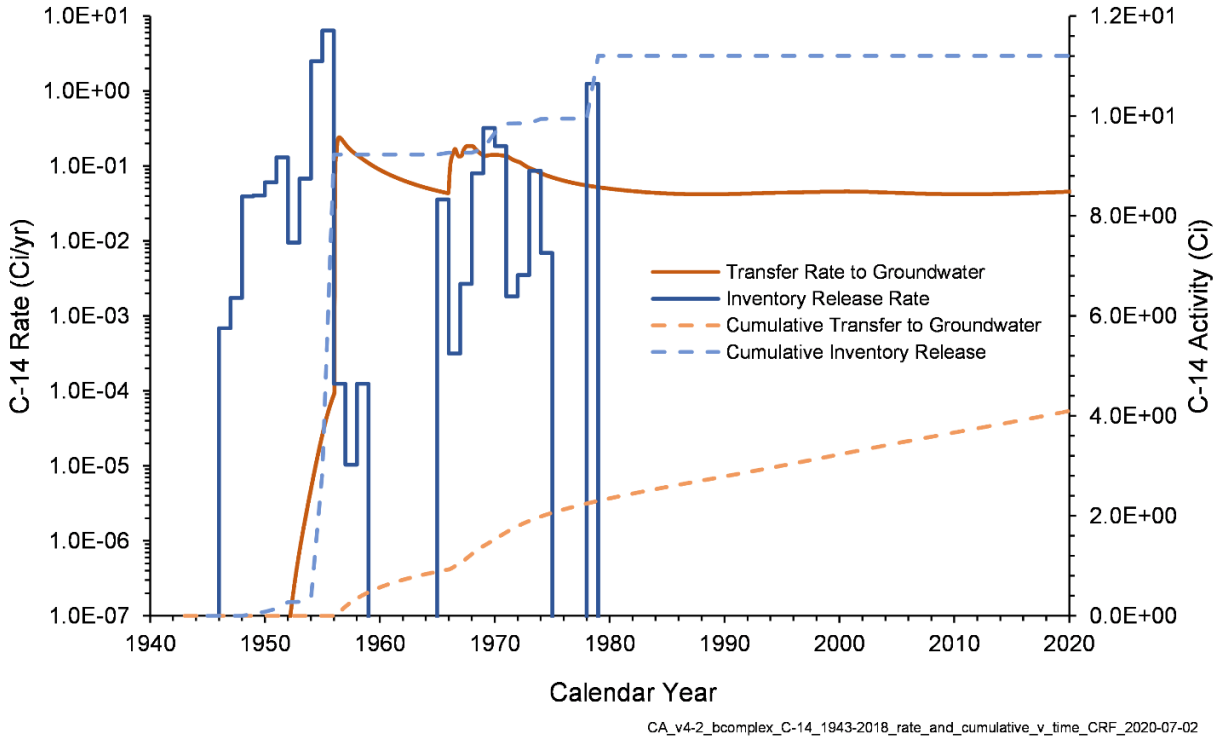

Figure 7-7. H-3 Inventory Release from Waste Sites and Transfer to Groundwater for the B Complex Model from 1943–2018

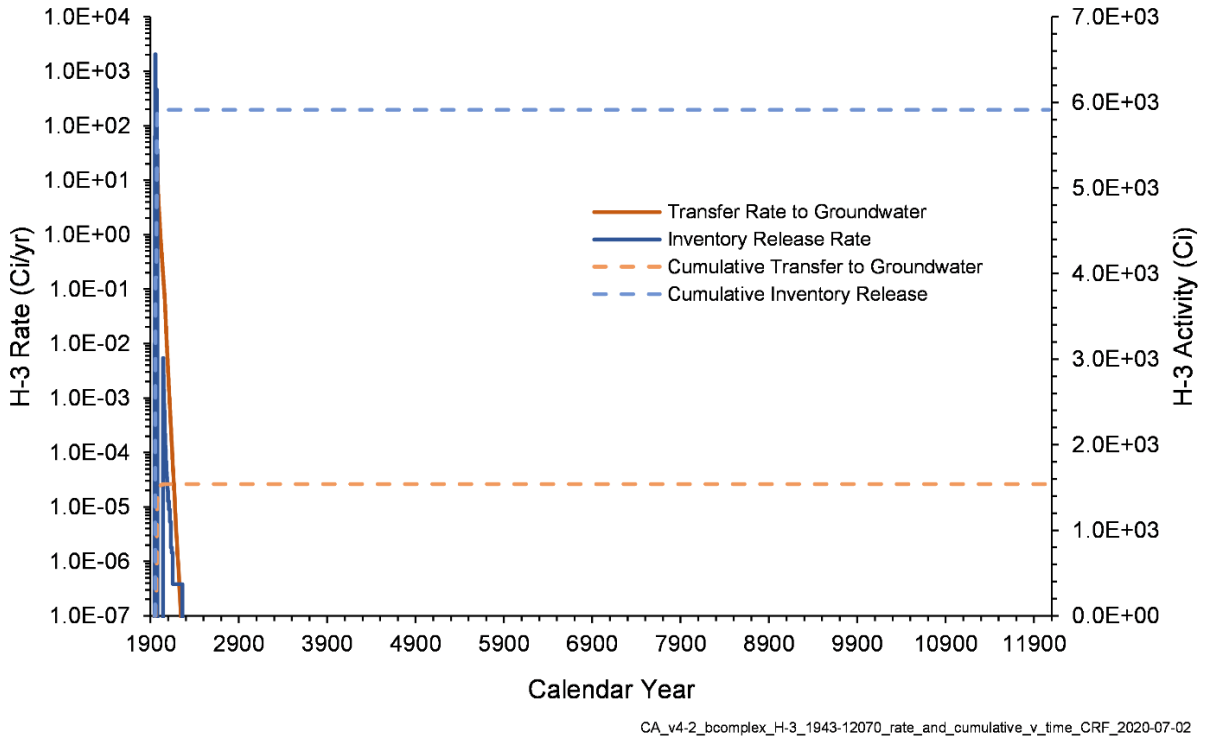

Figure 7-8. H-3 Inventory Release from Waste Sites and Transfer to Groundwater for the B Complex Model from 1943–12070

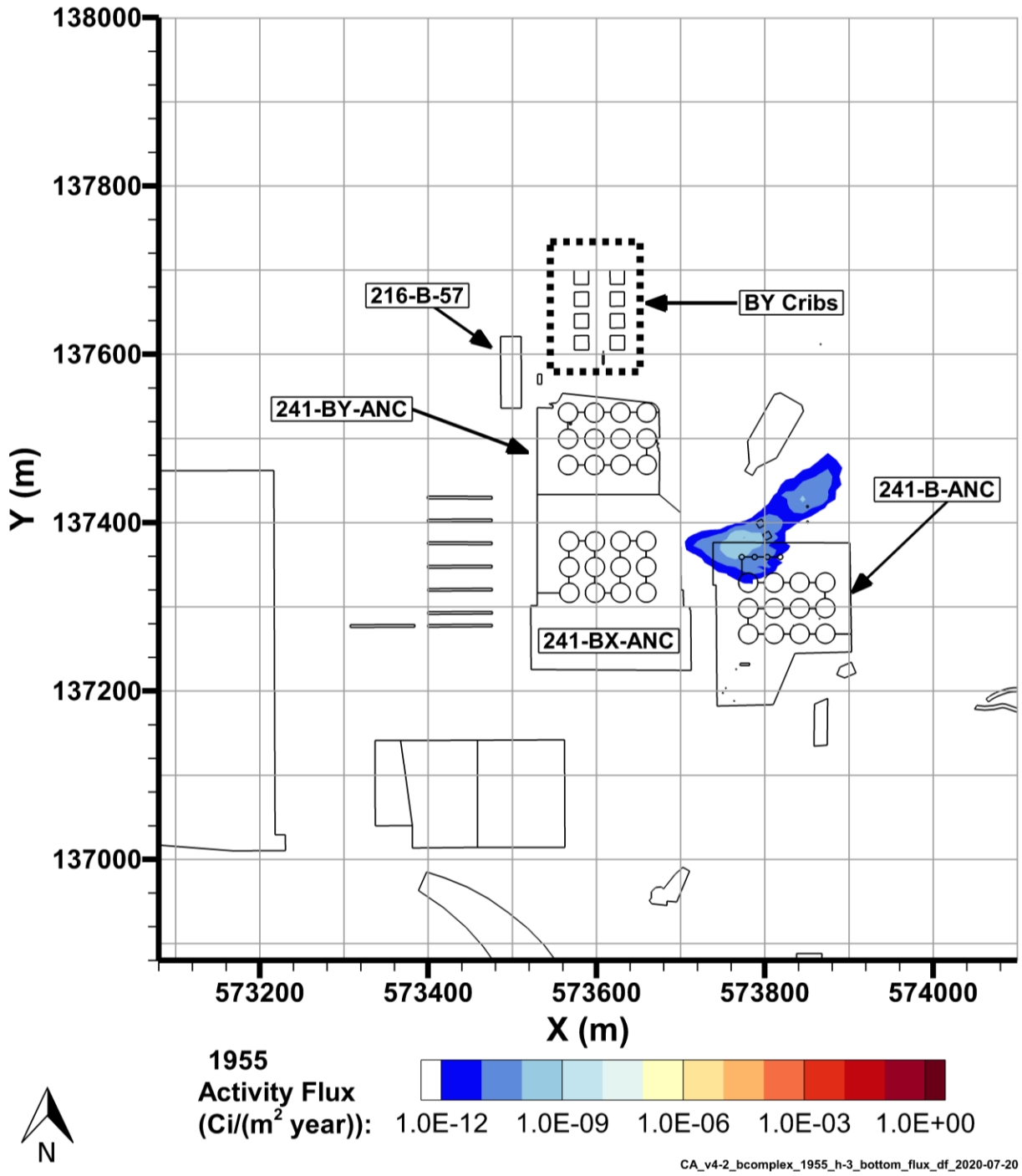

Note: the dashed black lines are used to indicate the waste sites that are collectively referred to as BY Cribs.

Figure 7-9. H-3 Flux to Groundwater, 1955

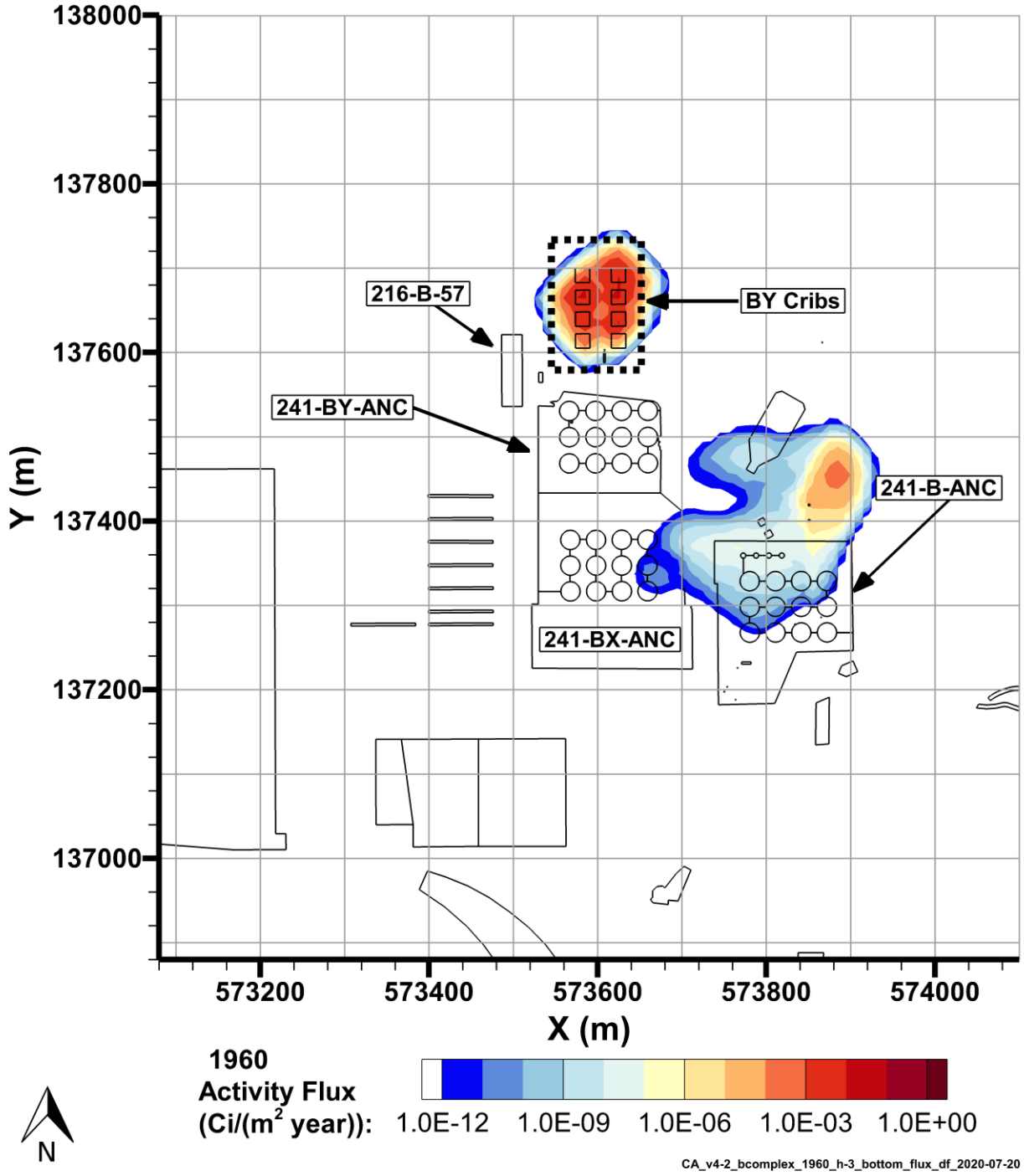

Note: the dashed black lines are used to indicate the waste sites that are collectively referred to as BY Cribs.

Figure 7-10. H-3 Flux to Groundwater, 1960

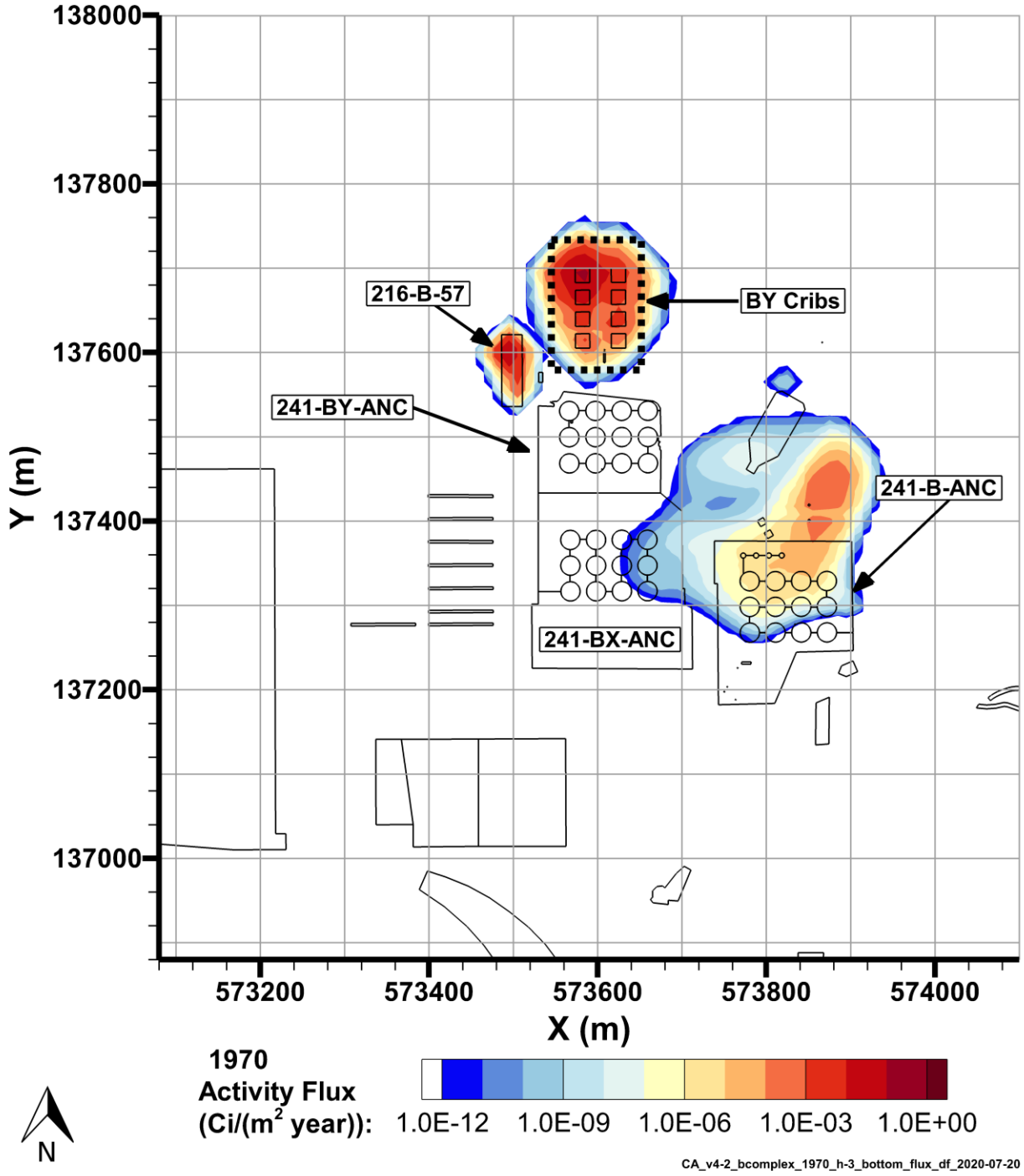

Note: the dashed black lines are used to indicate the waste sites that are collectively referred to as BY Cribs.

Figure 7-11. H-3 Flux to Groundwater, 1970

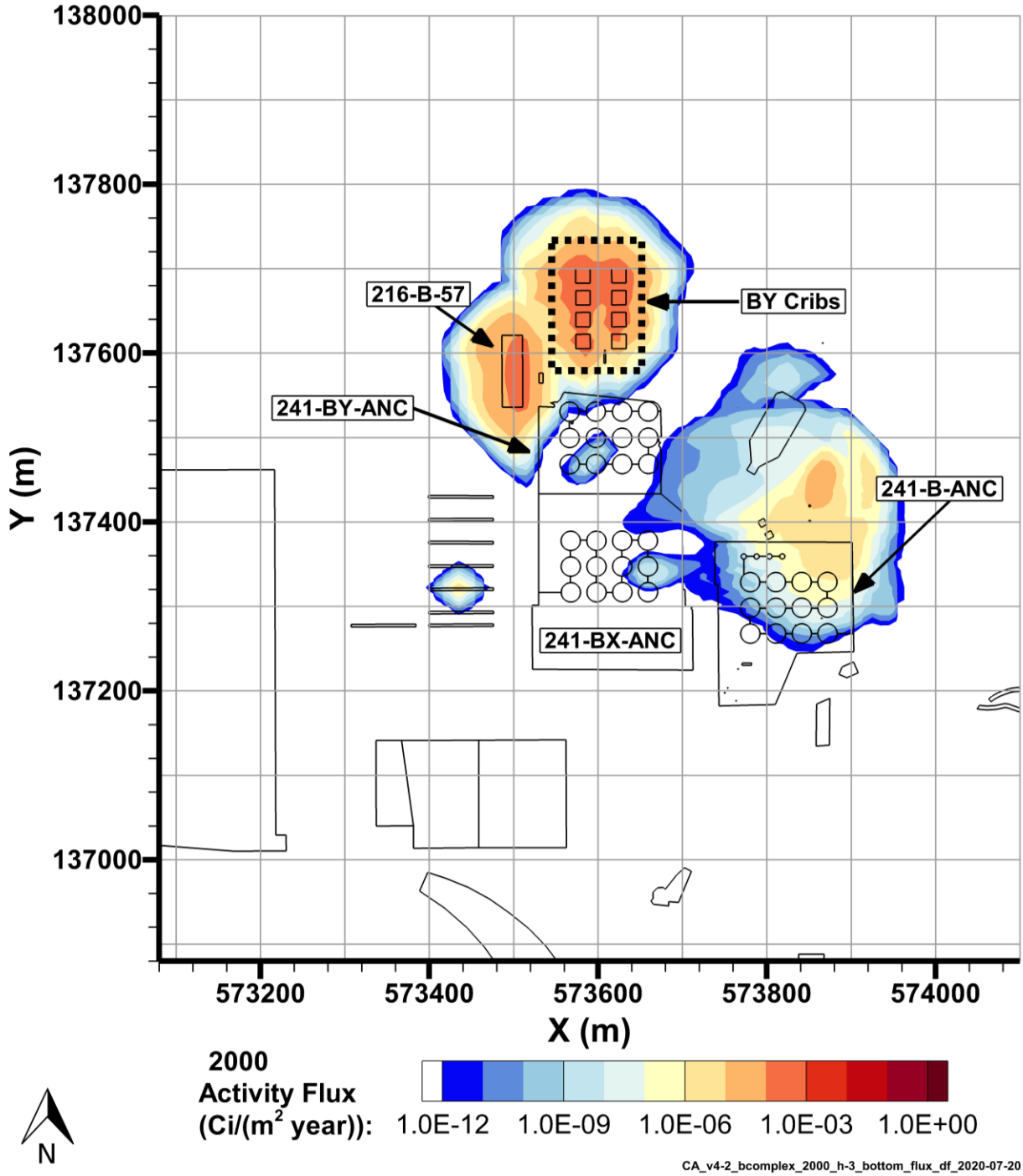

Note: the dashed black lines are used to indicate the waste sites that are collectively referred to as BY Cribs.

Figure 7-12. H-3 Flux to Groundwater, 2000

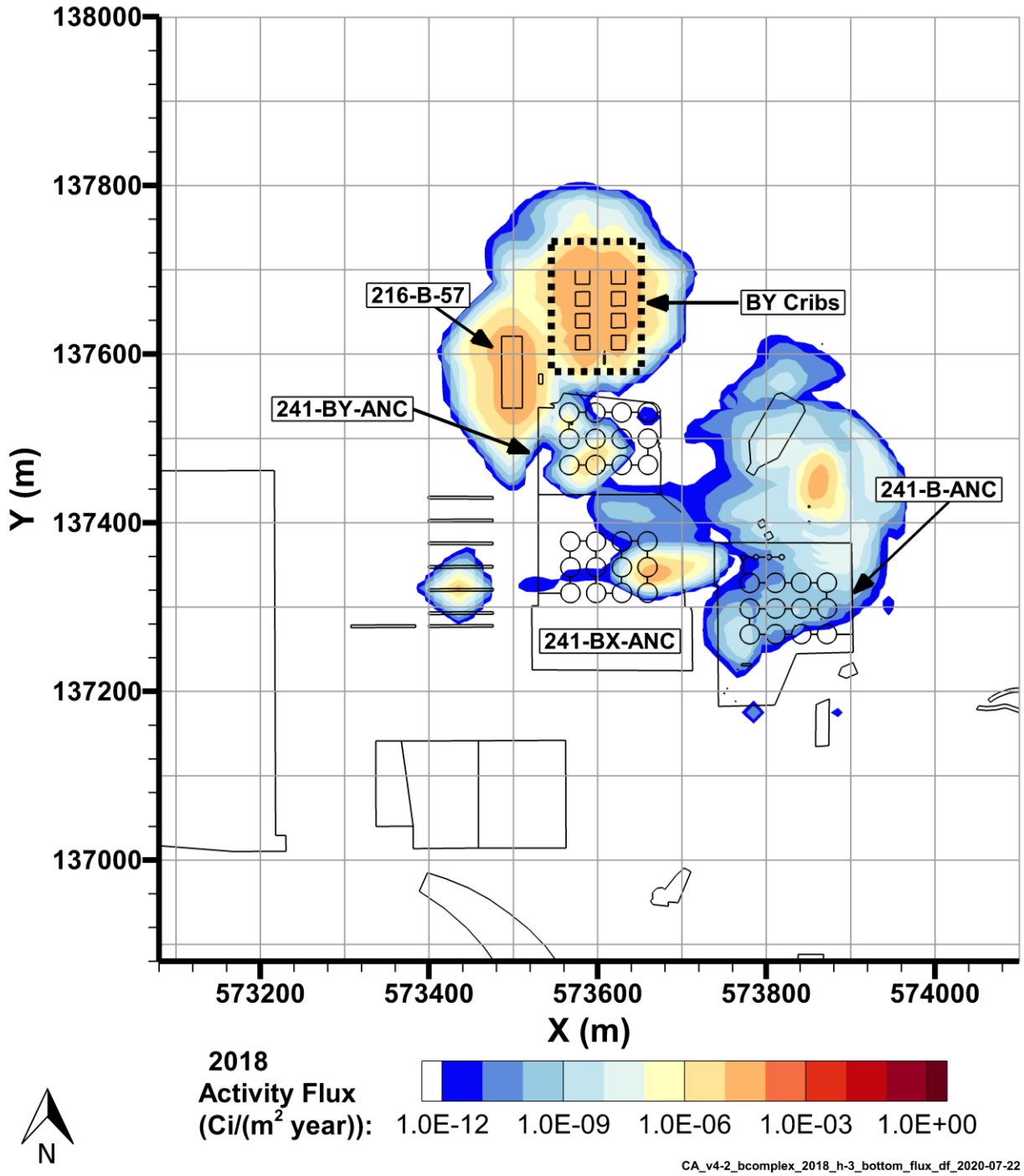

Note: the dashed black lines are used to indicate the waste sites that are collectively referred to as BY Cribs.

Figure 7-13. H-3 Flux to Groundwater, 2018

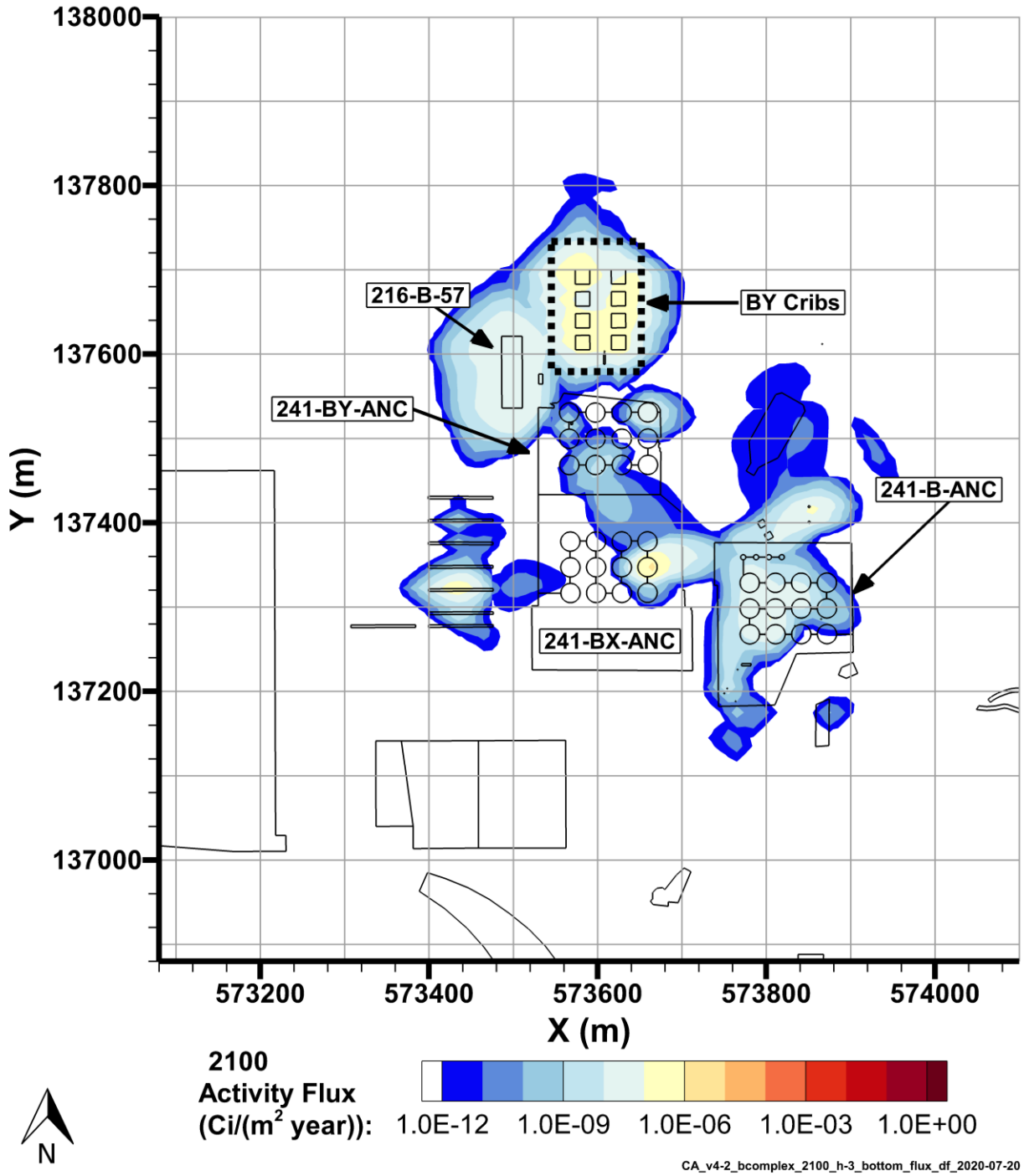

Note: the dashed black lines are used to indicate the waste sites that are collectively referred to as BY Cribs.

Figure 7-14. H-3 Flux to Groundwater, 2100

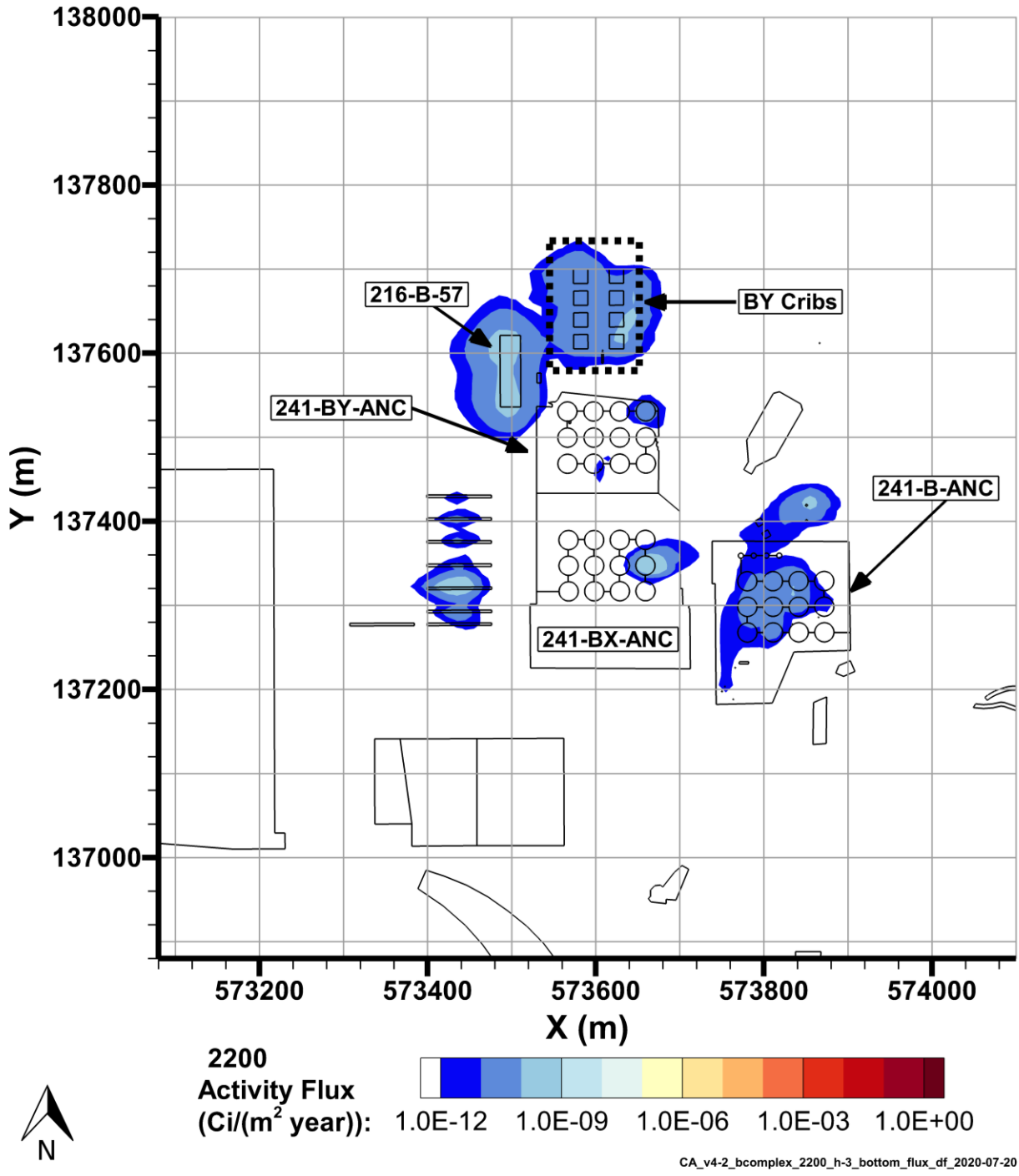

Note: the dashed black lines are used to indicate the waste sites that are collectively referred to as BY Cribs.

Figure 7-15. H-3 Flux to Groundwater, 2200

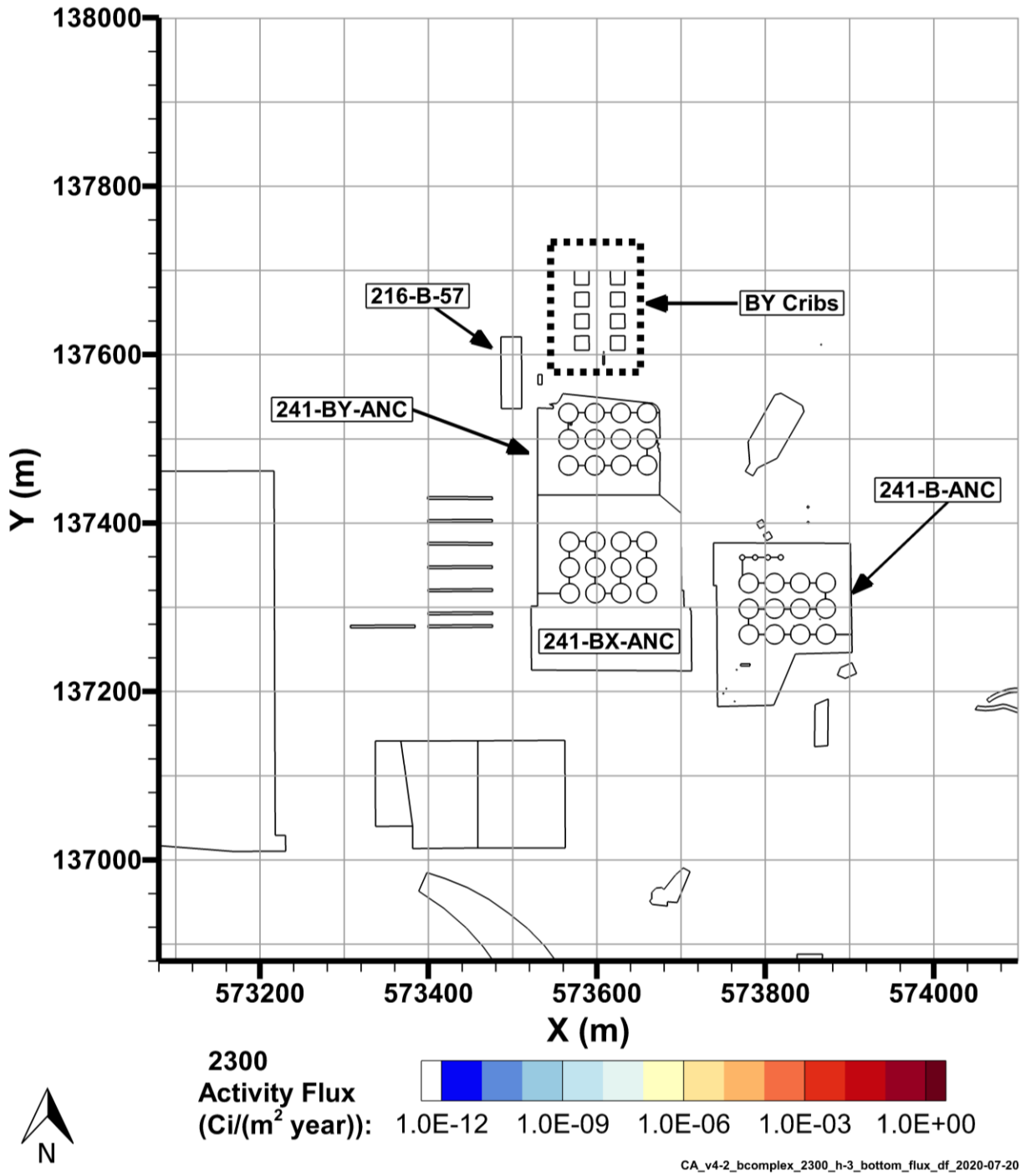

Note: the dashed black lines are used to indicate the waste sites that are collectively referred to as BY Cribs.

Figure 7-16. H-3 Flux to Groundwater, 2300

7.4 I-129 Fate and Transport Results

This model simulated release and transport of I-129. The cumulative discharge of I-129 into groundwater is shown aggregated by P2R grid cell in Figure 7-17 and Figure 7-18 for 1943–2018 and 2018–12070, respectively. The inventory released to the B Complex model and the transfer of I-129 to groundwater are

shown from 1943–2018 in Figure 7-19 and from 1943–12070 in Figure 7-20. Figure 7-21 through Figure 7-27 show the flux of I-129 to groundwater in Ci/yr. These figures are generated at times with peak fluxes (local maxima) and during periods with gradual decline, as shown in Figure 7-19 and Figure 7-20. A figure for 2018, Figure 7-23, is also included to demonstrate the initial flux conditions for the 2018–12070 simulation.

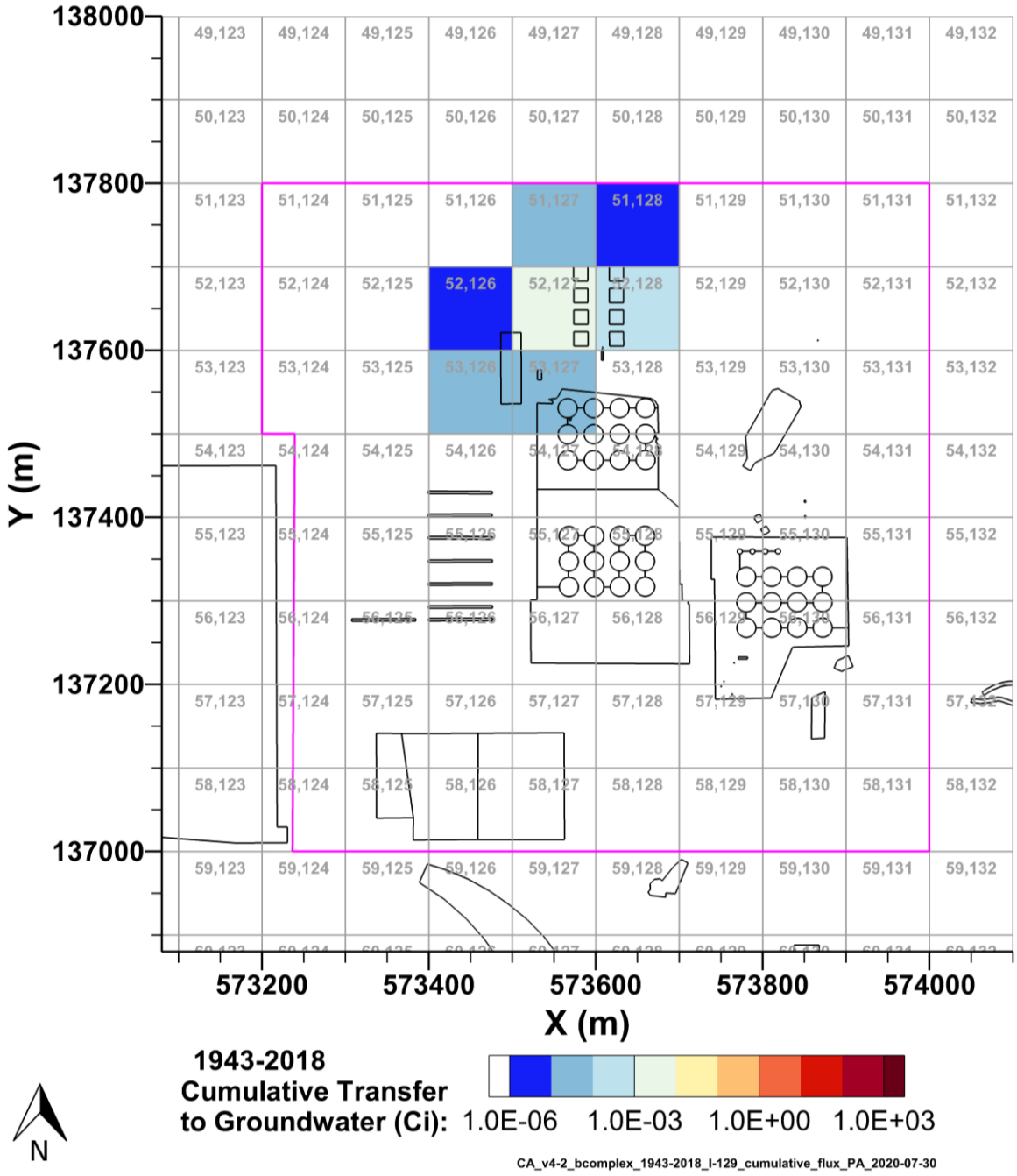

Note: source zone outlined in pink.

Figure 7-17. Cumulative I-129 Activity Discharged to Groundwater from the B Complex Model from 1943–2018 per P2R Grid Cell

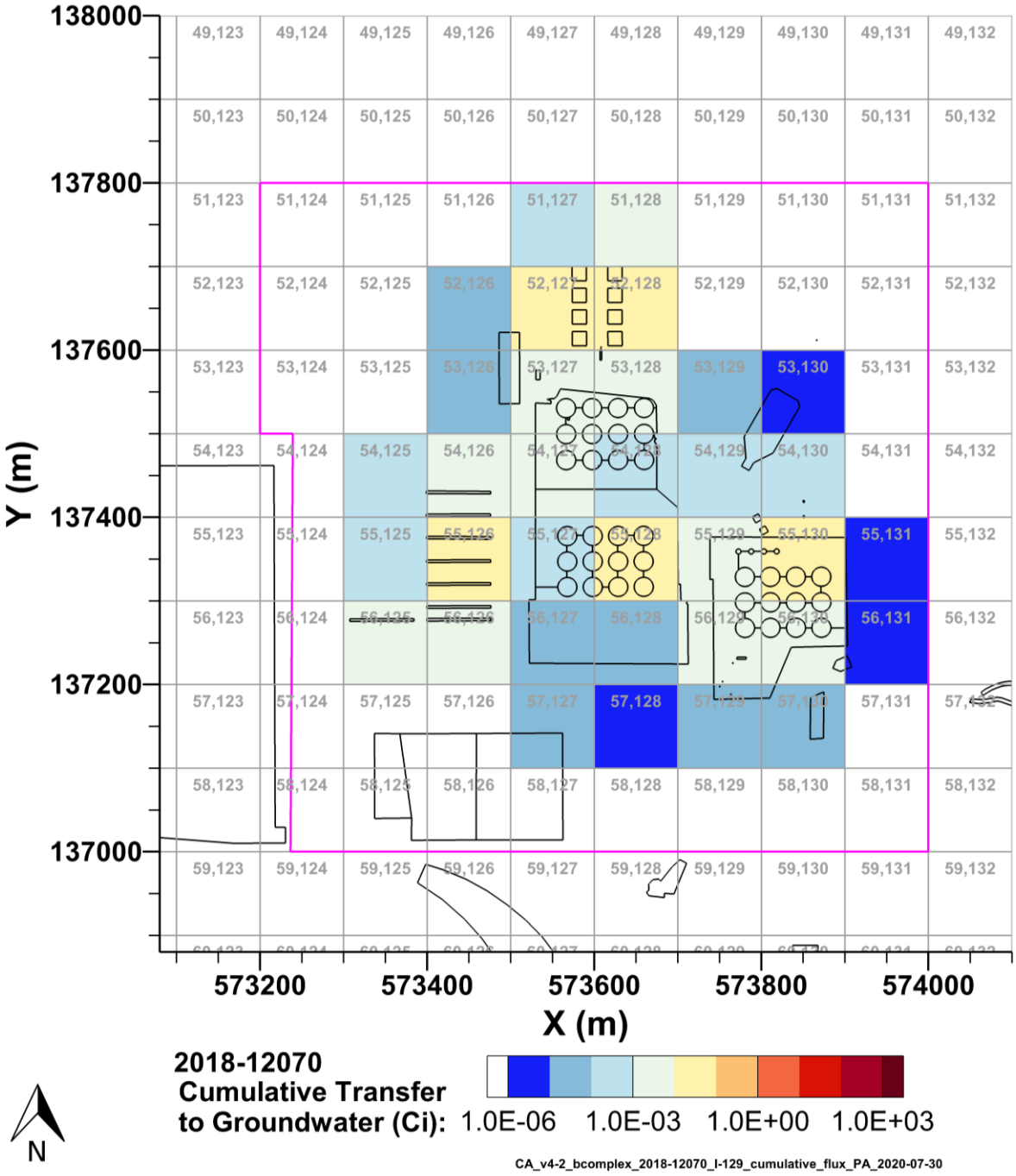

Note: source zone outlined in pink.

Figure 7-18. Cumulative I-129 Activity Discharged to Groundwater from the B Complex Model from 2018–12070 per P2R Grid Cell

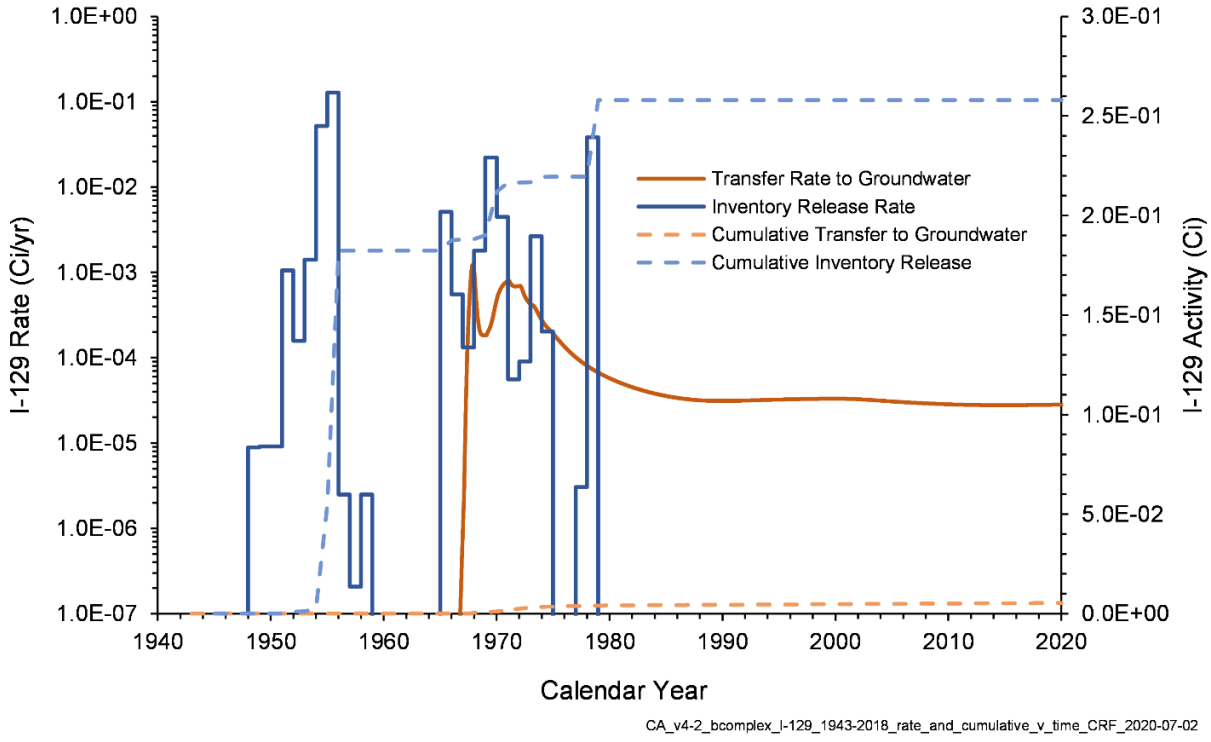

Figure 7-19. I-129 Inventory Release from Waste Sites and Transfer to Groundwater for the B Complex Model from 1943–2018

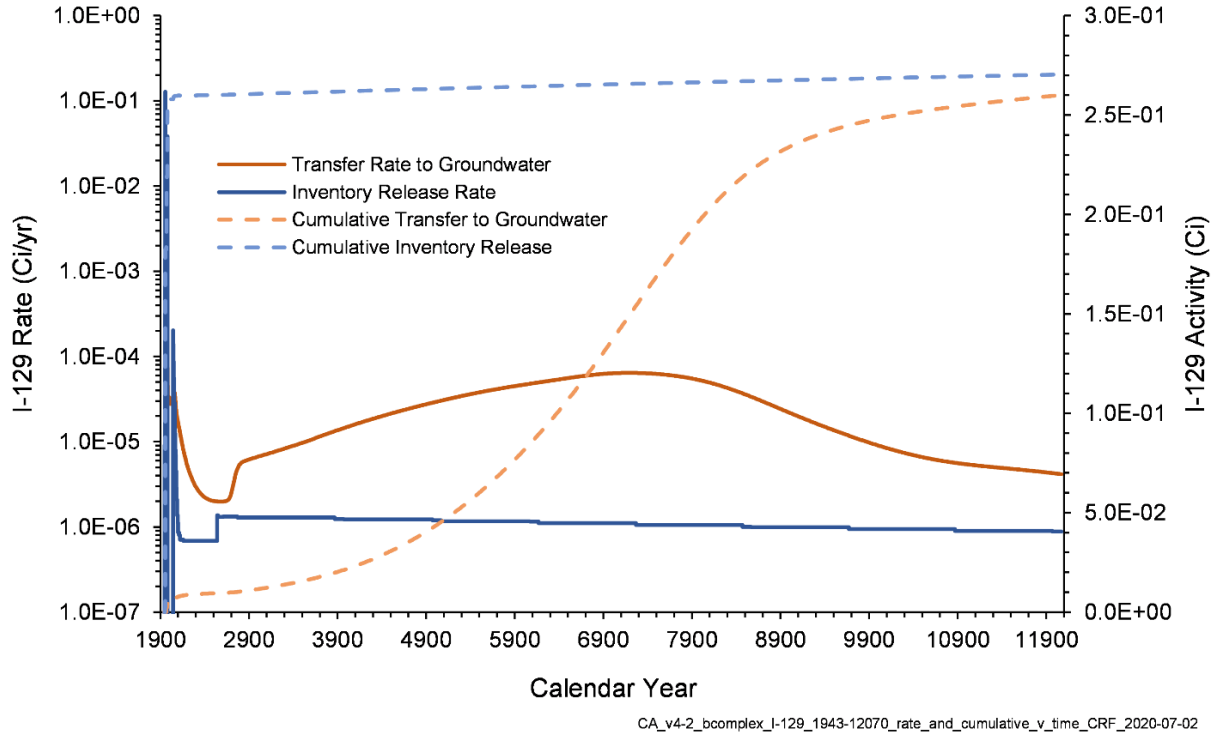

Figure 7-20. I-129 Inventory Release from Waste Sites and Transfer to Groundwater for the B Complex Model from 1943–12070

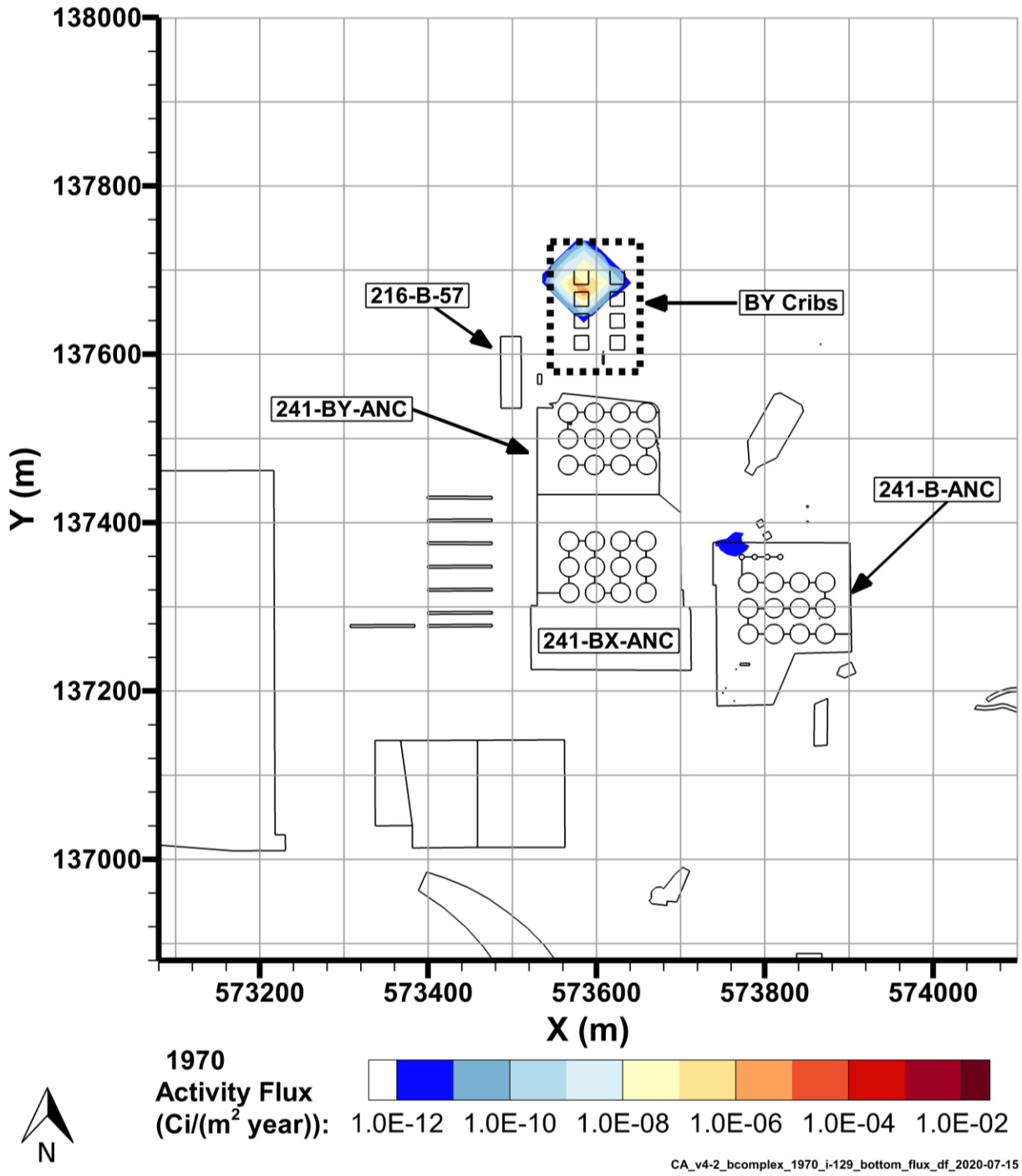

Note: the dashed black lines are used to indicate the waste sites that are collectively referred to as BY Cribs.

Figure 7-21. I-129 Flux to Groundwater, 1970

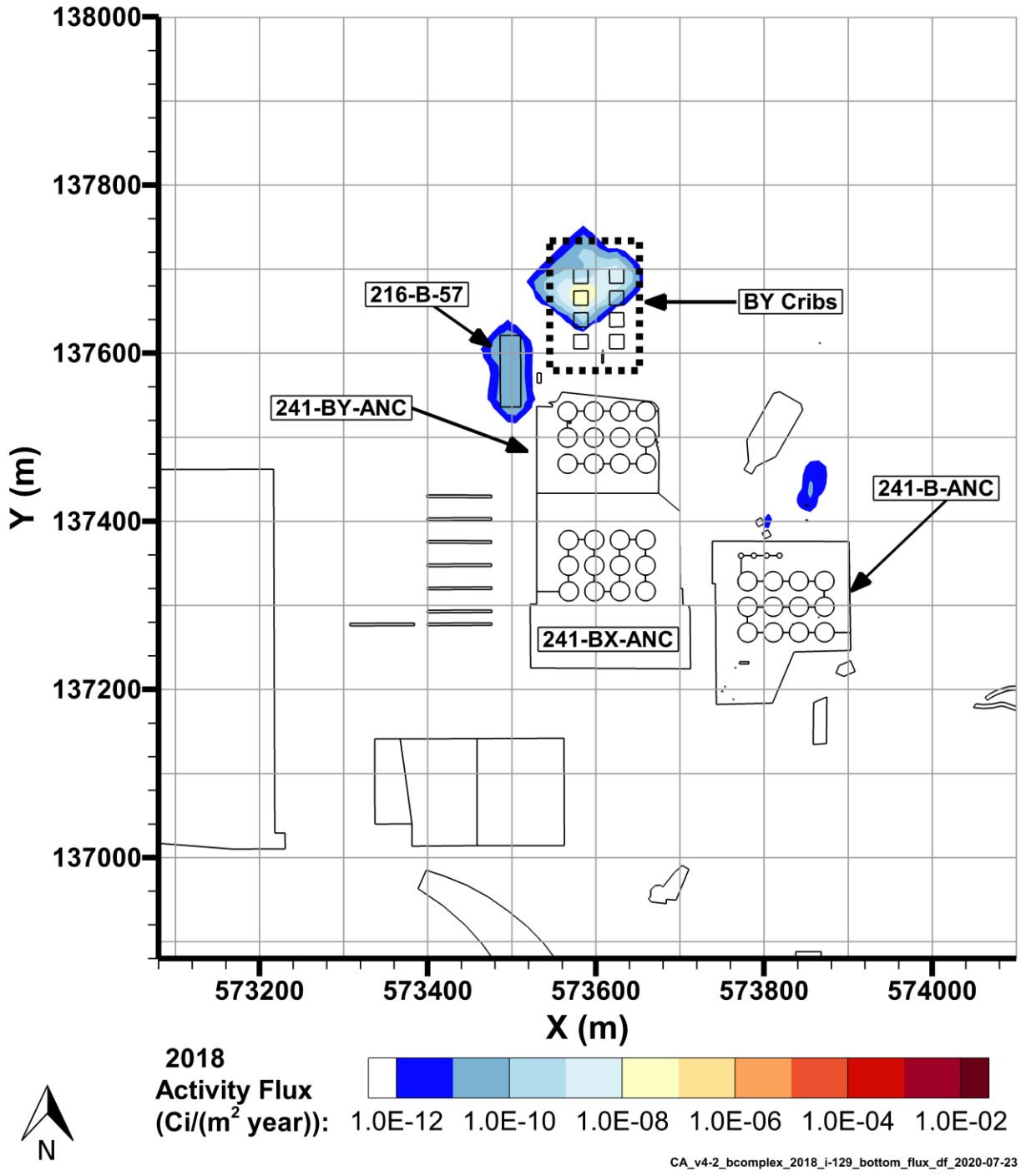

Note: the dashed black lines are used to indicate the waste sites that are collectively referred to as BY Cribs.

Figure 7-22. I-129 Flux to Groundwater, 2018

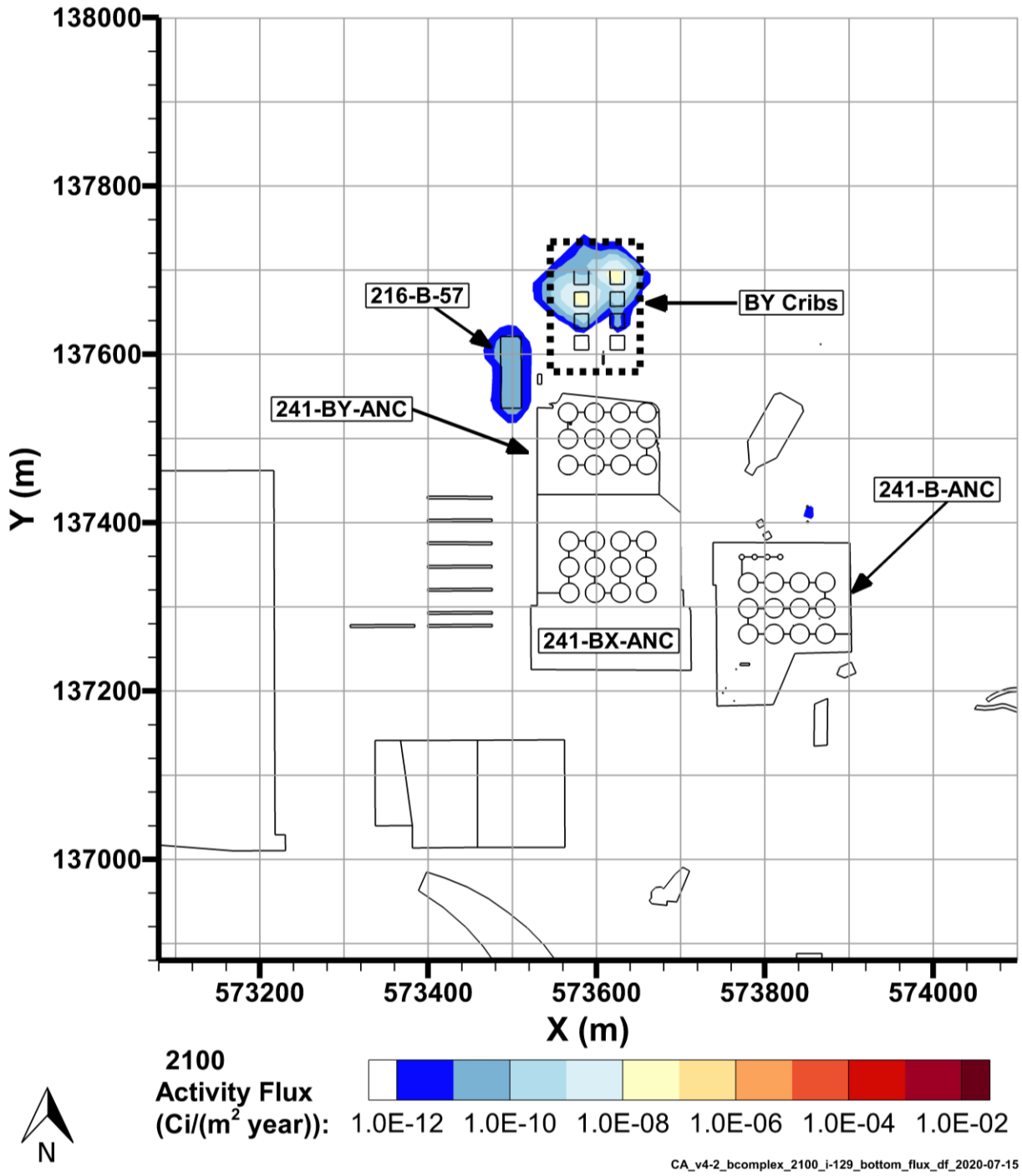

Note: the dashed black lines are used to indicate the waste sites that are collectively referred to as BY Cribs.

Figure 7-23. I-129 Flux to Groundwater, 2100

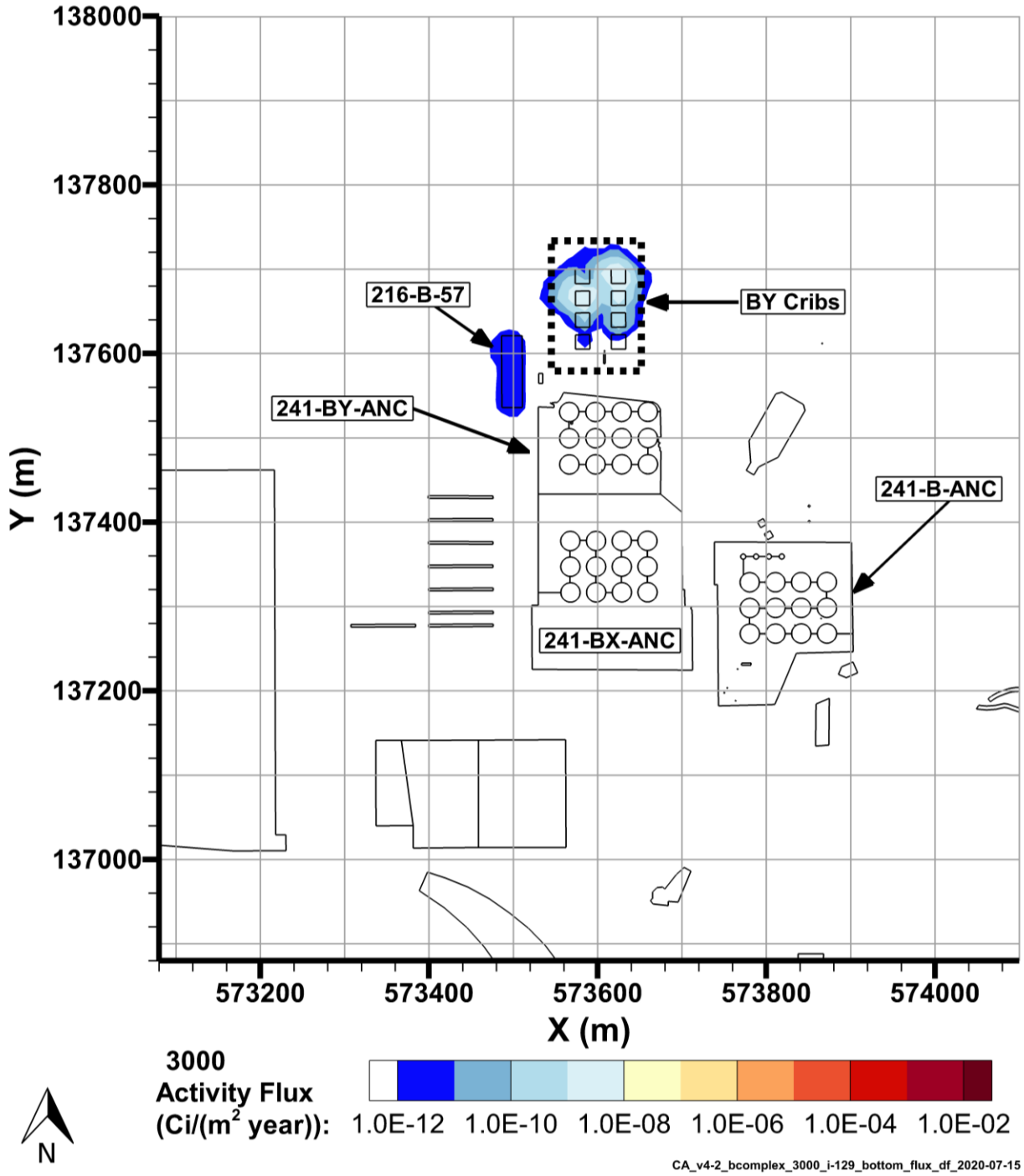

Note: the dashed black lines are used to indicate the waste sites that are collectively referred to as BY Cribs.

Figure 7-24. I-129 Flux to Groundwater, 3000

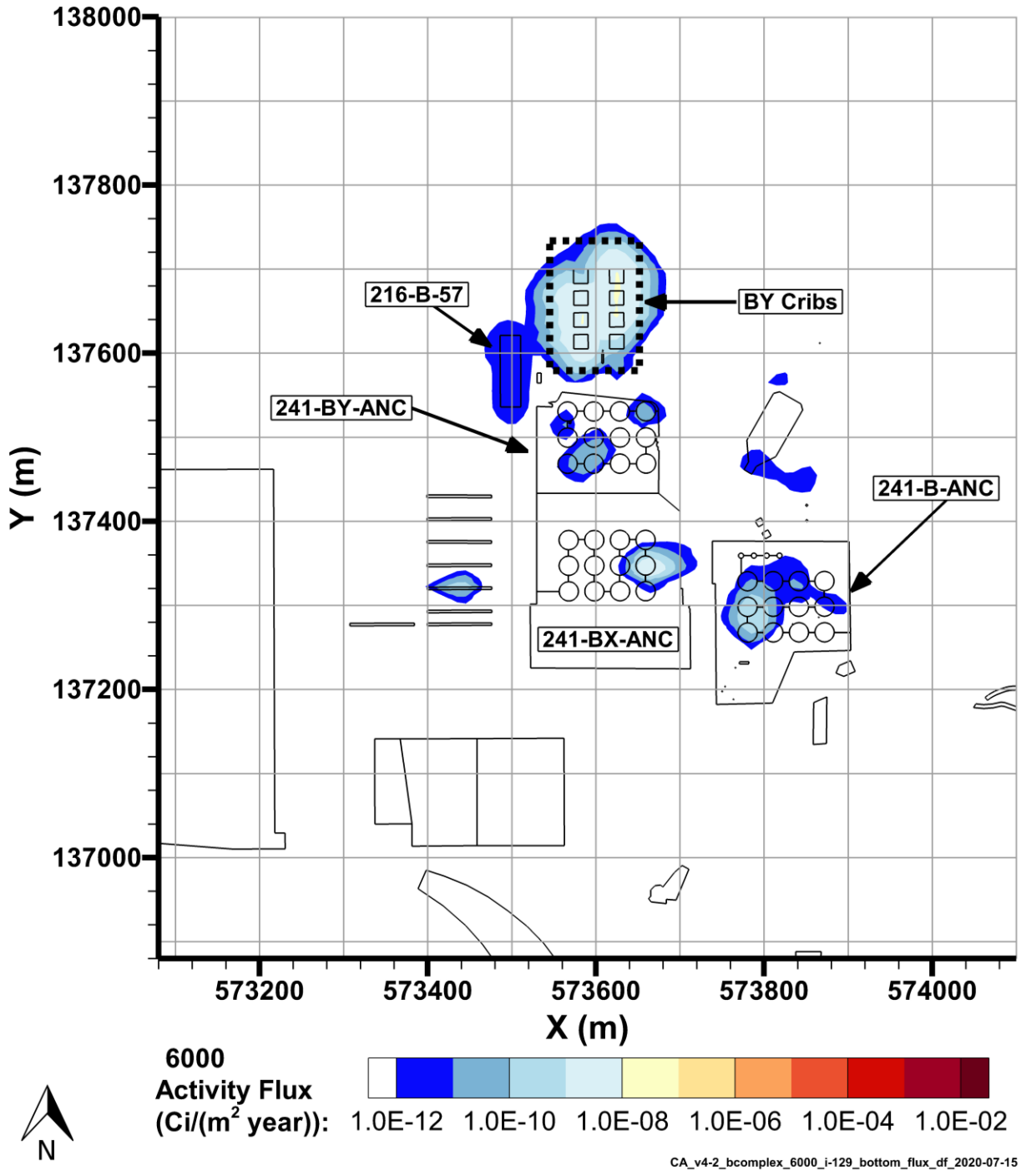

Note: the dashed black lines are used to indicate the waste sites that are collectively referred to as BY Cribs.

Figure 7-25. I-129 Flux to Groundwater, 6000

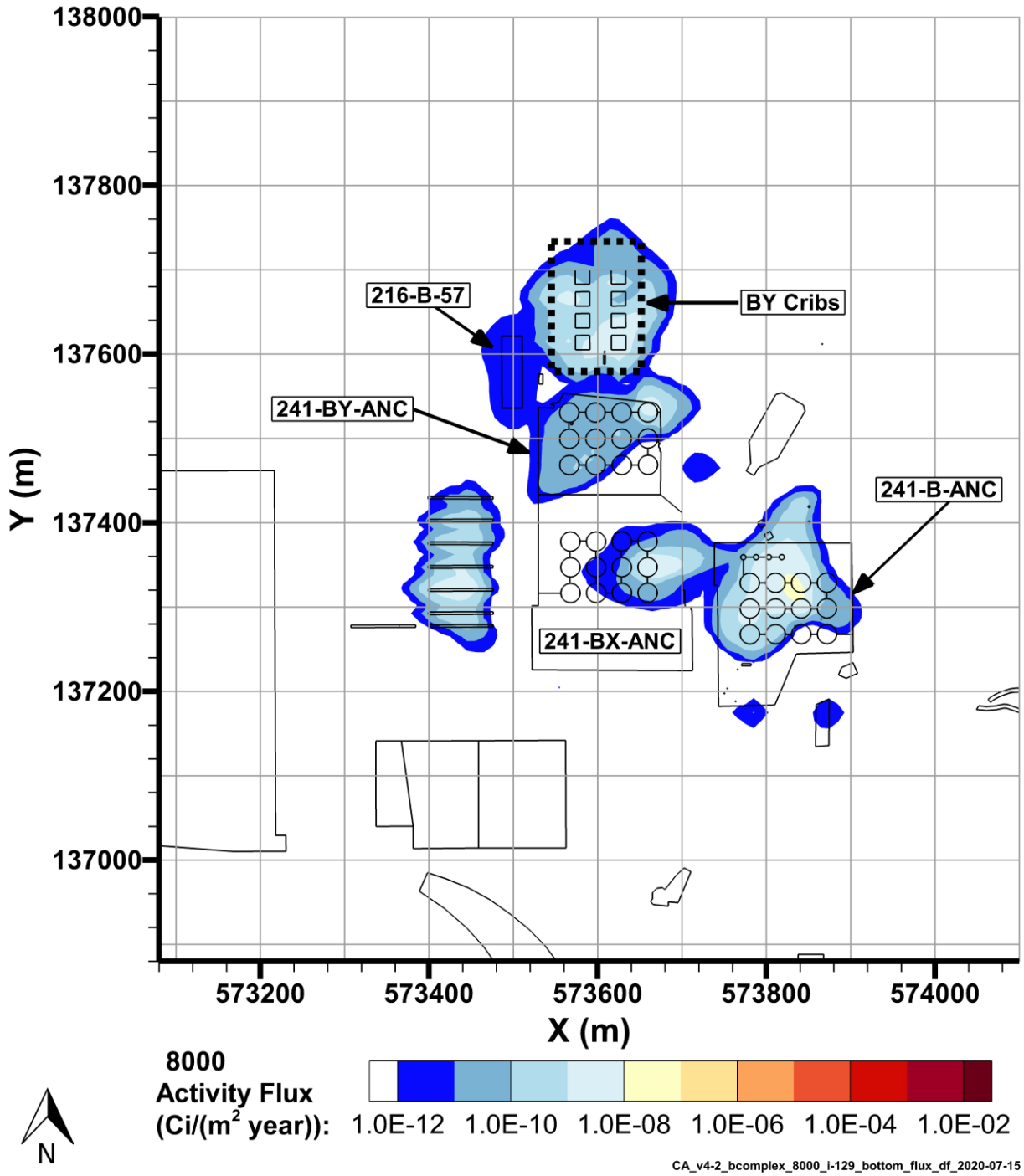

Note: the dashed black lines are used to indicate the waste sites that are collectively referred to as BY Cribs.

Figure 7-26. I-129 Flux to Groundwater, 8000

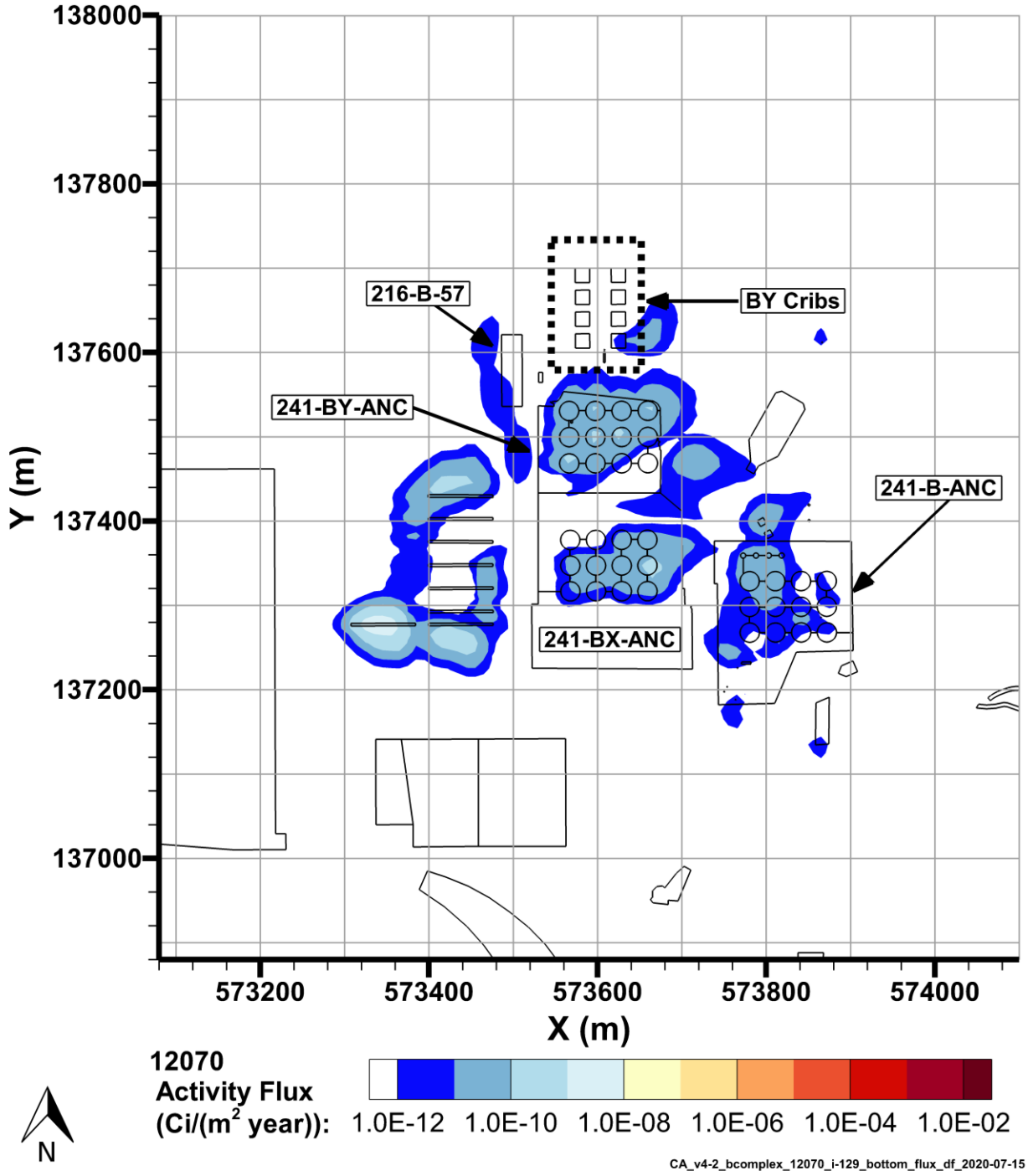

Note: the dashed black lines are used to indicate the waste sites that are collectively referred to as BY Cribs.

Figure 7-27. I-129 Flux to Groundwater, 12070

7.5 Np-237 Fate and Transport Results

This model simulated the release and transport of Np-237. No Np-237 was discharged to groundwater at a cumulative activity above 1.0E-6 Ci per P2R grid. The inventory released to the B Complex model and

the transfer of Np-237 to groundwater are shown from 1943–2018 in Figure 7-28 and from 1943–12070 in Figure 7-29.

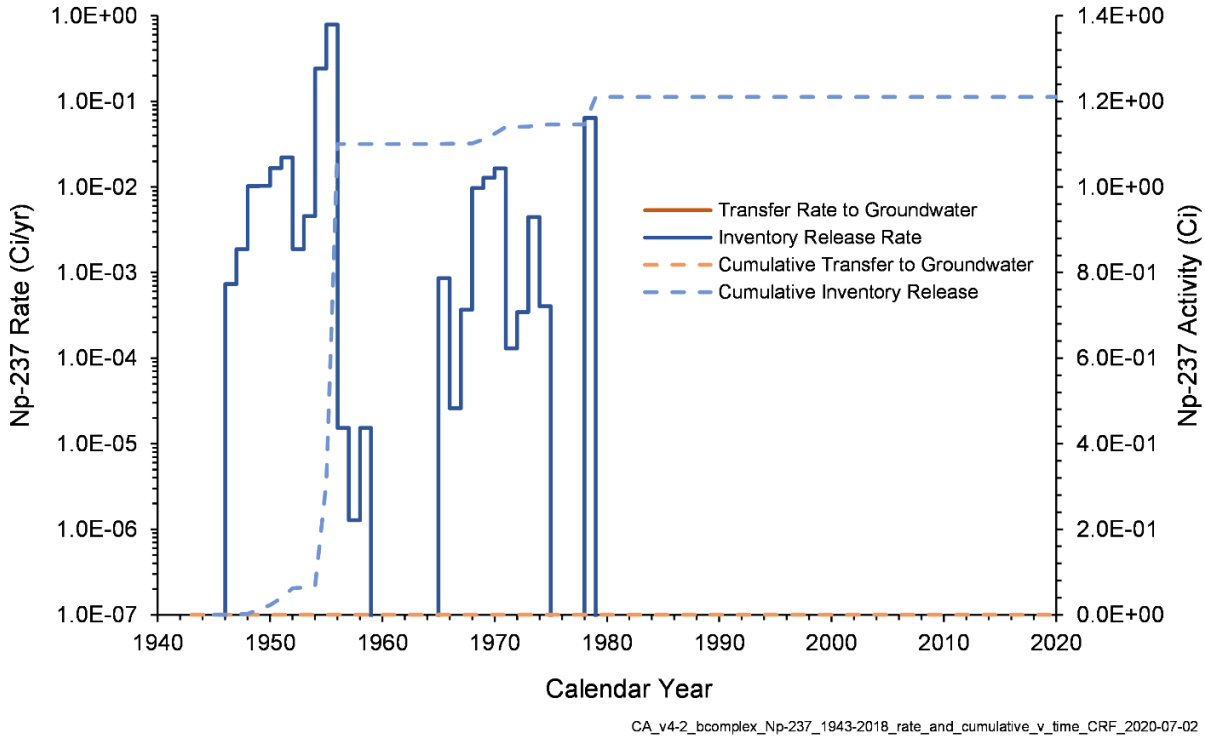

Figure 7-28. Np-237 Inventory Release from Waste Sites and Transfer to Groundwater for the B Complex Model from 1943–2018

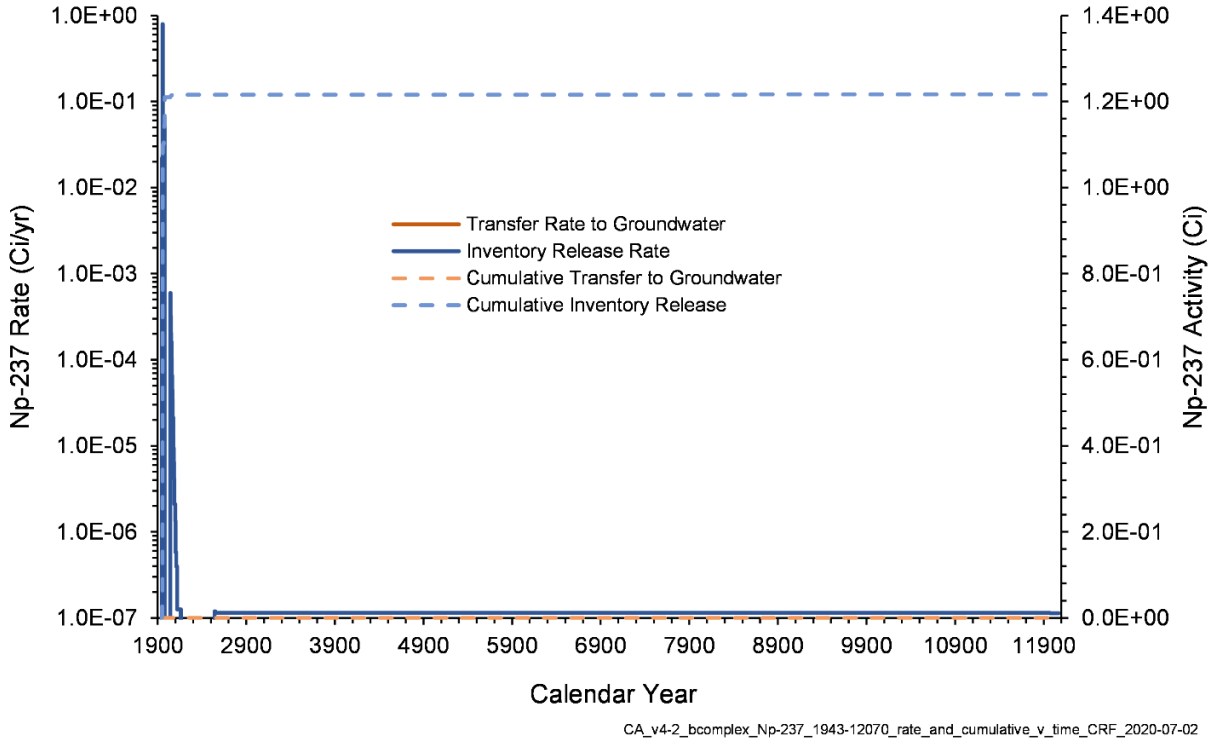

Figure 7-29. Np-237 Inventory Release from Waste Sites and Transfer to Groundwater for the B Complex Model from 1943–12070

7.6 Re-187 Fate and Transport Results

Due to a lack of inventory, transport of Re-187 was not calculated in this model.

7.7 Sr-90 Fate and Transport Results

This model simulated the release and transport of Sr-90. No Sr-90 was discharged to groundwater at a cumulative activity above 1.0E-6 Ci per P2R grid cell. The inventory released to the B Complex model and the transfer of Sr-90 to groundwater are shown from 1943–2018 in Figure 7-30 and from 1943–12070 in Figure 7-31.

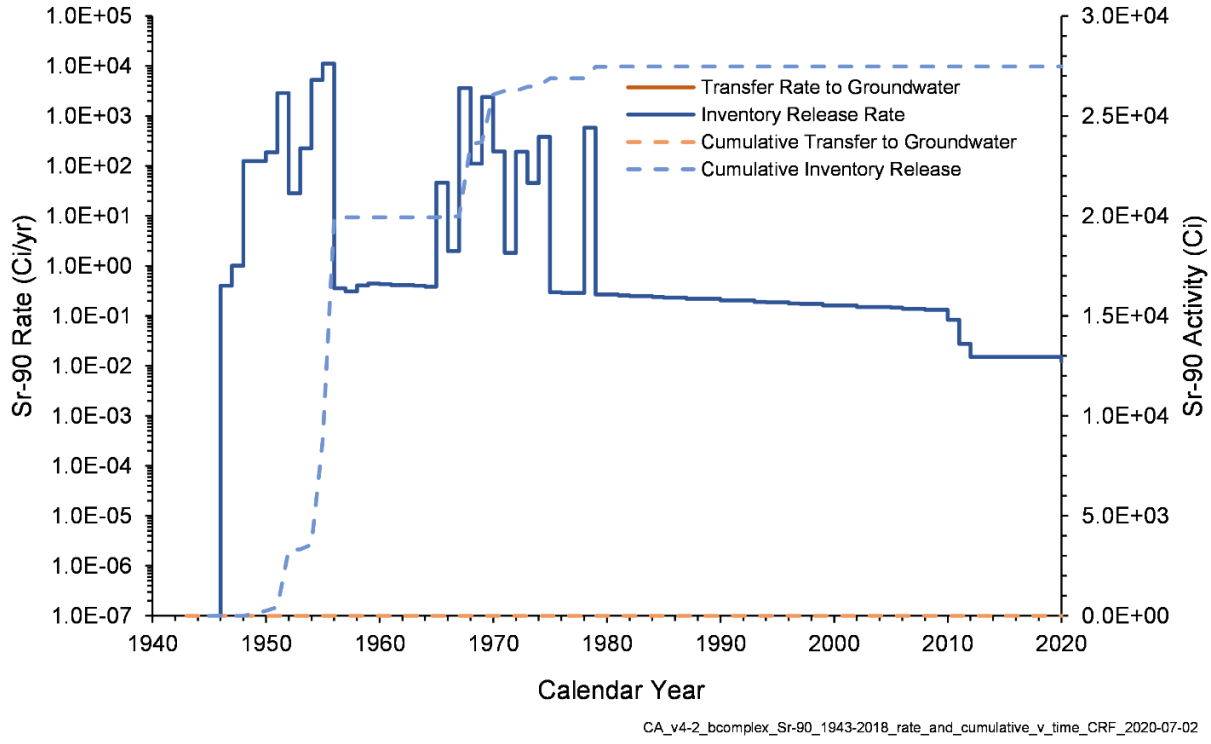

Figure 7-30. Sr-90 Inventory Release from Waste Sites and Transfer to Groundwater for the B Complex Model from 1943–2018

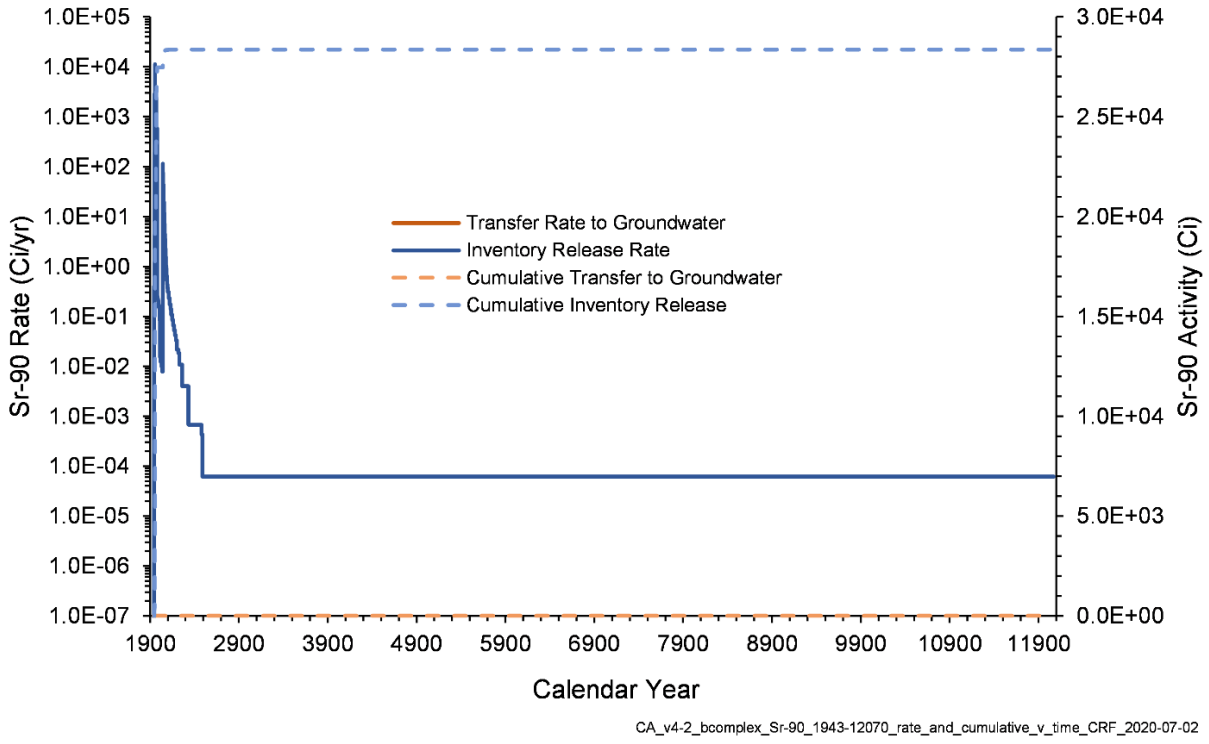

Figure 7-31. Sr-90 Inventory Release from Waste Sites and Transfer to Groundwater for the B Complex Model from 1943–12070

7.8 Tc-99 Fate and Transport Results

This model simulated release and transport of Tc-99. The cumulative discharge of Tc-99 into groundwater is shown aggregated by P2R grid cell in Figure 7-32 and Figure 7-33 for 1943–2018 and 2018–12070, respectively. The inventory released to the B Complex model and the transfer of Tc-99 to groundwater are shown from 1943–2018 in Figure 7-34 and from 1943–12070 in Figure 7-35. Figure 7-36 through Figure 7-43 show the flux of Tc-99 to groundwater in Ci/yr. These figures are generated at times with peak fluxes (local maxima) and during periods with gradual decline, as shown in Figure 7-34 and Figure 7-35. A figure for 2018, Figure 7-39, is also included to demonstrate the initial flux conditions for the 2018–12070 simulation.

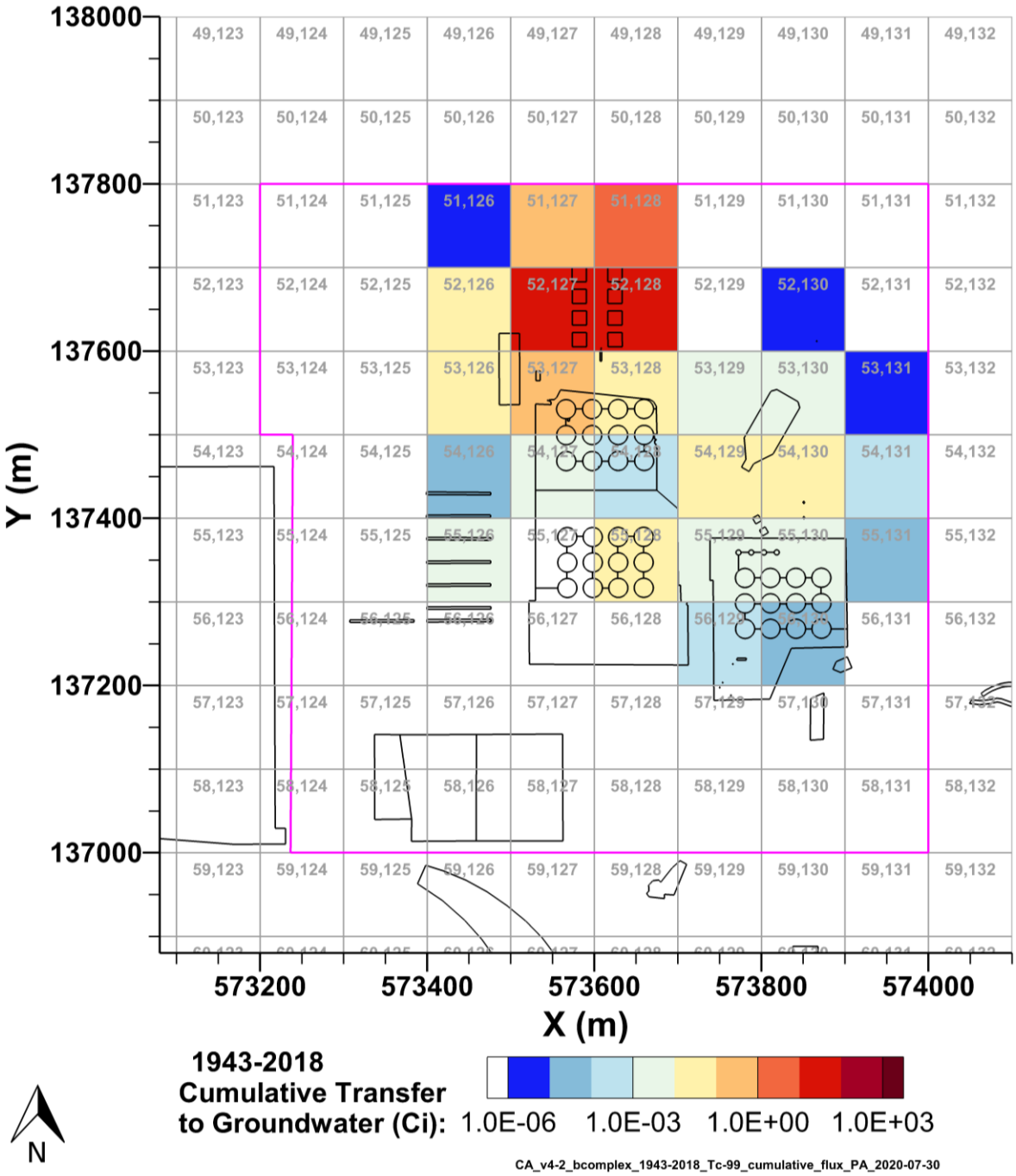

Note: source zone outlined in pink.

Figure 7-32. Cumulative Tc-99 Activity Discharged to Groundwater from the B Complex Model from 1943–2018 per P2R Grid Cell

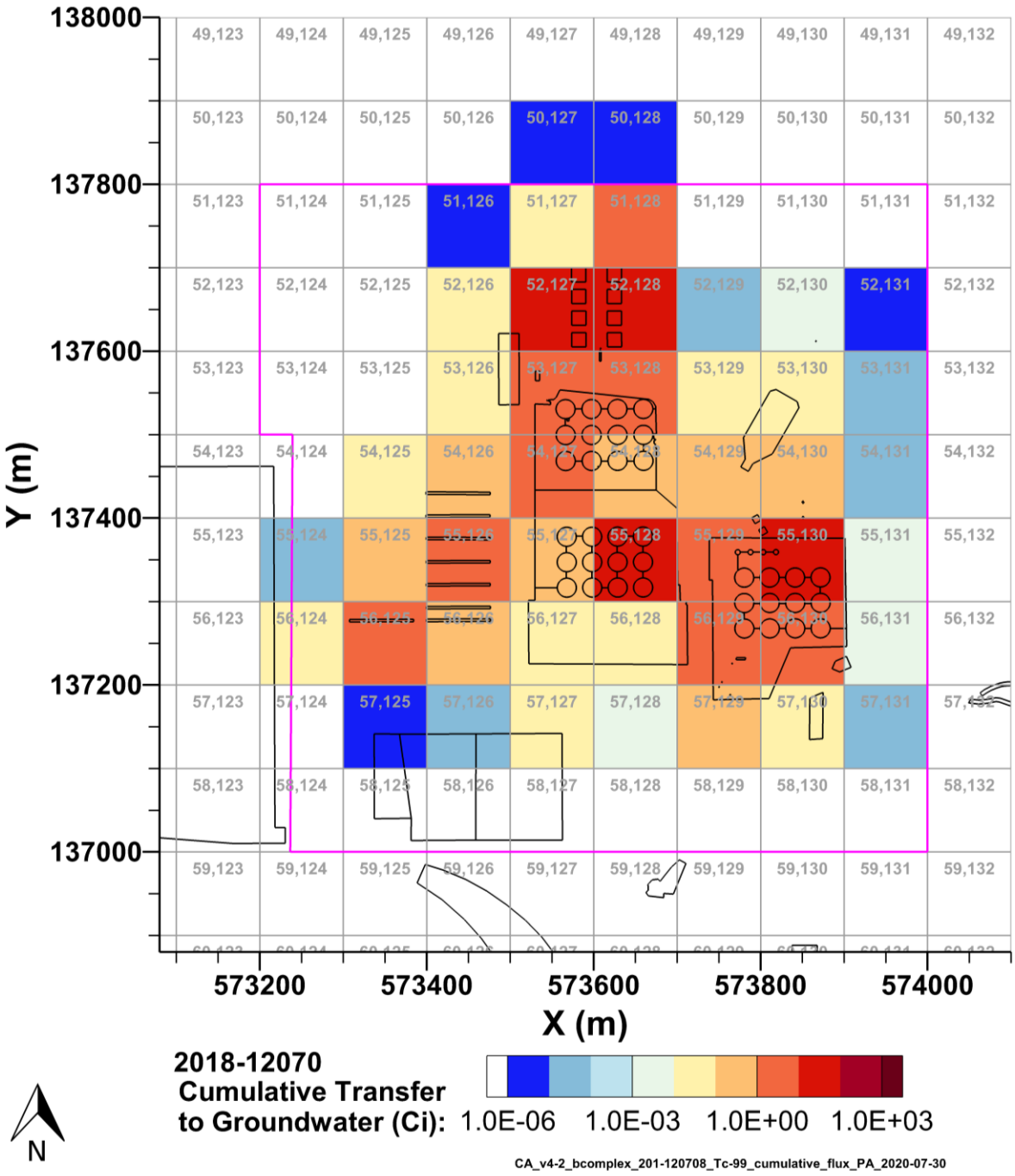

Note: source zone outlined in pink.

Figure 7-33. Cumulative Tc-99 Activity Discharged to Groundwater from the B Complex Model from 2018–12070 per P2R Grid Cell

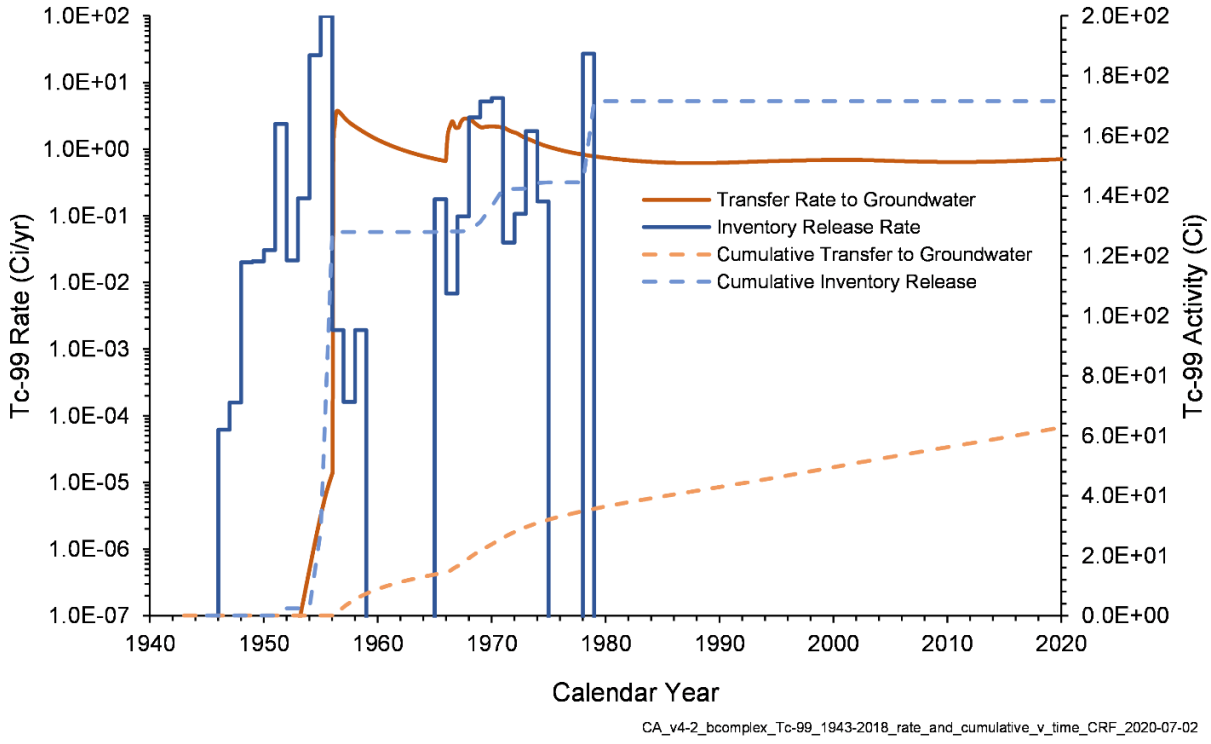

Figure 7-34. Tc-99 Inventory Release from Waste Sites and Transfer to Groundwater for the B Complex Model from 1943–2018

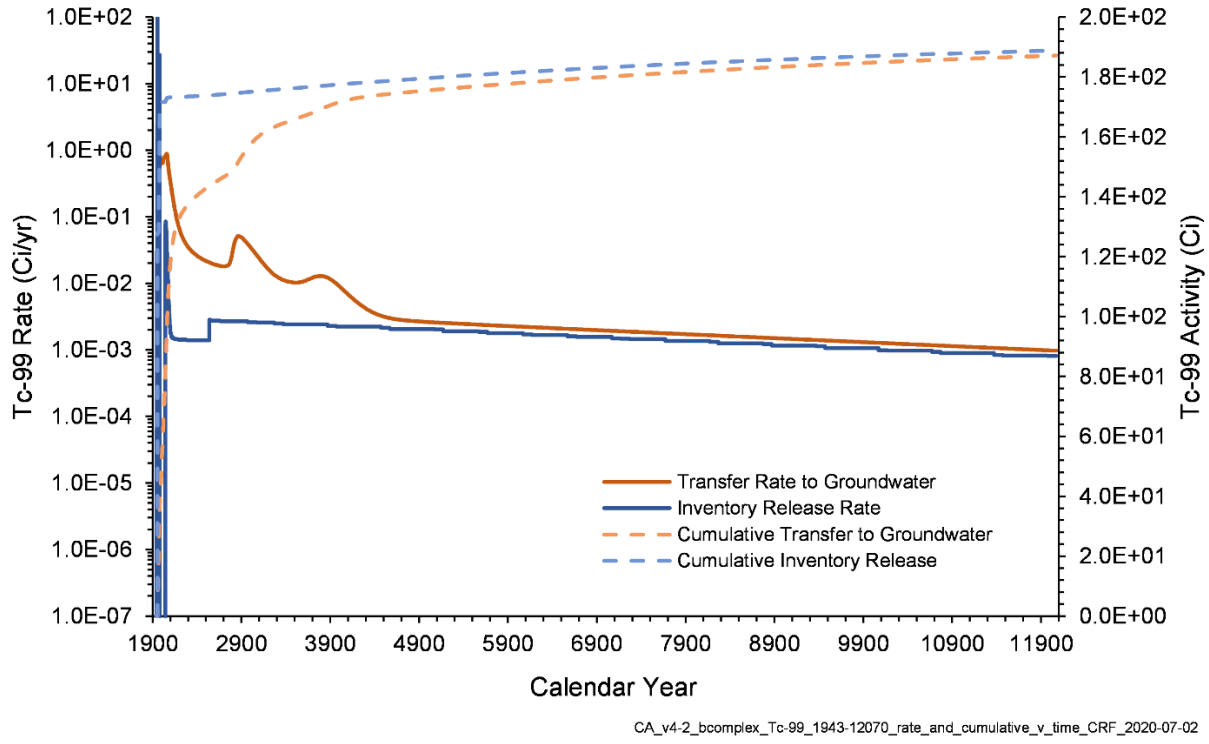

Figure 7-35. Tc-99 Inventory Release from Waste Sites and Transfer to Groundwater for the B Complex Model from 1943–12070

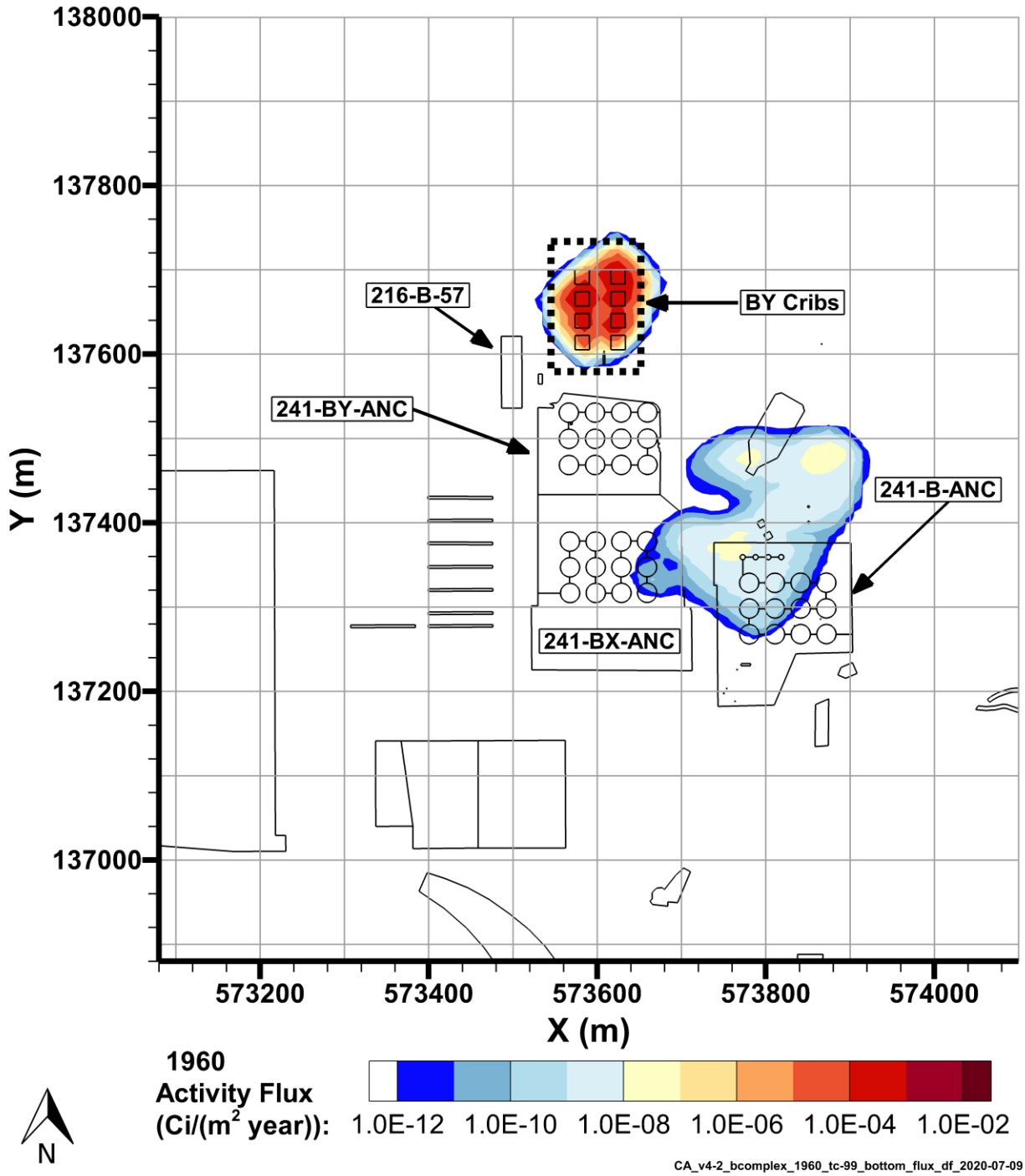

Note: the dashed black lines are used to indicate the waste sites that are collectively referred to as BY Cribs.

Figure 7-36. Tc-99 Flux to Groundwater, 1960

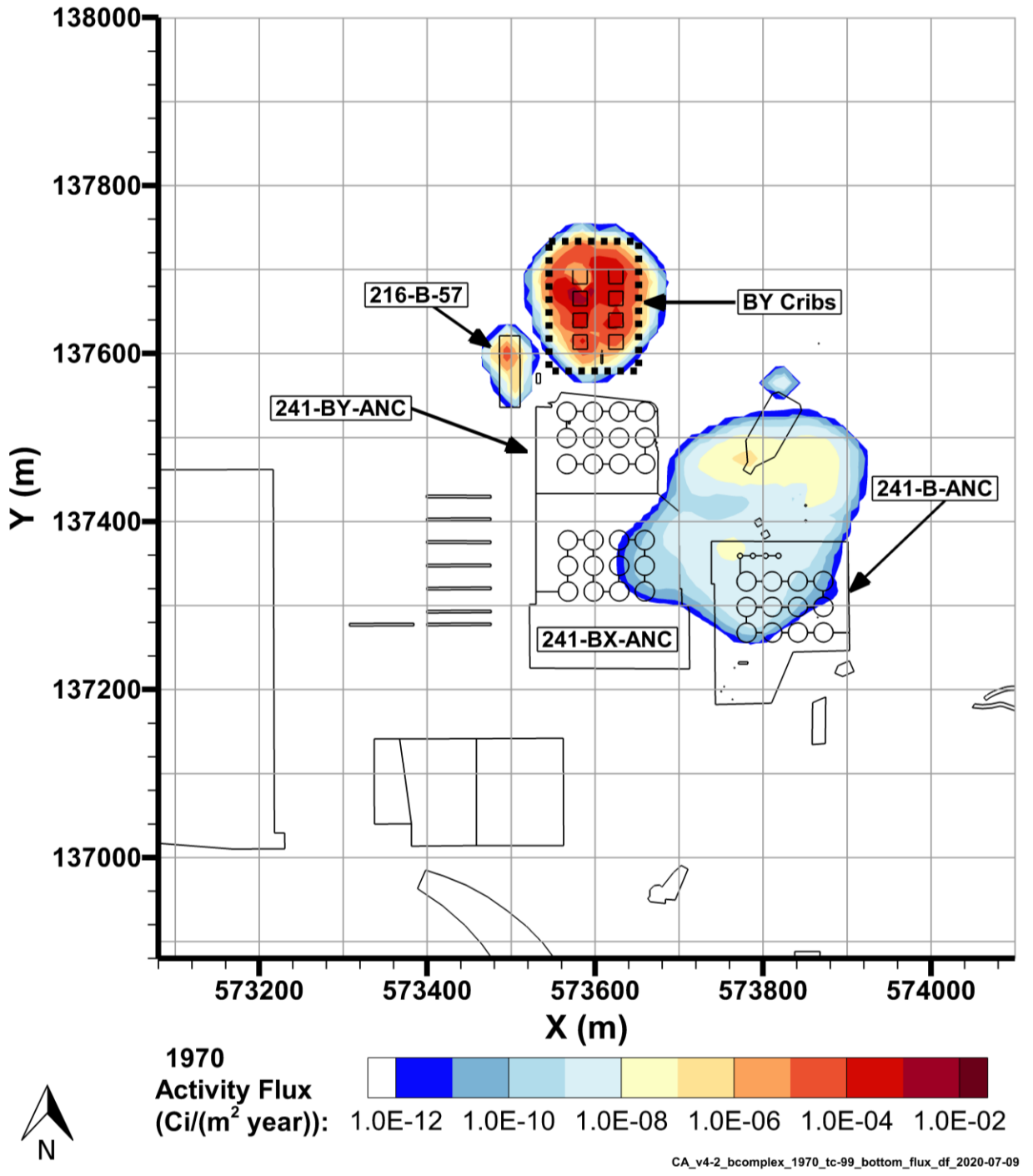

Note: the dashed black lines are used to indicate the waste sites that are collectively referred to as BY Cribs.

Figure 7-37. Tc-99 Flux to Groundwater, 1970

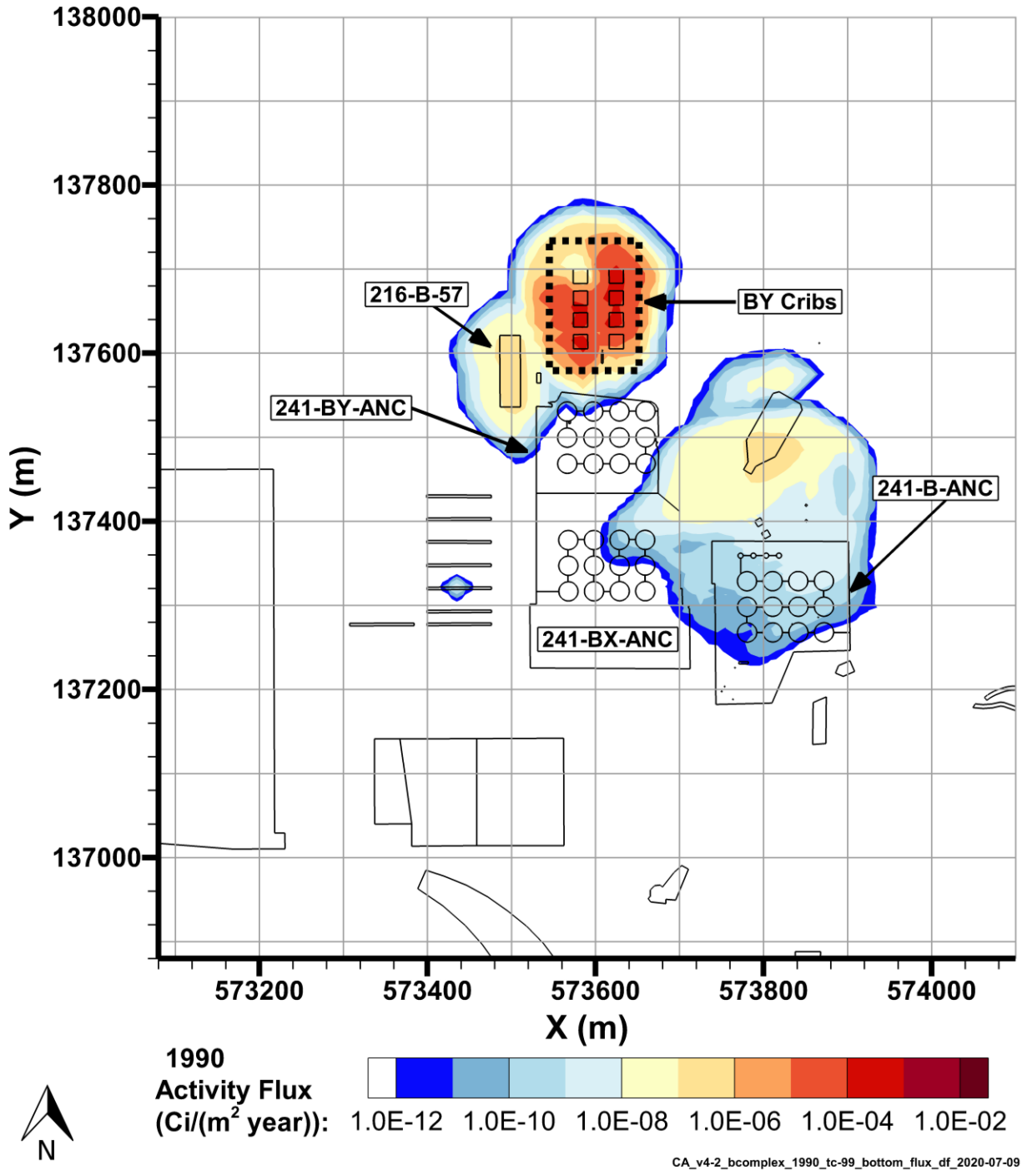

Note: the dashed black lines are used to indicate the waste sites that are collectively referred to as BY Cribs.

Figure 7-38. Tc-99 Flux to Groundwater, 1990

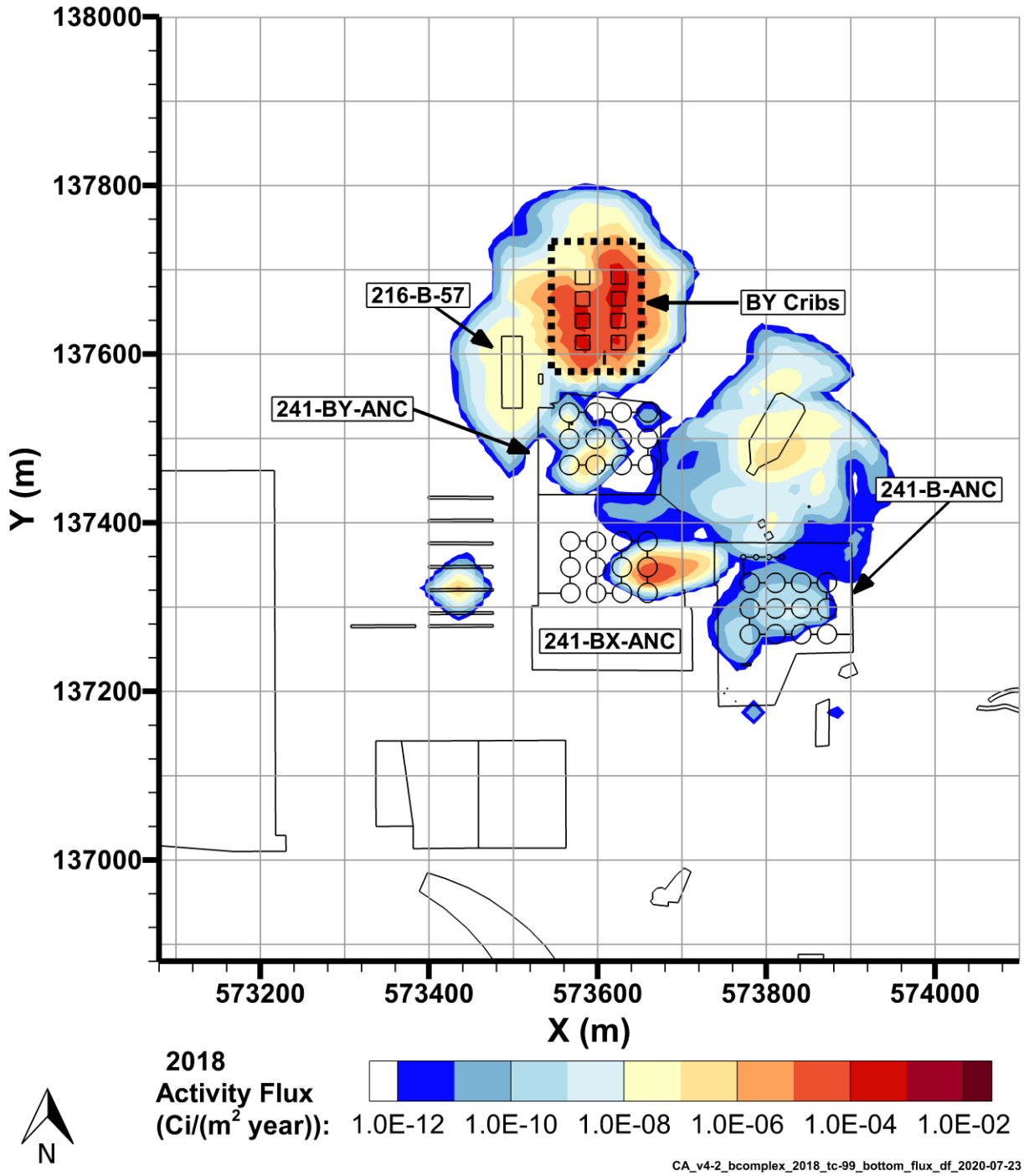

Note: the dashed black lines are used to indicate the waste sites that are collectively referred to as BY Cribs.

Figure 7-39. Tc-99 Flux to Groundwater, 2018

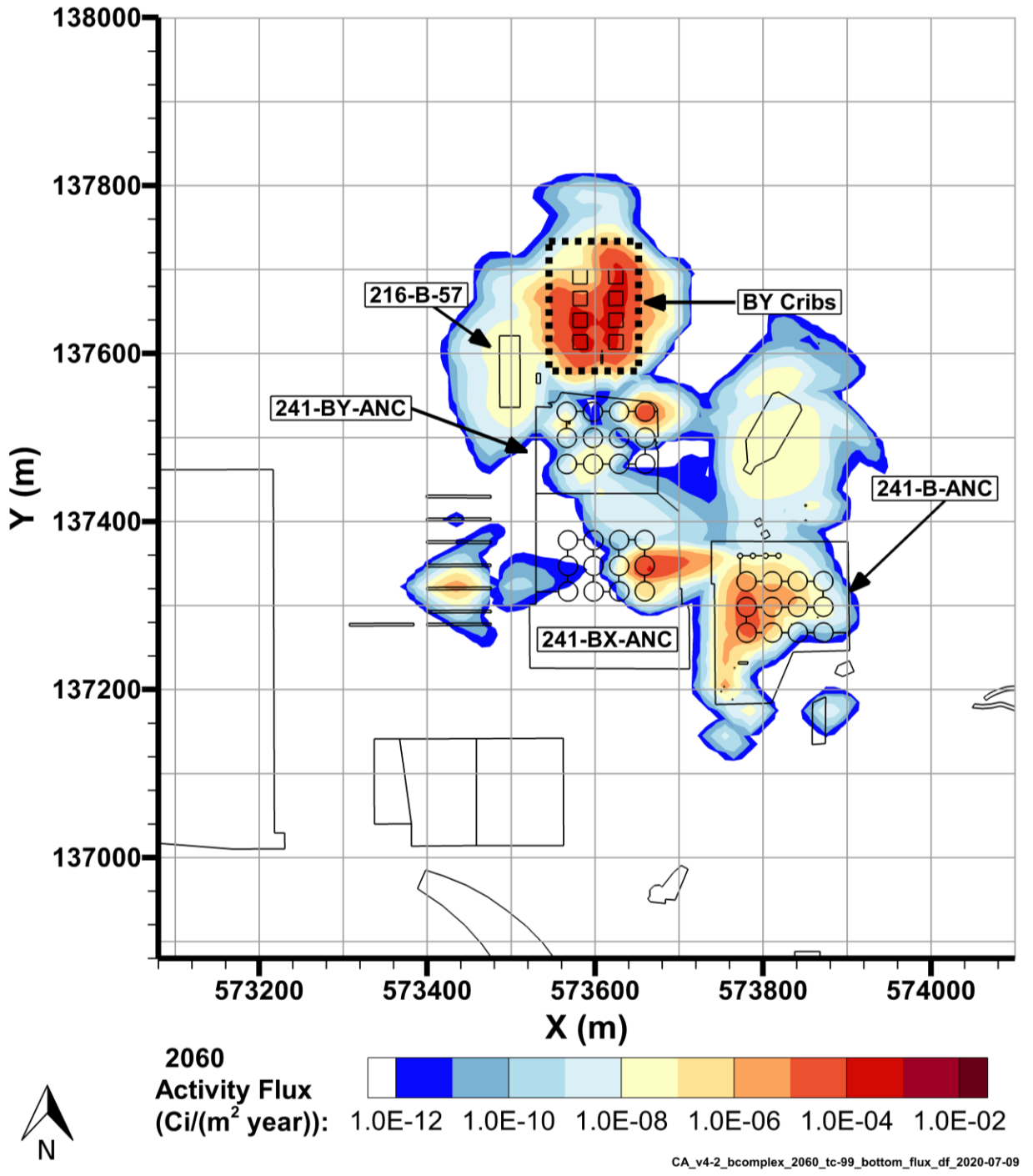

Note: the dashed black lines are used to indicate the waste sites that are collectively referred to as BY Cribs.

Figure 7-40. Tc-99 Flux to Groundwater, 2060

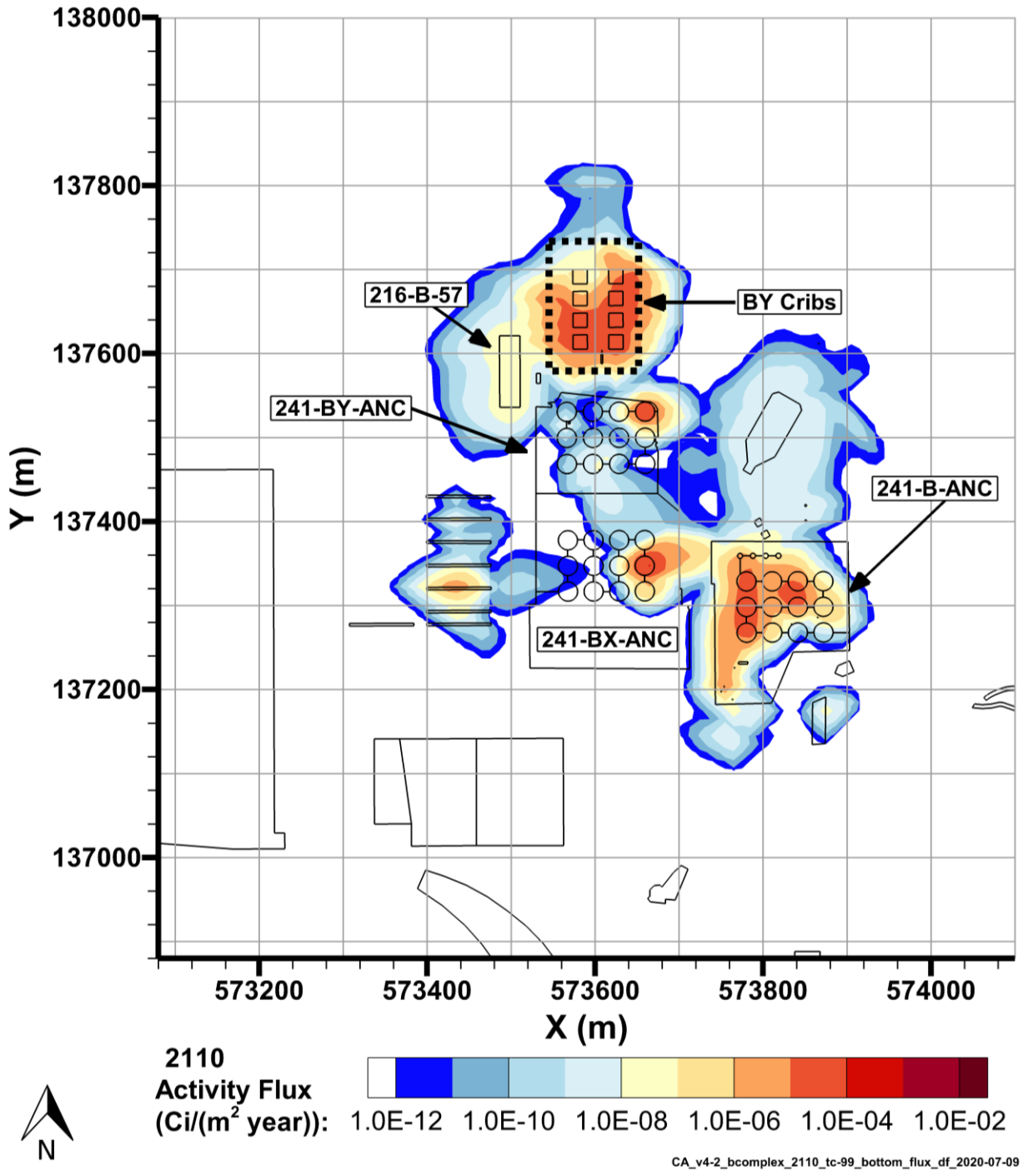

Note: the dashed black lines are used to indicate the waste sites that are collectively referred to as BY Cribs.

Figure 7-41. Tc-99 Flux to Groundwater, 2110

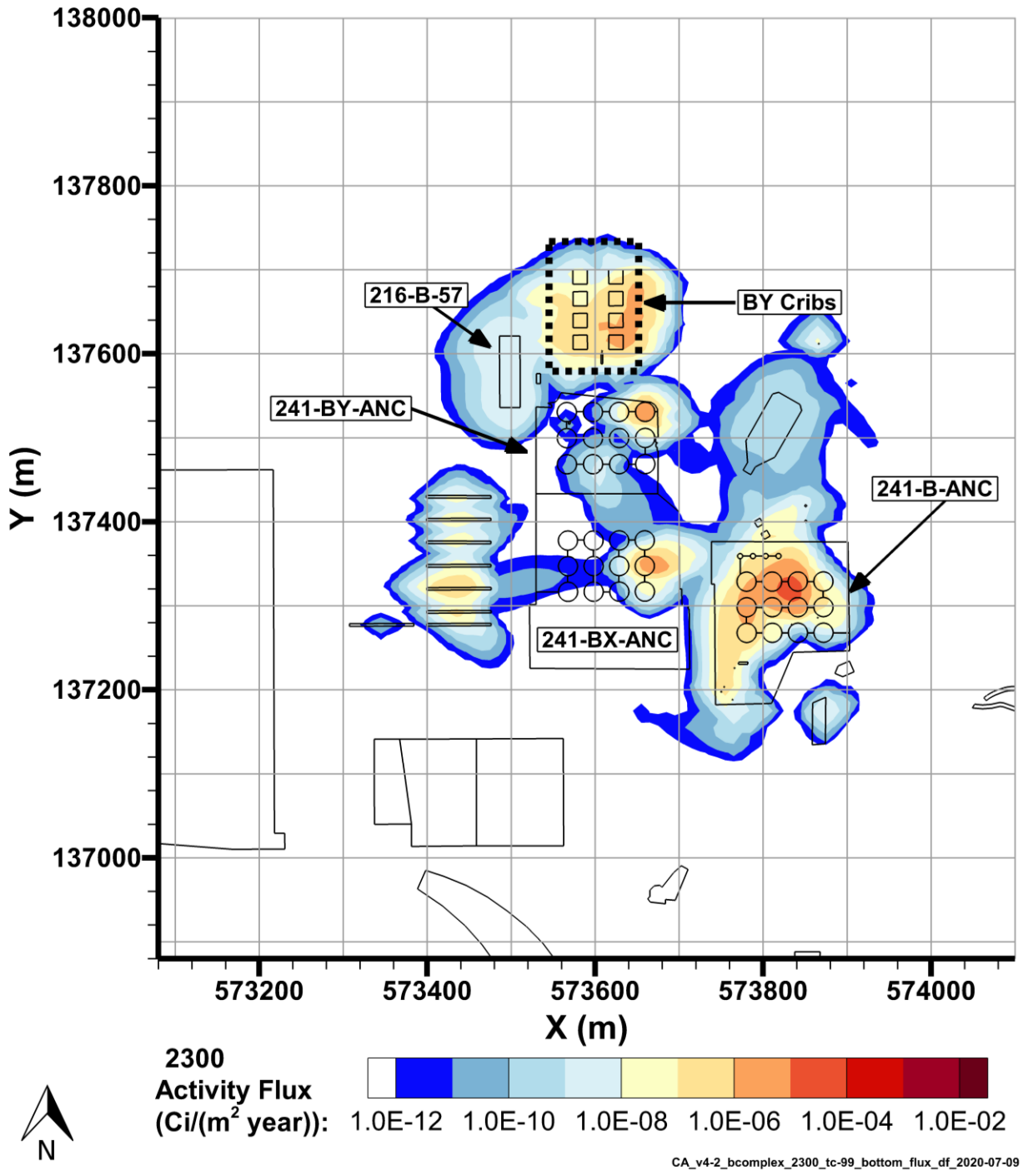

Note: the dashed black lines are used to indicate the waste sites that are collectively referred to as BY Cribs.

Figure 7-42. Tc-99 Flux to Groundwater, 2300

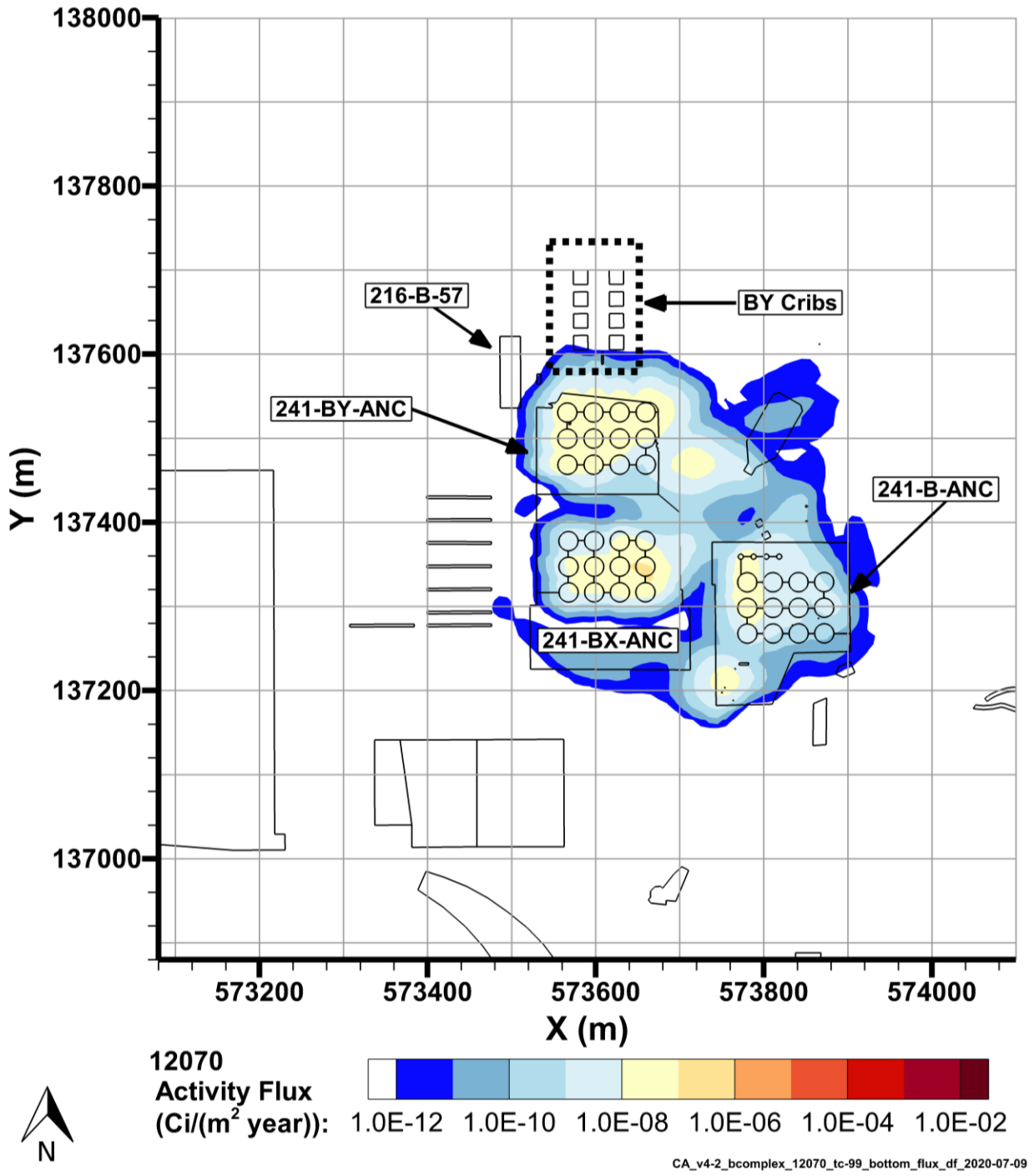

Note: the dashed black lines are used to indicate the waste sites that are collectively referred to as BY Cribs.

Figure 7-43. Tc-99 Flux to Groundwater, 12070

7.9 U-232 Fate and Transport Results

This model simulated the release and transport of U-232. No U-232 was discharged to groundwater at a cumulative activity above 1.0E-6 Ci per P2R grid cell at any point during modeling. The cumulative discharge of mobile U-232 into groundwater from 241-BX-102 is shown aggregated by P2R grid cell in

Figure 7-44 for 2018–12070. No mobile U-232 was discharged to groundwater at a cumulative activity above 1.0E-6 per P2R grid cell from 1943–2018. The inventory released to the B Complex model and the transfer of U-232 to groundwater are shown from 1943–2018 in Figure 7-45 and from 1943–12070 in Figure 7-46. The inventory released to the B Complex model from 241-BX-102 and the transfer of mobile U-232 to groundwater are shown from 1943–2018 in Figure 7-47 and from 1943–12070 in Figure 7-48.

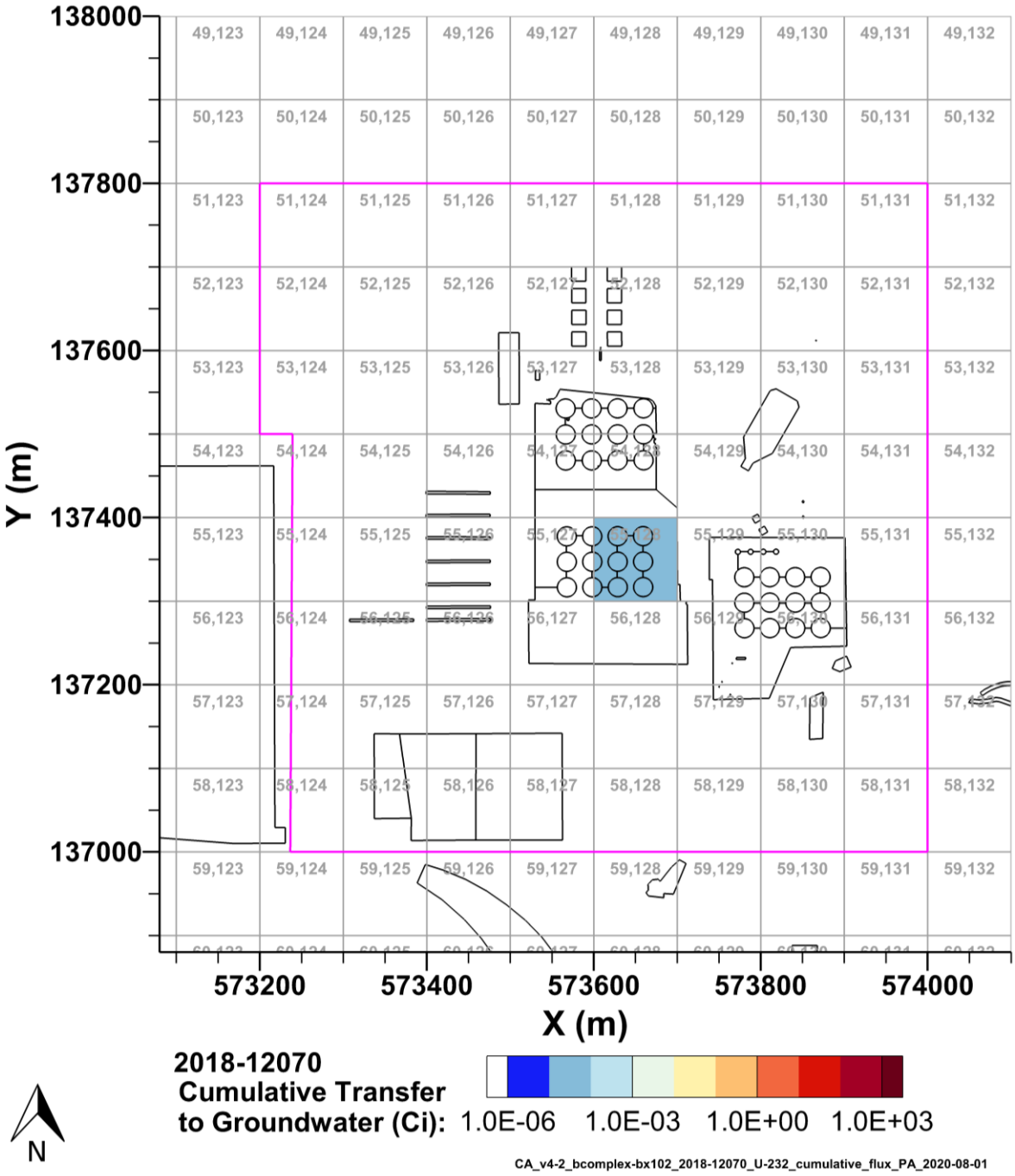

Figure 7-44. Cumulative Mobile U-233 Activity Discharged to Groundwater from 241-BX-102 in the B Complex Model from 2018–12070 per P2R Grid Cell

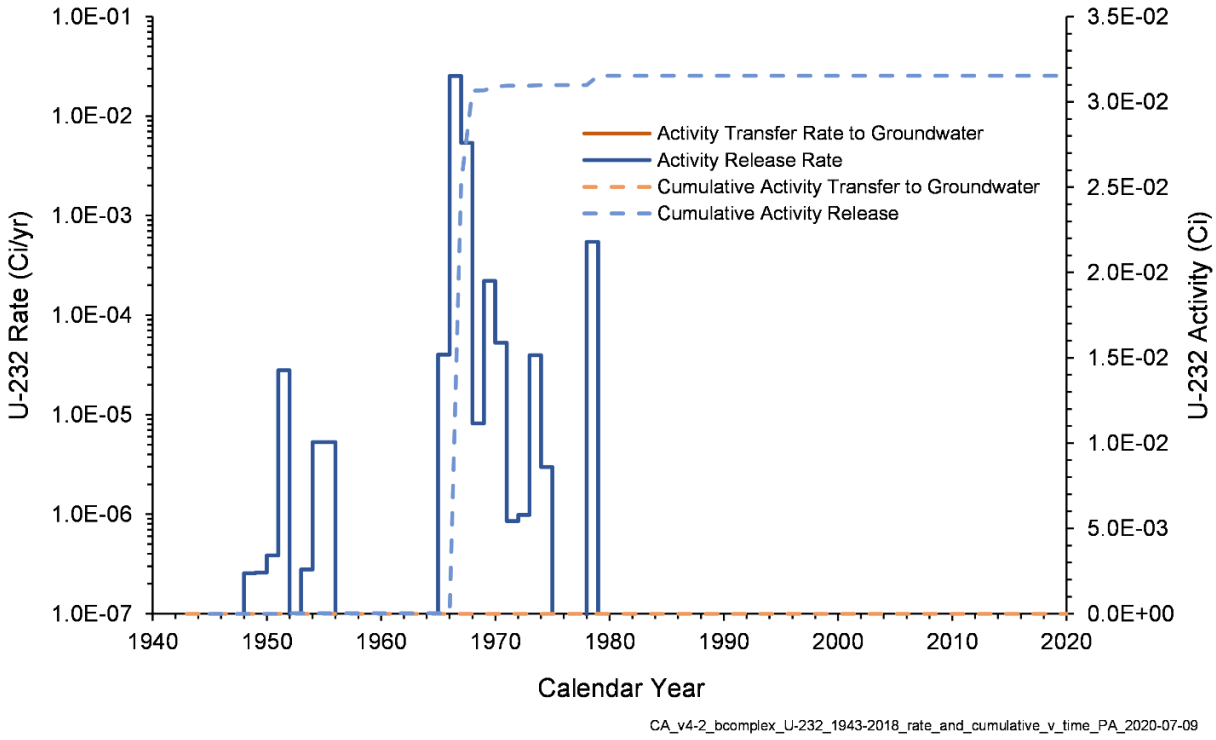

Figure 7-45. U-232 Inventory Release from Waste Sites and Transfer to Groundwater for the B Complex Model from 1943–2018

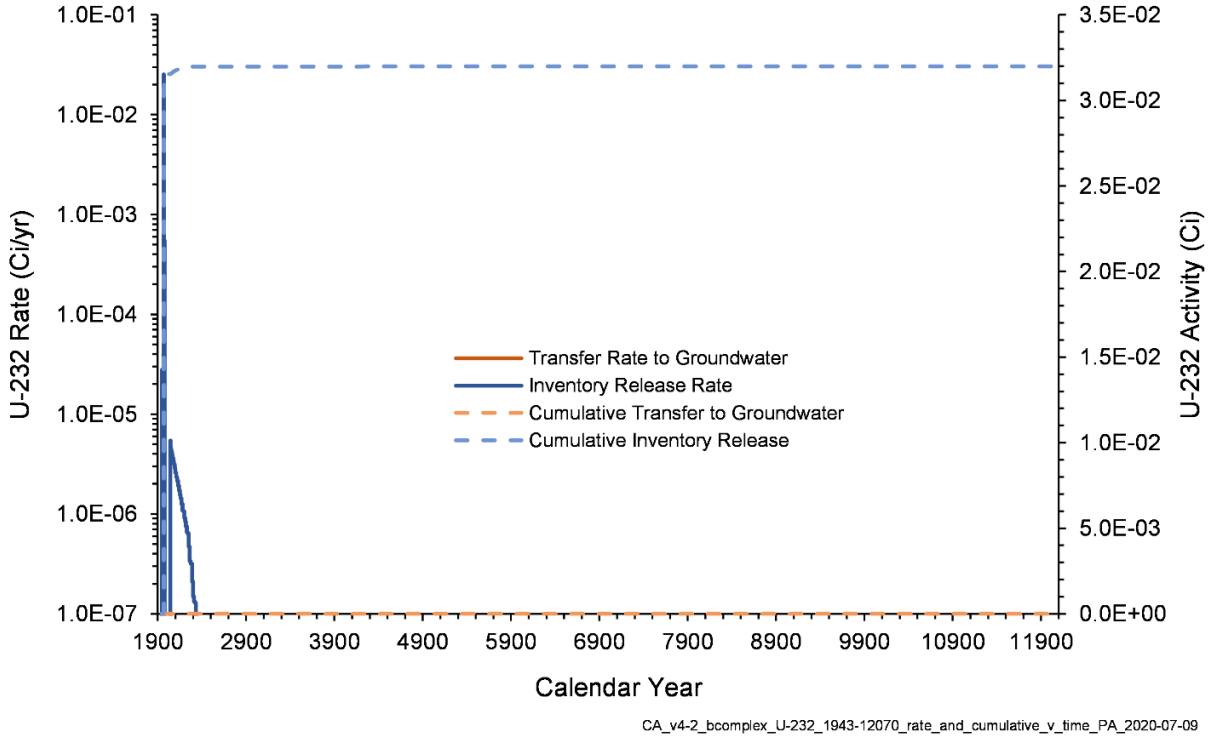

Figure 7-46. U-232 Inventory Release from Waste Sites and Transfer to Groundwater for the B Complex Model from 1943–12070

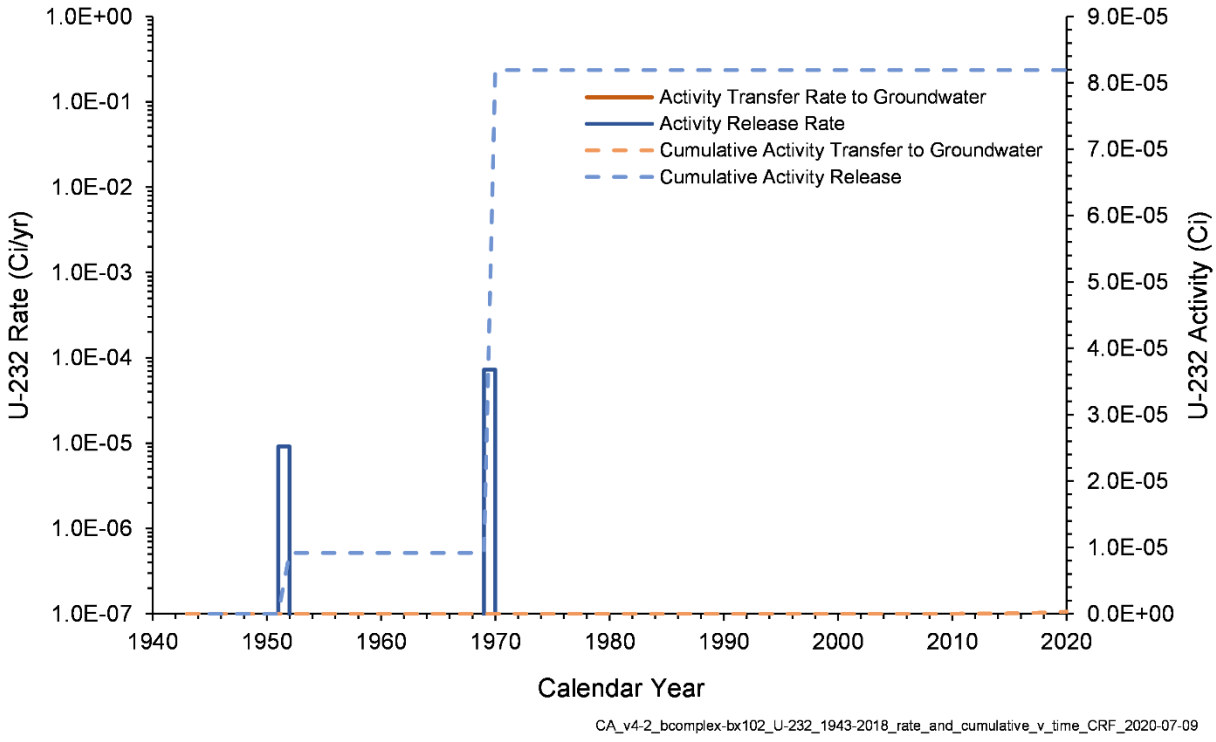

Figure 7-47. Mobile U-232 Inventory Release from 241-BX-102 and Transfer to Groundwater for the B Complex Model from 1943–2018

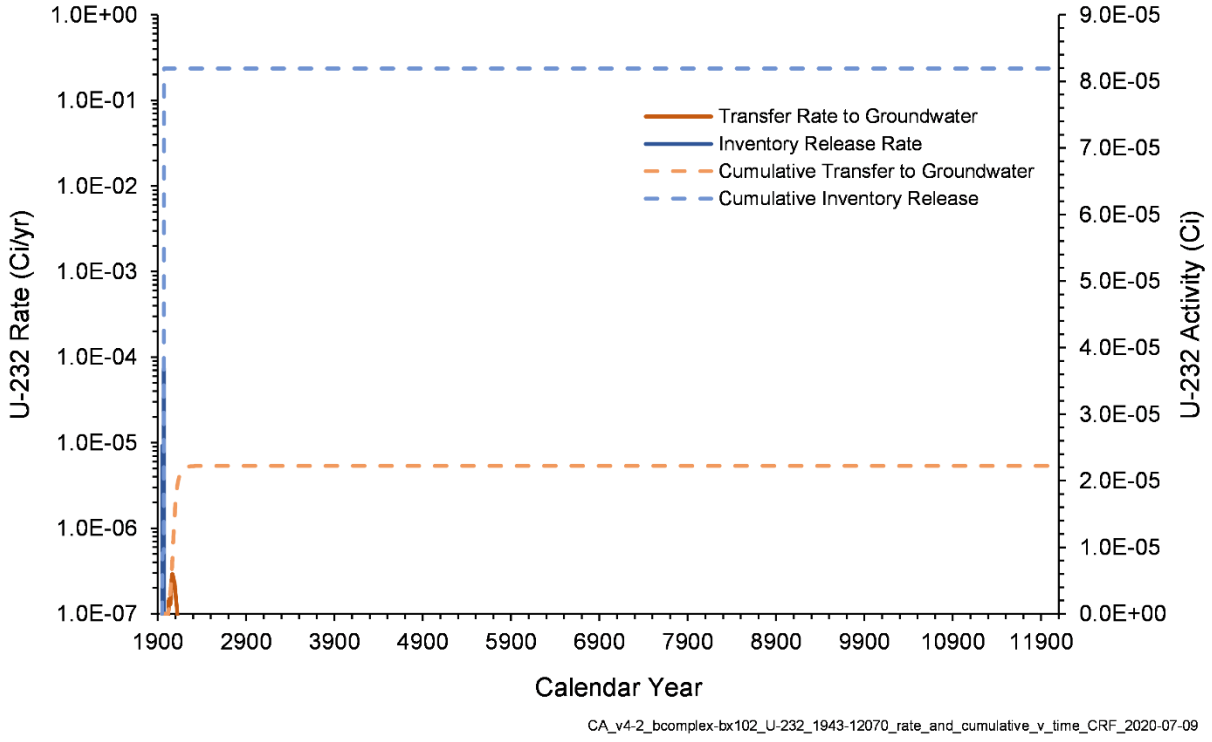

Figure 7-48. Mobile U-232 Inventory Release from 241-BX-102 and Transfer to Groundwater for the B Complex Model from 2018–12070

7.10 U-233 Fate and Transport Results

This model simulated the release and transport of U-233. The cumulative discharge of U-233 into groundwater is shown aggregated by P2R grid cell in Figure 7-49 and Figure 7-50 for 1943–2018 and 2018–12070, respectively. The cumulative discharge of mobile U-233 into groundwater from 241-BX-102 is shown aggregated by P2R grid cell in Figure 7-51 for 2018–12070. No mobile U-233 was discharged to groundwater at a cumulative activity above 1.0E-6 per P2R grid cell from 1943–2018. The inventory released to the B Complex model and the transfer of U-233 to groundwater are shown from 1943–2018 in Figure 7-52 and from 1943–12070 in Figure 7-53. The inventory released to the B Complex model from 241-BX-102 and the transfer of mobile U-233 to groundwater are shown from 1943–2018 in Figure 7-54 and from 1943–12070 in Figure 7-55.

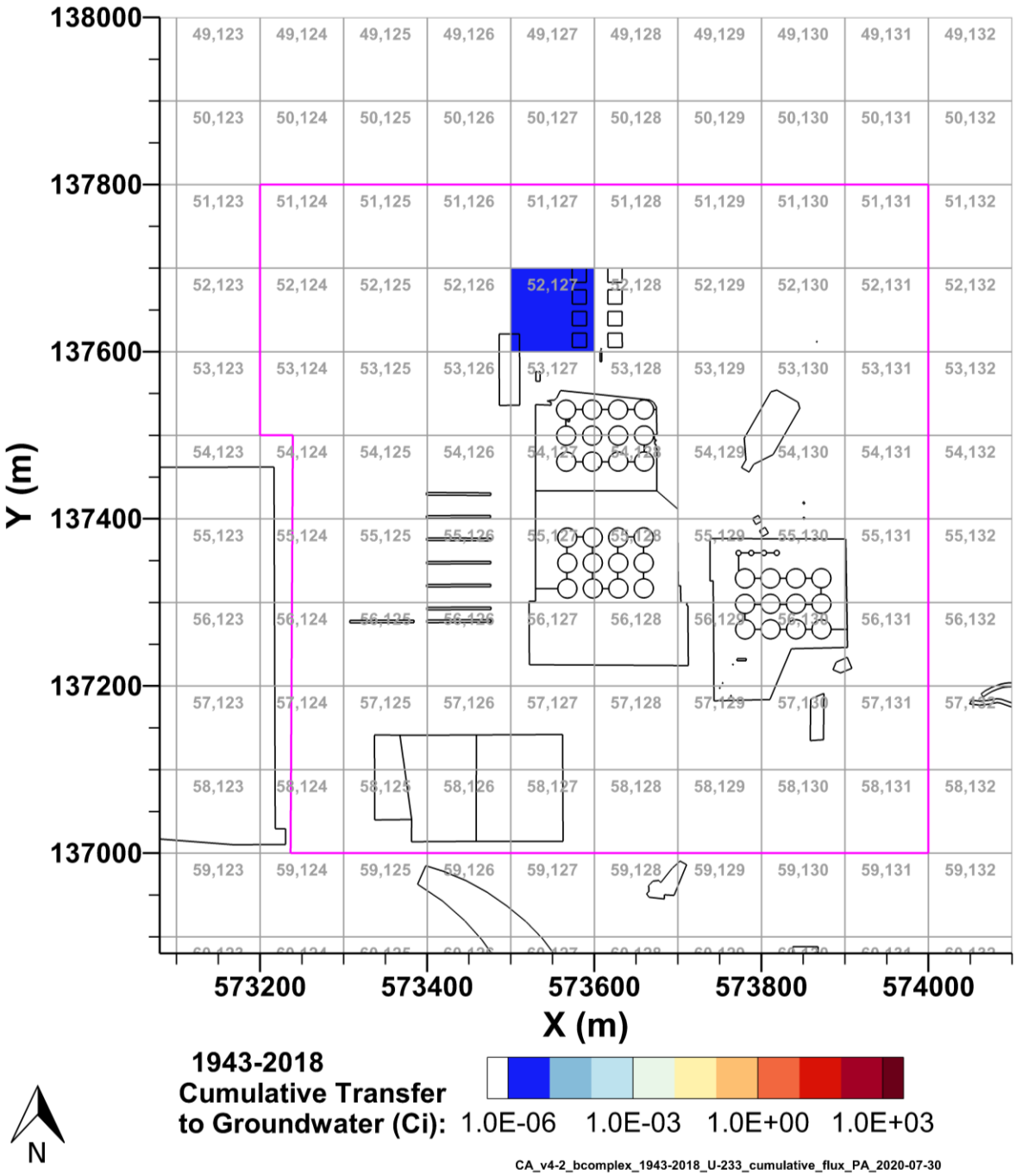

Note: source zone outlined in pink.

Figure 7-49. Cumulative U-233 Activity Discharged to Groundwater from the B Complex Model from 1943–2018 per P2R Grid Cell

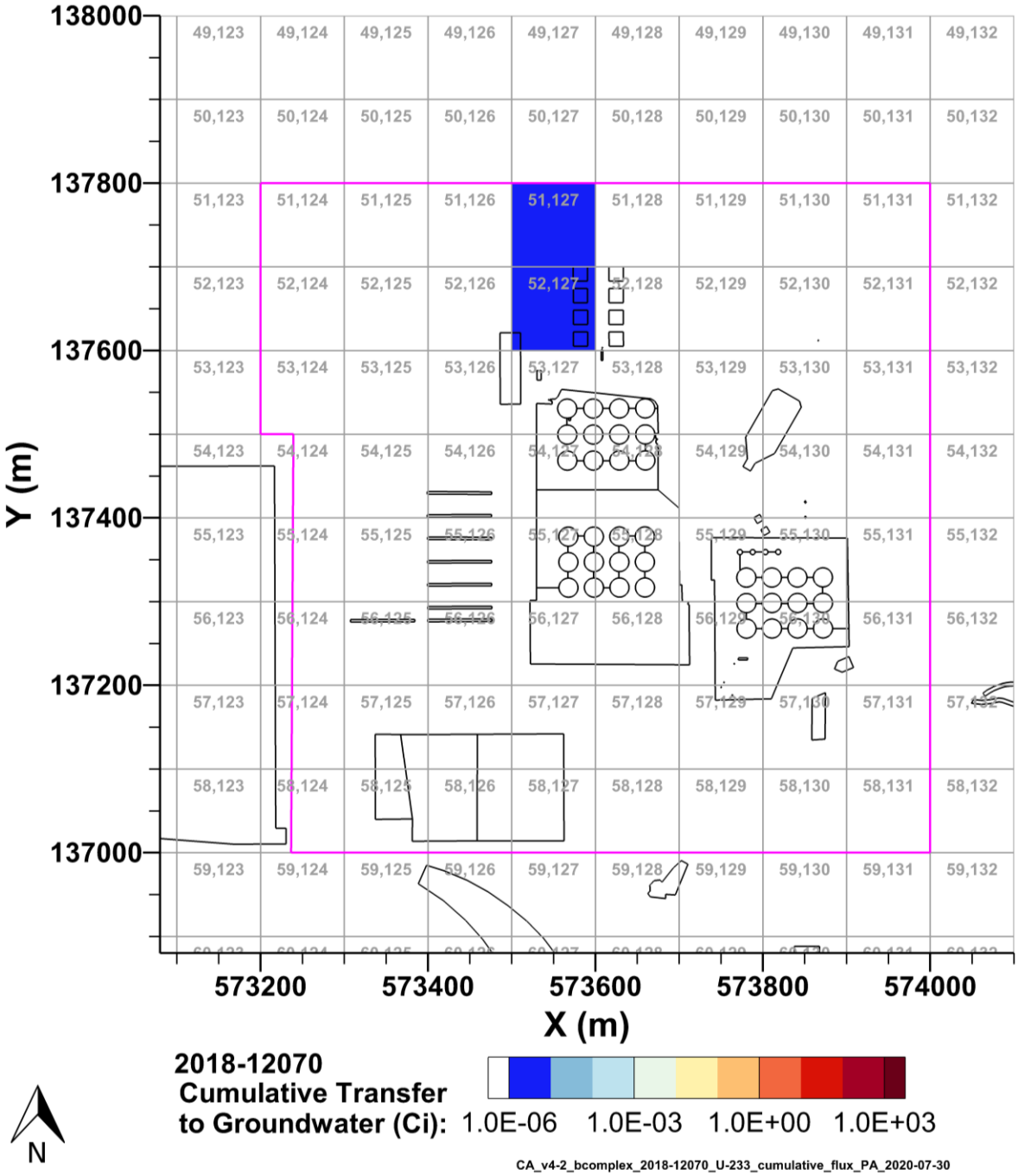

Note: source zone outlined in pink.

Figure 7-50. Cumulative U-233 Activity Discharged to Groundwater from the B Complex Model from 2018–12070 per P2R Grid Cell

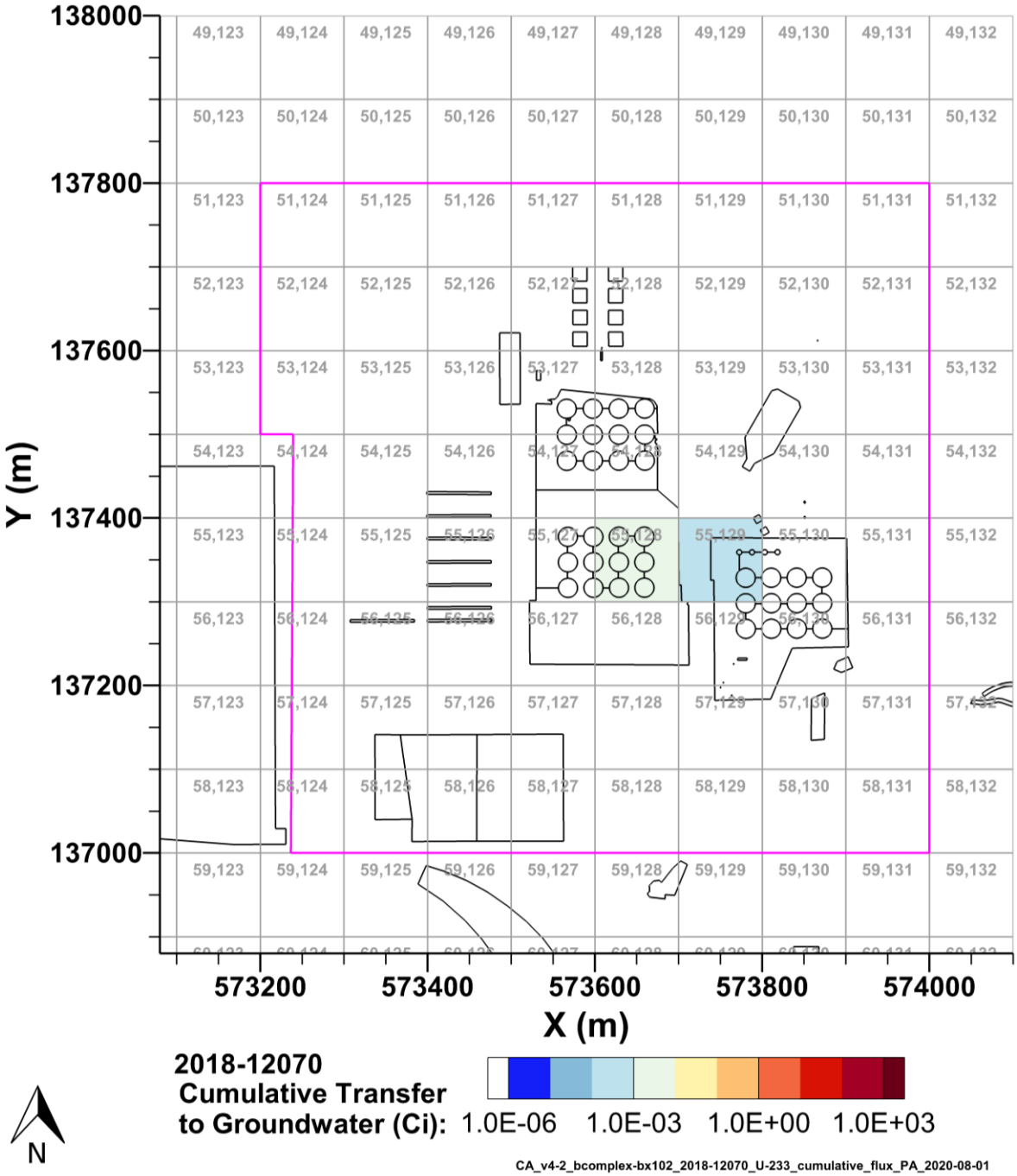

Figure 7-51. Cumulative Mobile U-233 Activity Discharged to Groundwater from 241-BX-102 in the B Complex Model from 2018–12070 per P2R Grid Cell

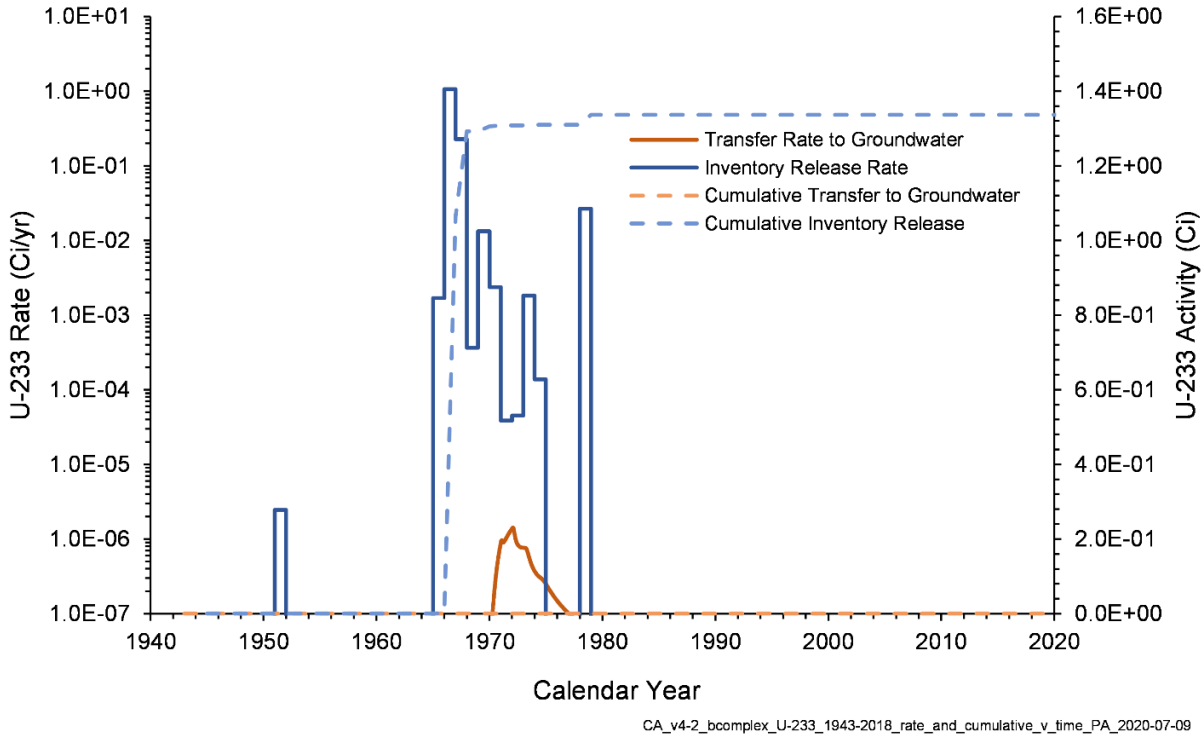

Figure 7-52. U-233 Inventory Release from Waste Sites and Transfer to Groundwater for the B Complex Model from 1943–2018

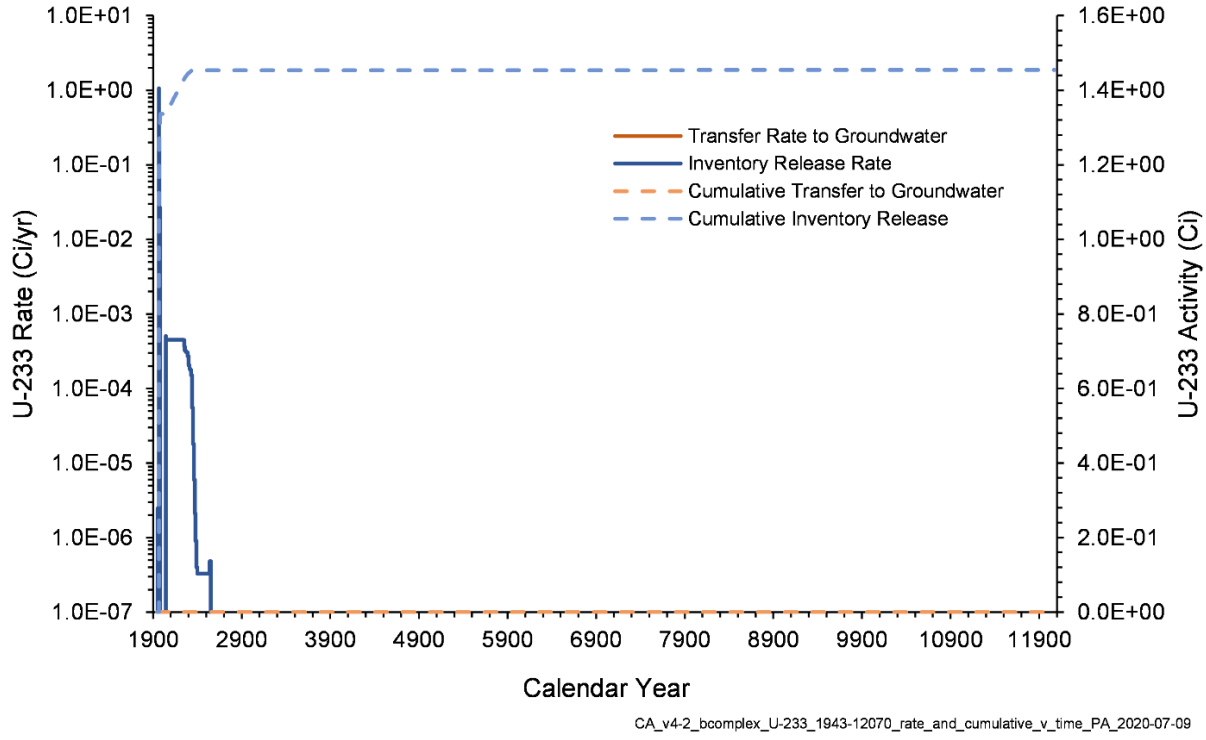

Figure 7-53. U-233 Inventory Release from Waste Sites and Transfer to Groundwater for the B Complex Model from 1943–12070

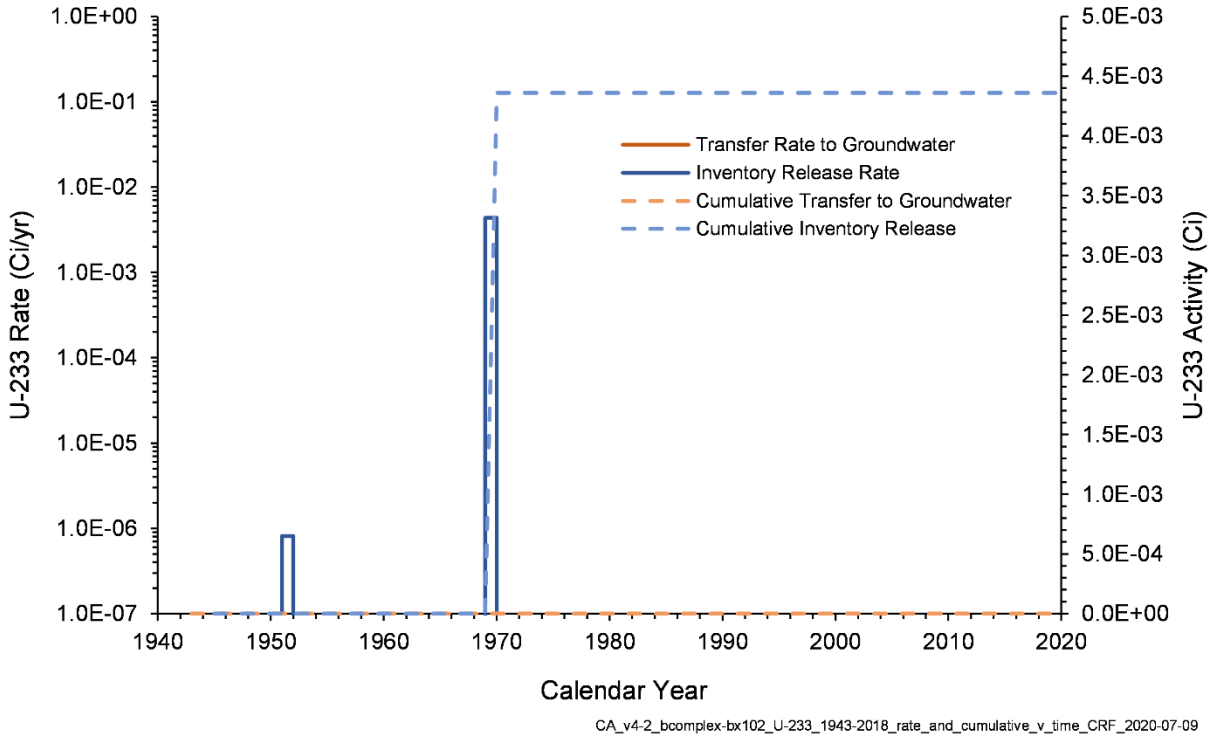

Figure 7-54. Mobile U-233 Inventory Release from 241-BX-102 and Transfer to Groundwater for the B Complex Model from 1943–2018

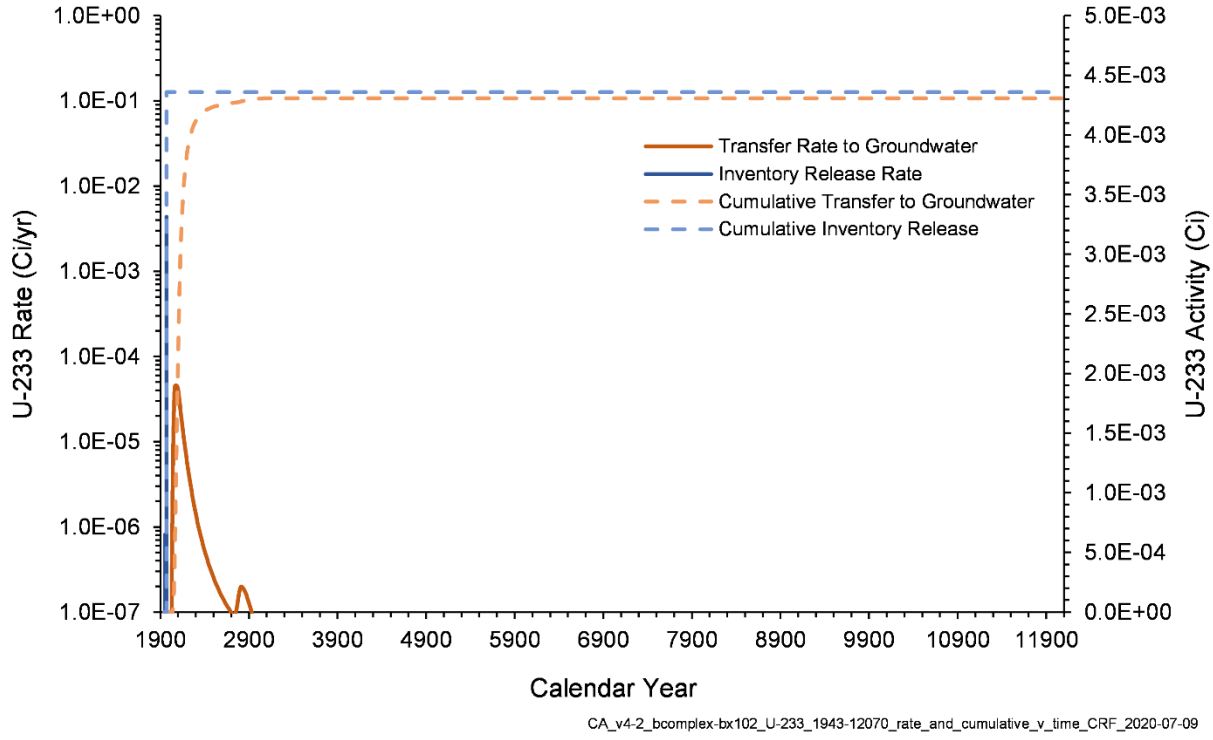

Figure 7-55. Mobile U-233 Inventory Release from 241-BX-102 and Transfer to Groundwater for the B Complex Model from 2018–12070

7.11 U-234 Fate and Transport Results

This model simulated the release and transport of U-234. The cumulative discharge of U-234 into groundwater is shown aggregated by P2R grid cell in Figure 7-56 and Figure 7-57 for 1943–2018 and 2018–12070, respectively. The cumulative discharge of mobile U-234 into groundwater from 241-BX-102 is shown aggregated by P2R grid cell in Figure 7-58 and Figure 7-59 for 1943–2018 and 2018–12070, respectively. The inventory released to the B Complex model and the transfer of U-234 to groundwater are shown from 1943–2018 in Figure 7-60 and from 1943–12070 in Figure 7-61. The inventory released to the B Complex model from 241-BX-102 and the transfer of mobile U-234 to groundwater are shown from 1943–2018 in Figure 7-62 and from 1943–12070 in Figure 7-63.

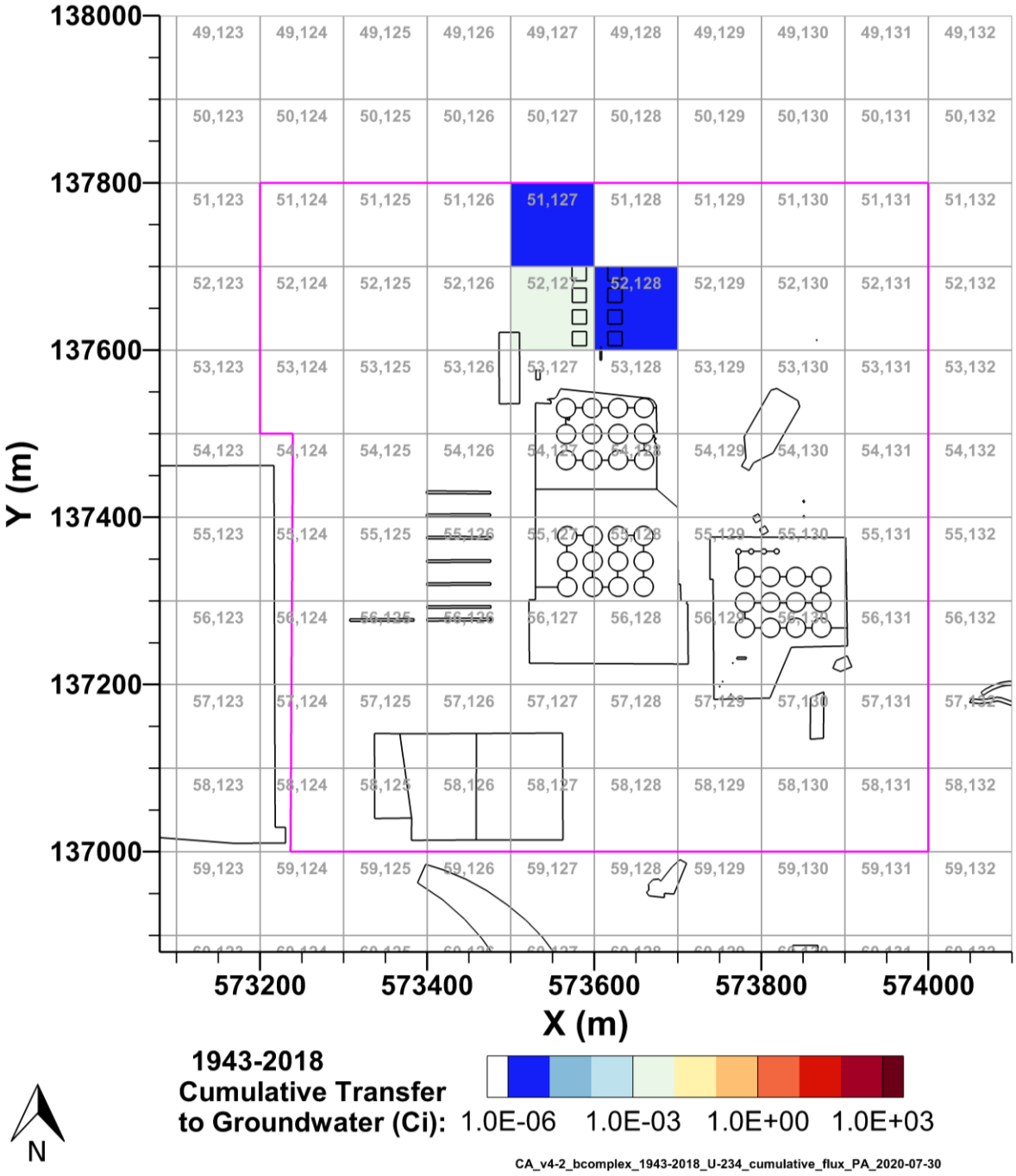

Note: source zone outlined in pink.

Figure 7-56. Cumulative U-234 Activity Discharged to Groundwater from the B Complex Model from 1943–2018 per P2R Grid Cell

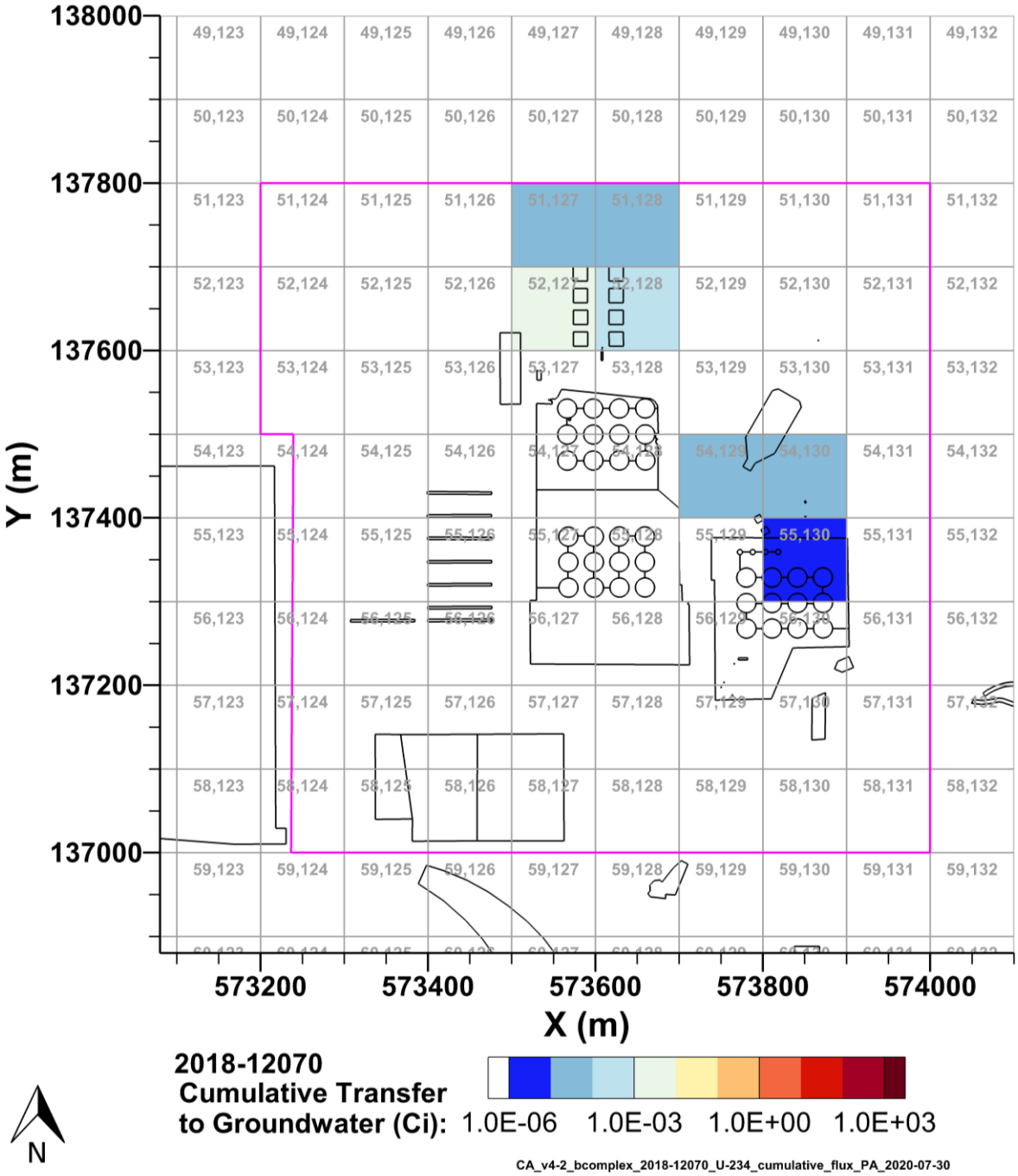

Note: source zone outlined in pink.

Figure 7-57. Cumulative U-234 Activity Discharged to Groundwater from the B Complex Model from 2018–12070 per P2R Grid Cell

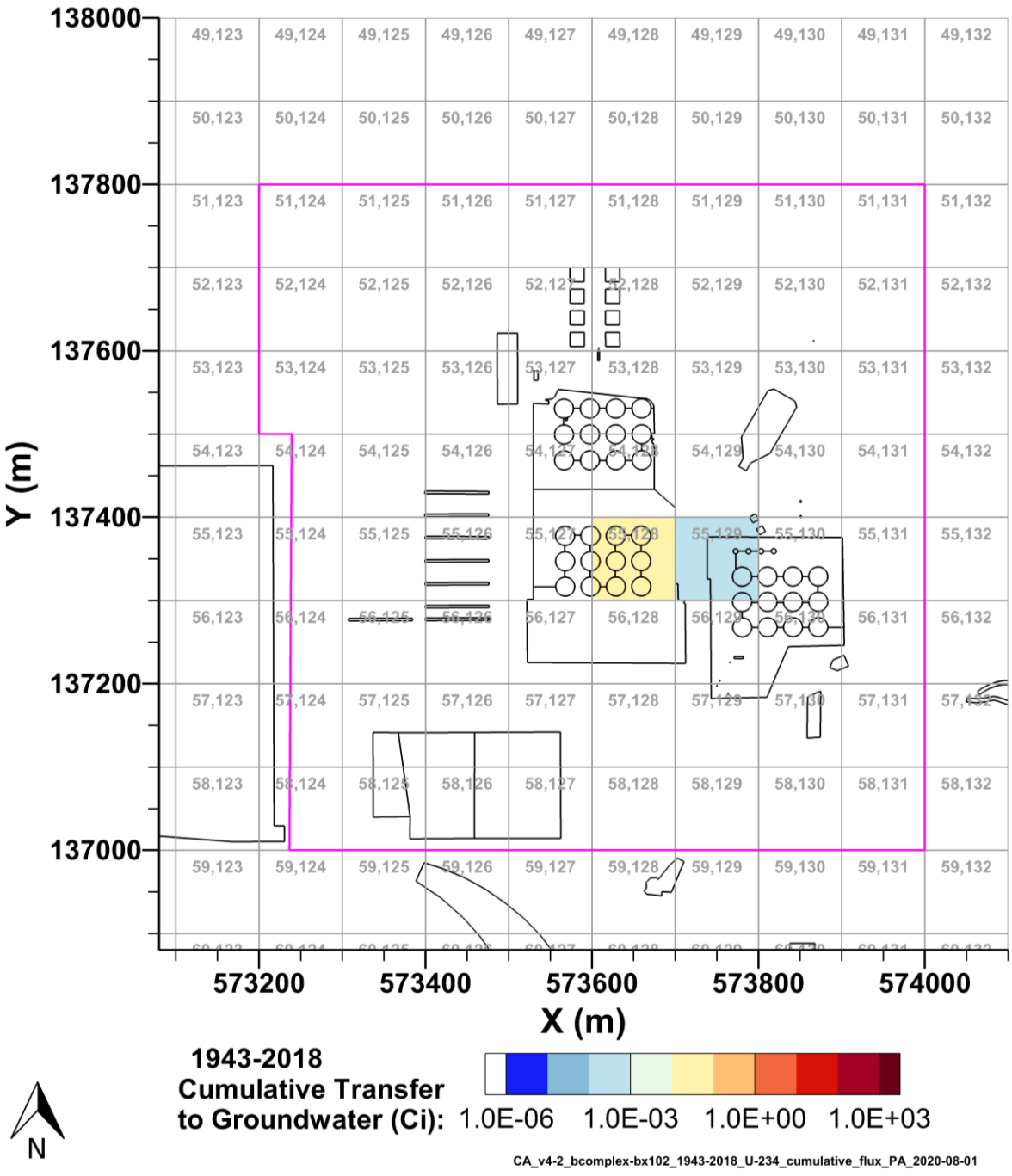

Figure 7-58. Cumulative Mobile U-234 Activity Discharged to Groundwater from 241-BX-102 in the B Complex Model from 1943–2018 per P2R Grid Cell

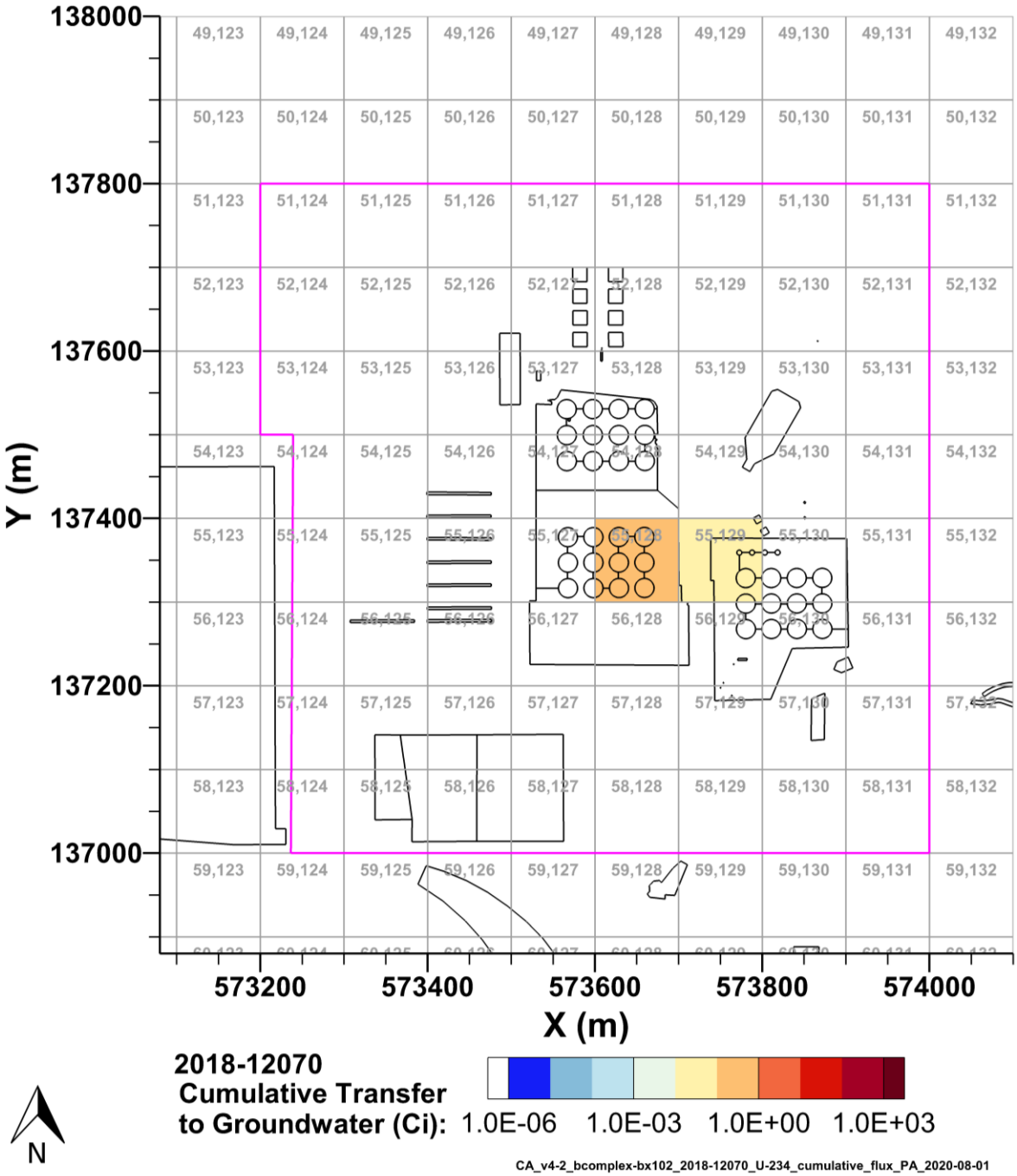

Figure 7-59. Cumulative Mobile U-234 Activity Discharged to Groundwater from 241-BX-102 in the B Complex Model from 2018–12070 per P2R Grid Cell

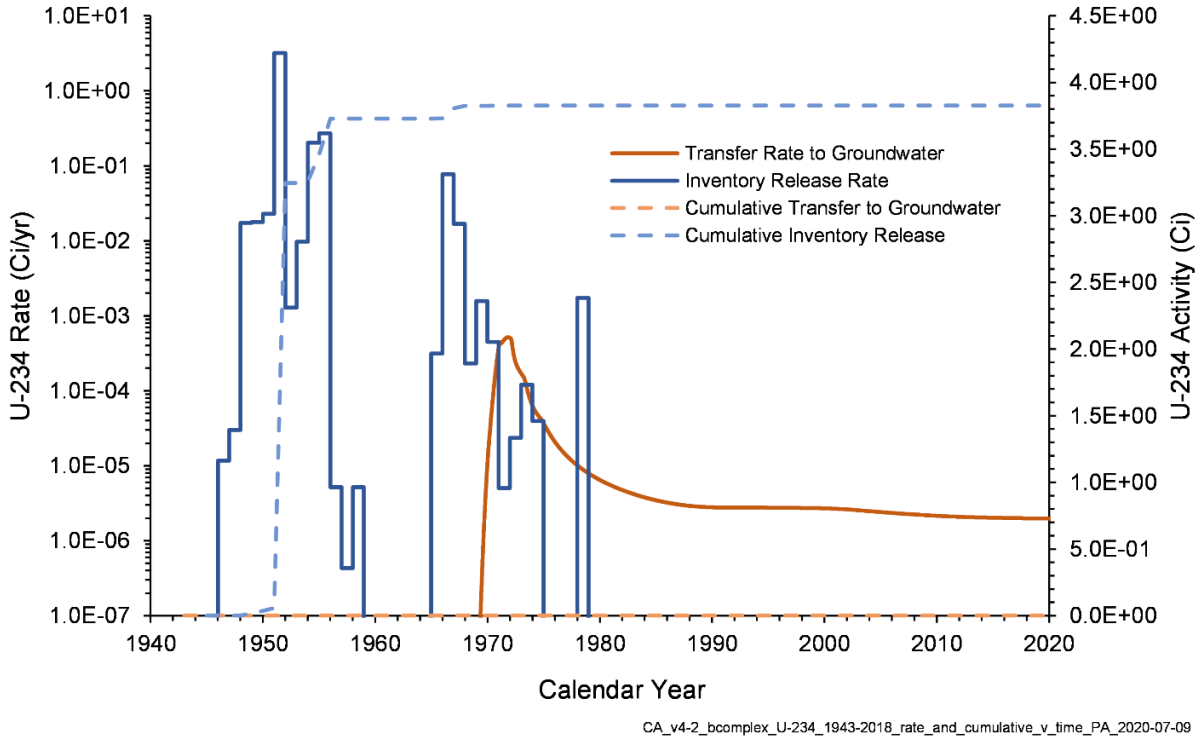

Figure 7-60. U-234 Inventory Release from Waste Sites and Transfer to Groundwater for the B Complex Model from 1943–2018

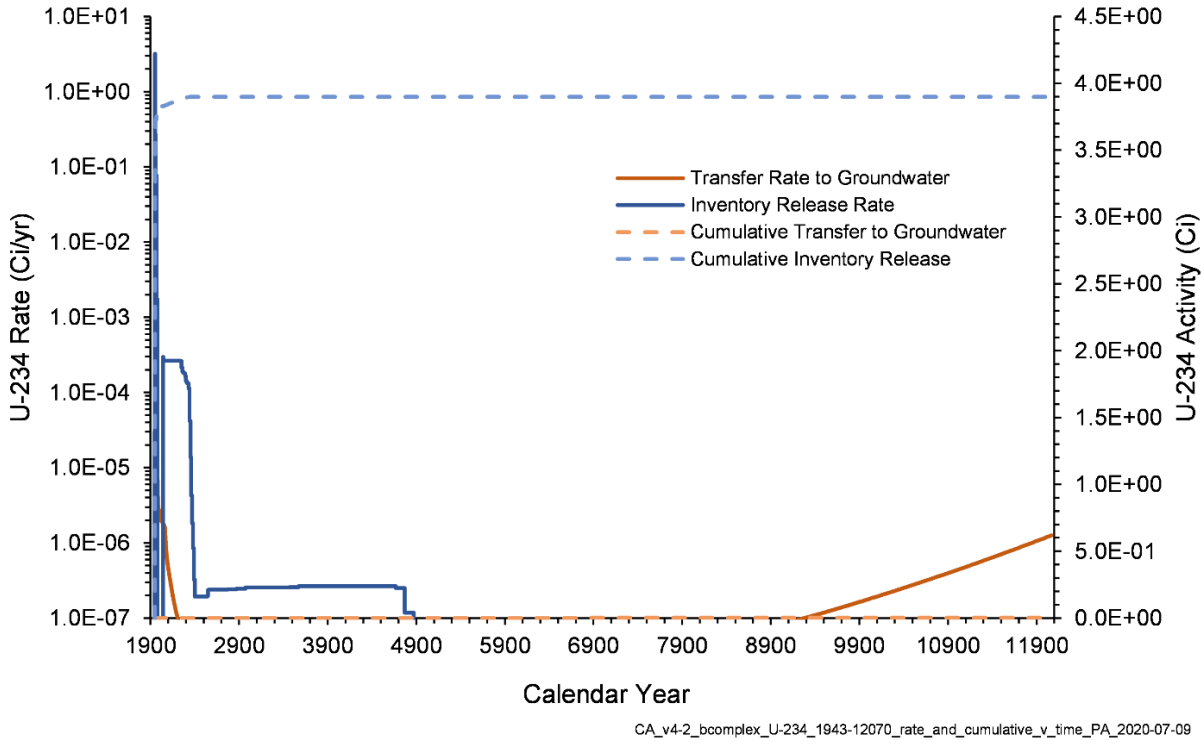

Figure 7-61. U-234 Inventory Release from Waste Sites and Transfer to Groundwater for the B Complex Model from 1943–12070

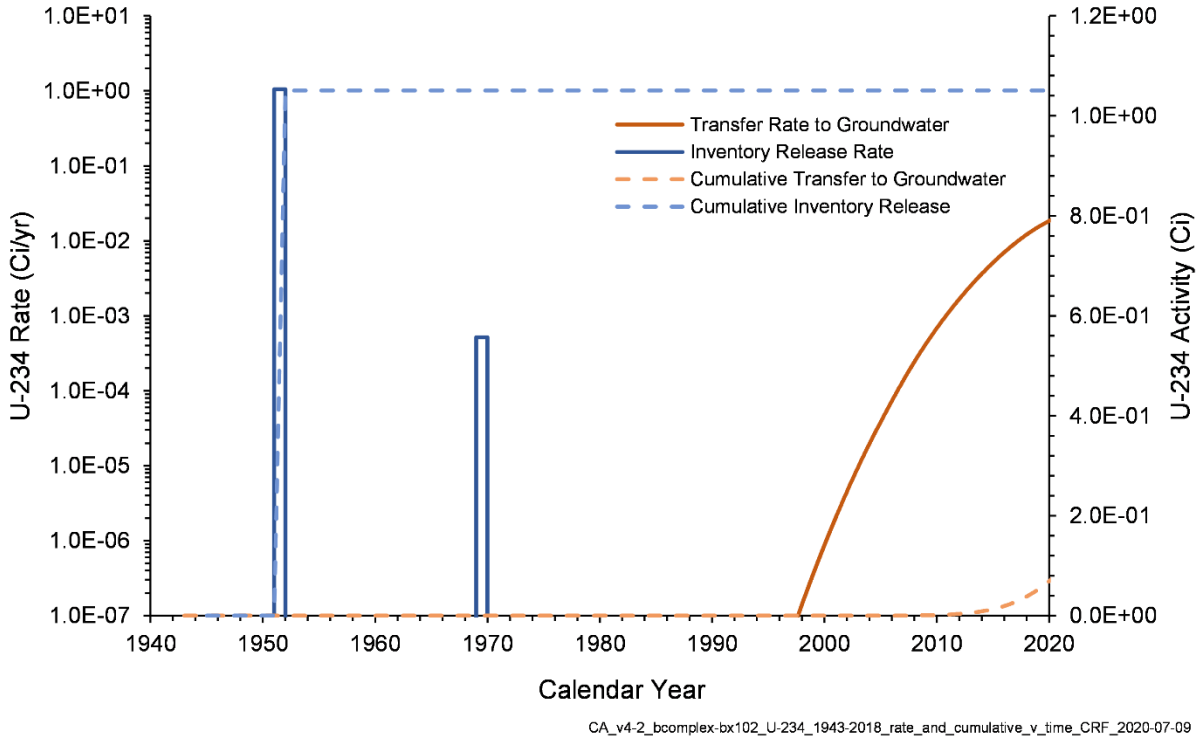

Figure 7-62. Mobile U-234 Inventory Release from 241-BX-102 and Transfer to Groundwater for the B Complex Model from 1943–2018

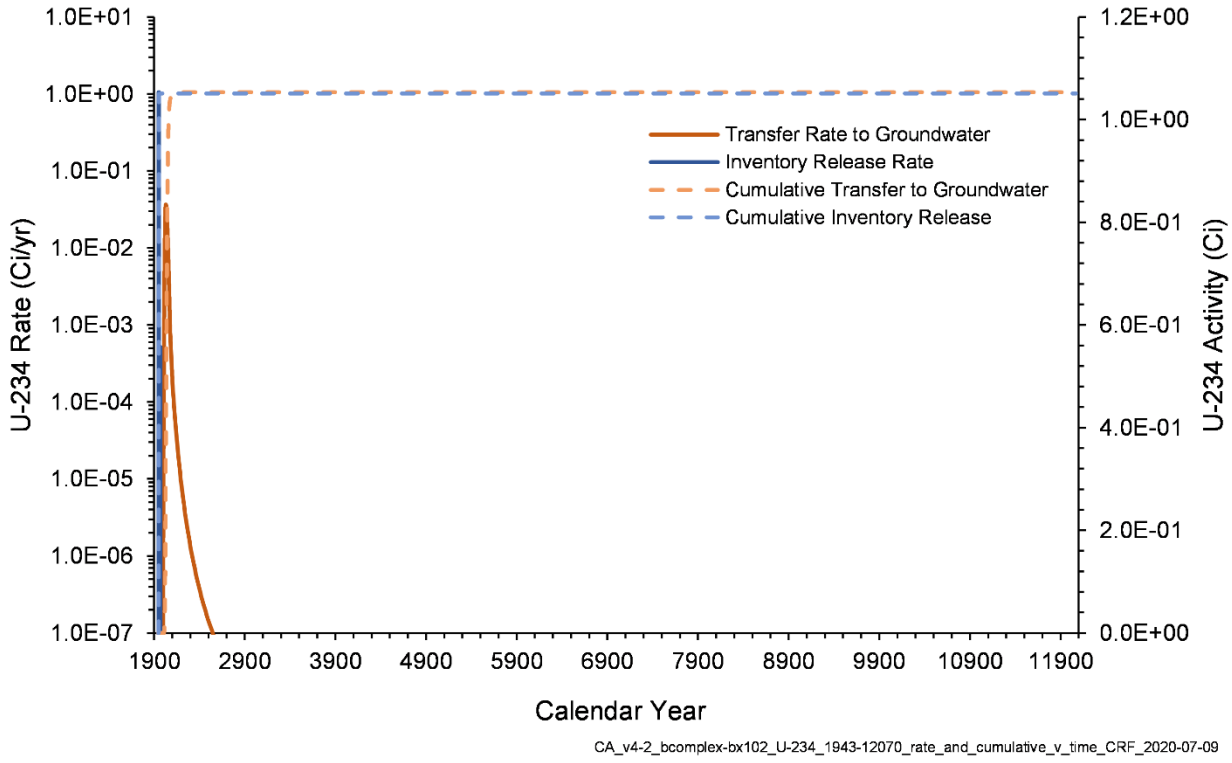

Figure 7-63. Mobile U-234 Inventory Release from 241-BX-102 and Transfer to Groundwater for the B Complex Model from 2018–12070

7.12 U-235 Fate and Transport Results

This model simulated the release and transport of U-235. The cumulative discharge of U-235 into groundwater is shown aggregated by P2R grid cell in Figure 7-64 and Figure 7-65 for 1943–2018 and 2018–12070, respectively. The cumulative discharge of mobile U-235 into groundwater from 241-BX-102 is shown aggregated by P2R grid cell in Figure 7-66 and Figure 7-67 for 1943–2018 and 2018–12070, respectively The inventory released to the B Complex model and the transfer of U-235 to groundwater are shown from 1943–2018 in Figure 7-68 and from 1943–12070 in Figure 7-69. The inventory released to the B Complex model from 241-BX-102 and the transfer of mobile U-235 to groundwater are shown from 1943–2018 in Figure 7-70 and from 1943–12070 in Figure 7-71.

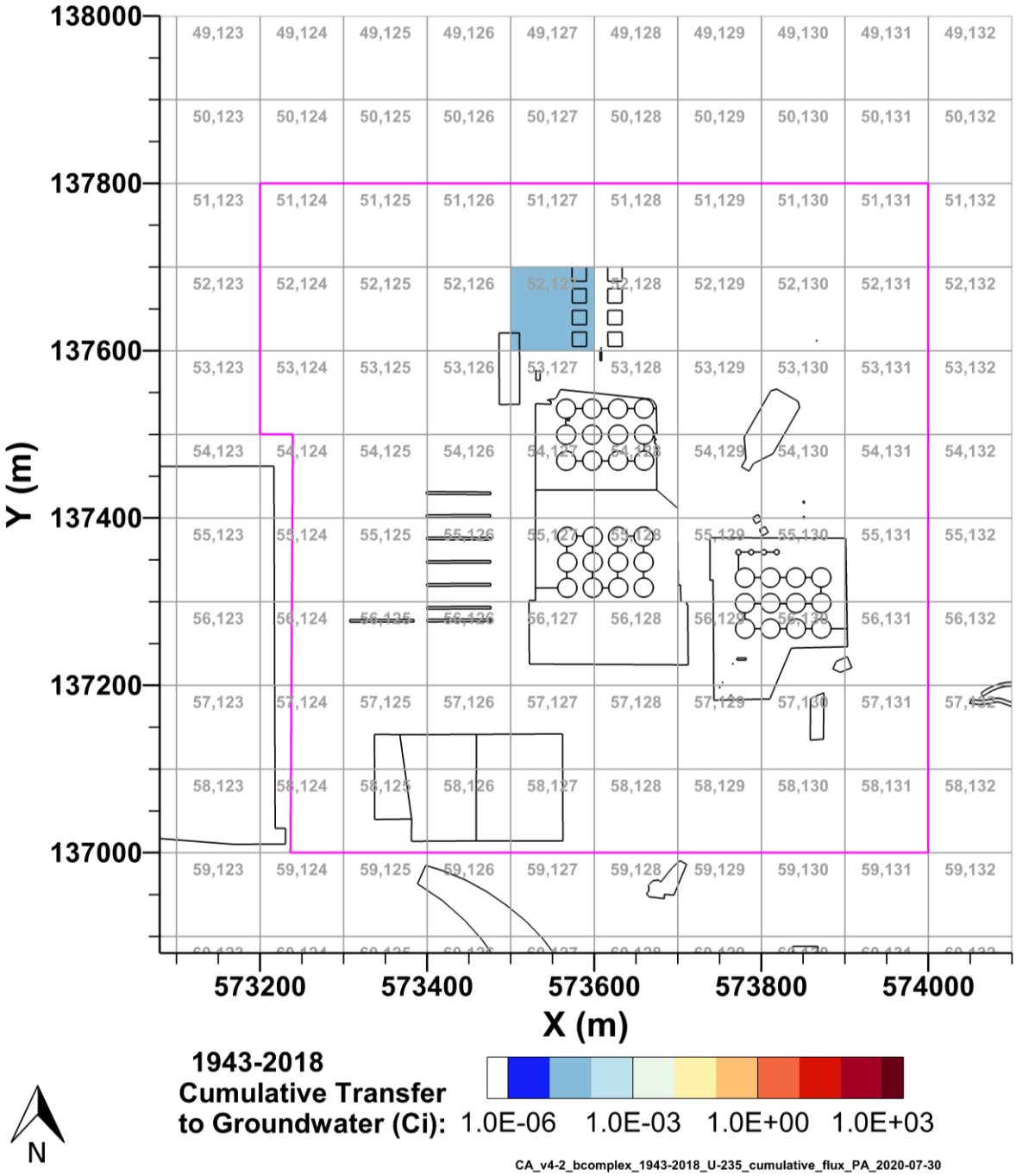

Note: source zone outlined in pink.

Figure 7-64. Cumulative U-235 Activity Discharged to Groundwater from the B Complex Model from 1943–2018 per P2R Grid Cell

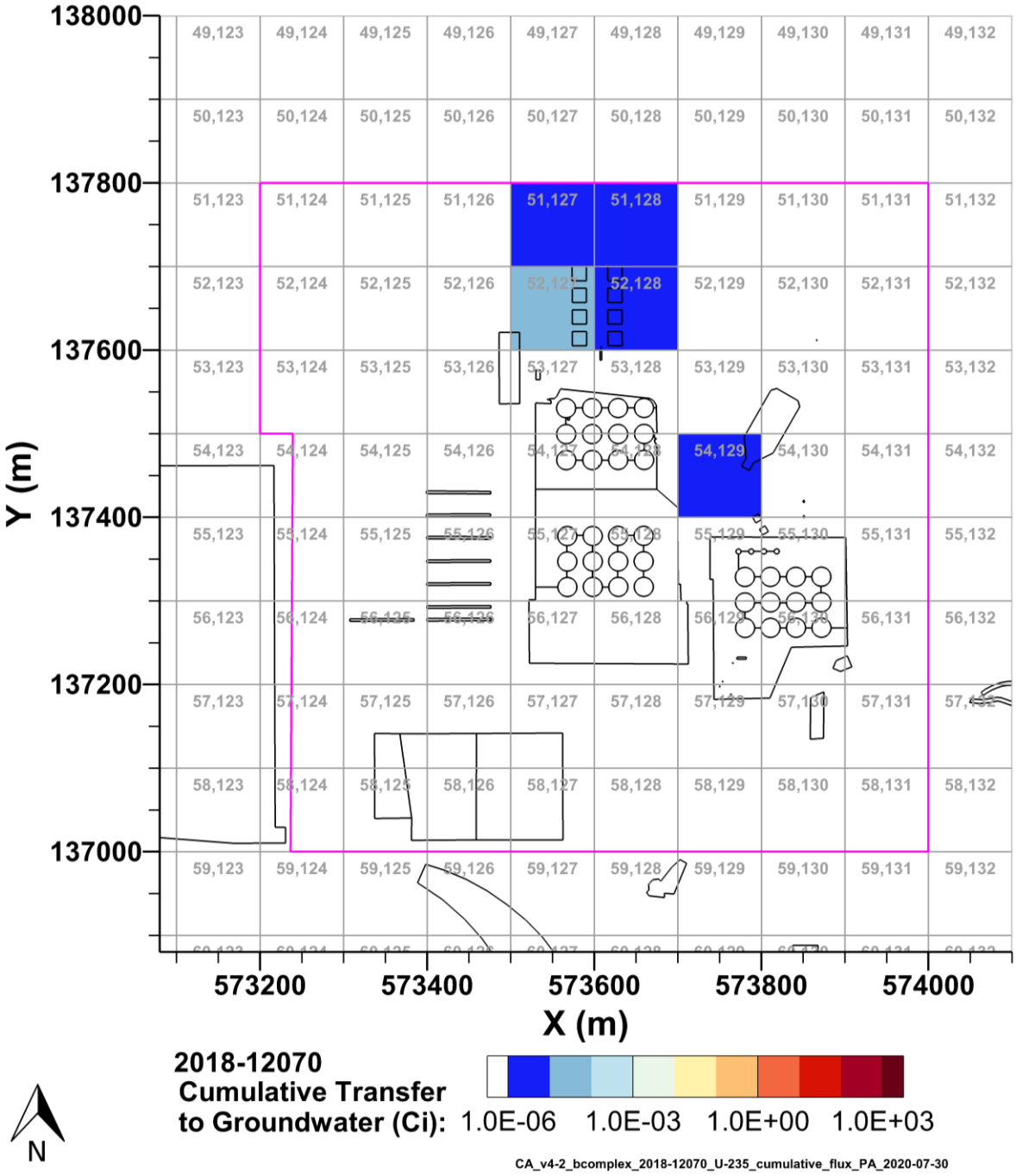

Note: source zone outlined in pink.

Figure 7-65. Cumulative U-235 Activity Discharged to Groundwater from the B Complex Model from 2018–12070 per P2R Grid Cell

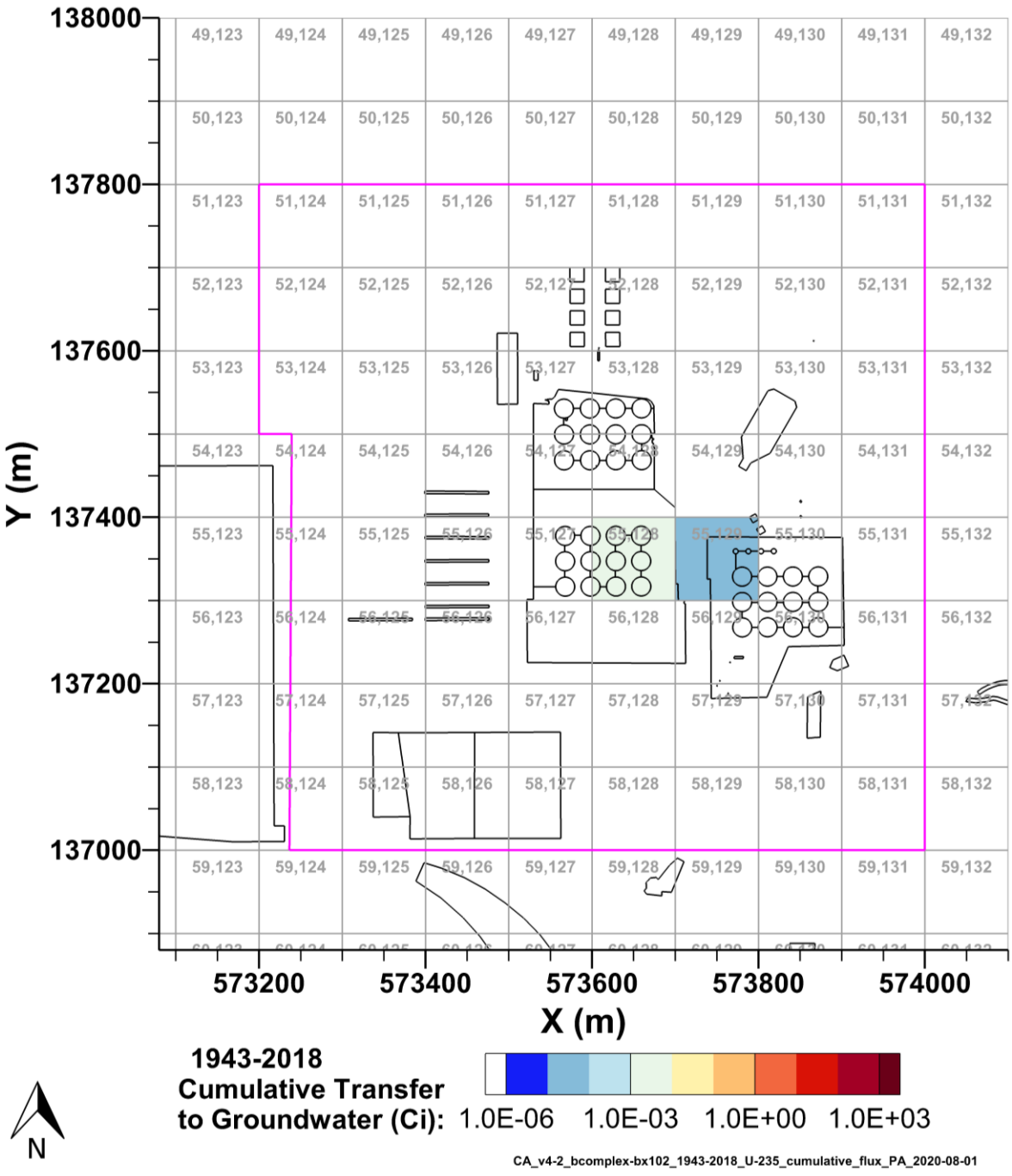

Figure 7-66. Cumulative Mobile U-235 Activity Discharged to Groundwater from 241-BX-102 in the B Complex Model from 1943–2018 per P2R Grid Cell

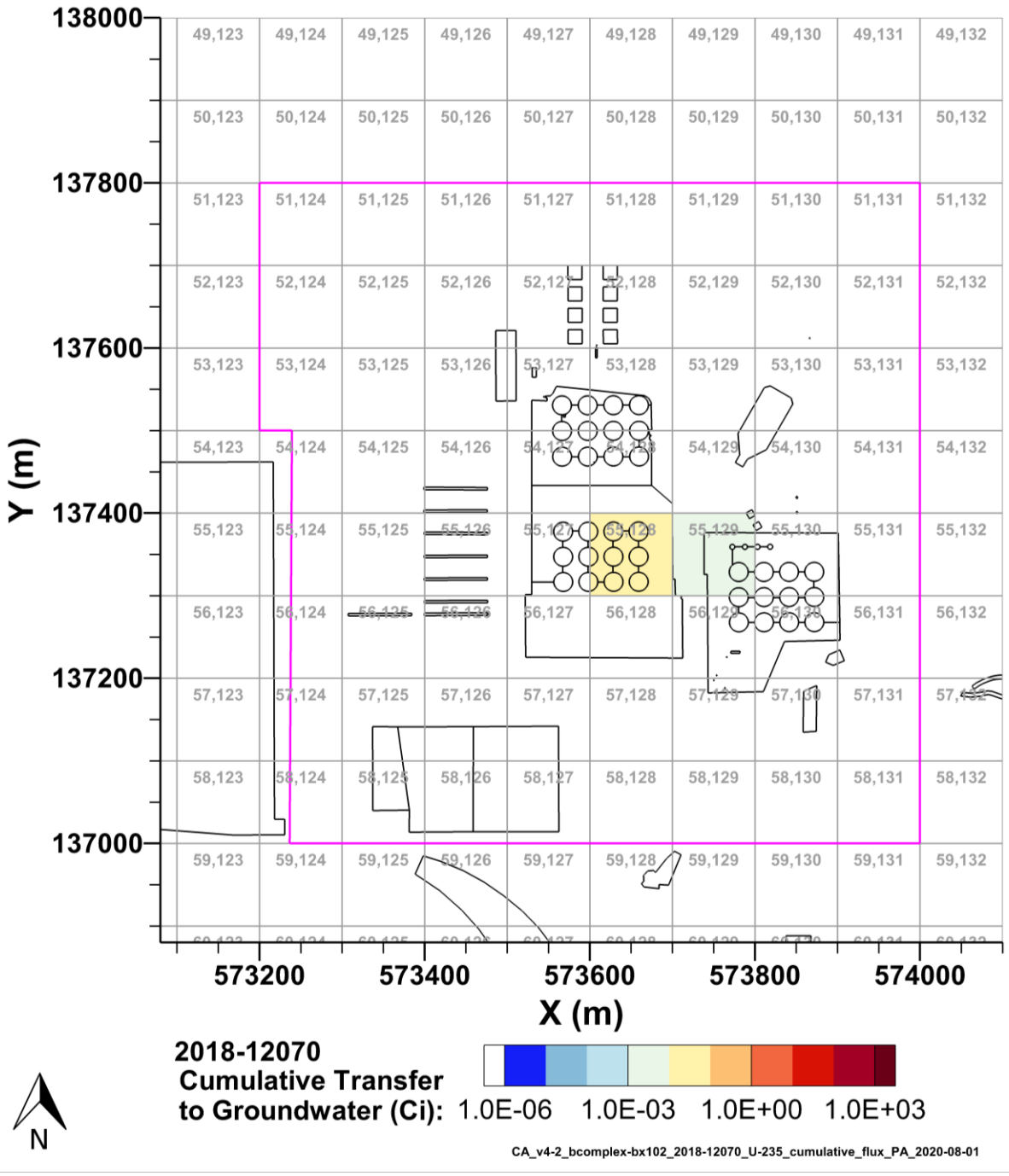

Figure 7-67. Cumulative Mobile U-235 Activity Discharged to Groundwater from 241-BX-102 in the B Complex Model from 2018–12070 per P2R Grid Cell

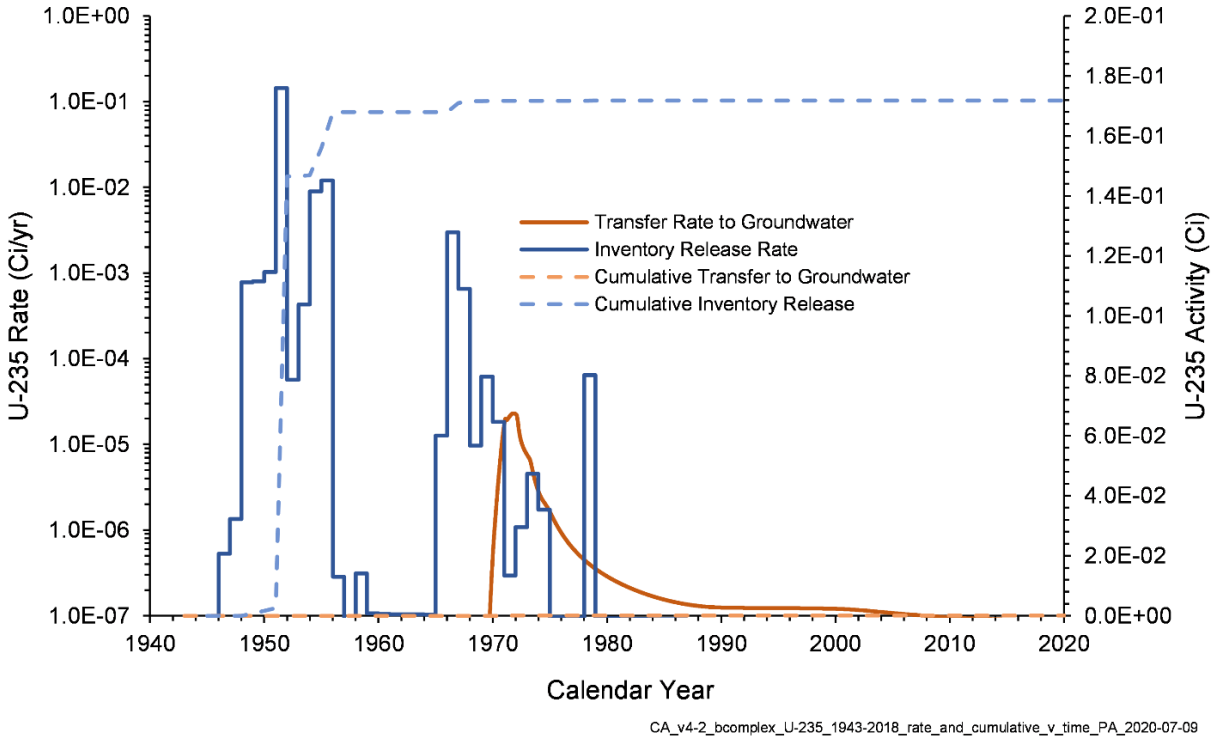

Figure 7-68. U-235 Inventory Release from Waste Sites and Transfer to Groundwater for the B Complex Model from 1943–2018

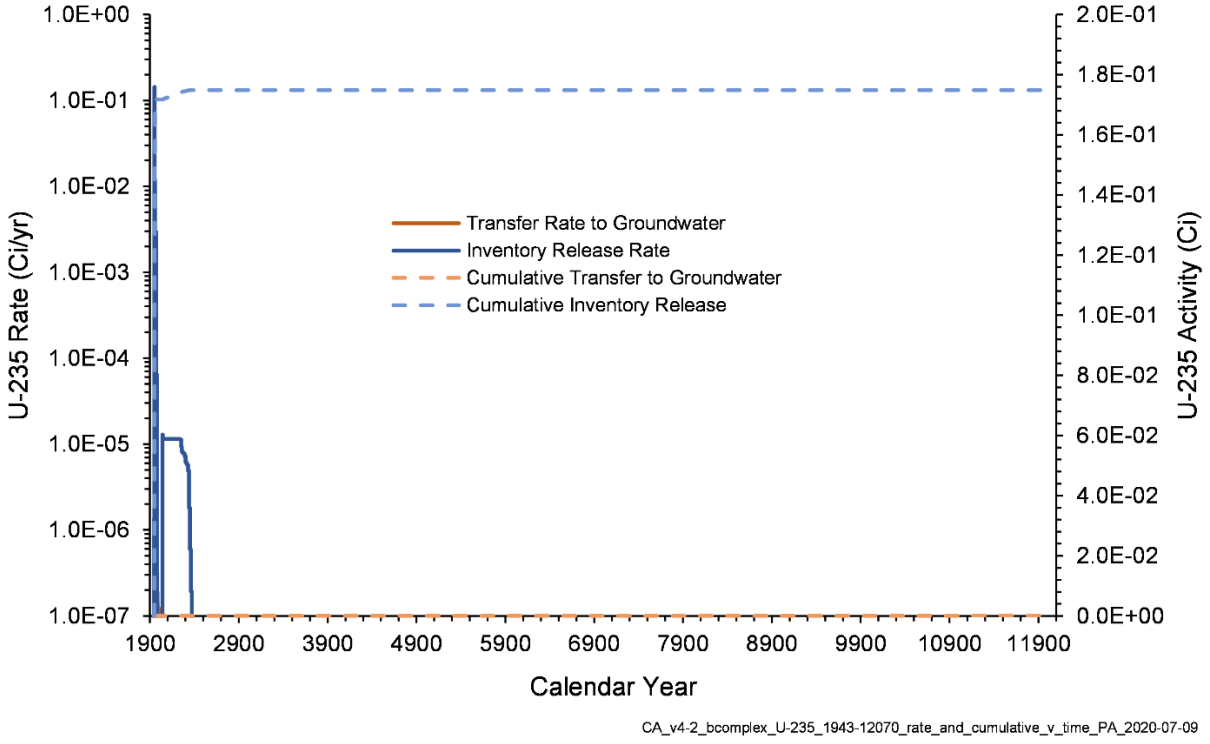

Figure 7-69. U-235 Inventory Release from Waste Sites and Transfer to Groundwater for the B Complex Model from 1943–12070

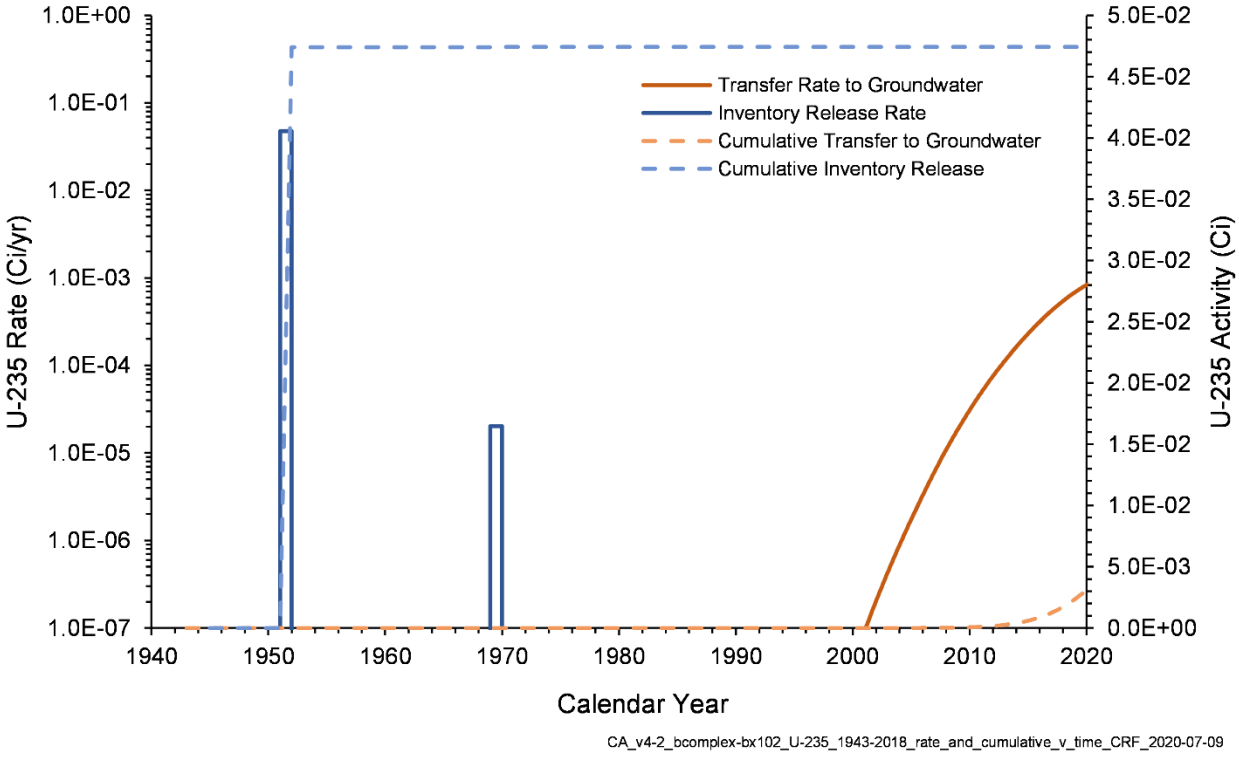

Figure 7-70. Mobile U-235 Inventory Release from 241-BX-102 and Transfer to Groundwater for the B Complex Model from 1943–2018

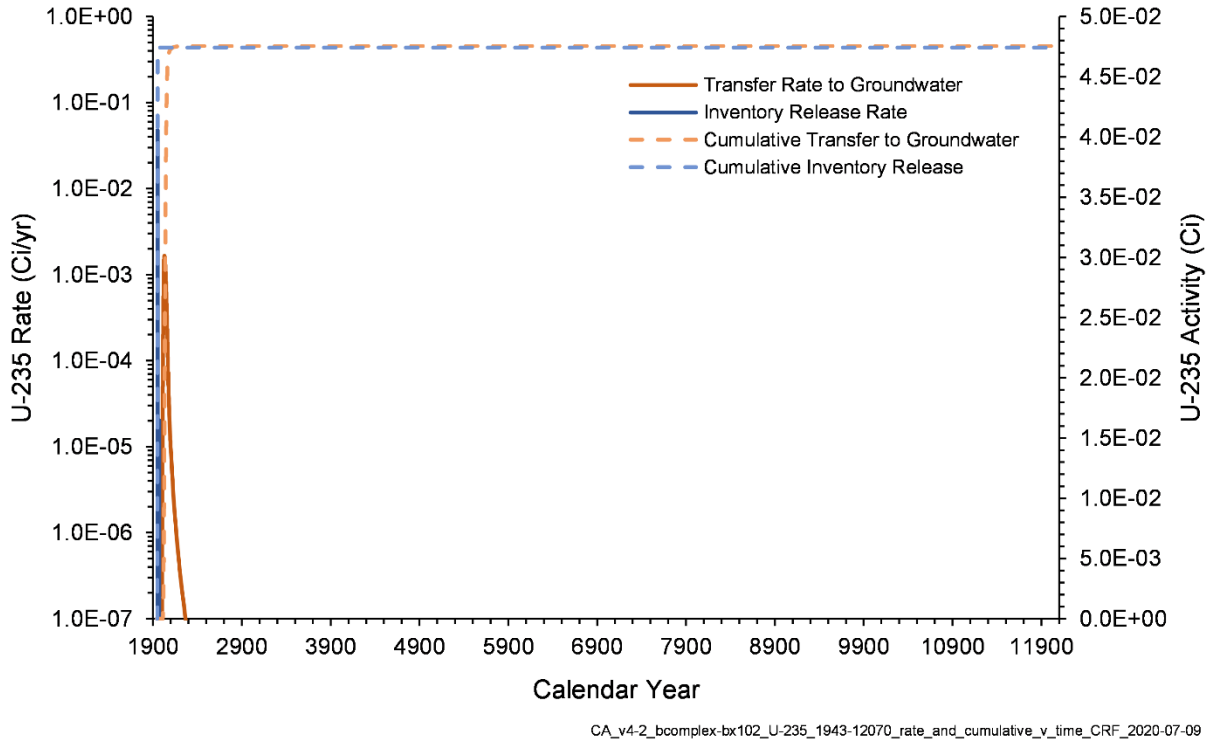

Figure 7-71. Mobile U-235 Inventory Release from 241-BX-102 and Transfer to Groundwater for the B Complex Model from 2018–12070

7.13 U-236 Fate and Transport Results

This model simulated the release and transport of U-236. The cumulative discharge of U-236 into groundwater is shown aggregated by P2R grid cell in Figure 7-72 and Figure 7-73 for 1943–2018 and 2018–12070, respectively. The cumulative discharge of mobile U-236 into groundwater from 241-BX-102 is shown aggregated by P2R grid cell in Figure 7-74 and Figure 7-75 for 1943–2018 and 2018–12070, respectively. The inventory released to the B Complex model and the transfer of U-236 to groundwater are shown from 1943–2018 in Figure 7-76 and from 1943–12070 in Figure 7-77. The inventory released to the B Complex model from 241-BX-102 and the transfer of mobile U-236 to groundwater are shown from 1943–2018 in Figure 7-78 and from 1943–12070 in Figure 7-79.

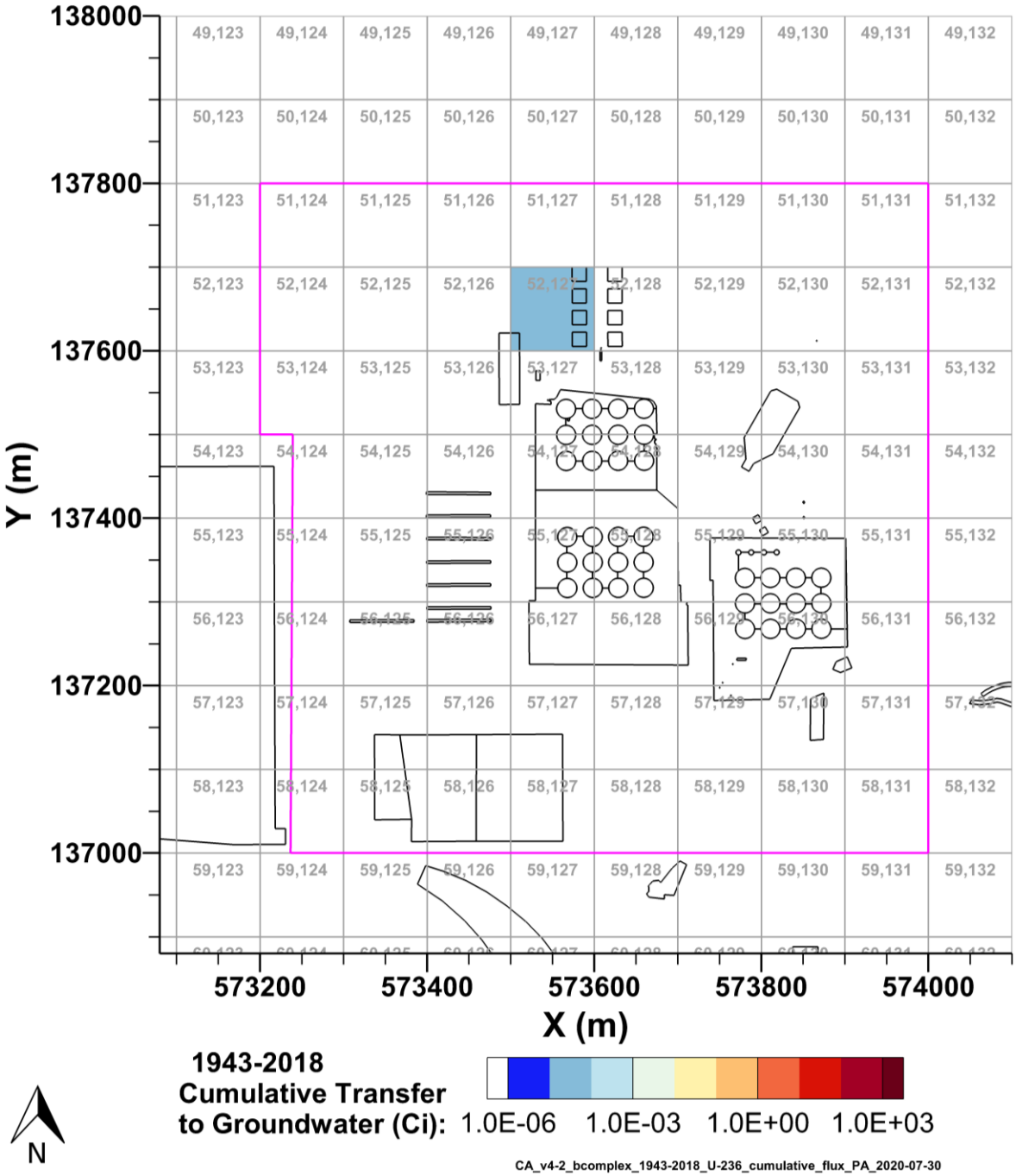

Note: source zone outlined in pink.

Figure 7-72. Cumulative U-236 Activity Discharged to Groundwater from the B Complex Model from 1943–2018 per P2R Grid Cell

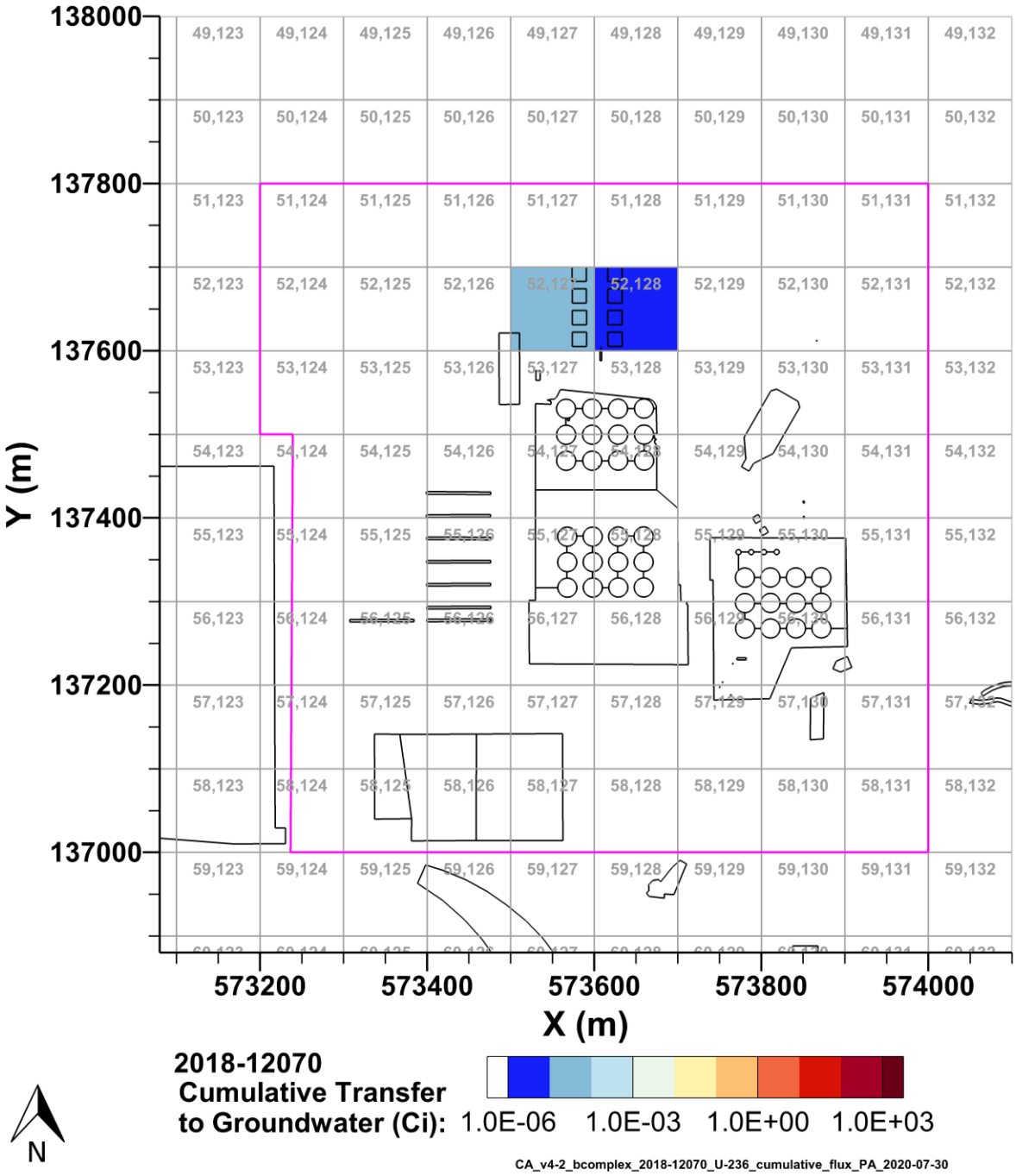

Note: source zone outlined in pink.

Figure 7-73. Cumulative U-236 Activity Discharged to Groundwater from the B Complex Model from 2018–12070 per P2R Grid Cell

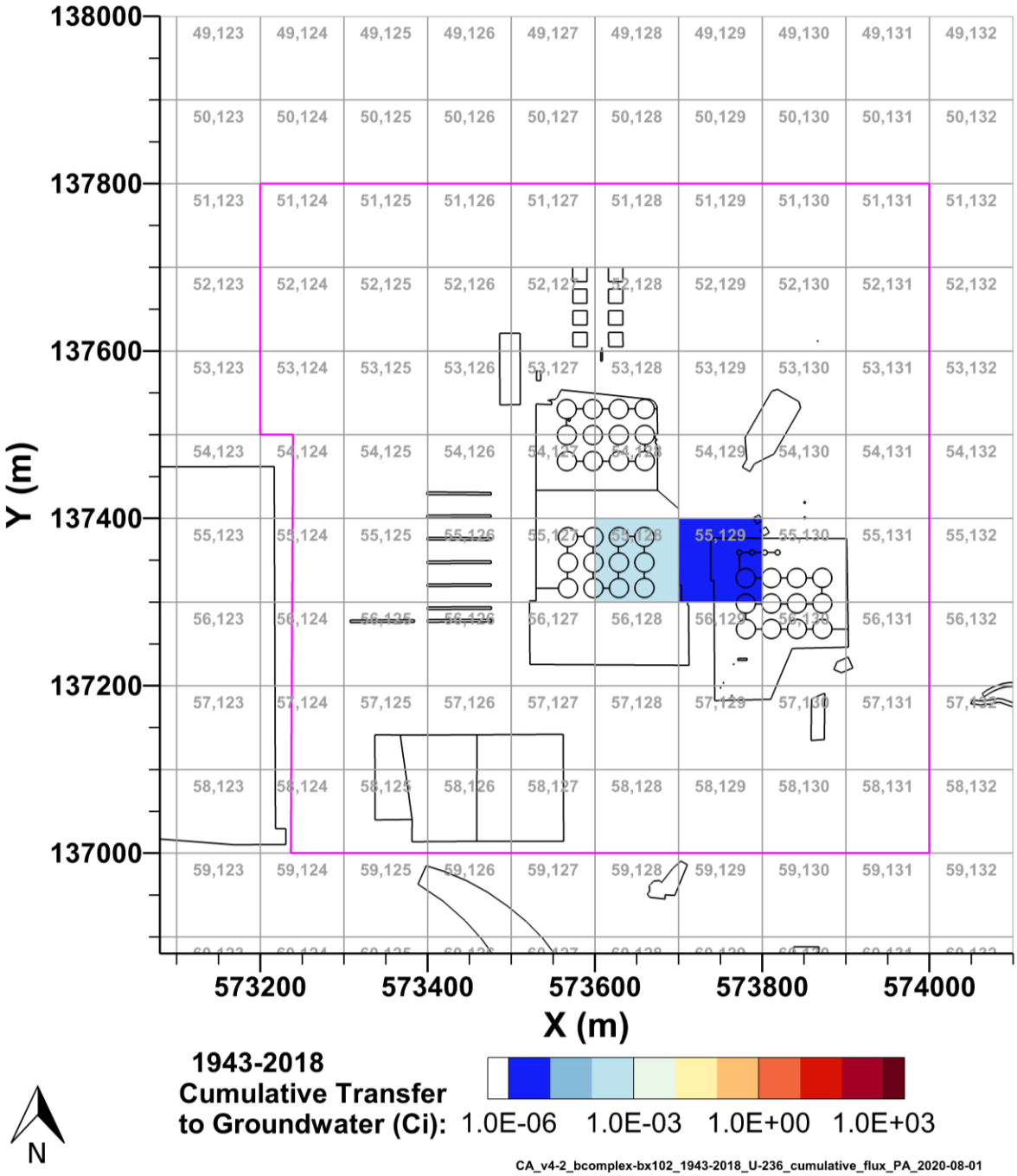

Figure 7-74. Cumulative Mobile U-236 Activity Discharged to Groundwater from 241-BX-102 in the B Complex Model from 1943–2018 per P2R Grid Cell

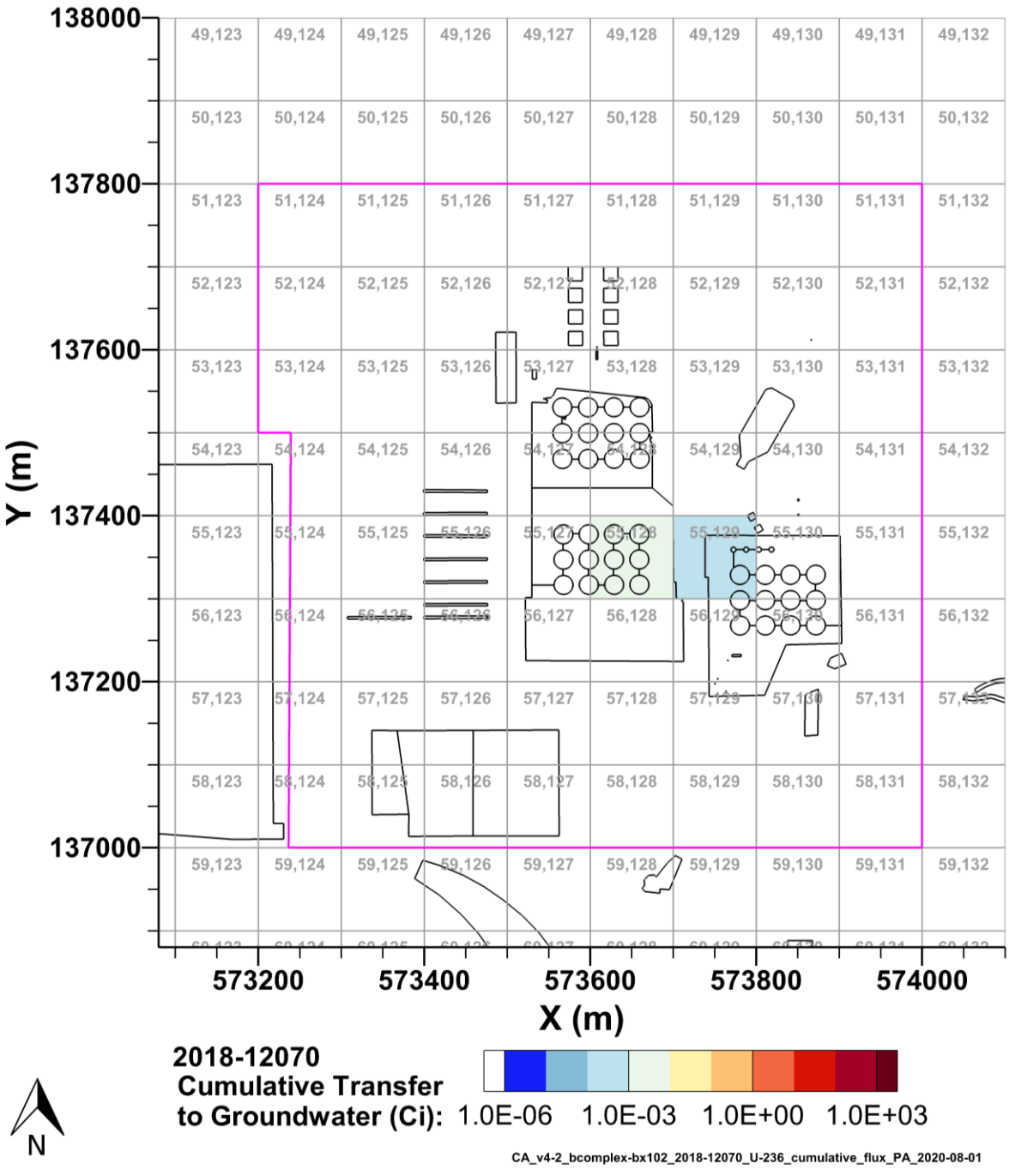

Figure 7-75. Cumulative Mobile U-236 Activity Discharged to Groundwater from 241-BX-102 in the B Complex Model from 2018–12070 per P2R Grid Cell

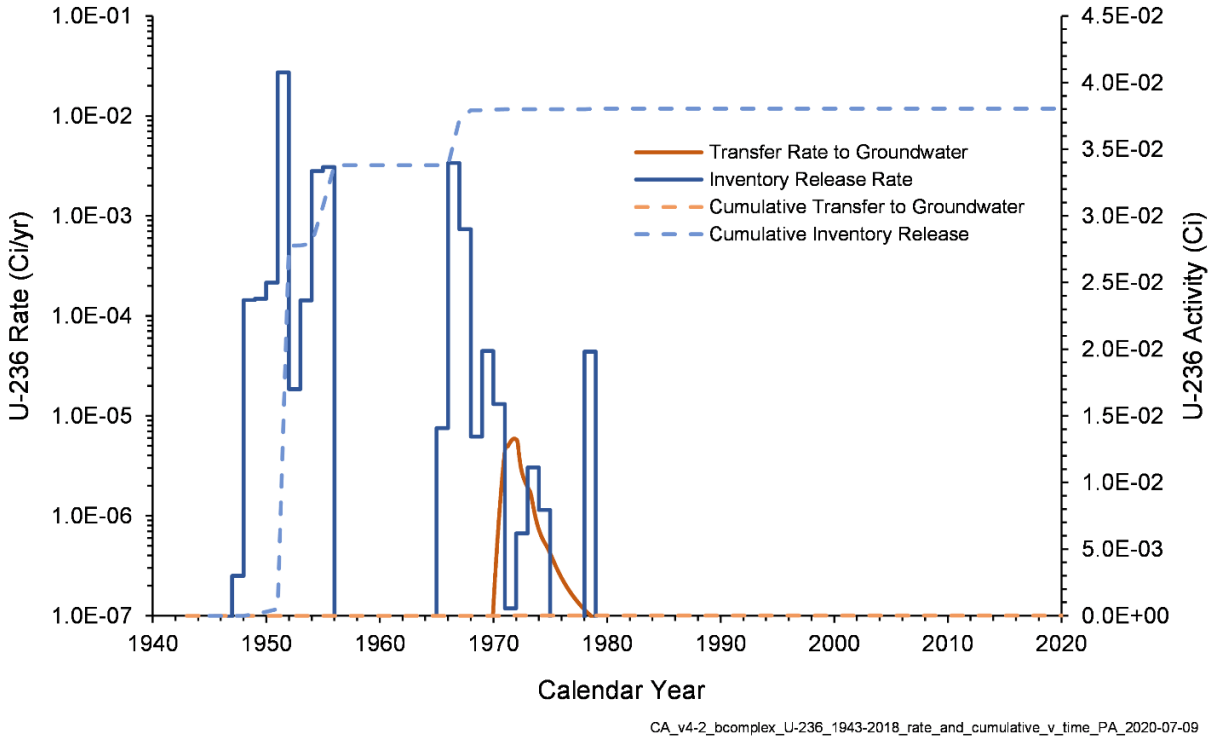

Figure 7-76. U-236 Inventory Release from Waste Sites and Transfer to Groundwater for the B Complex Model from 1943–2018

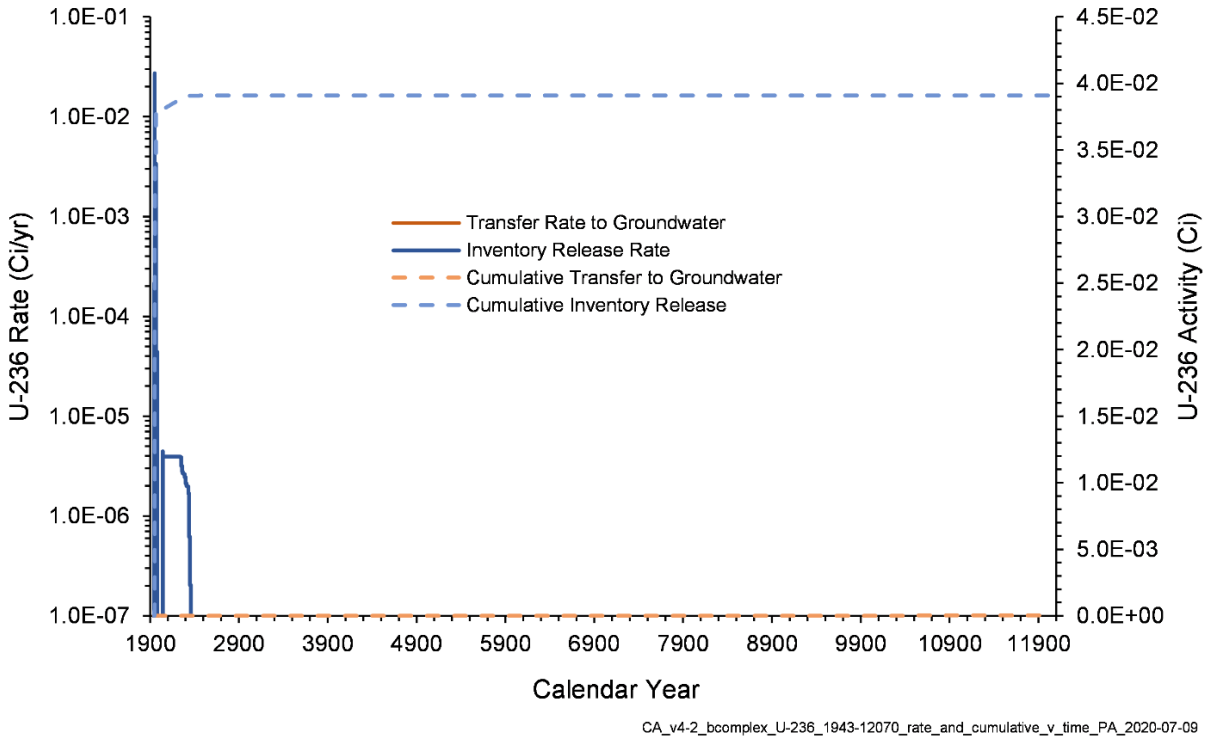

Figure 7-77. U-236 Inventory Release from Waste Sites and Transfer to Groundwater for the B Complex Model from 1943–12070

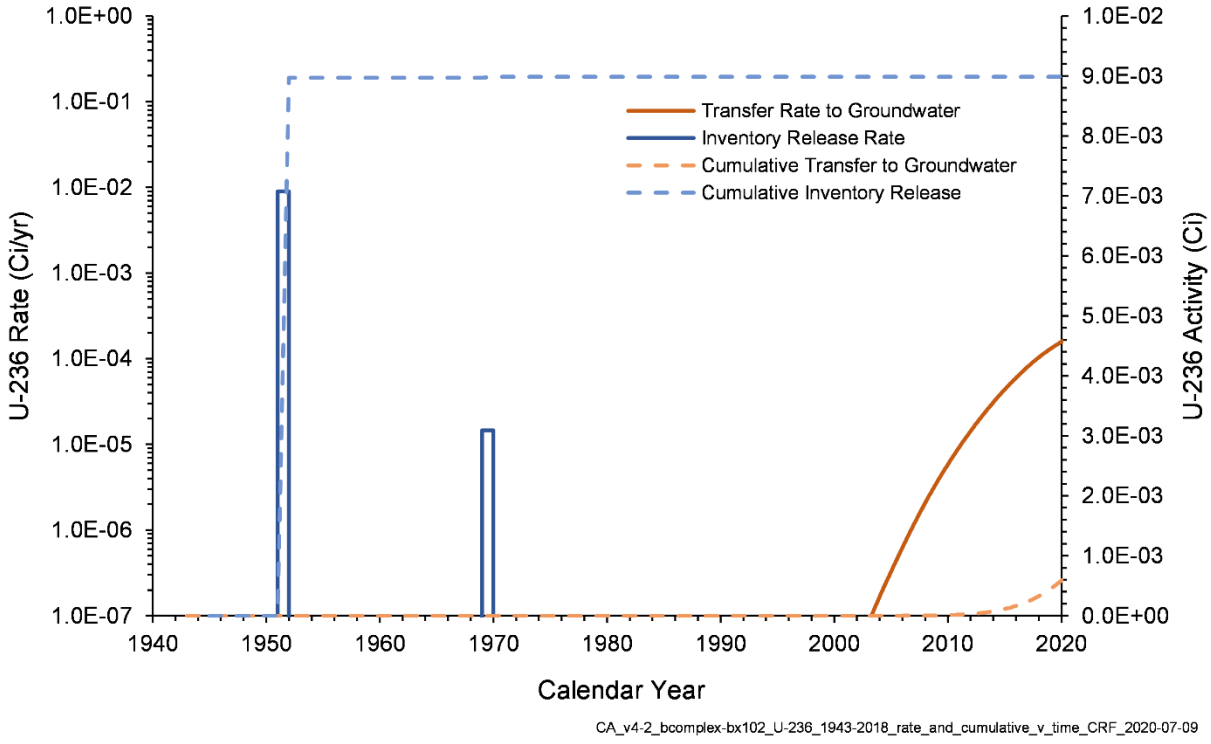

Figure 7-78. Mobile U-236 Inventory Release from 241-BX-102 and Transfer to Groundwater for the B Complex Model from 1943–2018

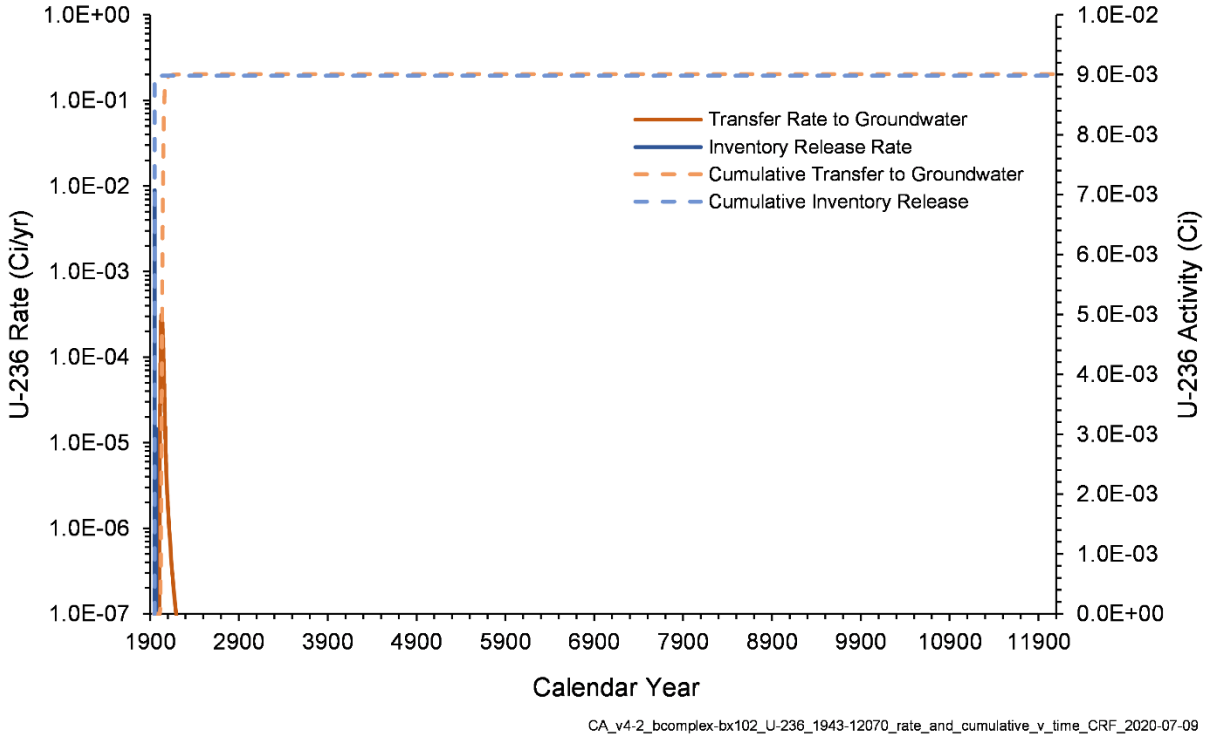

Figure 7-79. Mobile U-236 Inventory Release from 241-BX-102 and Transfer to Groundwater for the B Complex Model from 2018–12070

7.14 U-238 Fate and Transport Results

This model simulated release and transport of U-238. The cumulative discharge of U-238 into groundwater is shown aggregated by P2R grid cell in Figure 7-80 and Figure 7-81 for 1943–2018 and 2018–12070, respectively. The cumulative discharge of mobile U-238 into groundwater from 241-BX-102 is shown aggregated by P2R grid cell in and Figure 7-82 for Figure 7-83 1943–2018 and 2018–12070, respectively. The inventory released to the B Complex model and the transfer of U-238 to groundwater are shown from 1943–2018 in Figure 7-84 and from 1943–12070 in Figure 7-85. The inventory released to the B Complex model from 241-BX-102 and the transfer of mobile U-238 to groundwater are shown from 1943–2018 in Figure 7-86 and from 1943–12070 in Figure 7-87. Figure 7-88 through Figure 7-93 show the flux of mobile U-238 from 241-BX-102 groundwater in Ci/yr. These figures are generated at times with peak fluxes (local maxima) and during periods with gradual decline, as shown in Figure 7-86 and Figure 7-87. A figure for 2018, Figure 7-89, is also included to demonstrate the initial flux conditions for the 2018–12070 simulation.

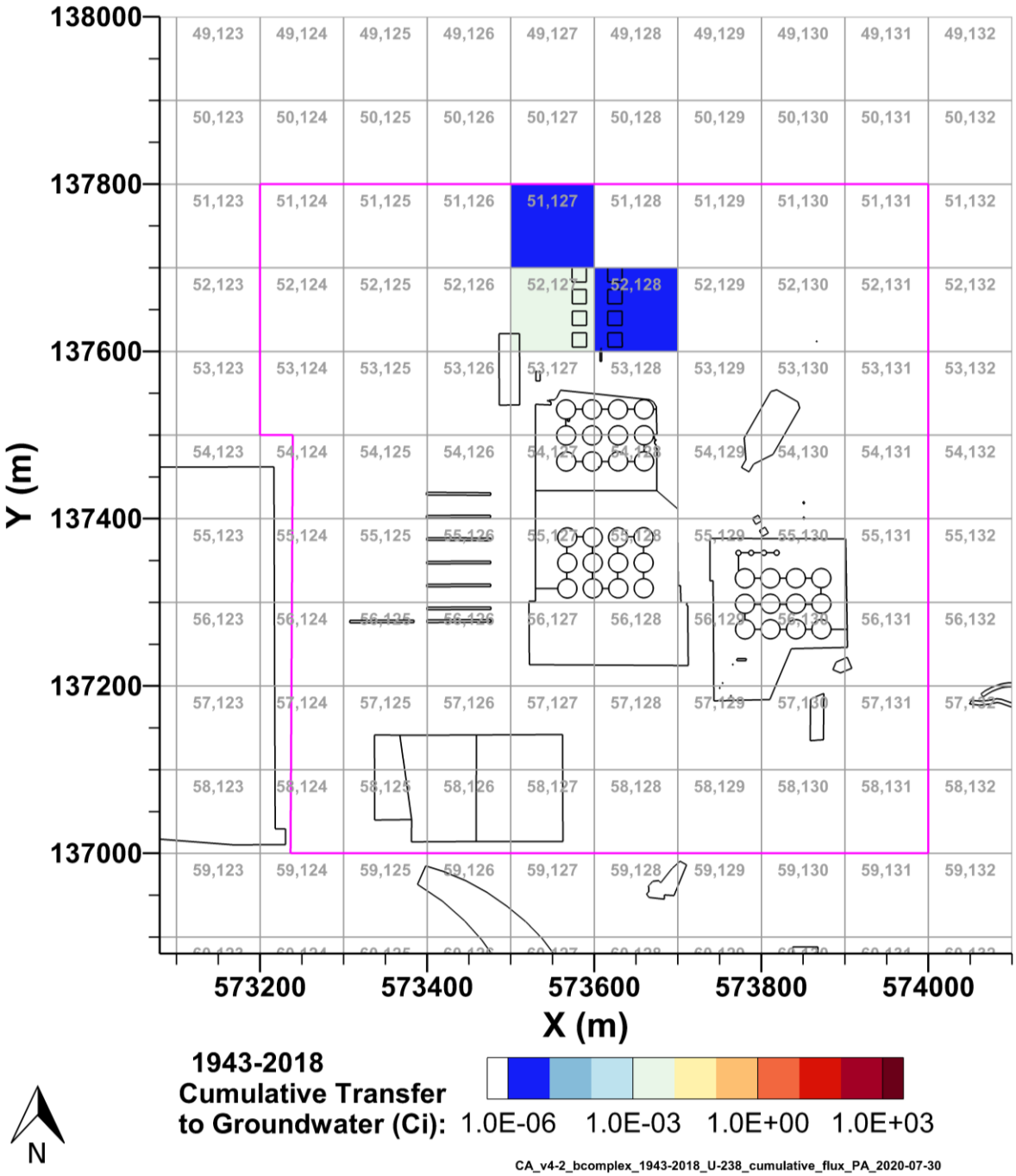

Note: source zone outlined in pink.

Figure 7-80. Cumulative U-238 Activity Discharged to Groundwater from the B Complex Model from 1943–2018 per P2R Grid Cell

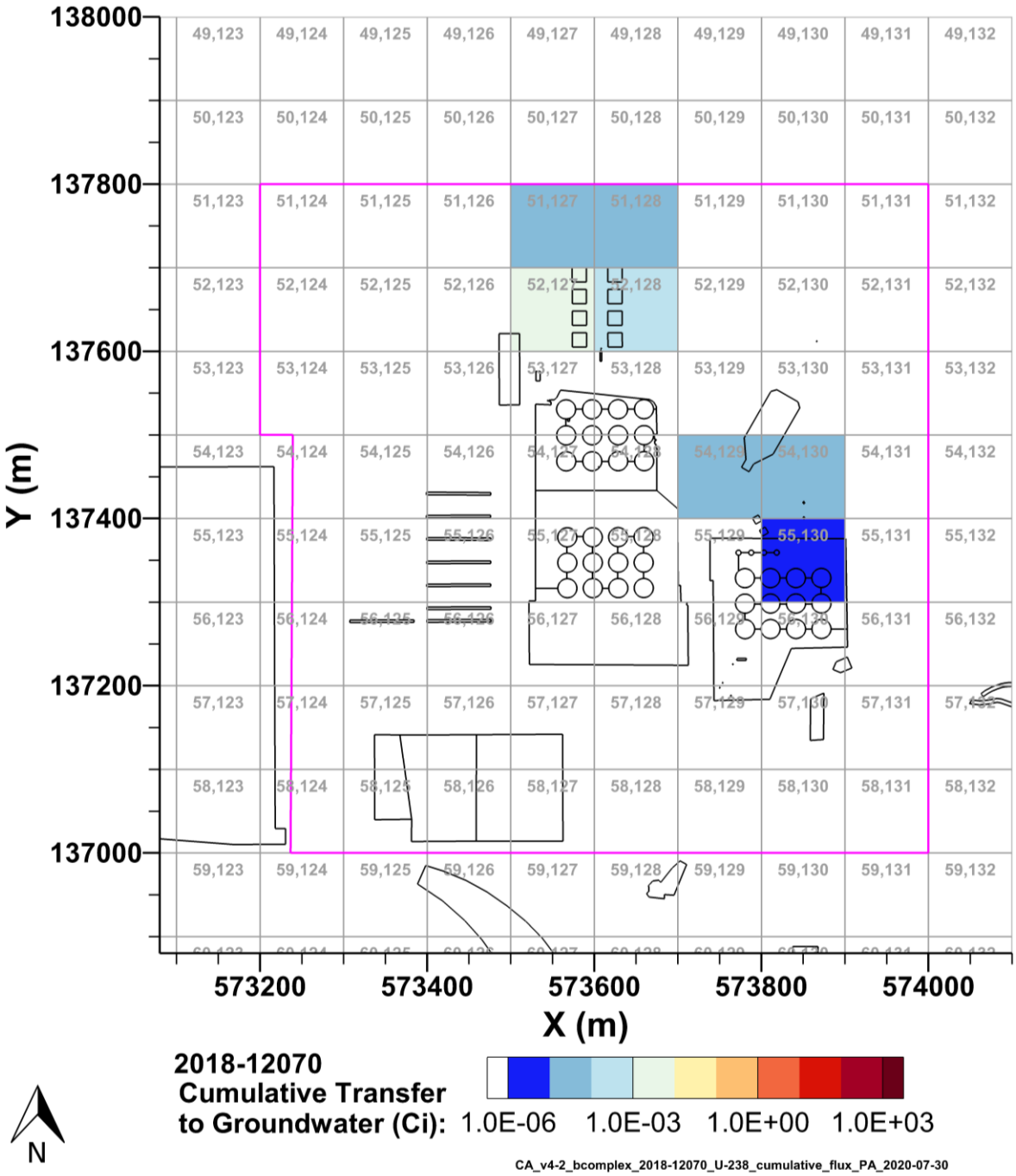

Note: source zone outlined in pink.

Figure 7-81. Cumulative U-238 Activity Discharged to Groundwater from the B Complex Model from 2018–12070 per P2R Grid Cell

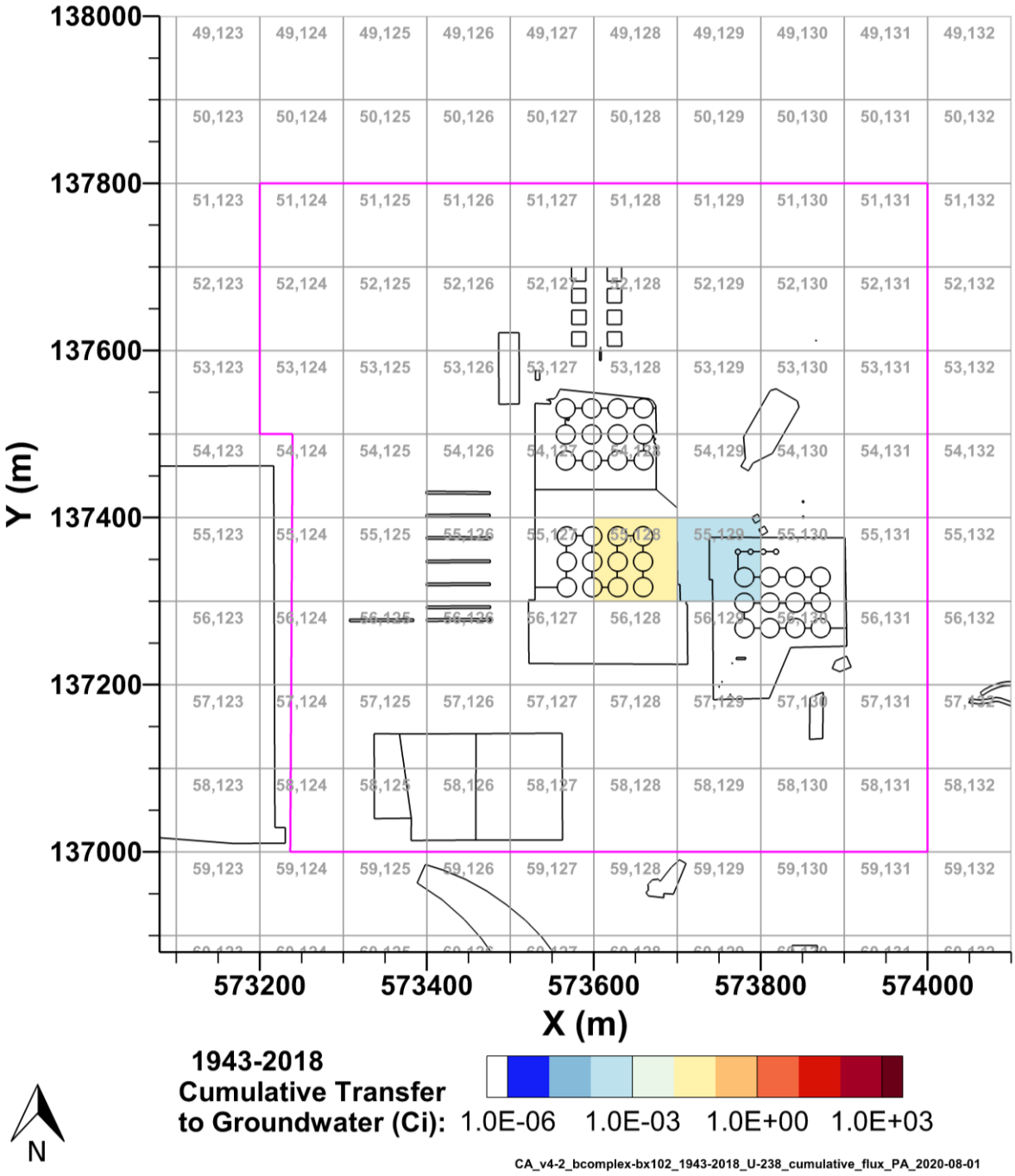

Figure 7-82. Cumulative Mobile U-238 Activity Discharged to Groundwater from 241-BX-102 in the B Complex Model from 1973–2018 per P2R Grid Cell

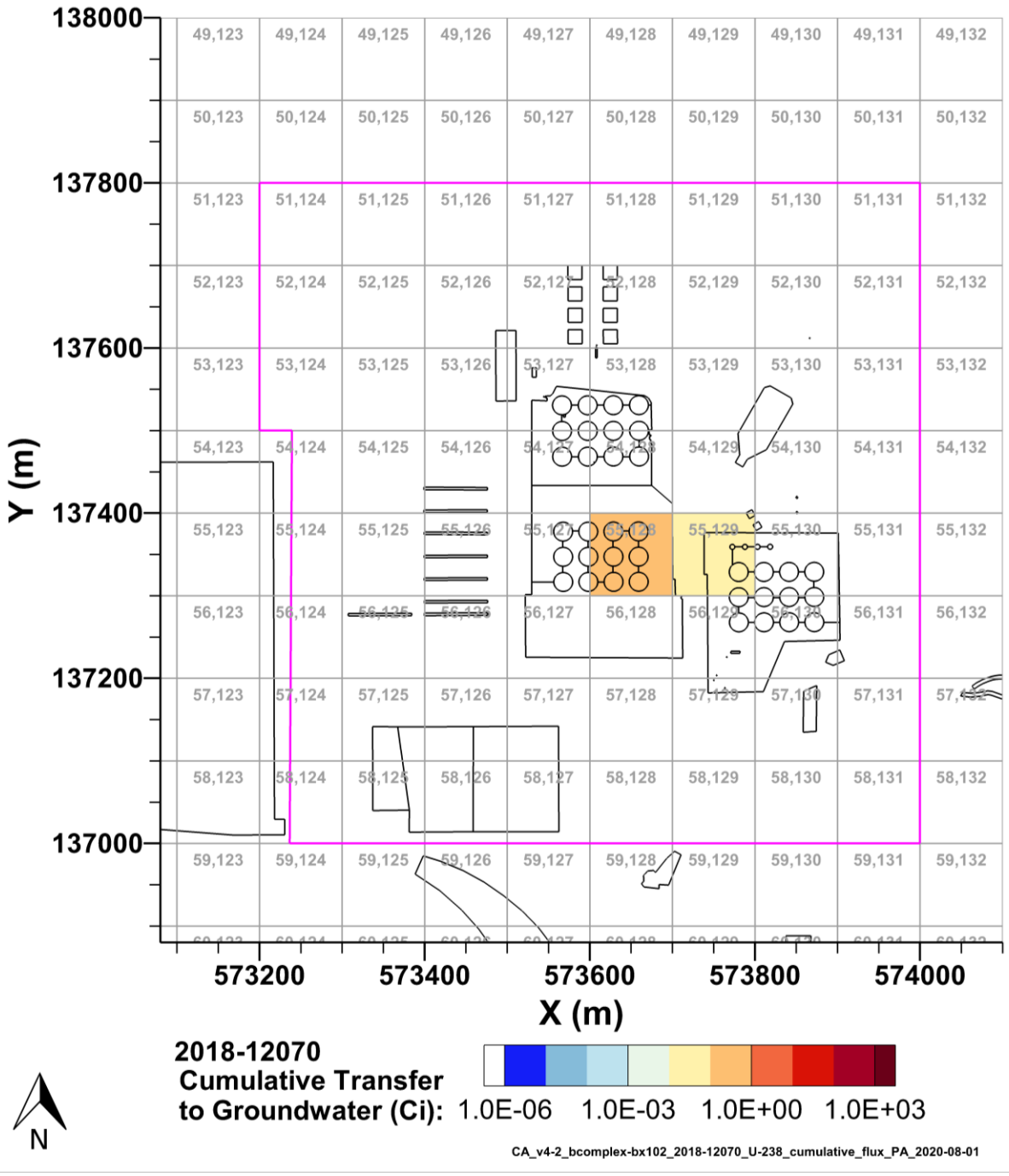

Figure 7-83. Cumulative Mobile U-238 Activity Discharged to Groundwater from 241-BX-102 in the B Complex Model from 2018–12070 per P2R Grid Cell

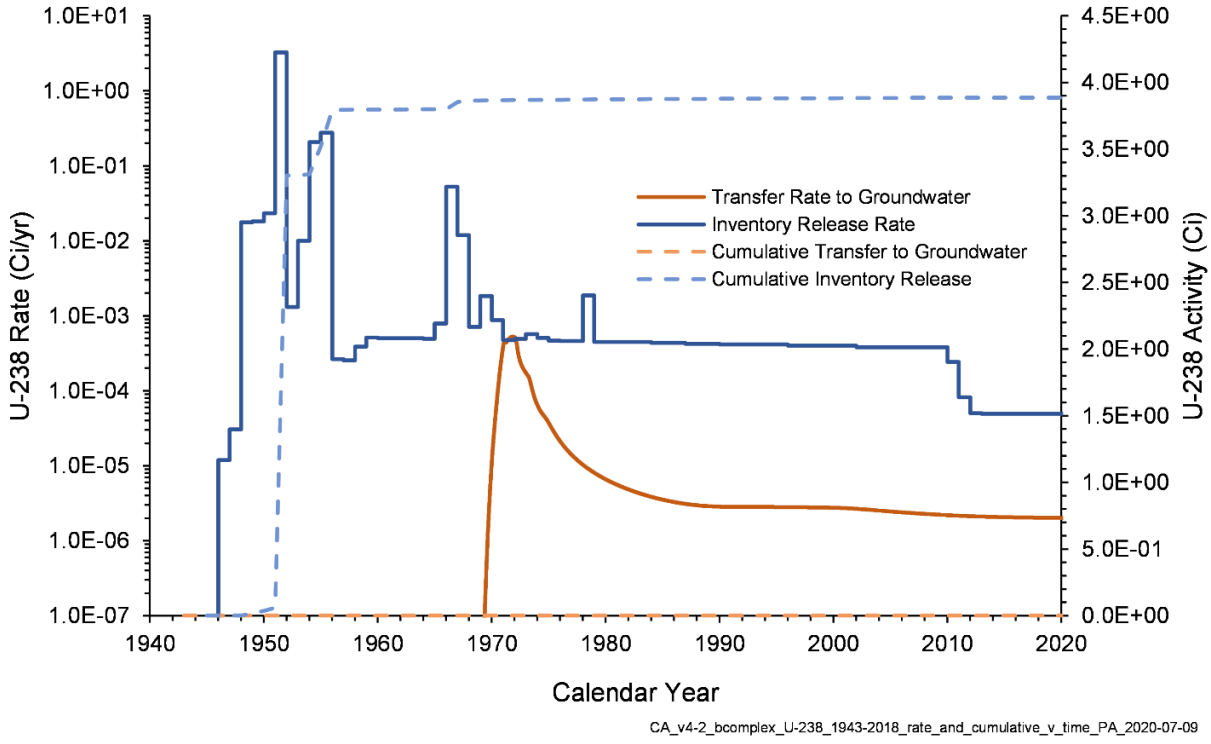

Figure 7-84. U-238 Inventory Release from Waste Sites and Transfer to Groundwater for the B Complex Model from 1943–2018

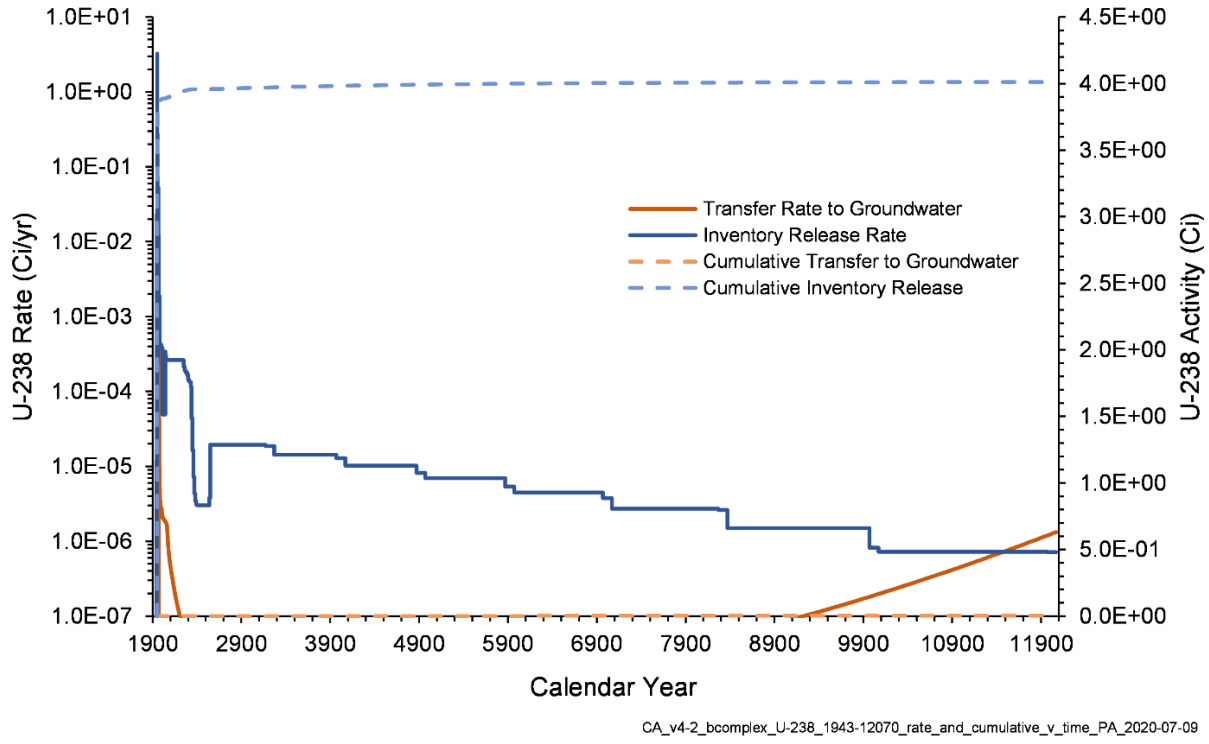

Figure 7-85. U-238 Inventory Release from Waste Sites and Transfer to Groundwater for the B Complex Model from 1943–12070

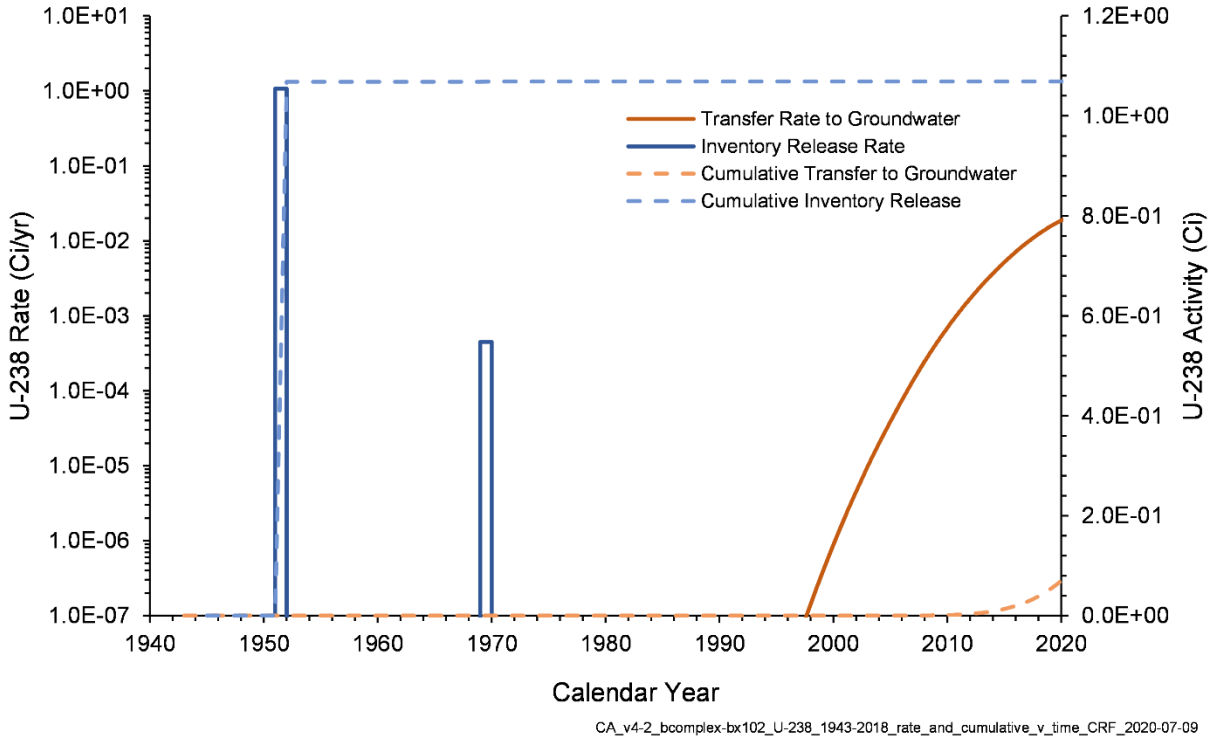

Figure 7-86. Mobile U-238 Inventory Release from 241-BX-102 and Transfer to Groundwater for the B Complex Model from 1943–2018

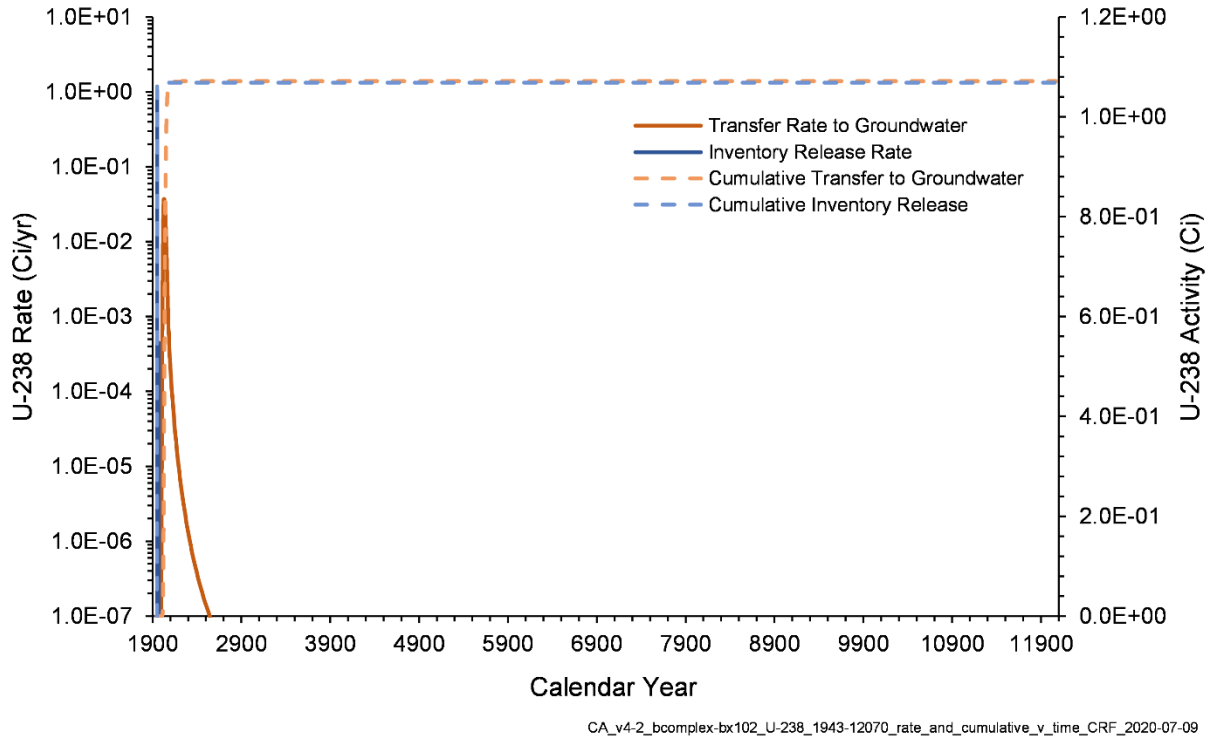

Figure 7-87. Mobile U-238 Inventory Release from 241-BX-102 and Transfer to Groundwater for the B Complex Model from 2018–12070

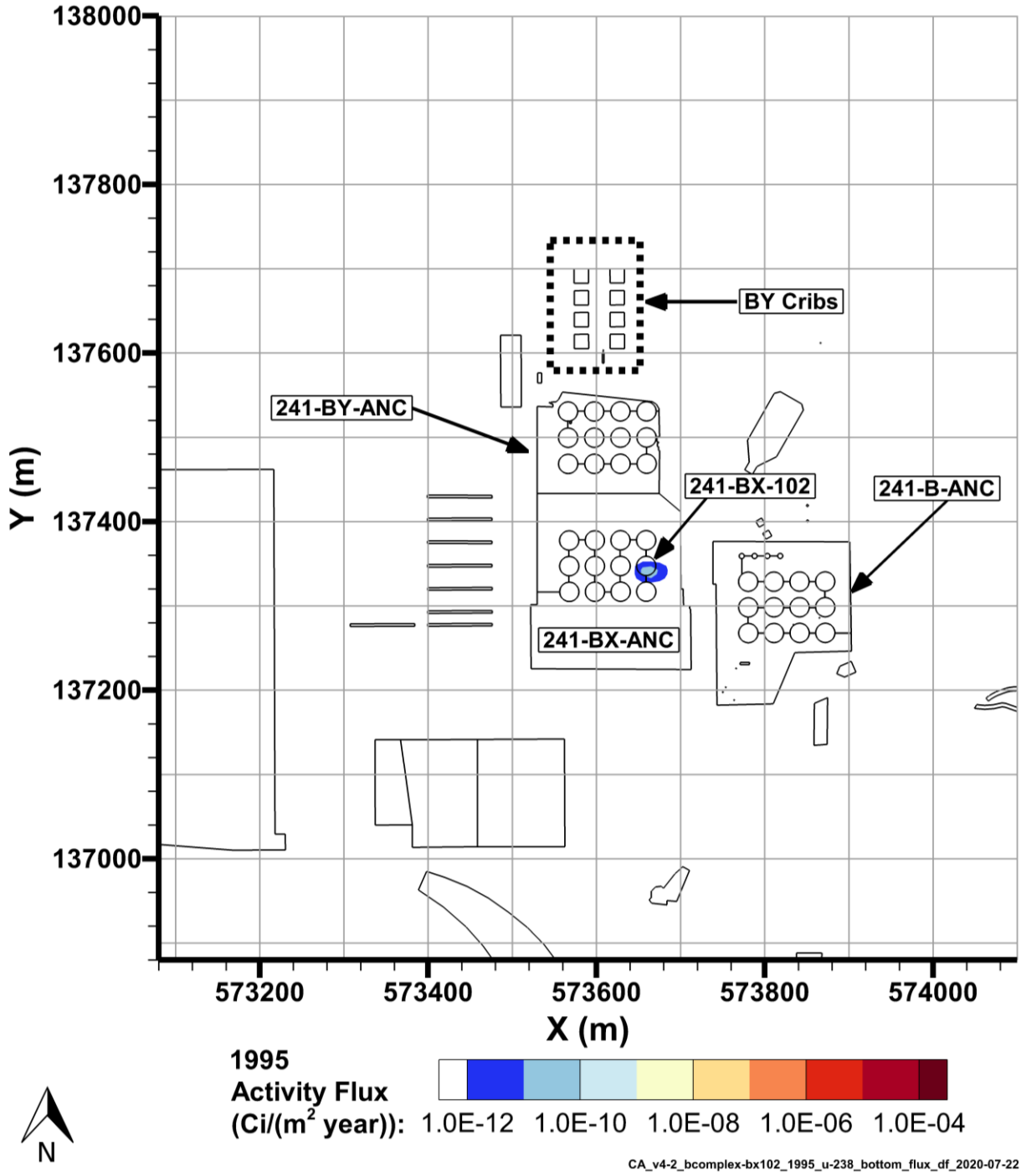

Note: the dashed black lines are used to indicate the waste sites that are collectively referred to as BY Cribs.

Figure 7-88. Mobile U-238 Flux to Groundwater, 1995

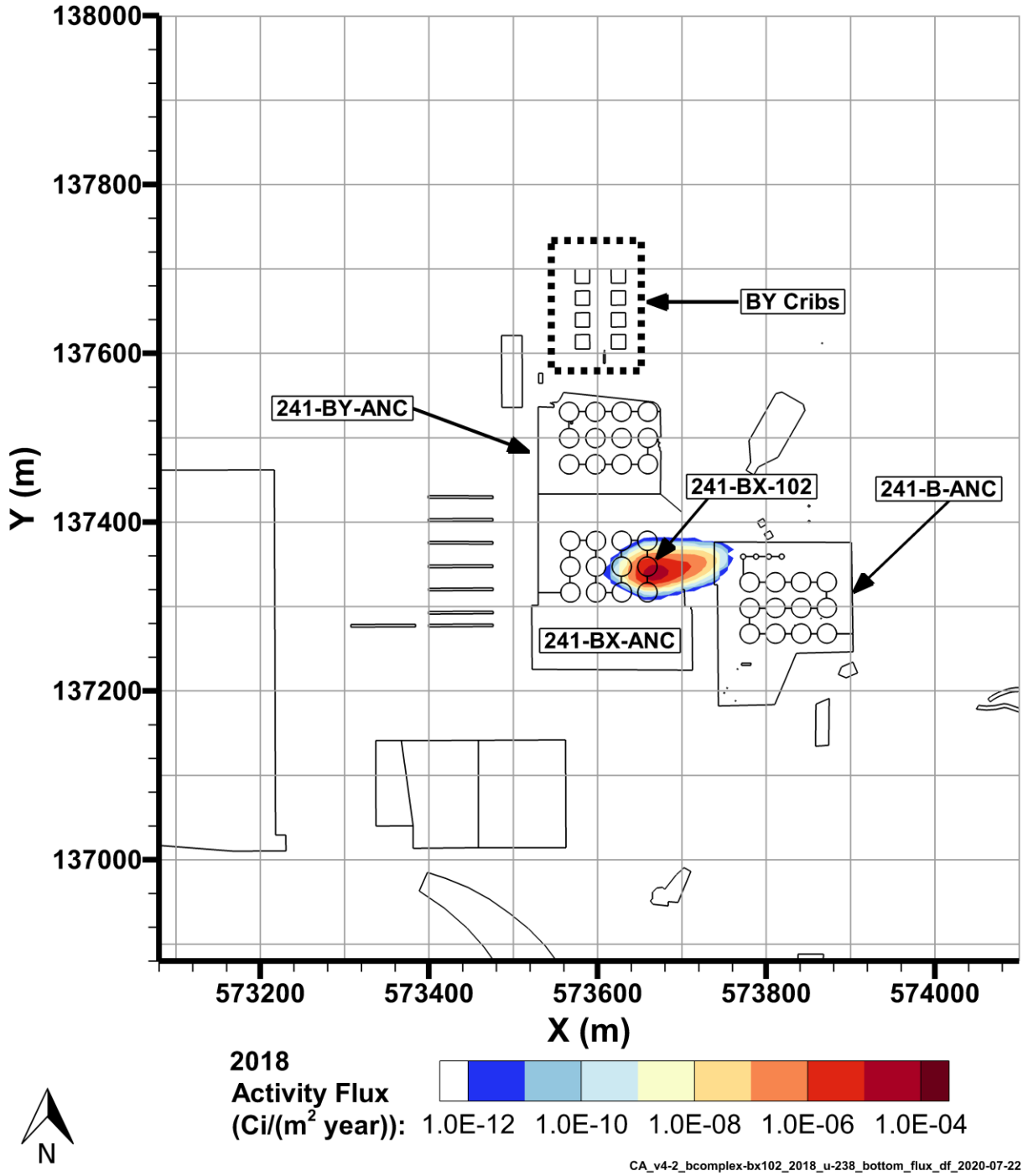

Note: the dashed black lines are used to indicate the waste sites that are collectively referred to as BY Cribs.

Figure 7-89. Mobile U-238 Flux to Groundwater, 2018

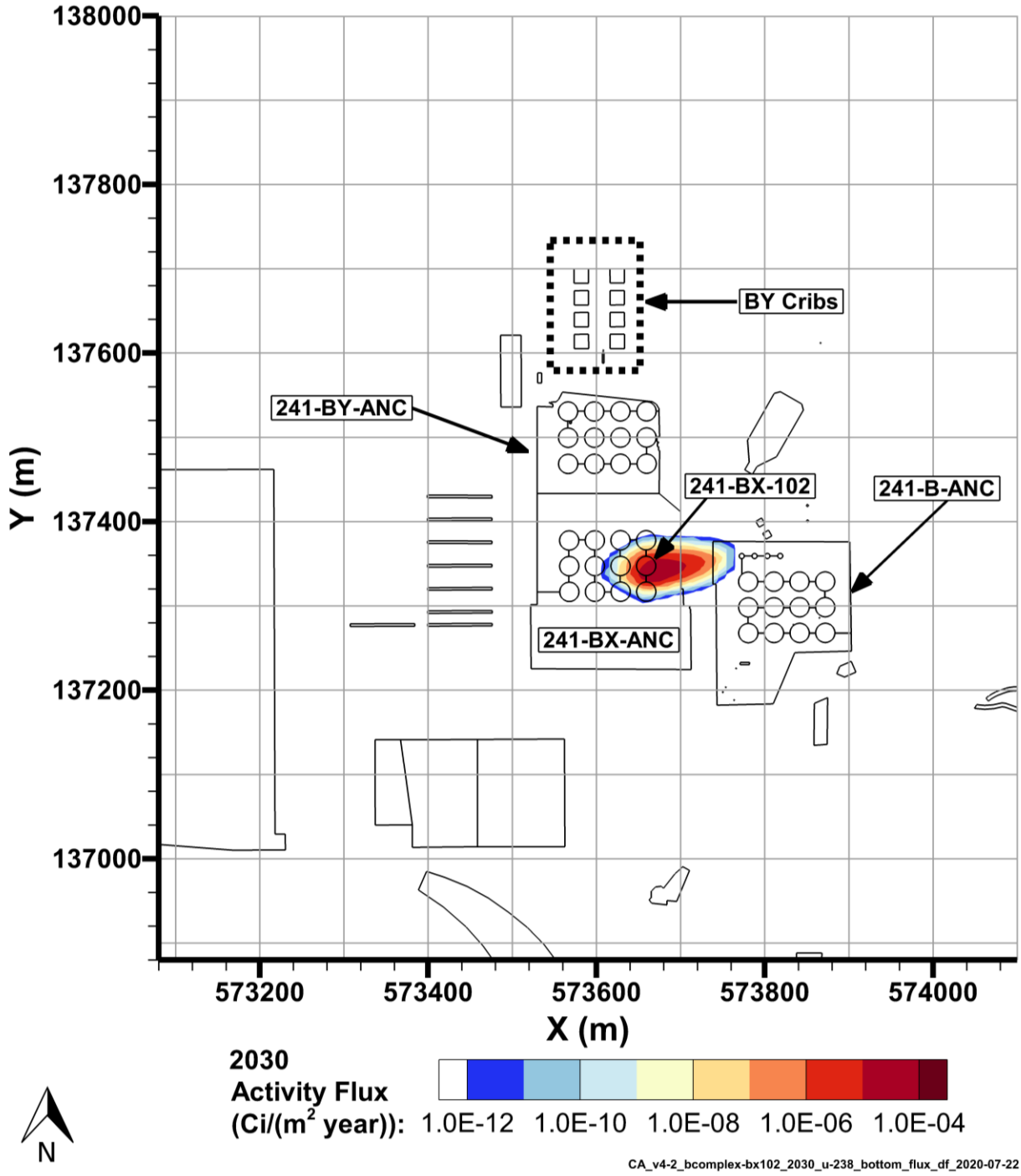

Note: the dashed black lines are used to indicate the waste sites that are collectively referred to as BY Cribs.

Figure 7-90. Mobile U-238 Flux to Groundwater, 2030

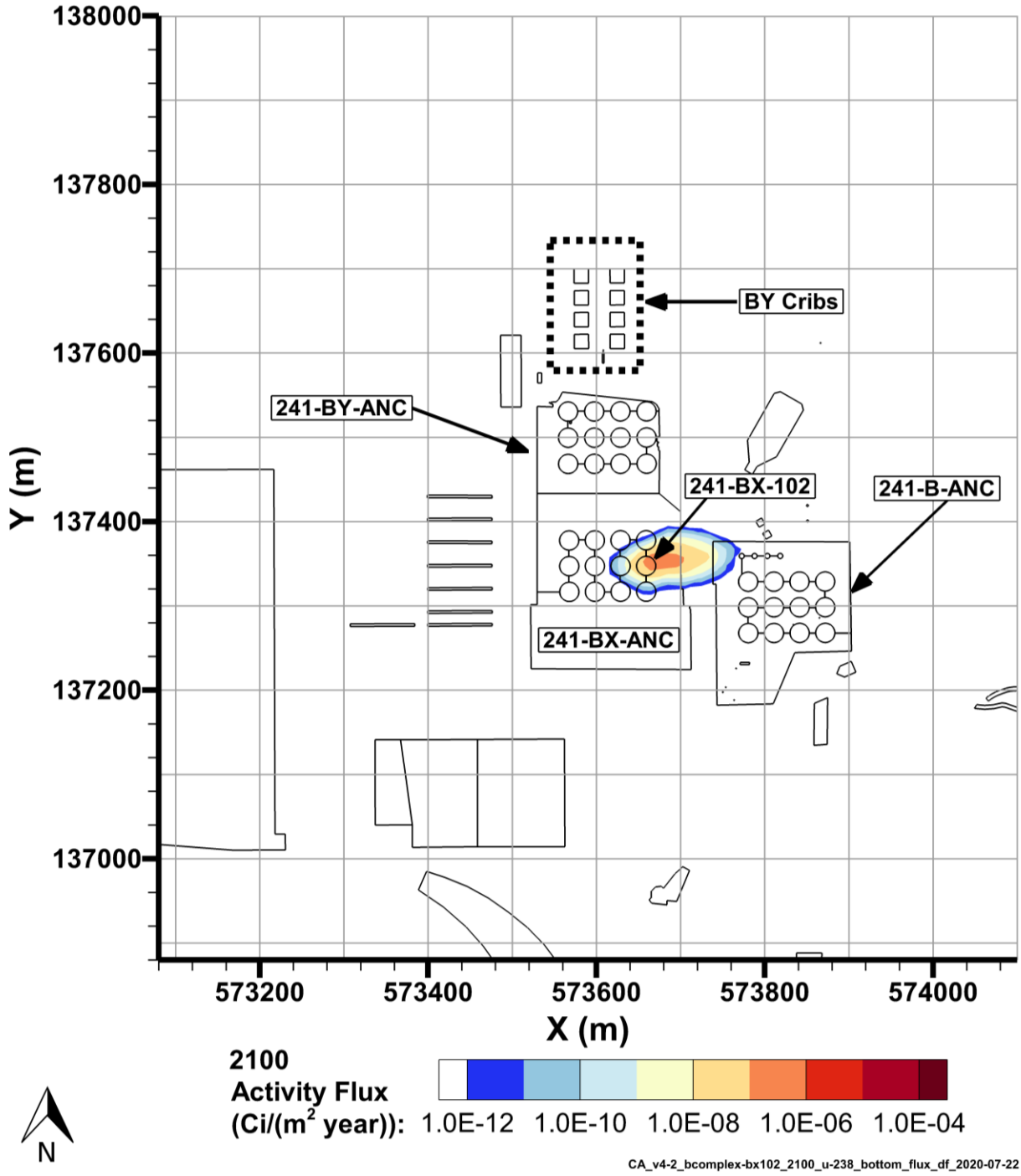

Note: the dashed black lines are used to indicate the waste sites that are collectively referred to as BY Cribs.

Figure 7-91. Mobile U-238 Flux to Groundwater, 2100

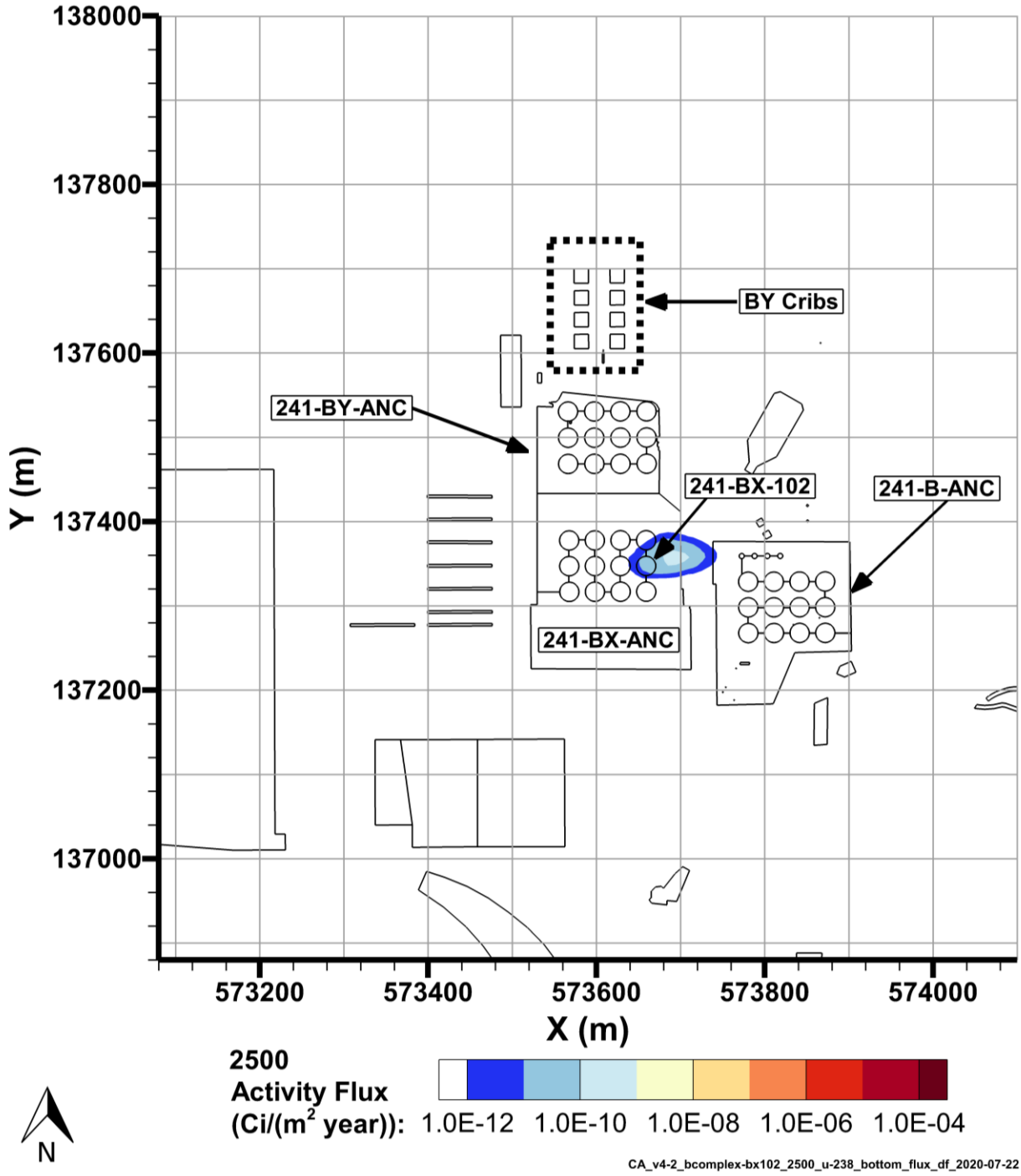

Note: the dashed black lines are used to indicate the waste sites that are collectively referred to as BY Cribs.

Figure 7-92. Mobile U-238 Flux to Groundwater, 2500

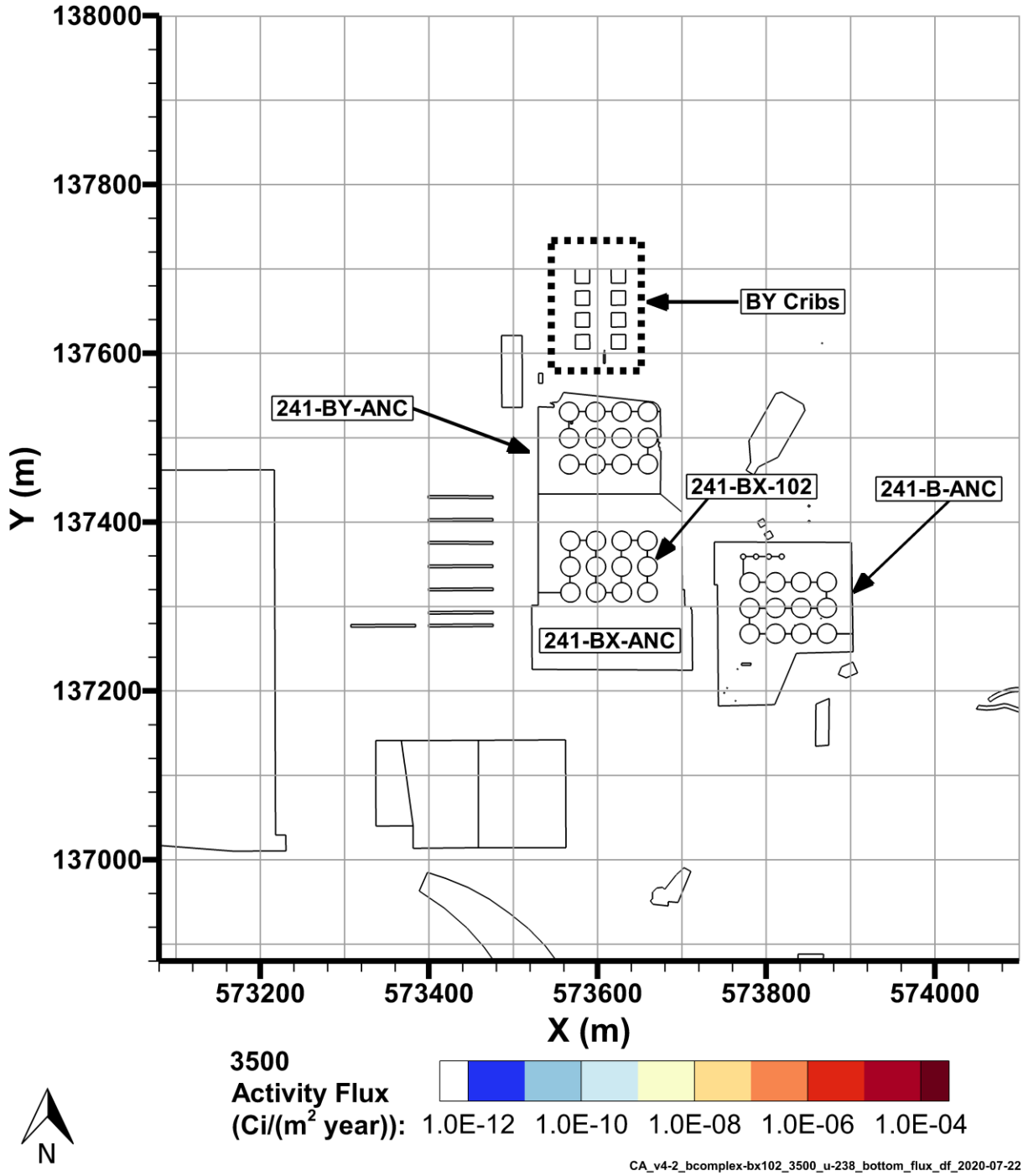

Note: the dashed black lines are used to indicate the waste sites that are collectively referred to as BY Cribs.

Figure 7-93. Mobile U-238 Flux to Groundwater, 3500

7.15 Ra-226 Fate and Transport Results

This model simulated the release and transport of Ra-226. No Ra-226 was discharged to groundwater at a cumulative activity above 1.0E-6 Ci per P2R grid cell at any point during modeling. The inventory

released to the B Complex model and the transfer of Ra-226 to groundwater are shown from 1943–2018 in Figure 7-94 and from 1943–12070 in Figure 7-95.

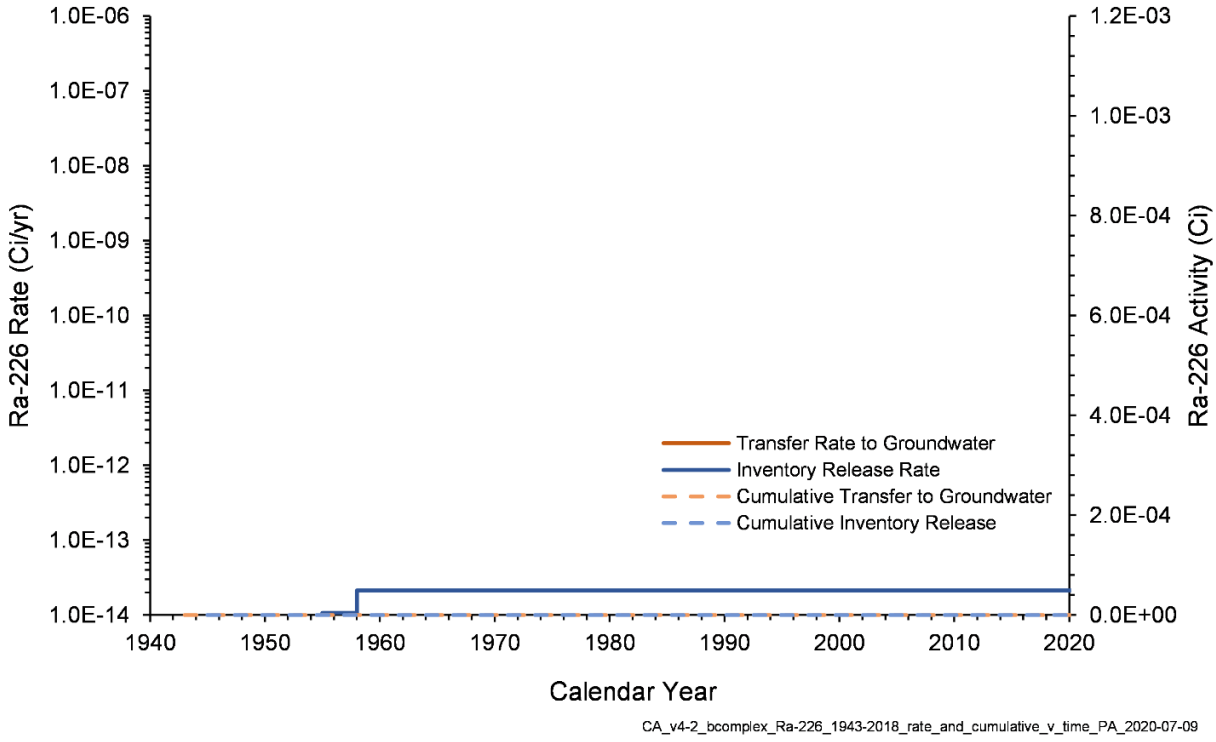

Figure 7-94. Ra-226 Inventory Release from Waste Sites and Transfer to Groundwater for the B Complex Model from 1943–2018

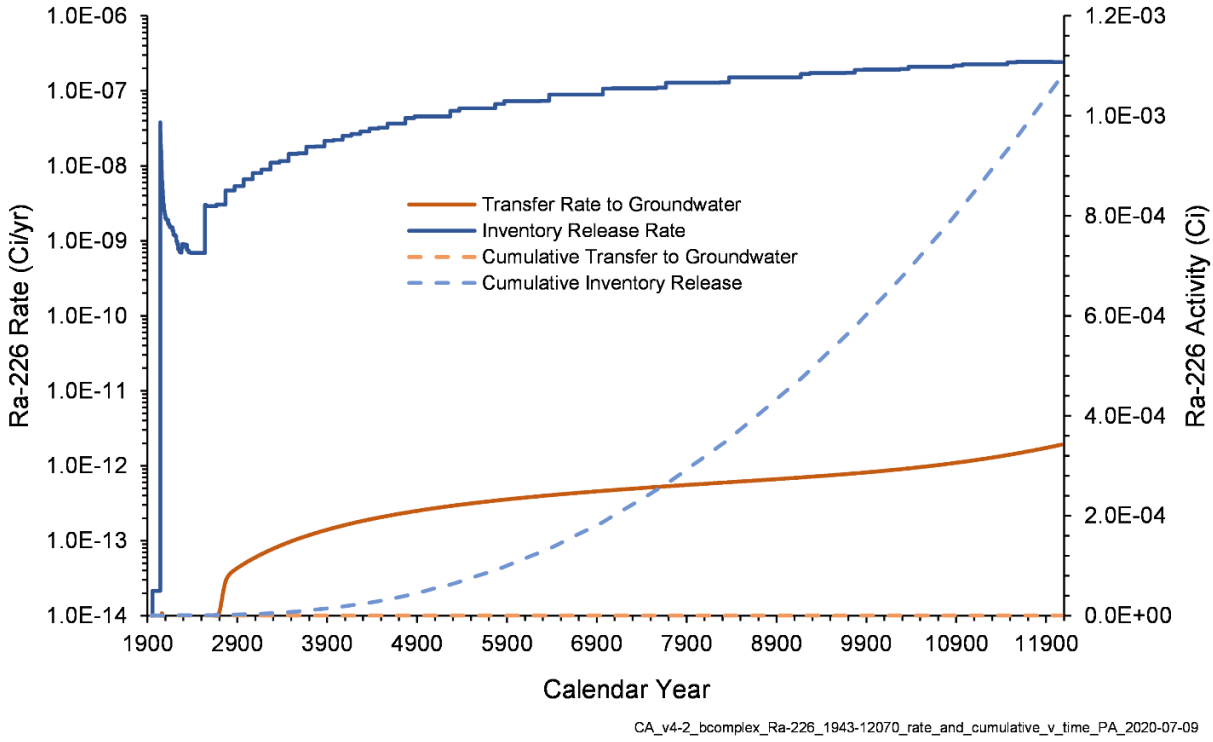

Figure 7-95. Ra-226 Inventory Release from Waste Sites and Transfer to Groundwater for the B Complex Model from 1943–12070

7.16 Th-230 Fate and Transport Results

This model simulated the release and transport of Th-230. No Th-230 was discharged to groundwater at a cumulative activity above 1.0E-6 Ci per P2R grid cell at any point during modeling. The inventory released to the B Complex model and the transfer of Th-230 to groundwater are shown from 1943–2018 in Figure 7-96 and from 1943–12070 in Figure 7-97. Figure 7-96 indicates no inventory was released from 1943–2018.

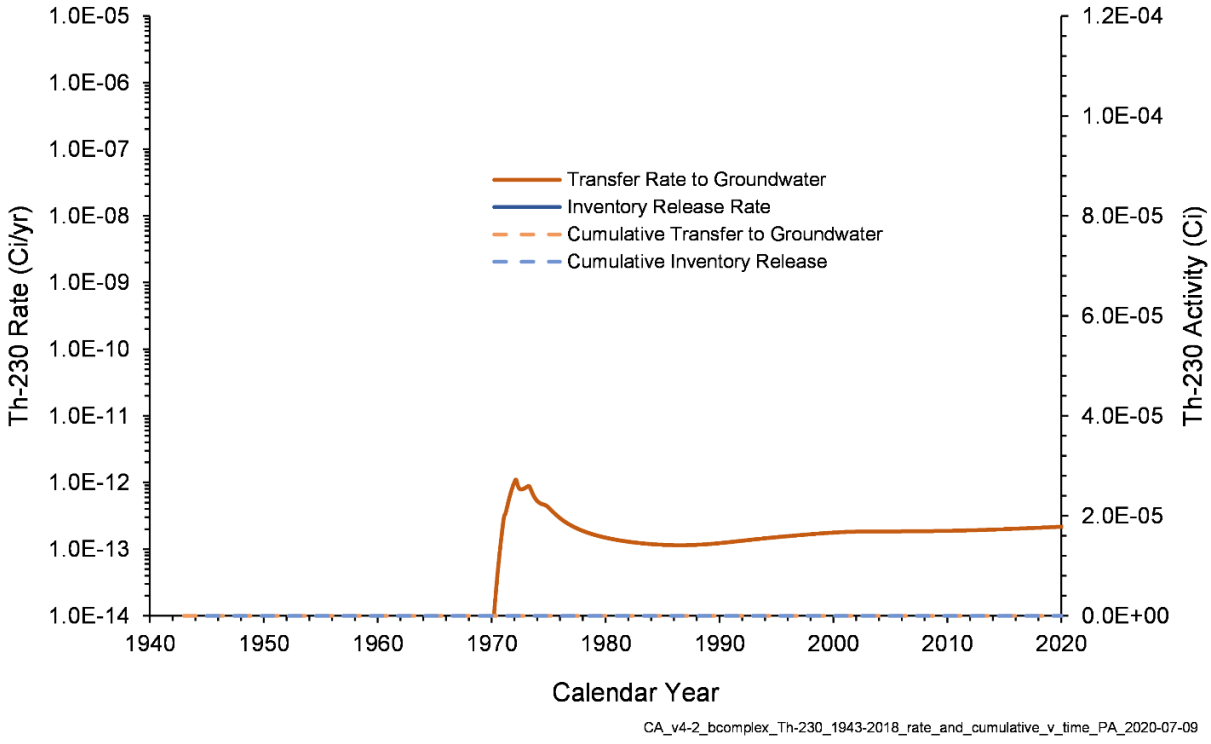

Figure 7-96. Th-230 Inventory Release from Waste Sites and Transfer to Groundwater for the B Complex Model from 1943–2018

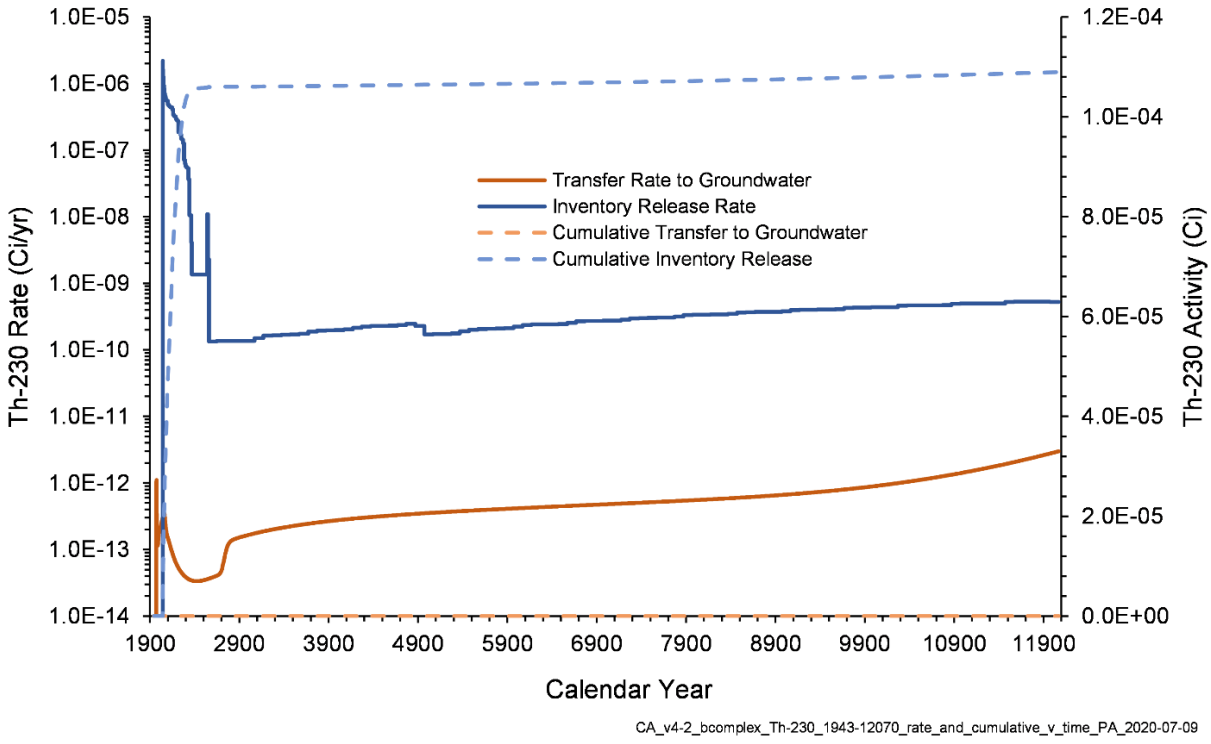

Figure 7-97. Th-230 Inventory Release from Waste Sites and Transfer to Groundwater for the B Complex Model from 1943–12070

8 References

CHPRC-00176, 2016, *STOMP Software Management Plan*, Rev. 4, CH2M HILL Plateau Remediation Company, Richland, Washington.

CHPRC-00211, 2016, *STOMP Software Test Plan*, Rev 3, CH2M HILL Plateau Remediation Company, Richland, Washington.

CHPRC-00222, 2016, *STOMP Functional Requirements Document* Rev 2, CH2M HILL Plateau Remediation Company, Richland, Washington.

CHPRC-00269, 2017, *STOMP Requirement Traceability Matrix*, Rev. 5, CH2M HILL Plateau Remediation Company, Richland, Washington.

CHPRC-00515, 2017, *STOMP Acceptance Test Report*, Rev. 5, CH2M HILL Plateau Remediation Company, Richland, Washington.

CHPRC-04032, 2020, *Composite Analysis / Cumulative Impact Evaluation (CACIE) Utility Codes Integrated Software Management Plan*, Rev. 1, CH2M HILL Plateau Remediation Company, Richland, Washington.

CP-57037, 2020, *Model Package Report: Plateau to River Groundwater Model Version 8.3*, Rev. 2, CH2M HILL Plateau Remediation Company, Richland, Washington. Available at: https://www.osti.gov/servlets/purl/1601635.

CP-60925, 2018, *Model Package Report: Central Plateau Vadose Zone Geoframework*, Rev. 0, CH2M HILL Plateau Remediation Company, Richland, Washington. Available at: https://www.osti.gov/servlets/purl/1432798.

CP-61786, 2019, *Inventory Data Package for the Hanford Site Composite Analysis*, Rev. 1, CH2M HILL Plateau Remediation Company, Richland, Washington. Available at: https://www.osti.gov/servlets/purl/1576745.

CP-62184, 2019, *Hanford Site Composite Analysis: Radionuclide Selection for Groundwater Pathway Evaluation*, Rev. 0, CH2M HILL Plateau Remediation Company, Richland, Washington. Available at: https://www.osti.gov/servlets/purl/1491467.

CP-62766, 2020, *Model Package Report: Composite Analysis Solid Waste Release Model (CASWR Model)*, Rev. 0, CH2M HILL Plateau Remediation Company, Richland, Washington. Available at: https://www.osti.gov/servlets/purl/1595469.

CP-63515, *Model Package Report: Central Plateau Vadose Zone Models*, Rev. 0 pending, CH2M HILL Plateau Remediation Company, Richland, Washington.

CP-63883, 2020*Vadose Zone Flow and Transport Parameters Data Package for the Hanford Site Composite Analysis*, Rev. 0, CH2M HILL Plateau Remediation Company, Richland, Washington. Available at: https://www.osti.gov/servlets/purl/1608425.

DOE O 414.1D Chg 1 (Admin Chg), 2013, *Quality Assurance*, U.S. Department of Energy, Washington, D.C. Available at: https://www.directives.doe.gov/directives-documents/400-series/0414.1-BOrder-d-admchg1.

DOE/RL-97-1047, 2002, *Hanford Site Historic District History of the Plutonium Production Facilities 1943-1990*, Rev. 0, U.S. Department of Energy, Richland Operations Office, Richland, Washington. Available at: https://www.osti.gov/servlets/purl/807939.

DOE/RL-2014-37, 2015, *Removal Action Work Plan for 200-DV-1 Operable Unit Perched Water Pumping / Pore Water Extraction*, Rev. 0, U.S. Department of Energy, Richland Operations Office, Richland, Washington. Available at: https://pdw.hanford.gov/document/0079128H.

DOE/RL-2018-66, 2019, *Hanford Site Groundwater Monitoring Report for 2018*, Rev. 0, U.S. Department of Energy, Richland Operations Office, Richland, Washington. Available at: https://pdw.hanford.gov/document/AR-03138.

ECF-200DV1-18-0036, 2019, *B-Complex Perched Zone Geoframework, 200 East, Hanford Site*, Rev. 0, CH2M HILL Plateau Remediation Company, Richland, Washington. Available at: https://pdw.hanford.gov/document/AR-03735.

ECF-HANFORD-15-0019, 2020, *Hanford Site-wide Natural Recharge Boundary Condition for Groundwater Models*, Rev. 2, CH2M HILL Plateau Remediation Company, Richland, Washington. Available at: https://www.osti.gov/servlets/purl/1633785.

ECF-HANFORD-19-0040, *Vadose Zone Model for B Plant Area for Composite Analysis*, Rev.0 pending, CH2M HILL Plateau Remediation Company, Richland, Washington.

ECF-HANFORD-17-0079, 2018, *Hanford Soil Inventory Model (SIM-v2) Calculated Radionuclide Inventory of Direct Liquid Discharges to Soil in the Hanford Site's 200 Areas*, Rev. 0, CH2M HILL Plateau Remediation Company, Richland, Washington. Available at: https://www.osti.gov/servlets/purl/1441375.

ECF-HANFORD-17-0120, 2017, *Preparation of the March 2017 Hanford Site Water Table and Potentiometric Surface Maps*, Rev. 0, CH2M HILL Plateau Remediation Company, Richland, Washington. Available at: https://pdw.hanford.gov/document/0066758H.

ECF-HANFORD-18-0035, 2020, *Central Plateau Vadose Zone Geoframework*, Rev. 0, CH2M HILL Plateau Remediation Company, Richland, Washington. Available at: https://www.osti.gov/servlets/purl/1603767.

ECF-HANFORD-19-0094, 2020, *Calculation of Moisture-Dependent Anisotropic Parameters Supporting the Hanford Site's Composite Analysis, Cumulative Impact Evaluation, and Performance Assessments*, Rev. 0, CH2M HILL Plateau Remediation Company, Richland, Washington. Available at: https://www.osti.gov/servlets/purl/1595470.

ECF-HANFORD-19-0112, 2020, *Solid Waste Release Calculations for the Composite Analysis Baseline Assessment*, Rev. 0, CH2M HILL Plateau Remediation Company, Richland, Washington. Available at: https://www.osti.gov/servlets/purl/1617041.

ECF-HANFORD-19-0121, 2020, *Selection of Vadose Zone Flow and Transport Properties with Gravel Fraction Corrections for the Hanford Site Composite Analysis and Cumulative Impact Evaluation*, Rev. 0, CH2M HILL Plateau Remediation Company, Richland, Washington. Available at: https://www.osti.gov/servlets/purl/1605425.

ECF-HANFORD-20-0006, 2020, *Composite Analysis Solid Waste Release Data Reduction of Activity Flux from Waste Sites to the Vadose Zone*, Rev. 0, CH2M HILL Plateau Remediation Company, Richland, Washington. Available at: https://www.osti.gov/servlets/purl/1644636.

EMDT-GR-0035, 2019, *Waste Site and Structure Footprint Shapefiles for Inclusion in Updated Composite Analysis*, Rev. 0, CH2M HILL Plateau Remediation Company, Richland, WA.

Farrow, C.R., M. Williams, M. Oostrom, P. Allena, and D. Fryar, 2019, "Prediction of Long-Term Contaminant Flux from the Vadose Zone to Groundwater for Fluctuating Water Table Conditions at the Hanford Site," AGU Fall Meeting Abstracts.

Green, T.R., J.E. Constantz, and D.L. Freyberg, 1996, "Upscaled Soil-Water Retention Using Van Genuchten's Function," Journal of Hydrologic Engineering 1(3):123–130.

Khaleel, R., T.C.J. Yeh, and Z. Lu, 2002, "Upscaled Flow and Transport Properties for Heterogeneous Unsaturated Media," Water Resources Research 38(5):11-1–11-12.

Mualem, Y., 1976, "A New Model for Predicting the Hydraulic Conductivity of Unsaturated Porous Media," *Water Resources Research* 12(3):513-522.

NQA-1, 2008, *Quality Assurance Requirements for Nuclear Facility Applications*, American Society of Mechanical Engineers, New York, New York.

NUREG/CR-5965, 1994, *Modeling Field Scale Unsaturated Flow and Transport Processes*, Office of Nuclear Regulatory Research, U.S. Nuclear Regulatory Commission, Washington, D.C.

Oostrom, M., M.J. Truex, M.L. Rockhold, and T.C. Johnson, 2017, "Deep Vadose Zone Contaminant Flux Evaluation at the Hanford BY-Cribs Site Using Forward and Imposed Concentration Modeling Approaches," Environmental Processes 4(4):771–797.

PNNL-11216, 1997, *STOMP: Subsurface Transport Over Multiple Phases Application Guide*, Pacific Northwest National Laboratory, Richland, Washington. Available at: http://stomp.pnl.gov/documentation/application.pdf.

PNNL-12030, 2000, *STOMP: Subsurface Transport Over Multiple Phases Version 2.0 Theory Guide*, Pacific Northwest National Laboratory, Richland, Washington. Available at: http://stomp.pnnl.gov/documentation/guides/theory.pdf.

PNNL-13895, 2003, *Hanford Contaminant Distribution Coefficient Database and Users Guide*, Rev. 1, Pacific Northwest National Laboratory, Richland, Washington.

PNNL-14702, 2006, *Vadose Zone Hydrogeology Data Package for Hanford Assessments, Rev. 1, Pacific Northwest National Laboratory*, Richland, Washington. Available at: https://www.pnnl.gov/main/publications/external/technical_reports/PNNL-14702rev1.pdf.

PNNL-15782, 2006, *STOMP: Subsurface Transport Over Multiple Phases Version 4.0: User's Guide*, Pacific Northwest National Laboratory, Richland, Washington. Available at: http://stomp.pnl.gov/documentation/userguide.pdf.

PNNL-17031, 2007, *A Site-Wide Perspective on Uranium Geochemistry at the Hanford Site*, Pacific Northwest National Laboratory, Richland, Washington.

PNNL-17154, 2008, *Geochemical Characterization Data Package for the Vadose Zone in the Single-Shell Tank Waste Management Areas at the Hanford Site*, Pacific Northwest National Laboratory, Richland, Washington.

PNNL-19277, 2010, *Conceptual Model of Uranium in the Vadose Zone for Acidic and Alkaline Wastes Discharged at the Hanford Site Central Plateau*, Pacific Northwest National Laboratory, Richland, Washington.

PNNL-25146, 2016, *Scale-Dependent Solute Dispersion in Variably Saturated Porous Media,* RPT-IGTP-009, Rev. 0, Pacific Northwest National Laboratory, Richland, Washington.

RPP-ENV-58782, 2016, *Performance Assessment of Waste Management Area C, Hanford Site, Washington*, Rev. 0, Washington River Protection Solutions, Richland, Washington.

RPP-RPT-47562, 2011, *Hanford BX-Farm Leak Assessments Report*, Rev. 0, Washington River Protection Solutions, Richland, Washington. Available at: https://pdw.hanford.gov/document/0071643H.

RPP-RPT-59197, 2016, *Analysis of Past Waste Tank Leaks and Losses in the Vicinity of Waste Management Area C, Hanford Site, Washington*, Rev. 1, Washington River Protection Solutions, Richland, Washington.

van Genuchten, M.T., 1980, "A Closed-form Equation for Predicting the Hydraulic Conductivity of Unsaturated Soils," *Soil Sci. Soc. Am. J.* 44(5):892-898. Available at: http://ars.usda.gov/sp2UserFiles/Place/53102000/pdf_pubs/P0682.pdf.

Ye, M., R. Khaleel, and T.C.J. Yeh, 2005, "Stochastic Analysis of Moisture Plume Dynamics of a Field Injection Experiment," Water Resources Research 41(3):W03013.1–W03013.13.

Yeh, T.C.J., R. Khaleel, and K.C. Carroll, 2015, "Flow Through Heterogeneous Geologic Media," Cambridge University Press, New York, New York.

Zhang, Z.F. and R. Khaleel, 2010, "Simulating Field-Scale Moisture Flow Using a Combined Power-Averaging and Tensorial Connectivity-Tortuosity Approach," Water Resources Research 46(9):W09505, 14 pp.

Zhang, Z.F., A.L. Ward, and G.W. Gee, 2003, "A Tensorial Connectivity–Tortuosity Concept to Describe the Unsaturated Hydraulic Properties of Anisotropic Soils," Vadose Zone Journal 2(3):313–321.

Appendix A

Checking Documentation for the B Complex Model

This page intentionally left blank.

Contents

This page intentionally left blank.

A1 Introduction

This appendix is a folder of portable document files. These files contain documentation of checks completed by the modeling team and from qualified employees outside of the modeling team.

This page intentionally left blank.

Model Check 2 – Transport XPRT Part A				
Model (full name):	B Complex			
Modeler Name:	Praveena Allena			
Peer Reviewer Name:	Sandra Mondragon			
Task/Action/Operation	***Modeler***		***Peer Reviewer***	
	Status	Comment	Status	Comment
Surface Card Checks				
Completed tool qualification check (Surface Flux Cards Check 1)	☒		☒	
Completed P2R fingerprint check (Surface Flux Cards Check 2)	☒		☒	
Completed *input_SS* fingerprint check (Surface Flux Cards Check 3)	☒		☒	
Completed check of Rad1 and Rad2 list in *rad#_surface_flux.txt* files and proper sequence (Surface Flux Cards Check 4)	☒		☒	
Completed comparison of *rad#_surface_flux.txt* files (Surface Flux Cards Check 5)	☒		☒	
Completed check on TSFF computation (Surface Flux Cards Check 6)	☒		☒	DeltaA = 9 DeltaB = 10
Completed check to ensure correct domain bottom is used (Surface Flux Cards Check 7)	☒		☒	
Completed check on correct use of P2R area (Surface Flux Cards Check 8)	☒		☒	
Completed check on correct STOMP-P2R grid mapping (Surface Flux Cards Check 9)	☒		☒	
Output Card Checks				
Completed tool qualification check (Output Cards Check 1)	☒		☒	
Completed *input.nij* fingerprint check (Output Cards Check 2)	☒		☒	
Completed *input.sij* fingerprint check (Output Cards Check 3)	☒		☒	

Model Check 2 – Transport XPRT Part A				
Model (full name):	B Complex			
Modeler Name:	Praveena Allena			
Peer Reviewer Name:	Sandra Mondragon			
Task/Action/Operation	***Modeler***		***Peer Reviewer***	
	Status	Comment	Status	Comment
Completed *input.top* fingerprint check (Output Cards Check 4)	☒		☒	
Completed *plot_times.txt* check (Output Cards Check 5)	☒		☒	
Completed comparison of *rad#_Output_Control.dat* files (Output Cards Check 6)	☒		☒	
Completed comparison of *rad#_Mass_Balance_Output_Control.dat* files (Output Cards Check 7)	☒		☒	
Completed comparison of *rad1_Output_Control.dat* and *rad1_Mass_Balance_Output_Control.dat* files (Output Cards Check 8)	☒		☒	
Completed spot check of specified node locations (Output Cards Check 9)	☒		☒	
Boundary Card Checks				
Completed high-level check of recharge plots (Boundary Conditions Card Check 1)	☒		☒	
Completed recharge spot check and time-series comparison. Write down the checked i,j locations and time-series comparison results (OK; not OK) (Boundary Conditions Card Check 2)	☒	RET Nodes checked: 11,15 – OK 26,32 – OK 46,119 – OK 69,36 - OK 86,81 - OK	☒	I, J Values: 13, 53 (group 00024) 33, 60 (group 00014) 53, 44 (group 00132) 65, 80 (group 00153) 71, 62 (group 00100)
After completion by both the modeler and peer-reviewer, the form should be moved to the CompletedForms folder. The form should not be signed until both have completed the check and all issues have been resolved.				
Date Completed	***Modeler: 03-23-2020***		***Peer Reviewer: 03-24-2020***	

Model Check 2 – Transport XPRT Part A				
Model (full name):	B Complex			
Modeler Name:	Praveena Allena			
Peer Reviewer Name:	Sandra Mondragon			
Task/Action/Operation	***Modeler***		***Peer Reviewer***	
	Status	Comment	Status	Comment
Name	Praveena Allena		Sandra Mondragon	
Signature			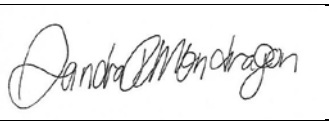	

Model Check 2 – Transport XPRT Part B				
Model (full name):	B Complex			
Modeler Name:	Praveena Allena			
Peer Reviewer Name:	Pedro Gutierrez			
Task/Action/Operation	***Modeler***		***Peer Reviewer***	
	Status	Comment	Status	Comment
Check list follows sections in CA-XPRT-2018-Input-File-Check-PartB-*.pptx Modelers: \CAVE\v4-2\supportfiles\CheckingDocs\xprt-PartB Peer Reviewers: \Rel.061\vadose\Peer-Checking-xprt-B\CheckingDocs				
Completed tool qualification checks (pages 11-17 of *CA-XPRT-2018-Input-File-Check-PartB-*.pptx*)	☒		☒	
Completed *ca-src2stomp.pl* tool input check (Pages 18-22)	☒		☒	
Completed *xprt_2018_input_gen.f for xprt-1 Simulations* tool input check (Pages 23-32)	☒		☒	
Completed *xprt_2018_input_gen.f for xprt-2 Simulations* tool input check (Pages 33-42)	☒		☒	
Completed Source Card site list comparison with maps (Page 43-45)	☒		☒	
Completed construction of all source-check spreadsheets (Page 49)	☒		☒	
Completed site areas comparison (Page 50)	☒		☒	
Completed operation years comparison (Page 51)	☒		☒	
Completed cumulative inventory comparison (Page 52)	☒		☒	
For sfarms model only: Completed special case check for SX-115 site (Page 53)	☐	NA	☐	NA

Model Check 2 – Transport XPRT Part B				
Model (full name):	B Complex			
Modeler Name:	Praveena Allena			
Peer Reviewer Name:	Pedro Gutierrez			
Task/Action/Operation	***Modeler***		***Peer Reviewer***	
	Status	Comment	Status	Comment
For bcomplex model only: Completed special case check for BX-102 site (Page 54)	☒		☒	
For tfarms model only: Completed special case check for T-106 site (Page 55-56)	☐	NA	☐	NA
Input File Check – xprt-1 simulation				
Completed Simulation Title Card Check (Page 59)	☒	Correction was made for date/time entries. Verified differences between old and new input file are only in this card (5/7/2020)	☒	Verified that date/time entries have been the only changes made in XPRT-1 (05/08/2020)
Completed Solution Control Card Check (Page 60-62)	☒		☒	
Completed Direct input_SS Copy Check (Page 63)	☒		☒	
Completed Water Table Boundary Check (Page 64)	☒		☒	
Completed Solute/Fluid Interaction Card Check (Page 65)	☒		☒	
Completed Solute/Porous Media Interaction Card Check (Page 66-67)	☒		☒	
Completed Initial Conditions Card Check (Page 68)	☒		☒	

Model Check 2 – Transport XPRT Part B				
Model (full name):	B Complex			
Modeler Name:	Praveena Allena			
Peer Reviewer Name:	Pedro Gutierrez			
Task/Action/Operation	***Modeler***		***Peer Reviewer***	
	Status	Comment	Status	Comment
Input File Check – xprt-2 simulation				
Completed Simulation Title Card Check (Page 71)	☒	Correction was made for date/time entries. Verified differences between old and new input file are only in this card (5/7/2020)	☒	Verified that date/time entries have been the only changes made in XPRT-2 (05/08/2020)
Completed Solution Control Card Check (Page 72-77)	☒		☒	
Completed Direct input_SS Copy Check (Page 75)	☒		☒	
Completed Water Table Boundary Check (Page 76)	☒		☒	
Completed Solute/Fluid Interaction Card Check (Page 77)	☒		☒	
Completed Solute/Porous Media Interaction Card Check (Page 78-79)	☒		☒	
Completed Initial Conditions Card Check (Page 80)	☒		☒	
After completion by both the modeler and peer-reviewer, the form should be moved to the CompletedForms folder. The form should not be signed until both have completed the check and all issues have been resolved.				
	Modeler		***Peer Reviewer***	
Date Completed	*05-07-2020*		*05-08-2020*	
Name	*Praveena Allena*		*Pedro E Gutierrez*	

Model Check 2 – Transport XPRT Part B				
Model (full name):	B Complex			
Modeler Name:	Praveena Allena			
Peer Reviewer Name:	Pedro Gutierrez			
Task/Action/Operation	***Modeler***		***Peer Reviewer***	
	Status	Comment	Status	Comment
Signature and Date	A.Praveena *05/08/2020*		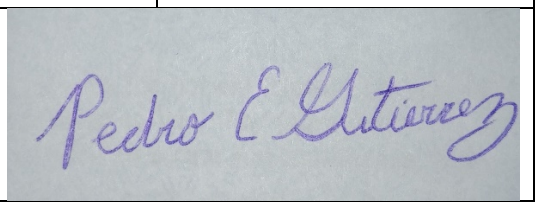	

Model Check 3 – Transport XPRT Part C				
Model (full name):	B Complex			
Modeler Name:	Praveena Allena			
Peer Reviewer Name:	Andrew Murphy			
Task/Action/Operation	***Modeler***		***Peer Reviewer***	
	Status	Comment	Status	Comment
Check list follows sections in CA-XPRT-MB-Input-File-Check-PartC-*.pptx Modelers: \CAVE\v4-2\supportfiles\CheckingDocs\xprt-PartC Peer Reviewers: \Rel.061\vadose\Peer-Checking-xprt-C\CheckingDocs				
Completed tool qualification checks (pages 12-13 of *CA-XPRT-MB-Input-File-Check-PartC-*.pptx*)	☒		☒	
Completed *xprt_mb_input_gen.f* tool input check (Pages 15-18)	☒		☒	
Input File Check – MB1 simulation				
Completed Simulation Title Card Check (Page 21)	☒		☒	
Completed Solution Control Card Check (Page 22-24)	☒		☒	
Completed Direct *input_XPRT-1* Copy Check (Page 25)	☒		☒	
Completed Solute/Fluid Interaction Card Check (Page 26)	☒		☒	
Completed Output Control Card Check (Page 27)	☒		☒	
Completed Surface Card Check (Page 28)	☒		☒	
Input File Check – MB2 simulation				
Completed Simulation Title Card Check (Page 31)	☒		☒	
Completed Solution Control Card Check (Page 32-234)	☒		☒	

Model Check 3 – Transport XPRT Part C				
Model (full name):	B Complex			
Modeler Name:	Praveena Allena			
Peer Reviewer Name:	Andrew Murphy			
Task/Action/Operation	***Modeler***		***Peer Reviewer***	
	Status	Comment	Status	Comment
Completed Direct *input_XPRT-1* Copy Check (Page 35)	☒		☒	
Completed Solute/Fluid Interaction Card Check (Page 36)	☒		☒	
Completed Output Control Card Check (Page 37)	☒		☒	
Completed Surface Card Check (Page 38)	☒		☒	
After completion by both the modeler and peer-reviewer, the form should be moved to the CompletedForms folder. The form should not be signed until both have completed the check and all issues have been resolved.				
	Modeler		***Peer Reviewer***	
Date Completed	***05/06/2020***		***05/07/2020***	
Name	***Praveena Allena***		***Andrew Murphy***	
Signature and Date				

Model Check 5– Transport XPRT Part E				
Model (full name):	B Complex			
Modeler Name:	Praveena Allena			
Peer Reviewer Name:	Brian Archuleta			
Task/Action/Operation	***Modeler***		***Peer Reviewer***	
	Status	Comment	Status	Comment
Check list follows sections in CA-XPRT-12070-Input-File-Check-PartE-*.pptx Modelers: \CAVE\v4-2\supportfiles\CheckingDocs\xprt-PartE Peer Reviewers: \Rel.061\vadose\Peer-Checking-xprt-E\CheckingDocs				
Completed "RTD sites on map" check (page 12 of *CA-XPRT-12070-Input-File-Check-PartE-*.pptx*)	☒		☒	
Completed qualification checks of all tools (pages 14-18)	☒		☒	
Completed *xprt_rtd_input_gen.f* tool input check (Pages 20-21)	☒		☒	
Completed *ca-rtdic.pl* tool input check (Pages 23-26)	☒		☒	
Completed *xprt_12070_input_gen.f* tool input check (Pages 28-31)	☒		☒	
Input File Check: xprt-1-rtd simulation				
Completed Simulation Title Card Check (Page 34)	☒		☒	
Completed Solution Control Card Check (Page 35)	☒		☒	
Completed Direct *input_XPRT-1* Copy Check (Page 36)	☒		☒	
Completed Output Control Card Check (Page 37)	☒		☒	
Input File Check: xprt-2-rtd simulation				
Completed Simulation Title Card Check (Page 40)	☒		☒	

Model Check 5– Transport XPRT Part E				
Model (full name):	B Complex			
Modeler Name:	Praveena Allena			
Peer Reviewer Name:	Brian Archuleta			
Task/Action/Operation	***Modeler***		***Peer Reviewer***	
	Status	Comment	Status	Comment
Completed Solution Control Card Check (Page 41)	☒		☒	
Completed Direct *input_XPRT-2* Copy Check (Page 42)	☒		☒	
Completed Output Control Card Check (Page 43)	☒		☒	
Input File Check: xprt-1-12070 simulation				
Completed Simulation Title Card Check (Page 46)	☒		☒	
Completed Solution Control Card Check (Page 47)	☒		☒	
Completed Direct *input_XPRT-1* Copy Check (Page 48)	☒		☒	
Completed Output Control Card Check (Page 49)	☒		☒	
Completed Initial Conditions Card Check – Part 1 (Page 51)	☒		☒	
Completed Initial Conditions Card Check – Part 2 (Page 52-53)	☒		☒	
Completed Initial Conditions Card Check – Part 3 (Page 54)	☒		☒	
Completed Initial Conditions Card Check – Part 4 (Page 55)	☒		☒	
Completed Initial Conditions Card Check – Part 5 (Page 56)	☒		☒	

Model Check 5– Transport XPRT Part E				
Model (full name):	B Complex			
Modeler Name:	Praveena Allena			
Peer Reviewer Name:	Brian Archuleta			
Task/Action/Operation	***Modeler***		***Peer Reviewer***	
	Status	Comment	Status	Comment
Completed Initial Conditions Card Check – Part 6 (Page 57-58)	☒		☒	
Input File Check: xprt-2-12070 simulation				
Completed Simulation Title Card Check (Page 61)	☒		☒	
Completed Solution Control Card Check (Page 62)	☒		☒	
Completed Direct *input_XPRT-1* Copy Check (Page 63)	☒		☒	
Completed Output Control Card Check (Page 64)	☒		☒	
Completed Initial Conditions Card Check – Part 1 (Page 66)	☒		☒	
Completed Initial Conditions Card Check – Part 2 (Page 67-68)	☒		☒	
Completed Initial Conditions Card Check – Part 3 (Page 69)	☒		☒	
Completed Initial Conditions Card Check – Part 4 (Page 70)	☒		☒	
Completed Initial Conditions Card Check – Part 5 (Page 71)	☒		☒	
Completed Initial Conditions Card Check – Part 6 (Page 72-73)	☒		☒	
After completion by both the modeler and peer-reviewer, the checker will move the form to the CompletedForms folder and will inform the modeler. The form should not be signed until both have completed all the checking and all issues have been resolved.				

Model Check 5– Transport XPRT Part E				
Model (full name):	B Complex			
Modeler Name:	Praveena Allena			
Peer Reviewer Name:	Brian Archuleta			
Task/Action/Operation	***Modeler***		***Peer Reviewer***	
	Status	Comment	Status	Comment
	Modeler		***Peer Reviewer***	
Date Completed	*05-14-2020*		*05-29-2020*	
Name	*Praveena Allena*		Brian Archuleta	
Signature and Date	APraveena *05-29-2020*		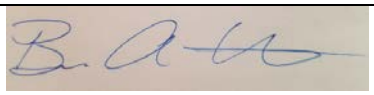 5-29-2020	

Appendix B

Cross-Sections of the Hydrostratigraphy in the B Complex Model

(Electronic Appendix)

This page intentionally left blank.

Contents

This page intentionally left blank.

B1 Introduction

This appendix is a folder containing two subfolders, SouthToNorth and WestToEast. Both contain images of cross-sections through the model showcasing the hydrostratigraphy; the first from south to north and the second from west to east.

The content of this electronic appendix is stored in the Environmental Modeling Management Archive (EMMA) indexed to this ECF by document number.

This page intentionally left blank.

Appendix C

Charts of Recharge to the B Complex Model as Defined by the Recharge Evolution Tool

(Electronic Appendix)

This page intentionally left blank.

Contents

This page intentionally left blank.

C1 Introduction

This appendix is a folder of images. Each image is a map of the annual recharge rate at the surface of the model, as assigned by the Recharge Evolution Tool, per grid cell in the model for each year where any recharge rate is different than the preceding year.

The content of this electronic appendix is stored in the Environmental Modeling Management Archive (EMMA) indexed to this ECF by document number.

This page intentionally left blank.

Appendix D

Software Installation and Checkout Forms

This page intentionally left blank.

Contents

This page intentionally left blank.

D1 Introduction

This appendix is a portable document file showing the completed Software Installation and Checkout form.

This page intentionally left blank.

CHPRC SOFTWARE INSTALLATION AND CHECKOUT FORM

Software Owner Instructions:

Complete Fields 1-13, then run test cases in Field 14. Compare test case results listed in Field 15 to corresponding Test Report outputs. If results are the same, sign and date Field 19. If not, resolve differences and repeat above steps.

Software Subject Matter Expert Instructions:

Assign test personnel. Approve the installation of the code by signing and dating Field 21, then maintain form as part of the software support documentation.

GENERAL INFORMATION:

1. Software Name: STOMP (Subsurface Transport Over Multiple Phases) Software Version No.: Bld 6

EXECUTABLE INFORMATION:

2. Executable Name (include path):

Following STOMP serial and parallel mode executable files in directory [REDACTED]/bin on head node and each compute node (compute-0-0 through compute-0-8, inclusive):

MD5 File Signature	Executable File Name
4a0f738b74620bc8df4d05290b513a44	eSTOMP1-chprc06-20200204-gaia.x
6536b8e12d8c5b83dca76f2c947b6153	stomp-wae-bcg-chprc06i.x
e0cdf04bc1a2f6c55c5a1b499939f663	stomp-wae-bcg-chprc06l.x
86c58db6fac5d1b4e6cbe13041b2568b	stomp-wae-bcg-chprc07i.x
6e72340bb39f6056e232fe5ff241c4d4	stomp-wae-bd-chprc06i.x
3f837a0fb8d9f47dbcada686f542d7fc	stomp-wae-bd-chprc06l.x
7e5b4cc36a8991b3d5a8ea2ed155ce47	stomp-wae-cgsq-chprc06i.x
00a898c0c3ec06817485781ad1c9ec46	stomp-wae-cgsq-chprc06l.x
f18ff5ab5667065d8ab12657344fb6a0	stomp-wae-cgst-chprc06i.x
061af86cf21ad8435b046d0efabe971b	stomp-wae-cgst-chprc06l.x
3c8111a9855dc0e430bf3c8a7abcf37e	stomp-w-bcg-chprc06i.x
20436d615a94955a2ce8eecdb8cba546	stomp-w-bcg-chprc06l.x
8b3df29df21d040189c3e2a50ef823bb	stomp-w-bd-chprc06i.x
066a289a75aedb933eb2536da5d7d1ff	stomp-w-bd-chprc06l.x
c8e62ad7a0d9b6fca39d8a8952ef5d8e	stomp-w-cgsq-chprc06i.x
28ad16806e1307aca51fd7bf89793e75	stomp-w-cgsq-chprc06l.x
6c25051016db2fe1f883a7caaaab1e97	stomp-w-cgst-chprc06i.x
ff9ff6f29b3469419ffaece87d7e772b	stomp-w-cgst-chprc06l.x
0c3e3fba40f5b93e71bcf9586432fd27	stomp-w-r-bcg-chprc06i.x
78492aee80a8c2d0a4e82aabf4a9c213	stomp-w-r-bcg-chprc06l.x
84b129786aba9c4be884e15e45a67389	stomp-w-r-bd-chprc06i.x
e990f1566c8099a8d54508de3da9cd88	stomp-w-r-bd-chprc06l.x
18a589a2b55aab2db290efea19b39351	stomp-w-r-cgsq-chprc06i.x
6569959476772a137df35ce874821889	stomp-w-r-cgsq-chprc06l.x

3. Executable Size (bytes): MD5 signatures above uniquely identify each executable file **COMPILATION INFORMATION:**

4. Hardware System (i.e., property number or ID):

Tellus Subsurface Modeling Platform (serial STOMP executables) and compiled directly on Gaia for eSTOMP.

5. Operating System (include version number):

[REDACTED] 2.6.18-308.4.1.el5 #1 SMP Tue Apr 17 17:08:00 EDT 2012 x86_64 x86 64 x86 64 GNU/Linux (for serial STOMP executables).

INSTALLATION AND CHECKOUT INFORMATION:

6. Hardware System (i.e., property number or ID):

GAIA Subsurface Flow and Transport Modeling Platform (Linux Cluster)

CHPRC SOFTWARE INSTALLATION AND CHECKOUT FORM (continued)

1. Software Name: STOMP (Subsurface Transport Over Multiple Phases) Software Version No.: Bld 6

7. Operating System (include version number):

[REDACTED] 3.10.0-693.5.2.el7.x86_64 #1 SMP Fri Oct 20 20:32:50 UTC 2017 x86_64 x86 64 x86 64 GNU/Linu

8. Open Problem Report? (●) No ( ) Yes PR/CR No.

TEST CASE INFORMATION:

9. Directory/Path:

[REDACTED]/test/stomp/build-6 on head node and each compute node of Gaia

10. Procedure(s):

CHPRC-00211 Rev 3, STOMP Software Test Plan

11. Libraries:

N/A (static linking)

12. Input Files:

Input files for ITC-STOMP-1, ITC-STOMP-2, and ITC-STOMP-2
(Baseline for comparison are results files from ATC-STOMP-1, ATC-STOMP-2, and ATC-STOMP-3 prepared on Tellus during acceptance testing)

13. Output Files:

plot.* files produced by STOMP in testing

14. Test Cases:

ITC-STOMP-1, ITC-STOMP-2, and ITC-STOMP-3

15. Test Case Results:

All PASS, all tests run, on all nodes of Gaia.

16. Test Performed By: WE Nichols

17. Test Results: (●) Satisfactory, Accepted for Use ( ) Unsatisfactory

18. Disposition (include HISI update):

Accepted, entry added to HISI. Installation applicable to all approved Gaia users who have completed STOMP required reading training assignment. Includes all acceptance tested STOMP executables EXCEPT eSTOMP reactive transport (will test this later).

Prepared By:

19.			
WILLIAM NICHOLS (Affiliate) Digitally signed by WILLIAM NICHOLS (Affiliate) Date: 2020.02.05 11:27:03 -08'00'	WE Nichols	
Software Owner (Signature)	Print	Date

20. Test Personnel:

	WE Nichols	
Sign	Print	Date
Sign	Print	Date
Sign	Print	Date

Approved By:

21.		
N/R (per CHPRC-00211 Rev 1)		
Software SME (Signature)	Print	Date

Appendix E

Radionuclide Arrival to the Groundwater Through Time for Plateau to River Grid Cells in the B Complex Model

(Electronic Appendix)

This page intentionally left blank.

Contents

E1 Introduction

This appendix is a folder of portable document files. These files contain charts showing the radionuclide transfer to groundwater from the model in different configurations, as indicated by the figure titles on the charts.

The content of this electronic appendix is stored in the Environmental Modeling Management Archive (EMMA) indexed to this ECF by document number.

1

2 This page intentionally left blank.

3